New constrained amino acids and peptide nucleic acid building blocks for the construction of bio-polymers

Alexandra Gresika

UNIVERSITÉ CÔTE D'AZUR

ÉCOLE DOCTORALE
SCIENCES FONDAMENTALES ET APPLIQUÉES

THÈSE DE DOCTORAT

Nouveaux synthons contraints de type α-amino acides et PNA en vue de l´élaboration de bio-foldamères

New constrained amino acids and peptide nucleic acid building blocks for the construction of biopolymers

Alexandra Gresika

Molécules Bioactives

Présentée en vue de l'obtention du grade de docteur en Chimie
d'Université Côte d'Azur
Dirigée par : Nadia Patino
Soutenue le : 16.11.2018

Devant le jury, composé de :
Muriel Amblard, Directrice de Recherche CNRS, IBMM UMR 5247, Université de Montpellier
Karine Alvarez, Chargée de Recherche CNRS, AFBM UMR 7257, Université Aix-Marseille
Mohamed Mehiri, Maître de Conférences, ICN UMR 7272, Université Côte d'Azur
Nadia Patino, Professeur des Universités, ICN UMR 7272, Université Côte d'Azur

New constrained α–amino acids and peptide nucleic acid building blocks for the construction of bio-polymers.

The purpose of this thesis concerned the development of two kinds of constrained oligomeric structures, based either on unnatural cyclic α-amino acids derivatives or on cyclic Peptide Nucleic Acid (PNA) dimers, in view of analyzing their propensity to adopt pre-organized conformations mimicking the active conformations of proteins or nucleic acids. The first part of this thesis reports on the elaboration of new cyclic α-amino-acids (6-substituted 4-oxopipecolic acids) building blocks, their potential use in the synthesis of constrained homogenous and heterogeneous peptidomimetics as well as their limitations in this use. As part of this work, a new methodology has been developed for the synthesis of N-protected 6-substituted 4-oxo-pipecolic acids residues. The second part of this thesis reports on the elaboration of constrained α-PNA dimers (*di*-α-PNA), in which the side-chains of two consecutive α-PNA monomers are "stapled" *via* a lactam bridge. A synthetic orthogonal strategy has been first developed in liquid-phase then applied to the solid-phase synthesis of models "stapled" di-α□PNA incorporating thymine nucleobases.

Keywords: foldamers; constrained peptidomimetics; constrained Peptide Nucleic Acids; Nucleic Acid analogs; stapled Peptide Nucleic Acids; pre-organized structures; peptide synthesis; solid-phase.

Nouveaux dérivés d'acides α-aminés et de Peptide Nucleic Acids (PNA) contraints pour la construction de bio-polymères.

Le but de cette thèse a concerné le développement de deux types de structures oligomériques contraintes, basées soit sur des dérivés non naturels d'acides aminés cycliques, soit sur des dimères cycliques de Peptide Nucleic Acids (PNA), en vue d'analyser leur tendance à adopter des conformations pré-organisées, imitant les conformations actives des protéines ou des acides nucléiques. La première partie de cette thèse a trait à l'élaboration de synthons clefs dérivant d'acides α-aminés cycliques non naturels (acides 4-oxopipécoliques 6-substitués), à leur utilisation potentielle dans la synthèse de peptidomimétiques contraints, homogènes et hétérogènes, ainsi qu'à leurs limites dans cette utilisation. Dans le cadre de ce travail, une nouvelle voie de synthèse permettant d'accéder à des résidus N-protégés d'acides 4-oxo-pipécoliques 6-substitués a été mise au point. La deuxième partie de cette thèse concerne l'élaboration de dimères d'α-PNA (*di*-α-PNA) cycliques, dans lesquels les chaînes latérales de deux monomères d'α-PNA consécutifs sont «agrafées» via un pont lactame. Une stratégie de synthèse a tout d'abord été développée en phase liquide, puis appliquée à la synthèse en phase solide de di-α-PNA «agrafés» modèles, incorporant des bases nucléiques thymine.

Mots-clés: foldamères ; peptidomimétiques contraints ; PNA contraints ; analogues d'Acides Nucléiques ; PNA agrafés ; structures pré-organisées ; synthèse peptidique ; phase-solide.

Thanks to my family and friends.

Acknowledgements

This scientific work was carried out from 1. October 2015 to 1. October 2018 at the University Côte d'Azur in the "Institut de Chimie de Nice" under the supervision of Prof. Nadia Patino. I thank Professor Nadia Patino to provide me the opportunity to take part on her research and the support during this three years. Thank you for being my second mom in the ICN.

As well, I thank the director of the group, Dr. Rachid Benhida to welcome me to the research group "Chimie de Molecules Bioactives" and the jury to read and judge my thesis.

I thank the "Ministère de l´Education Nationale" and the University Côte d'Azur for their financial support, Dr Lionel Massi and Dr Marc Gaysinski for LC-MS and NMR analyses and Dr. Mohamed Mehiri for his chemical expertise.

All thanks go to the students at the Institute for their encouragement, support and open ear, special thanks go to Anto, Nelli, Mauro, Gabriela, Anita and Oleksander - You were always there for me, in good and bad days.

I would like to express my sincere thanks to my parents and family for their affection and encouragement.

ABREVIATIONS

aeg-PNA	*N*-(2-aminoethyl)-glycine-peptide nucleic acid
Glu	Glutamic acid
Asp	Aspartic acid
Lys	Lysine
Gly	Glycine
Ser	Serine
Orn	Ornithine
Val	Valine
β-ala	beta-alanine
Trp	Tryptophane
Ile	Isoleucine
T_m	Melting point
Arg	Arginine
GPNA	L-g-Glutamyl-p-nitroanilide/ L-Glutamic acid 5-(4-nitroanilide)
dmg-PNA	*(α,α*-dimethyl)glygly-peptide nucleic acid
Aib-Pro	α- aminoisobutyric acid-Proline
IR	Infrared spectroscopy
DMMP	Dimethyl methylphosphonate
Trt-Cl	Trityl chloride

AcCl	Acetyl chloride
TEA	Triethylamine
NEt_3	Triethylamine
DIPEA	*N,N*-Diisopropylethylamine
MeOH	Methanol
DCM	Dichlormethane
n-BuLi	butyllithium
THF	Tetrahydrofuran
MeCN	Acetonitrile
TFA	Trifluoro acetic acid
H_2O =	Water
HCl	Hydrochloric acid
Fmoc-Cl	9-Fluorenylmethyl chloroformate
Boc_2O	Di-*tert*-butyldicarbonate
Alloc-Cl	Allyl chloroformate
Allyl-Br	Allyl bromide
DBF	Dibenzofuran
DMF	Dimethylformamide
Me_3SnOH	Trimethyltin hydroxide
1,2-DCE	1,2-Dichloroethane
LiOH	Lithium hydroxide
NaOH	Natrium hydroxide
iPrOH	isopropyl alcohol
r.t	room temperature
Br_2	Bromine
$CHCl_3$	Chloroform
EtOAc	Ethyl acetate

Et_2O	Diethyl ether
DMSO	Dimethyl sulfoxide
IPA	isopropyl alcohol
TLC	thin-layer chromatography
HBTU	2-(1*H*-benzotriazol-1-yl)-1,1,3,3-tetramethyluronium hexafluorophosphate
DCC	*N,N*-Dicyclohexylcarbodiimide
EDC	1-Ethyl-3-(3-dimethylaminopropyl)carbodiimide
DMAP	4-Dimethylaminopyridine
CDI	Carbonyldiimidazole
DIC	Diisopropylcarbodiimide
HOBt	Hydroxybenzotriazole
PyBOP	benzotriazol-1-yl-oxytripyrrolidinophosphonium hexafluorophosphate
DhbtOH	3-Hydroxy-1,2,3-benzotriazin-4(3H)-one
Pyr	Pyridine
Ac_2O	Acetic anhydride
FmocOSu	*N*-(9-Fluorenylmethoxycarbonyloxy)succinimide
Fm =	Fluorenylmethoxycarbonyl
PG	protecting group
Pd	Palladium
MeI	Methyl iodide
Bzl	benzyl
ESI-MS	electrospray ionization mass spectrometry
HRMS	High-resolution mass spectrometry
MBHA resine	4-Methylbenzhydrylamine hydrochloride resine
TFMSA	Trifluoromethanesulfonic acid
TIPS	Triisopropylsilane

Content

General Introduction

Protein-Protein and Protein-Nucleic Acid (NA) Interactions play crucial roles in numerous biological processes, constituting relevant targets in various diseases. In this context, structures mimicking bioactive peptide conformations, called foldamers, have emerged as important tools for the modulation of these interactions. Indeed, by adopting well-suited pre-organized conformations, they can target large surface areas and mimic protein regions involved in such interactions. The search for new pre-organized structures mimicking the active conformations of proteins is now an area in full expansion since advances in the field have demonstrated their potential for the discovery of next generation therapeutics.

On the other hand, Nucleic Acids (NA) analogs constitute also an intense research area, since they are able to inhibit or modulate gene expression, by forming a complex with complementary DNA or RNA target, *via* Watson-Crick base pairing. In this context, due to their high DNA/RNA binding strength, Peptide Nucleic Acids are considered as devices of choice in diagnostics applications and molecular biology studies. However, as most of NA analogs, they present some limitations that hinder their application as therapeutics, such as poor cellular uptake and off-target effects and the search for PNA analogs overcoming these problems is still relevant.

The purpose of this thesis fit into these two research domains and concerns the elaboration of two different kinds of constrained structures, based either on unnatural constrained α-amino acid derivatives or on constrained Peptide Nucleic acid (PNA) analogs, for studying their propensity to adopt pre-organized conformations, to define them and, in the case of PNA analogs, to study their DNA *vs* RNA specificity.

This manuscript is divided in three parts:

The first part focuses on the development of new constrained peptide mimics, starting from unnatural cyclic α-amino-acid residues, namely “6-substituted 4-oxopipecolic acid” residues. A first chapter, bibliographic, recalls protein secondary structures and

their implications, in particular in Protein/Protein and Protein/NA interactions. Afterward, several mimics of protein secondary structures are described as well as their biological applications. The second chapter is devolved to the synthesis of 6-substituted 4-oxopipecolic acid building blocks required for the construction of peptidomimetic structures, and to the attempts made to synthetize these latter.

The second part of this manuscript is dedicated to our second goal, *i.e.* the development of constrained PNA analogs. A first bibliographic chapter presents the different classes of Nucleic Acids mimics described in the literature, their applications in antisense oligonucleotide therapies and their limitations. A particular attention will be paid to the "Peptide Nucleic Acids" family. The second chapter is dedicated to our works and describes the synthesis of stapled di-α-PNA blocks, both in liquid- and solid-phase, and their structural characterization.

The third part of the manuscript assembles the experimental protocols and the characterization of all the synthetized products. NMR spectra of some molecules are given in Annex I.

Part I

"6-substituted 4-oxopipecolic acid" building blocks for the development of new constrained peptidomimetics

I.-Bibliography

I.-1. Introduction

By using only 20 proteinogenic amino acids, the nature can achieve an endless variety of proteins, which can perform many complex functions essential for the foundation of life. Proteins adopt complex secondary, tertiary and quaternary structures, depending on their primary sequences and further extern influences. Their intrinsic structure is closely related to their biological functions. Many Protein-Protein (PPI) and Protein-Nucleic Acids interactions play essential roles in numerous biological processes representing thus relevant targets for various diseases. These interactions often involve highly structured short peptide sequences of proteins. Chemists have recently begun to design synthetic oligomers that approach the structural and functional complexities of the interacting sequences of proteins to disrupt these interactions. The structure and folding of these synthetic oligomers control their conformation and carry out unsurpassed chemical functions. In the following chapters, several mimetics of protein secondary structures, their biological application and therapeutic potential are described.[1,2,3]

I.-2. Protein structure

Proteins have different shapes and molecular weights and their structure is constructed by four levels (Figure 1):[4]

1) **Primary structure:** linear α-amino acid sequence

2) **Secondary structure:** local conformation of a polypeptide chain, depending on the hydrogen bonding network. The two main types are the α-helix and the ß-sheet, but other conformations are known, among them PolyProline helices of type II and turns.

3) **Tertiary structure:** overall three-dimensional shape of the entire protein. It is fashioned by many stabilizing forces due to bonding interactions between the side-chain groups of the amino acid residues of the protein.
4) **Quaternary structure:** Aggregation from two to several polypeptide chains (subunits)

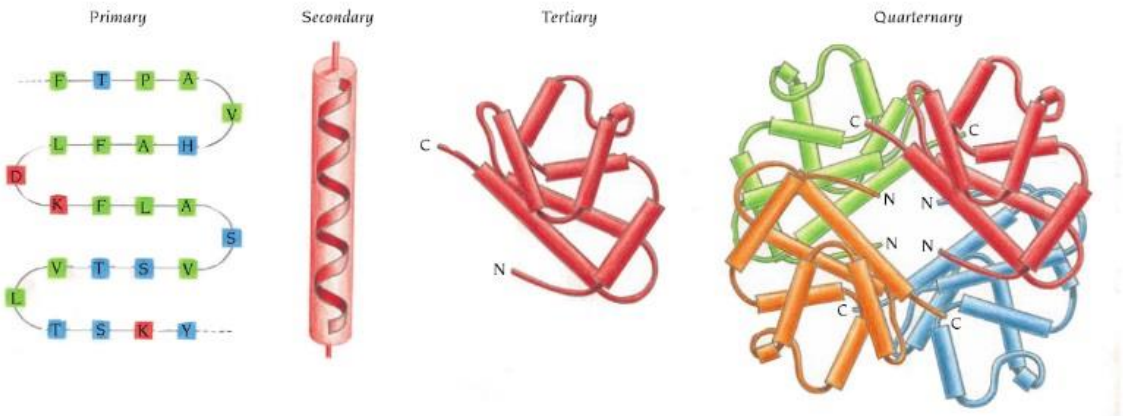

Figure 1: Four levels of protein structure.[4]

I.-2.1 Secondary structures

The secondary structures are defined by the three torsional angles, which are presented in Figure 2. Torsional angle omega (ω) between C_1 and N´ partial double bond, psi (ψ) C_α and CO single bond and phi (ϕ) N and C_α single bond.[5]

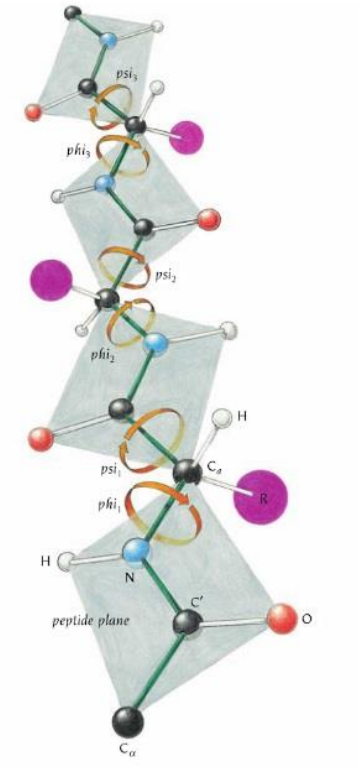

Figure 2: Definition of torsional angles psi (ψ), phi (ϕ) and omega (ω).[4]

The specific *(ψ) and (ϕ)* torsional angles defining the most common secondary structures are presented in table 1.

Table 1:Torsional angles (Φ and Ψ) for α-helix, β-sheets, turns, PPI and PPII.[6,5]

secondary structure	**Φ°**	**Ψ°**
Parallel β-sheet	-119	113
Antiparallel β-sheet	-139	135
α-helix	-58	-47
β-turn Type I	-60	-30
PPI	-83	158
PPII	-78	149

I.-2.1.1 α-helix

The α-helix structure is the most common secondary structure in proteins. In 1948, Pauling discovered this coiled structure, that is stabilized by a network of intra-molecular hydrogen bonds between the C=O groups of residues "*i*" and the NH groups of residues "(*i+4*)" (Figure 3).[7] The α-helix has 3.6 residues per turn and the screw sense is essentially right-handed. Two other helices, π– and $3_{10,}$ exist in which hydrogen bonds established with residues "*i*" and "(*i+5*)" or "(*i+3*)", respectively (Figure 3).[4,8,9]

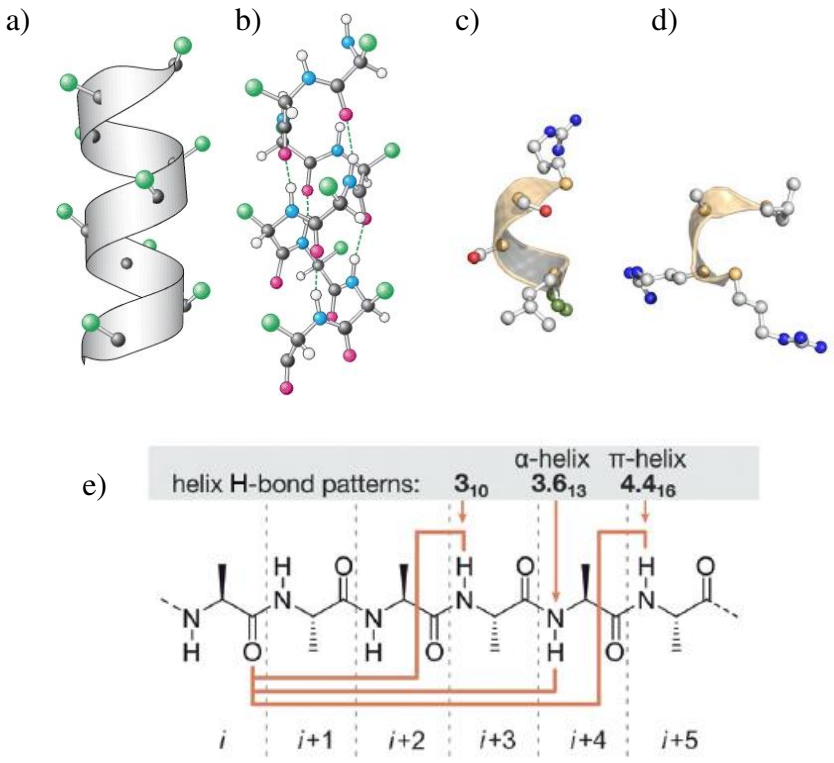

Figure 3: Illustration of α-helix a) Ribbon depiction (green points = amino acid residues) b) side-view of stick and ball version c) 3_{10}-helix d) π-helix. c) and d) illustration with PyMol. e) Helix H-bond patterns.[9,10]

I-2.1.2 β-sheets/β-strands

β-sheets represent an important motif of secondary structure in proteins and arise when segments of polypeptide chains, called β-strands, are connected laterally by at least two or three backbone hydrogen bonds (Figure 4).[4]

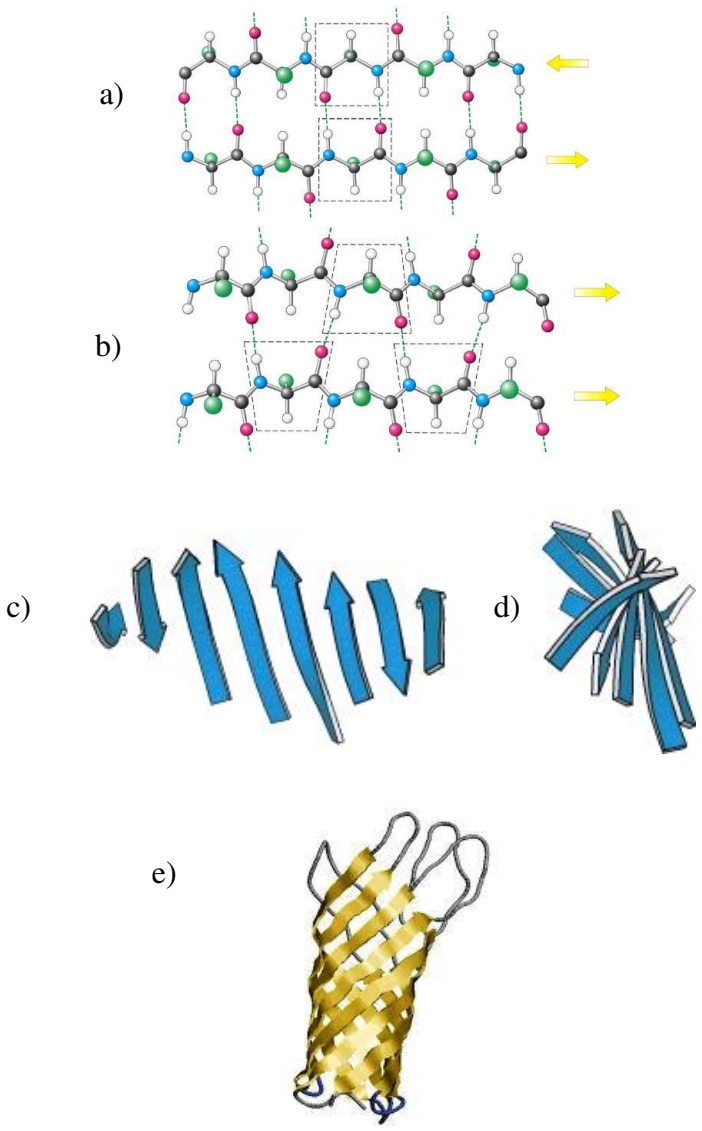

Figure 4: Illustration of β-strands and sheets. a) antiparallel b) parallel; c) and d) Twist of β–sheets. β-strands are illustrated as blue arrows e) β-barrel structure.[10]

The two β-strands in connection can be orientated in the same direction (N-terminal to C-terminal), giving parallel β-sheets or in opposite direction (N-terminal to C-terminal following C-terminal to N-terminal), giving antiparallel β-sheets (Figure 4 a and b). A mixed combination of antiparallel and parallel β-strands may exist. β sheets can be relatively flat but mostly adopt a somewhat twisted and coiled conformation (Figure 4c and d). Additionally, they can fold upon themselves giving bended or bulged or closed

shape, as beta-barrel (Figure 4e). This latter motif is, for example, characteristic of fatty acid-binding proteins, which are important for lipid metabolism.[4,10]

I-2.1.3 Polyproline: PPI and PPII

Polyproline motif is one of the major structural elements found in unfolded proteins and since 1993, it has been advocated as secondary structure motif, like the α-helix and β-sheet. It may adopt two helicoidal secondary structures, defined as polyproline I (PPI) and polyproline II (PPII) helices (Figure 5). PPI and PPII are known since 1951 by Pauling.[11] The polyproline II helix (PPII, poly-Pro II) is left-handed and polyproline I helix (PPI, poly-Pro I) is right-handed. PPI contains all *cis* peptide bonds and is more compact compared to PPII with all *trans* peptide bonds.[12,13,9]

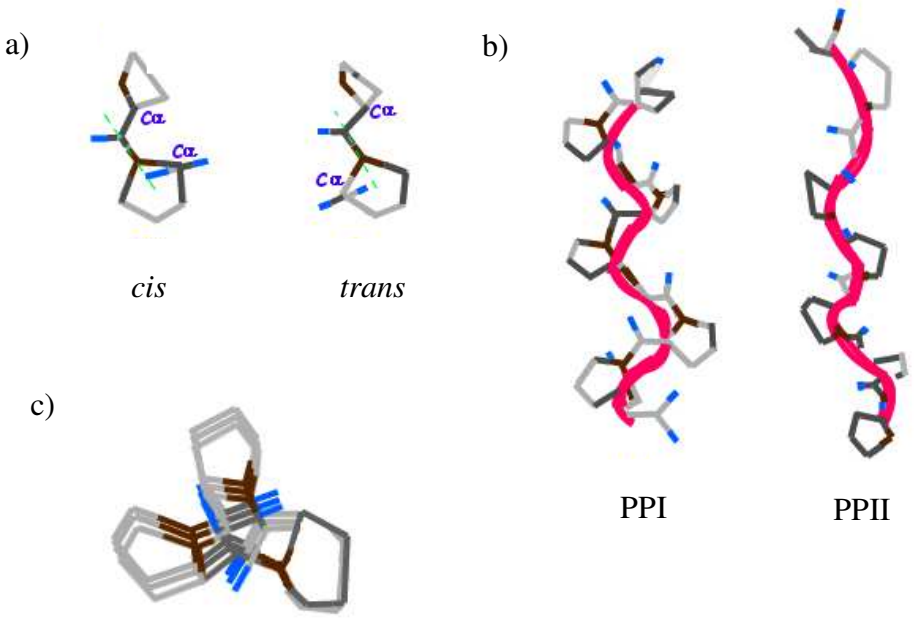

Figure 5: Illustration of a) and b) PPI (left) and PPII (right) structure and c) View of N-terminal of PPI structure.[9]

The polyproline type II (PPII) helix is a prevalent conformation in unfolded proline-rich proteins. It is found predominantly in collagen and commonly observed in fibrous proteins.[12] It is known to play important roles in a wide variety of biological processes.[12]

I-2.1.4 Turn motives/loops

Turns connect consecutive secondary motifs in proteins and reverse the direction of the protein backbone. Globally, turn structures imply two to six amino acids and are classified according to the hydrogen-bond pattern between the carboxyl group of the residue at position "*i*" and the amide proton at position "*i+n*". This forms three families: γ–, β–, and α-turns, with three, four, five amino acids in length, respectively (n = 2, 3, and 4; Figure 6).[14, 10]

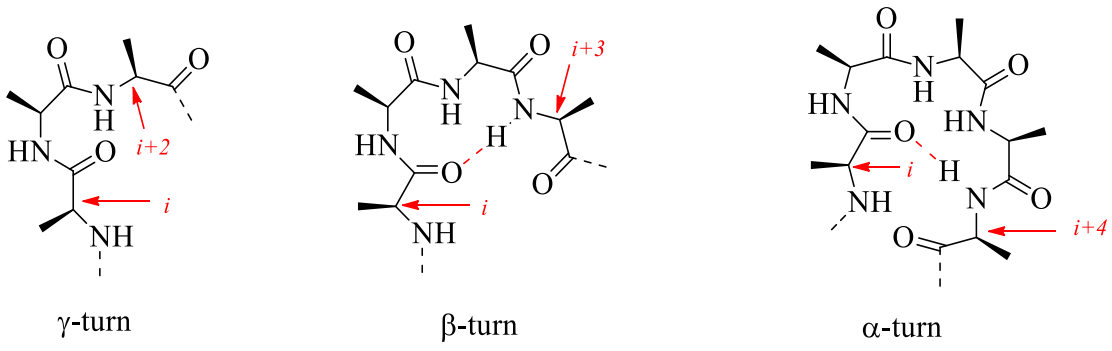

Figure 6: Definition of α-, β- and γ-turns (reverse turns).[10]

In other cases, more elaborate structures are responsible for chain reversals. These structures are called *loops*, they do not have regular, periodic structures (Figure 7). Nonetheless, loop structures are often rigid and well defined.[10]

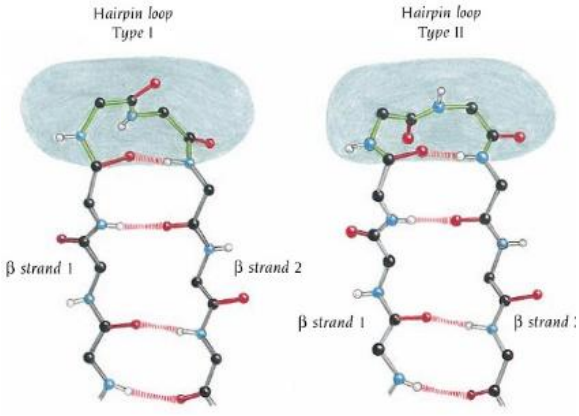

Figure 7: Illustration of Hairpin loop Type I and Hairpin loop Type II. They differ in the orientation of one amide group.[4,10]

Moreover, secondary structures that connect the consecutive hydrogen bonded antiparallel β-strands with loops/turns represent β-hairpins (Figure 8).[15]

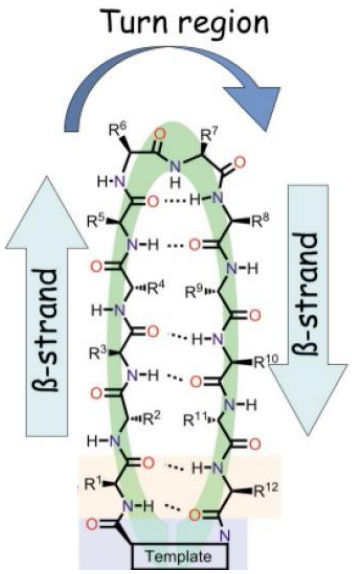

Figure 8: β-hairpin structure.[15]

Turns and loops invariably lie on the surfaces of proteins and thus often participate in interactions between proteins and other molecules.[10]

I.-3. Protein-Protein- and Protein-Nucleic acid interactions

I.-3.1 Protein-Protein Interactions (PPIs)

In many biological functions, the communication between proteins is essential, that makes PPIs important molecular targets with strong therapeutic value. Today, the modulation (inhibition or stabilization) of PPIs involved in relevant critical molecular communications is considered as a therapeutic strategy in various diseases and is useful for understanding biological mechanisms. However, PPIs are extremely difficult to target because of their high surface areas, normally flat and featureless. In general, PPIs involve two protein domains (domain–domain) or a short linear sequence of one protein and a domain of the other one (peptide-domain) (Figure 9). In the two cases, many new studies have revealed a high organization level of these interfaces.[16,17,18] It is known that diseases can be caused by aberrant PPIs, by loss of essential interactions or through the formation or/and stabilization of protein complexes at an inappropriate time or location.[18,19]

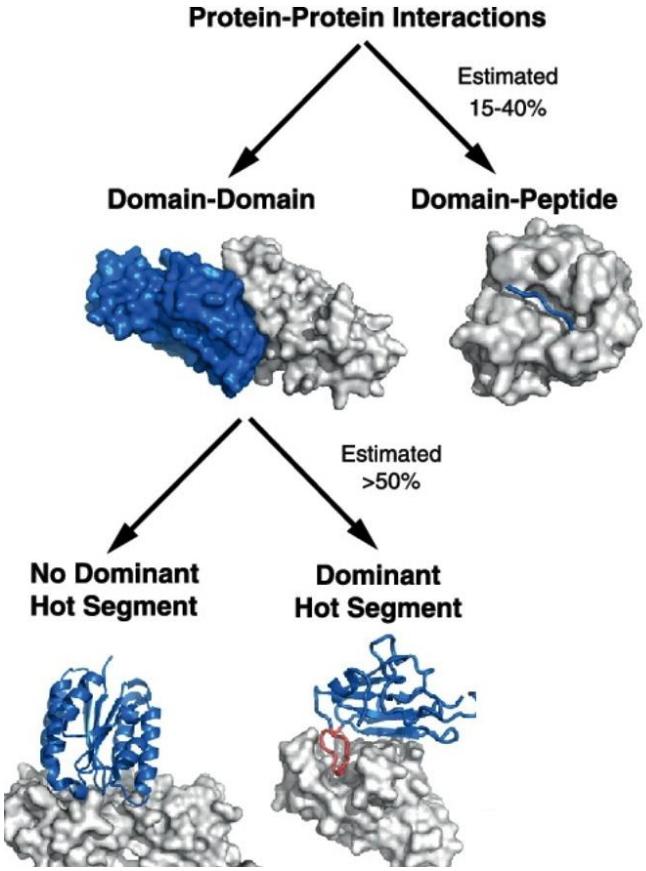

Figure 9:Two categories of PPIs: domain-mediated and peptide-mediated.[20]

Normally 40% of interacting peptides adopt a α-helix conformation and 30% of proteins contain β-strands/sheets motives, which constitute important recognition motives in some protein–protein interactions (PPIs), as in HIV protease-ligands recognition and are implied in neurologic disorders related to in Alzheimer's disease.

The inhibition of PPI constitutes an area of intense research. The most general approaches to inhibit PPIs are primary based on protein topologies (Figure 10). Peptidomimetics have shown their considerable potential in drug design by targeting PPIs.[16] One of their main applications is their interaction with an active conformation of a short linear peptide sequence located at the surfaces of a globular protein domain (peptide-domain interactions). However, domain-domain interactions also involve "hot segments", which are divided in dominant and no dominant segments (Figure 9).

London *et al.* defined "hot segments" as continuous epitopes contributing to the majority of the binding energy.[17,20]

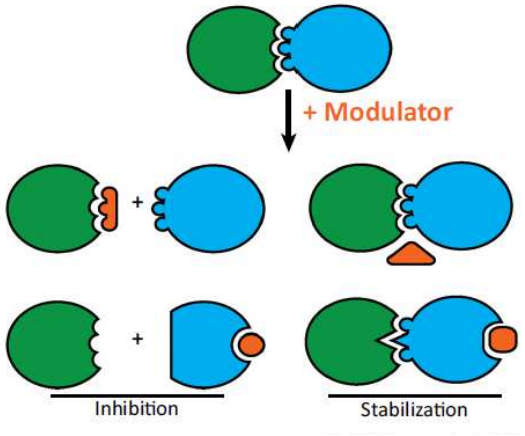

Figure 10: Modulators of PPIs.[19]

I.-3.2 Protein-Nucleic-acid Interactions

Protein-/Nucleic Acid interactions play an essential role in all mechanisms of genes expression and modulation. Structural, biochemical and molecular-genetic studies have proven that interactions between Proteins and Nucleic Acids are significant and are formed by:[21,22,23]

1) Electrostatic interactions (salt-bridges): Interaction between negative charged phosphate groups of DNA and positive charged side chains of proteins

2) Dipolar interactions (hydrogen bonding): Interaction between protein side chains (amino acids) and exposed edges of base pairs (major and minor groove)

3) Dispersion forces (aromatic ring stacking)

4) Entropic or hydrophobic interactions

The networks of specific and non-specific interactions established in DNA-protein- or RNA-protein complexes are intrinsically linked to the 3D-structures of these complexes.

I.-3.2.1 Protein-DNA Interactions

DNA-binding proteins are often used in many major cellular processes to organize and compact the chromosomal DNA and to regulate and effect the processes of transcription, DNA replication, and DNA recombination. The most spacious feature of DNA (A-form and B-form) is the recognition of major and minor grooves by proteins (Figure 11). The structural element employed most frequently is the α-helix, β-ribbons, β-sheets and loops are found less frequently. Considering Figure 11, in the B-DNA helix, the most common DNA form, the major groove is wide enough to accommodate an α-helix and the minor groove, on the other hand, is deep and narrow and thus less accessible to secondary structures such as an α-helix. In A-DNA helix, the opposite is correct. The minor groove is shallow and broad whereas the major groove is very deep and narrow. In general, however, one might expect proteins to directly decode DNA sequences via interactions in the major groove but discriminate among RNA sequences via interactions in the minor groove. This appears for the most part to be the case.[24,25,23]

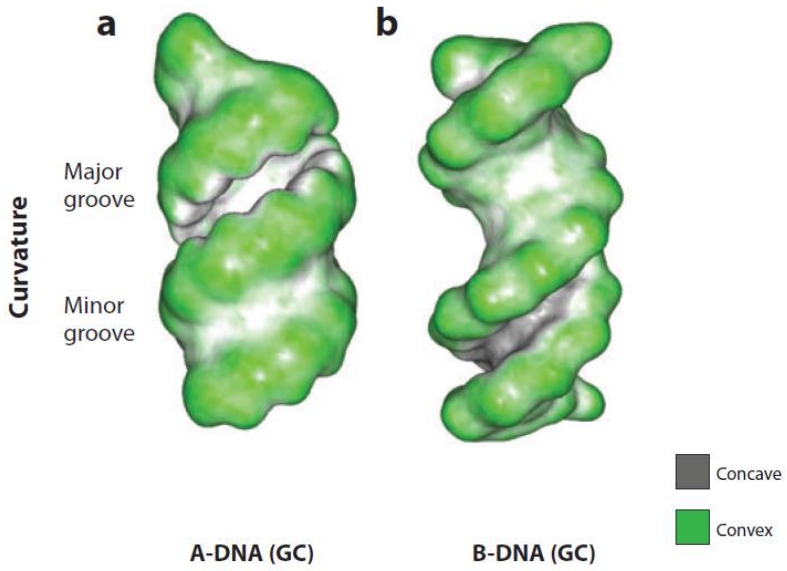

Figure 11: Molecular shape of A- and B-DNA. Convex surface in green and concave surface in dark grey.[25]

On one side, interactions between proteins and DNA can occur *via* the protein recognition of a sequence dependent DNA shape (shape readout), but on the other side, it can occur *via* recognition of the chemical signature of the DNA bases (base readout). That means the contact in the minor and major grooves of DNA is made *via* the formation of hydrogen bonds between nucleic bases and amino acids, directly or water-mediated, and *via* hydrophobic contacts.[25] In Figure 12, several DNA-binding domains of proteins are illustrated the zinc finger-eukaryotic transcription factors, the helix-turn/loop-helix characteristic of most prokaryotic regulatory proteins, the leucine zipper, β-sheet proteins that facilitate the binding to nucleic acids. In reference 23,24 and 26, more DNA-binding proteins are illustrated and explained.[23,24,26]

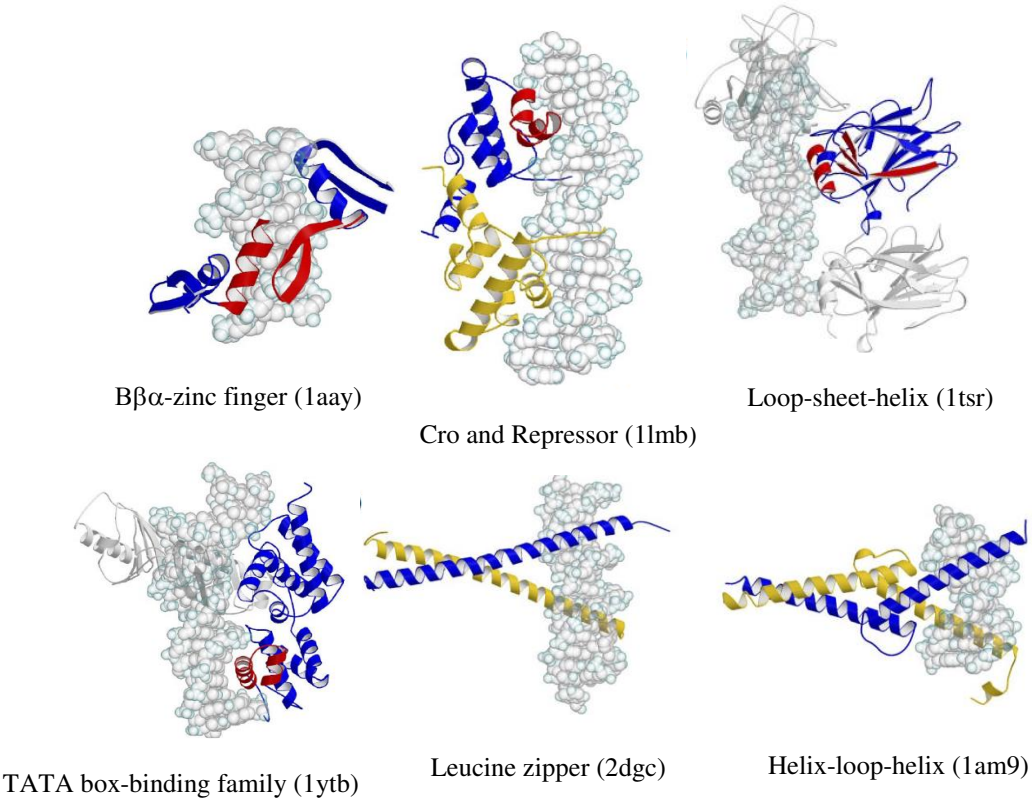

Figure 12: Examples of DNA binding motives in red. The protein binds as a dimer. One monomer is colored in blue and the other in yellow. The DNA is illustrated as space filling model. PDB codes are bracketed.[26]

I.-3.2.2 Protein-RNA Interactions

Specific interactions between RNA and proteins take part in many aspects of RNA biology. These RNA-binding Proteins (RBP) are involved in important mechanisms like transcription, translation, RNA trafficking, and packaging processes, which have important values for the development of potential therapeutic drugs. If we have a look to the major groove of the dsRNA, which correspond to the A-form of DNA (Figure 11), we realize that it is too narrow and deep to allow penetration by an α-helix or β-strand without extensive distortion.[27,28] The RNA recognition motif (RRM), constructed of 100 amino acids, is the most common and studied binding domain. Approximately 500 human proteins, that means 2% of human genoms contain this

protein binding domain.[29] An example is presented in Figure 13. RRM has a mixed α- and β-architecture and recognizes single strand RNAs *via* its β-sheets domain.[30]

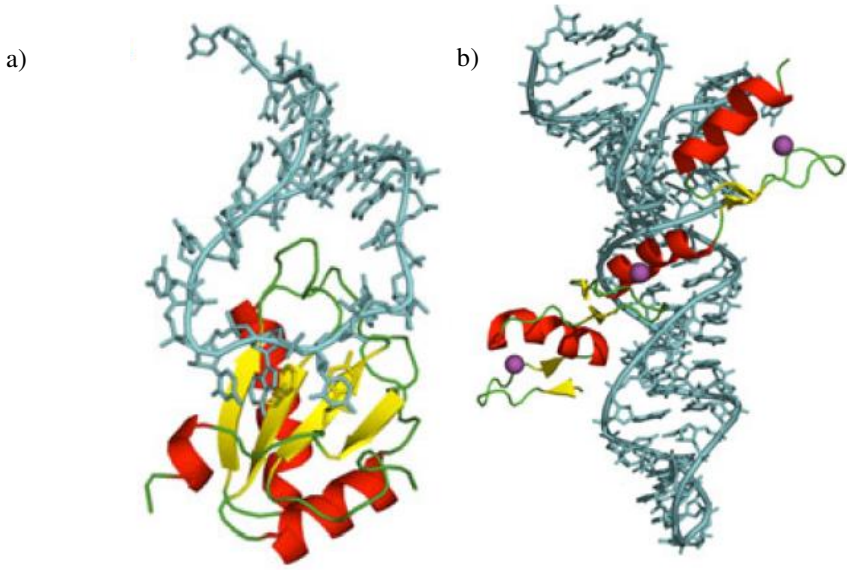

Figure 13: Protein are shown as ribbons (red = helices, yellow = sheets, green = loops). The structural figures are presented by PyMOL. The RNA is presented in blue (cyan stick model). a) RRM in complex with ssRNAs. 3. Crystal structure of the U1A spliceosomal protein RNA hairpin complex (PDB:1URN). Solution structure of RBD of Fox-1 in complex with UGCAUGU (PDB:2ERR). b) RNA binding by ZF proteins. Solution structure of the RBD of Fox-1 in complex with UGCAUGU (PDB entry 2ERR). Crystal structure of three-finger polypeptide from TIFIIIA in complex with truncated 5S RNA (61 nt) (PDB:1UN6). Protein side chain forming base specific contacts with GGU are shown in green. Zn2+ are shown in magenta.[30]

Mostly zinc finger domains bind to DNA, but some of them are also known to recognize RNA. In general, they are constructed from 30 amino acids and contain two cysteine and two histidine residues, following the sequence X_2-Cys-$X_{2,3}$-Cys-X_{12}-His-$X_{3,4,5}$. This sequence can fold in stable β-hairpin and α-helix structures because of the formation of Zn^{2+} complexes.[29] An examples of these RBP is presented in Figure 13, illustrating the crystal structure of the three-finger polypeptide from TIFIIA with 5S RNA.[30]

The minor or shallow groove of dsRNA should be accessible to α-helices and β-strands (Figure 11). But the functional groups of nucleic acid bases are not diverse enough among different nucleotides to allow effective discrimination.

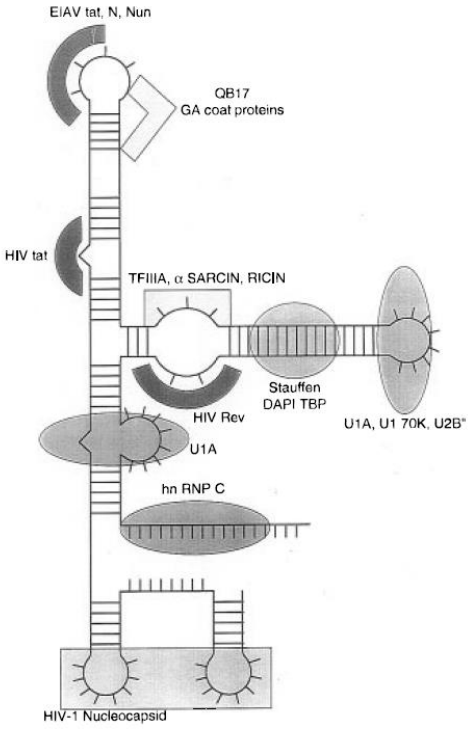

Figure 14: RNA binding proteins do not target dsRNA in sequence-specific manner. These recognize single-stranded regions or sites of local distortions induced in double-helical regions by RNA hairpins (U1A, U1 70K, EIAV Tat, N,...), bulges (HIV Tat), or internal loops (U1A, HIV Rev, TFIIIA, ...).[27]

That is the reason why, all known sequence-specific proteins only recognize ssRNAs and hairpin loops, because the functional groups of nucleic bases are free. However, dsRNA is only recognized if there is structural distortion in the double helix, like internal loops or bulges, allowing access to the major groove (Figure 14).[27] There are specific proteins, that are known to bind with high affinity and specificity to these disordered RNA sites. Arginine-rich motives (ARM), which are sequences of 10-15 amino acids in length rich in arginine and lysine residues, have been shown to bind in α-helical, β-hairpin and extended conformations, depending to the RNA sequence.[27,29]

The most common ARM/ARN complexes are the BIV Tat-TAR RNA, HIV Rev/-RRE and N-peptide/-box B-complexes shown in Figure 15.[28,30]

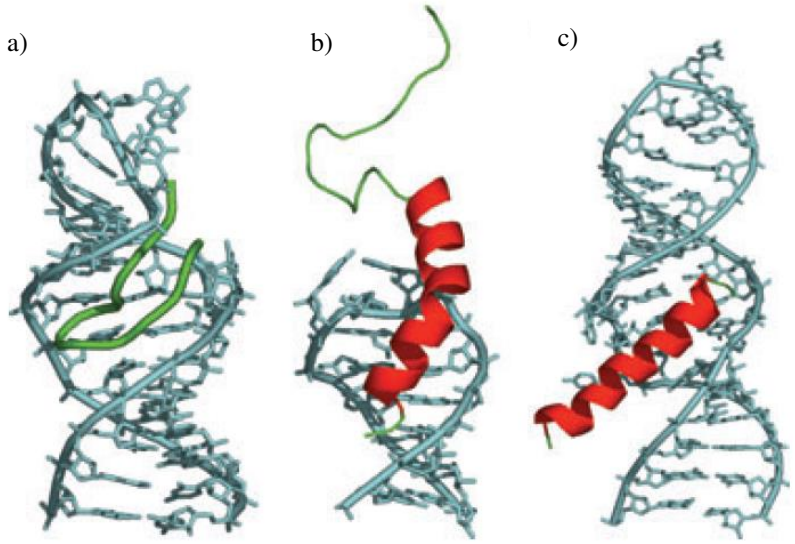

Figure 15: RNA-peptide complexes.: a) The bovine immunodeficiency virus (BIV) Tat-TAR peptide-RNA complex b) The bacteriophage λ N peptide-box B RNA complex c) HIV-1 Rev peptide RRE RNA complex.[28]

Today, inhibitors of protein-protein or protein/nucleic acids interactions have a strong therapeutic value. Mimicking the conformation of the binding domain of proteins is considered as a promising strategy. In the next section, we will present - non-exhaustively - some constrained structures mimicking the interacting sequences (or domains) of proteins. Their therapeutic potential is illustrated by several examples in the following chapters.

I.-4. Designed molecules to mimicking protein secondary structures

The defined peptide sequences of proteins involved in PPI seem ideal candidates as inhibitors of these PPI. However, these short sequences, which are highly structured inside the protein rarely adopt defined conformations when they are isolated, and they are often flexible (Figure 16).

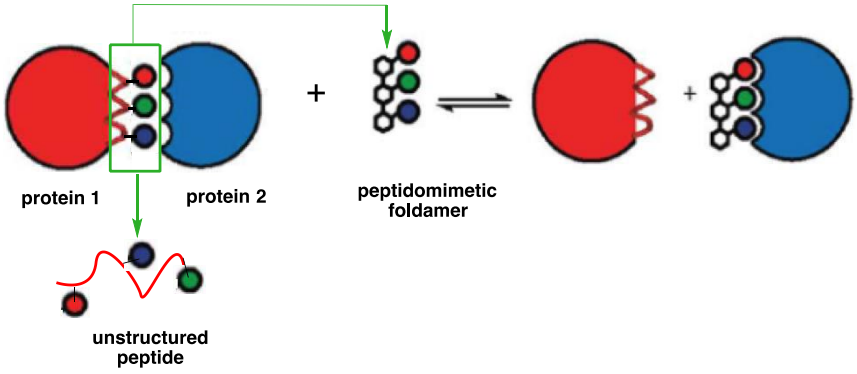

Figure 16: Inhibition of PPIs with secondary structure mimetics.[31]

Many different techniques have been developed to stabilize or pre-organize them into their bioactive conformation (Figure 17). Generally, α-helices are stabilized by the introduction of unnatural amino acids, *N*-terminal capping or side-chain (*i, i+4 or i+7/i+11*) cyclization. Turn motives are stabilized by the introduction of *D*-amino acids or proline, by *N*-methylation or macrocyclization. β-sheets are stabilized by side-chain interactions (disulfide bonds, tryptophan zipper), macrocyclization or turn mimetics.[32,31]

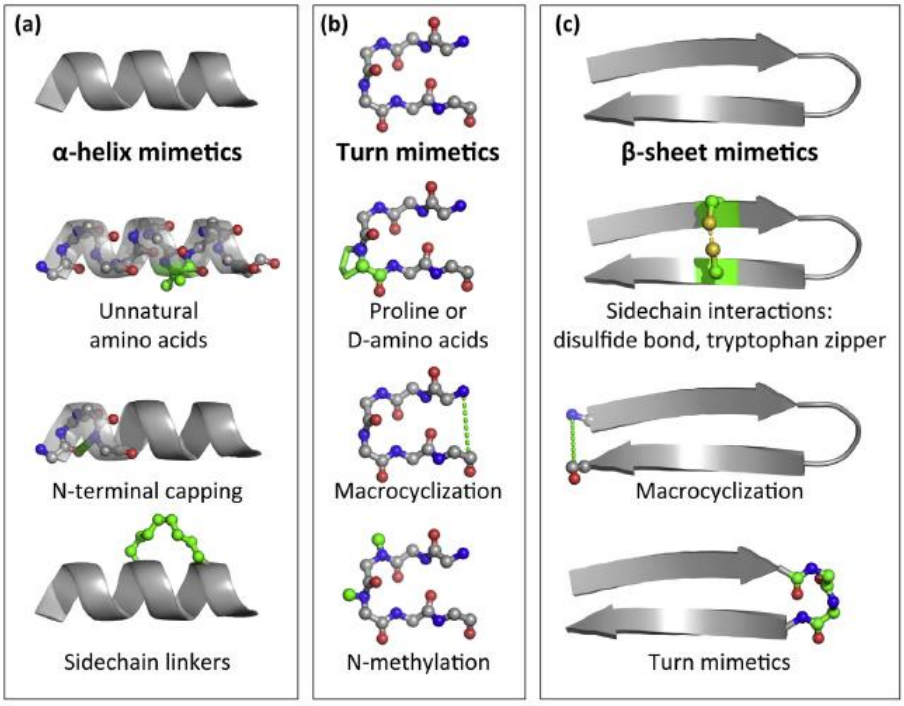

Figure 17: Stabilization-techniques of peptide secondary structures a) α-helices b) turns c) β-sheets.[32]

Peptide-based drugs are significantly prevented by their degradation by proteases, negligible membrane permeability or oral bioavailability, high clearance and metabolic instability. Numerous constrained secondary structures have been developed to overcome these drawbacks. Special examples are presented in the following chapters.

I.-4.1 Foldamers

Foldamers are sequence-specific oligomers based on monomeric repetitive units, folding into well-defined conformations because of noncovalent forces. They are synthetically accessible, amenable to modifications and are predictable and stable in their folding pattern. Based on this, foldamers are used to mimic natural folding of biopolymers. Their structures are controlled by the conformational preferences of the monomer units themselves.[33,34] Foldamers displaying conformational propensities to

proteins and nucleic acids are defined as "biotic" foldamers.[33,34]"Biotic" foldamers are biopolymers, which are constituted by non-natural amino acid units or/and with unusual functions that replace the amide moiety. On the contrary, "abiotic" foldamers are constructed mostly by aromatic rich sequences, which gain new importance, because of their remarkable properties, high stability of folding and relative ease of synthesis. Their robust structures are built by repulsive and attractive interactions. Specific examples of "biotic" and "abiotic" foldamers are shown in Figure 18.[1,2,3]

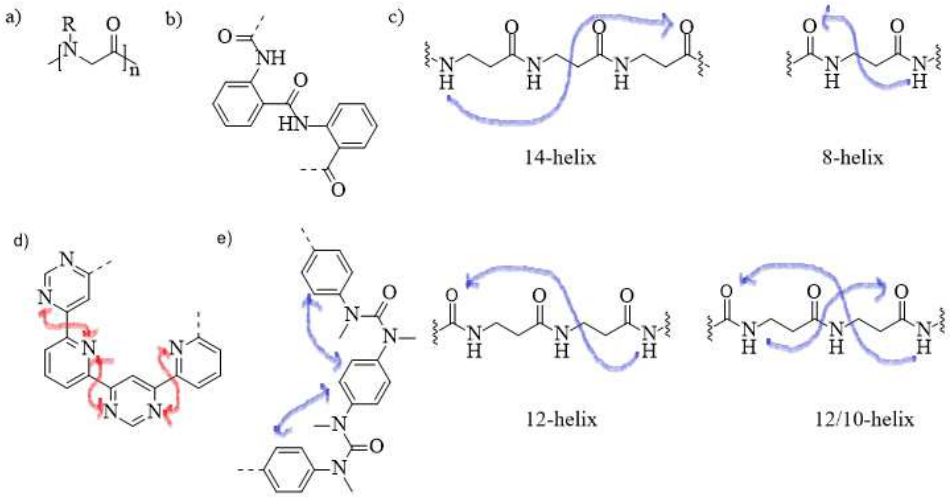

Figure 18: Examples of "biotic" and "abiotic" foldamers. **Biotic foldamers***: a) Peptoids c) ß-Peptides.* ***Abiotic foldamers****: b)Aromatic oligoamides d) Aza-aromatic oligomers e)Tertiary aromatic ureas. Arrows represent intramolecular repulsive and attactive interactions.*[2,3]

Moreover, two kind of foldamers exist: homogenous foldamers are built by the same monomer unit, in contrast to heterogonous foldamers, which contain different monomer units (Figure 19). [34]

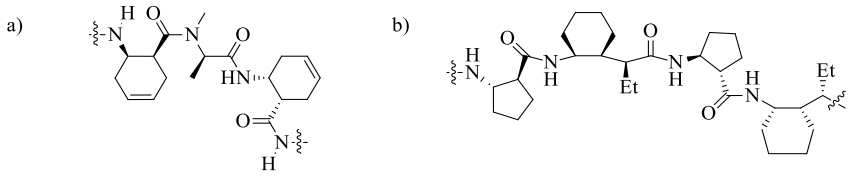

Figure 19:Examples for a) homogeneous b) heterogonous foldamer.[34]

In the following part, we will focus on biotic foldamers. Most of them have been designed for the inhibition of relevant PPIs, involved in various diseases. Nevertheless, some of them have been elaborated for their application as cell penetrating peptides (CPPs), for drug delivery, and as AMP (antimicrobial peptides), to disrupt microbial cell membranes. The structural requirements for peptides targeting cellular or microbial membranes are usually lower than those interacting with specific targets such as proteins.[35]

I.-4.1.1 "Biotic" Foldamers

In 1996, Seebach *et al.* and Gellman *et al*. reported the first peptide foldamer constituted by β-amino acids (10/12-helix).[36,37] These kind of foldamers are described in the literature as β-peptides. They can adopt a variety of helical secondary structures, depending on the nature of side-chains. Since then, many different kinds of aliphatic peptide foldamers (α–, β– and γ–peptide foldamers) have been described (Figure 20).[38,39,40]

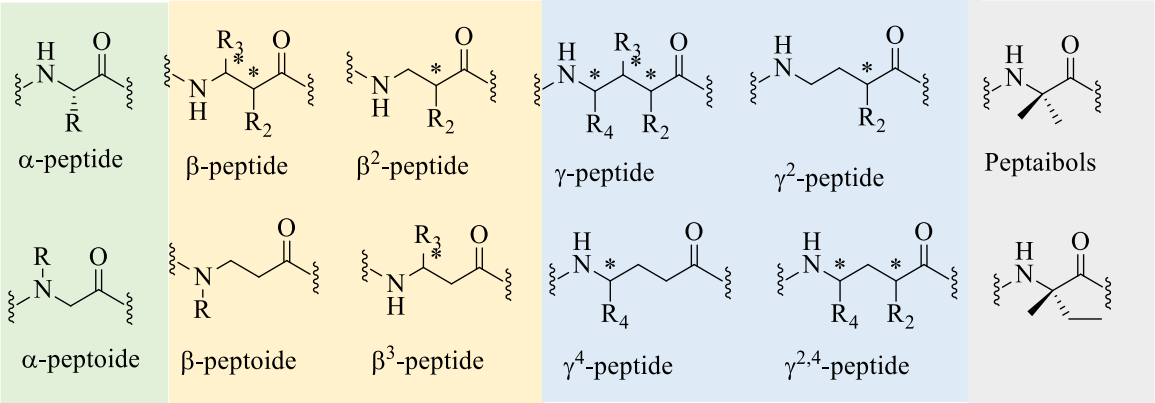

Figure 20: Structure of aliphatic peptide foldamers.[34]

β-peptide helices are named according to the number of atoms contained in the ring closed by the helix specific hydrogen bond and include 8-helix, 10-helix, 10/12-helix, 12-helix and 14-helix (Figure 21).[38,41]

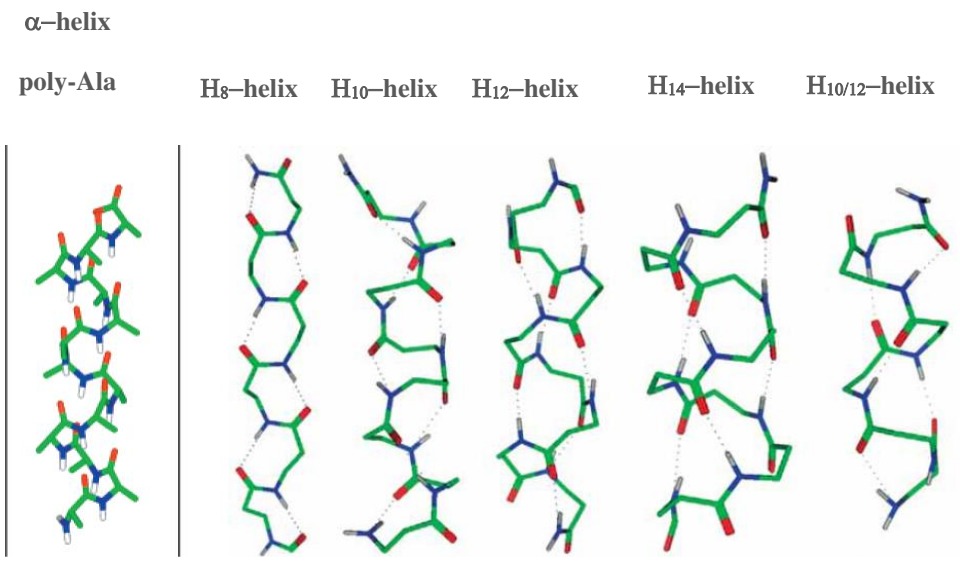

Figure 21.: Helical secondary structures of β-peptides compared to α-helix poly-Ala.[39]

β-amino acids are much more versatile than α-amino acids and because of that, peptides can adopt various secondary structures. Schepartz *et al.* developed β³-peptides **1** that

are more attractive than α-amino peptides counterparts, because of their enhanced conformational and proteolytic stability. These β^3-peptides **1** are used as inhibitors of the p-53-hDM2 interaction (Figure 22).[42,41]

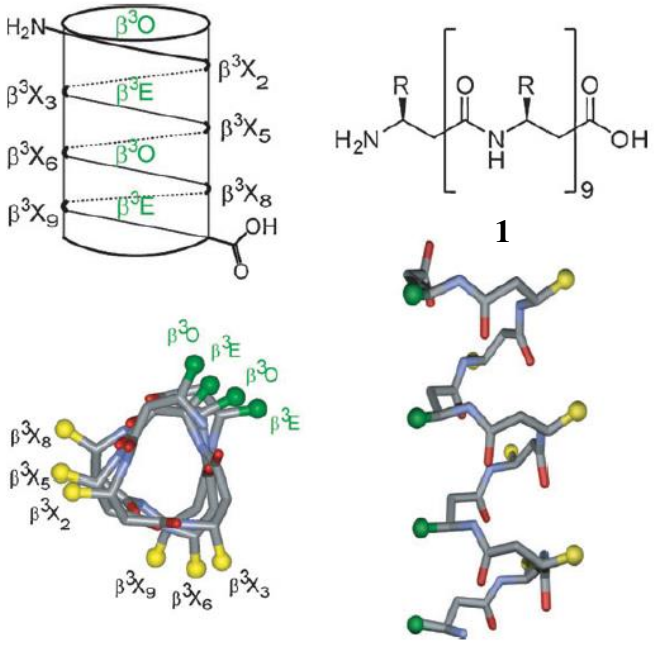

Figure 22: β³-peptide foldamers as inhibitors of p53-hDM2 interaction. Side-chains orientation in helices.[31]

Homo-oligomers of γ-peptides have received less attention, but they display a versatility comparable to that of β-peptides. In 1998, Seebach *et al*. and Hanessian *et al.* developed γ-amino acid oligomers, which formed defined 14-helical structures in solutions.[43,44] Afterwards, Hofmann *et al.* confirmed in 2003 with *ab initio* calculations that 14-helical and 9-helical are the most stable conformations. With further calculations, they showed that unsubstituted γ-peptides could also give, mixed helices, the 22/24 and 14/12-helices being the more stable (Figure 23).[45]

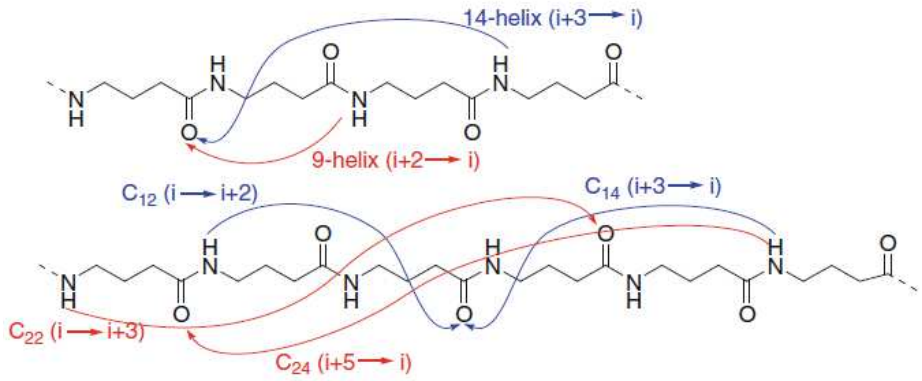

Figure 23: H-bondings in 14-helix or 9-helix (top) and in mixed helices: 14/12 helix or 24/22 helix (bottom).[45]

The Hanessian and Seebach groups studied the folding behavior of γ--peptides substituted on positions γ^4-, γ^3-, γ^2-, $\gamma^{2,4}$- and $\gamma^{2,3,4}$. Surprisingly, γ^4-, $\gamma^{2,4}$- and $\gamma^{2,3,4}$--peptides all fold into the same 14-helix while γ^3--and γ^2-peptides appear to adopt a flexible structure that is therefore hard to determine. From these results, it clearly appears that a single substituent at the γ^4-position is sufficient to promote a robust 14--helix in γ-peptides.[46,43,44] Since then, many mimics of γ^4-amino acids have been elaborated with the goal to form foldameric structures (Figure 24).

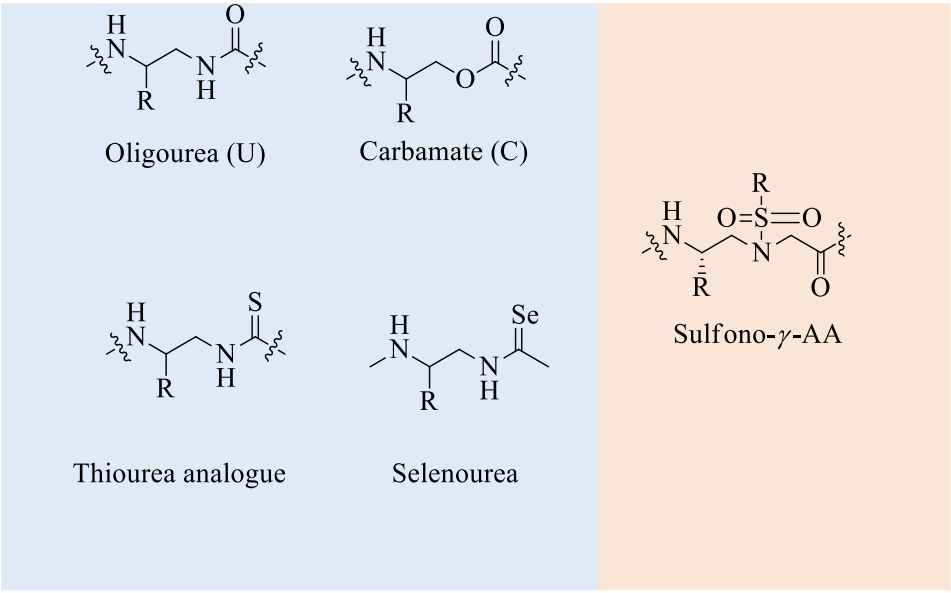

Figure 24: Selected γ4-amino acid isosteres.[34]

One of these mimics is based on the urea motif. It is one of the strongest H-bond pillars and this leads to a strong restriction of the backbone flexibility. Céline Douat *et al.* have developed amphiphilic helical oligourea foldamers, mimicking the histidine-rich peptide LAH4 for the transport of DNA into cells (Figure 25).[47]

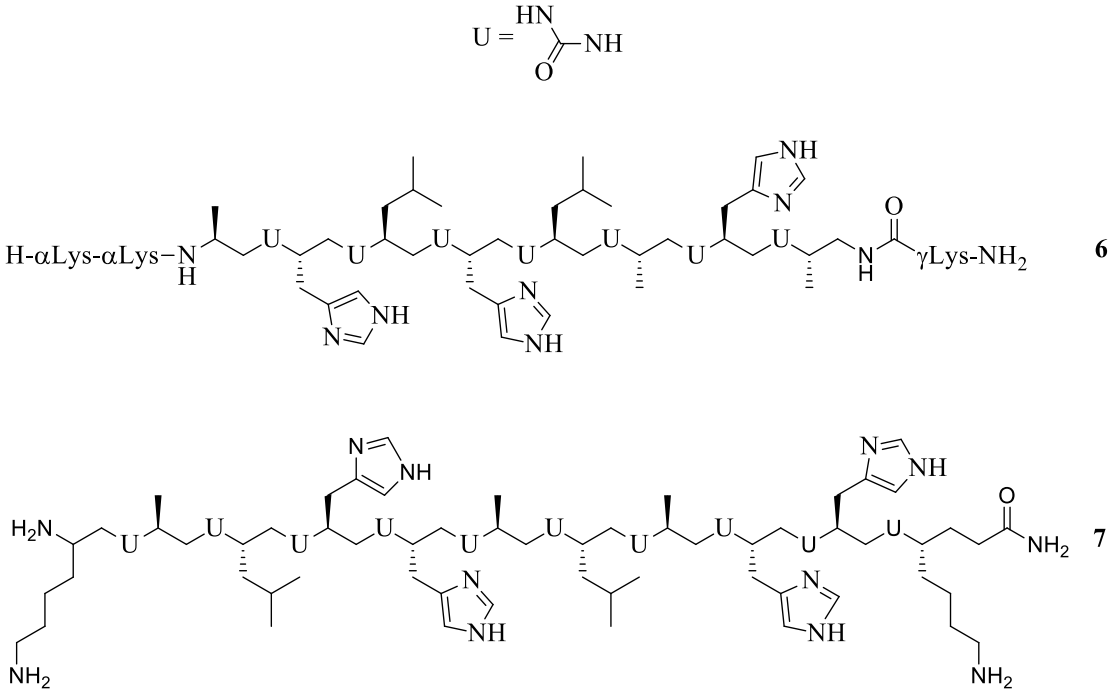

Figure 25: Structure of pH-responsive amphiphilic oligoureas, mimics of CPP LAH4, for NA cell delivery [47]

New families of foldamers based on α-, β-, γ-aminoxy acids have also been developed (Figure 26). Because of the presence of N-O bonds, α–, β- and γ– aminoxy acids shows unusual torsional characteristics and endow extra rigidity. Peptides containing aminoxy acid residues adopt several well-defined secondary structures, such as α–N-O turns (which feature an eight-membered-ring hydrogen bond), β-N-O turns (a nine-membered-ring hydrogen bond), γ-N-O turns (a ten-membered-ring hydrogen bond), $1.8_{(8)}$ helices (consecutive homochiral α-N-O turns), 7/8 helices (alternating α-N-O turns and γ-turns), $1.7_{(9)}$ helices (consecutive β-N-O turns), reverse turns (consecutive

heterochiral α–N-O turns) and sheet-like structures. α-aminoxy acids, which are β-amino acid analogs in which the β–carbon is replaced by a oxygen atom, have been successfully used for the design of anion receptors and channels (Figure 26).[48,49]

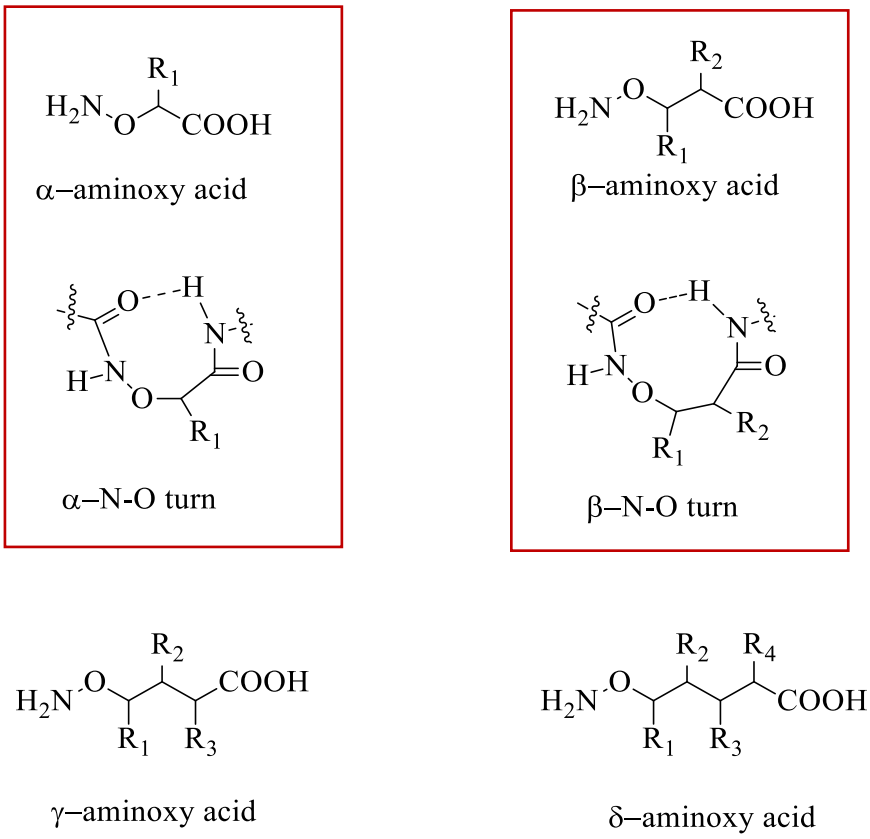

Figure 26: α–, β–, γ– and δ-aminoxy oligomer structures and illustration of α– and β–N-O turns.[49]

Foldamers based on mixed α, β, γ– amino acid, such as α/β–, α/γ–, and β/γ-peptides, also exist that broadens the potential in medicinal chemistry (Figure 29). [50,39] Indeed, the number of foldamers is vastly larger if we include heterogeneous backbones than if we are limited to homogeneous backbones.

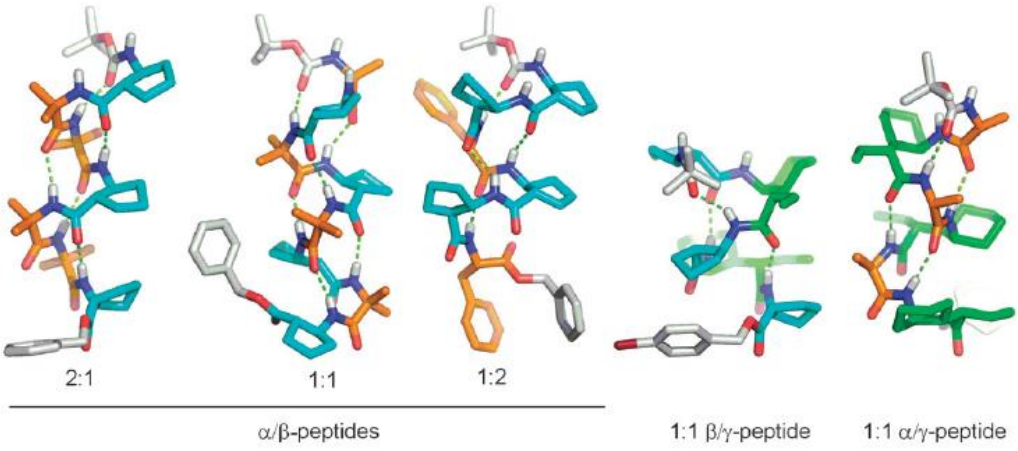

Figure 27: Crystal structure of helical heterogeneous peptide backbones (α–, β– and γ-amino acid residues = orange, cyan, green, respectively).[2]

α/β-peptide foldamers known since 2004, have led to the discovery of new helical secondary structures. In 2007, Choi *et al*. developed α/β-peptide foldamers displaying 11-helical and 14/15-helical secondary structures, starting from β–amino acids ACPC (2-aminocyclopentanecarboxylic acid) and α-amino acids (Ala or Aib) (Figure 30). Additionally, their torsion angels were determined.[48,51]

a)

b)

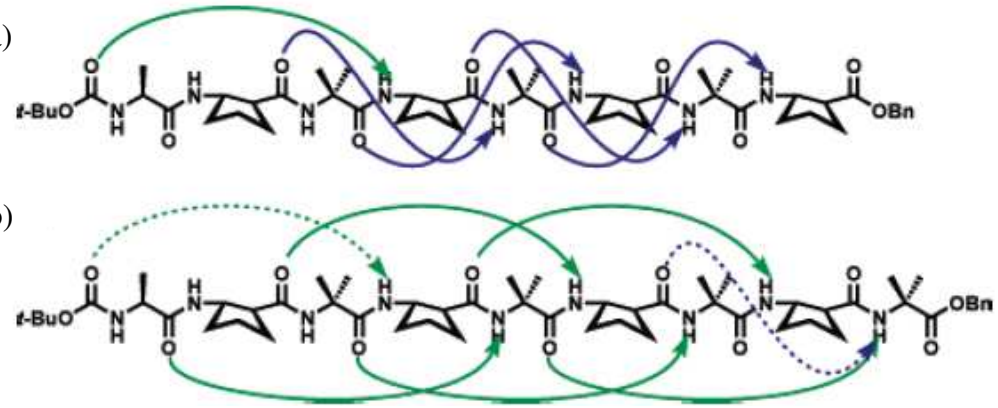

	α-residue		β-residue		
	Φ	Ψ	Φ	Θ	Φ
11-helix	-55(3)	-40(6)	-96(4)	94(6)	-88(7)
14/15-helix	-62(7)	-38(3)	-126(11)	83(6)	-119(15)

Figure 28: Intramolecular hydrogen bonding pattern: 14/15 helical (green), 11-helical (blue). dotted arrows: possible H-bonding interactions. Torsion angles (deg) from α/β-peptide 1-3 (unfolded c-terminal residues excluded) are given in the table.[51]

In 2007, Gellman *et al*. applied β– and α/β–peptide foldamers for the inhibition of PPI involving the Bcl-2 family. They designed a 14/15 helical foldamer to mimic the *N*-terminal region of the Bak segment and published its crystal structure (Figure 29).[52,53,54]

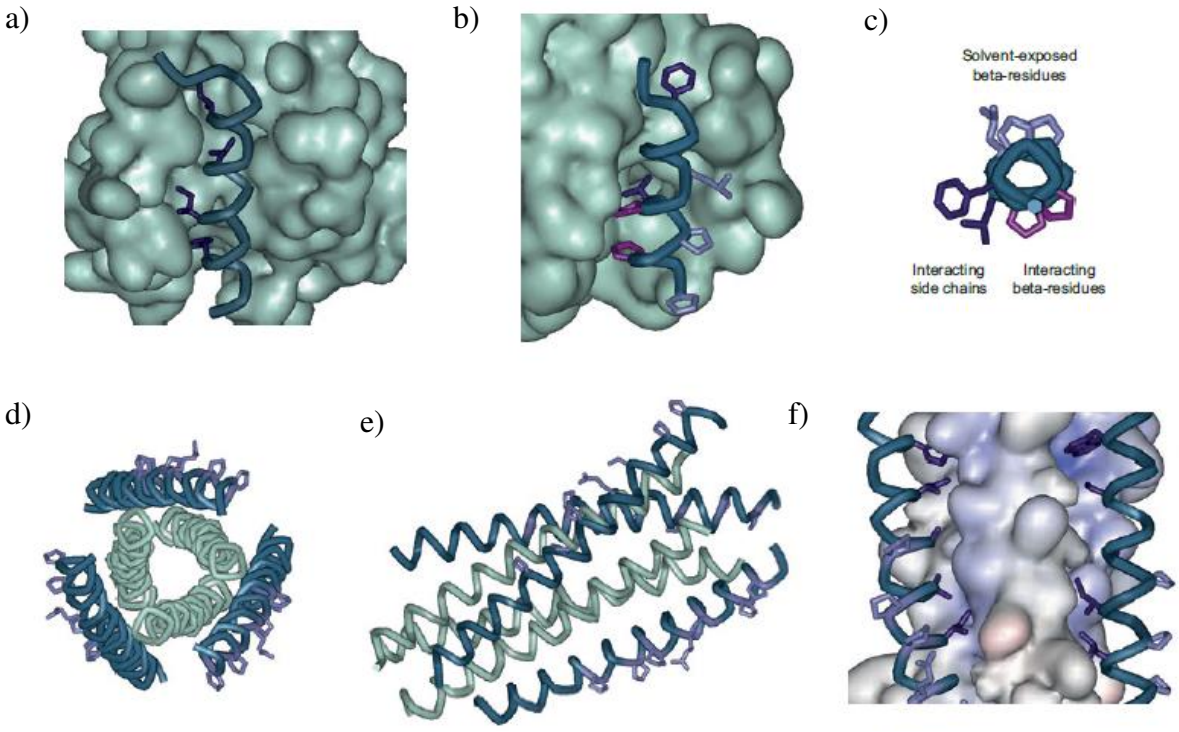

Figure 29: Foldamers for inhibition of PPIs. a) X-ray structure of the pro-apoptotic (α/β+α)-protein BIM interacting with Bcl-$_{XL}$ (PDB:3FDL). This interaction triggers cytochrome C release, leading to apoptosis *b) Chimeric Mimic of BIM-peptide binds to BH3 domain, already illustrated in a) (PDB:3FDM) c) Top view of α/β-foldamer mimicking BIM (PDB:3FDM). d) Top view and e) lateral view of six-helix bundle, which is formed by N-terminal heptad repeat domain (NHR) α-peptides (green) and α/β-foldamer (blue). The β-residues are illustrated in purple. f) Close view of X-ray crystal structure of α/β-inhibitor interacting with NHR core helices (PDB:3G7A). The interfacial residues are in purple, the β-residues in light purple.*[53]

Concerning mixed α/γ- and β/γ-foldamers, Baldauf *et al.* carried out in 2006 *ab initio* calculations proving, that mixed α/γ-peptides form especially 12-helices and mixed 12/10 or 18/20-helices (Figure 30).[55]

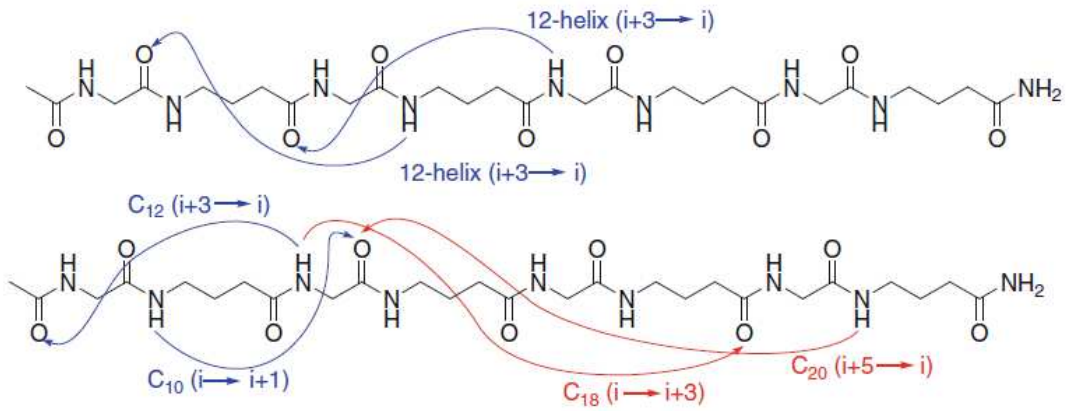

Figure 30: H-bonding in 12-helix (top) and in mixed helices (12/10 or 18/20-botton).[55]

β/γ-peptide foldamers form especially 11- and 13-helices and mixed 11/13 or 20/22 helices (Figure 31). [55]

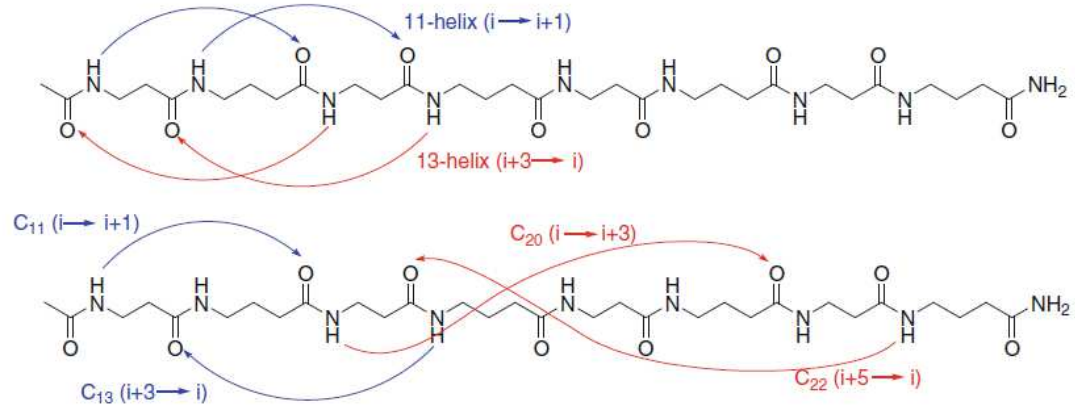

Figure 31:H-bonding in 11-helix and 13-helix (top) and in mixed helices (11/13 helix or 20/22 helix-bottom). [55]

Sharma and Kunwar *et al*. reported several interesting α/γ– and β/γ-peptide foldamers with sugar side chains that adopt 12/20 and 11/13 helices in solution. But recently, they reported as well α/ε-peptide foldamers, which form 14/12-helices (Figure 32).[56,57]

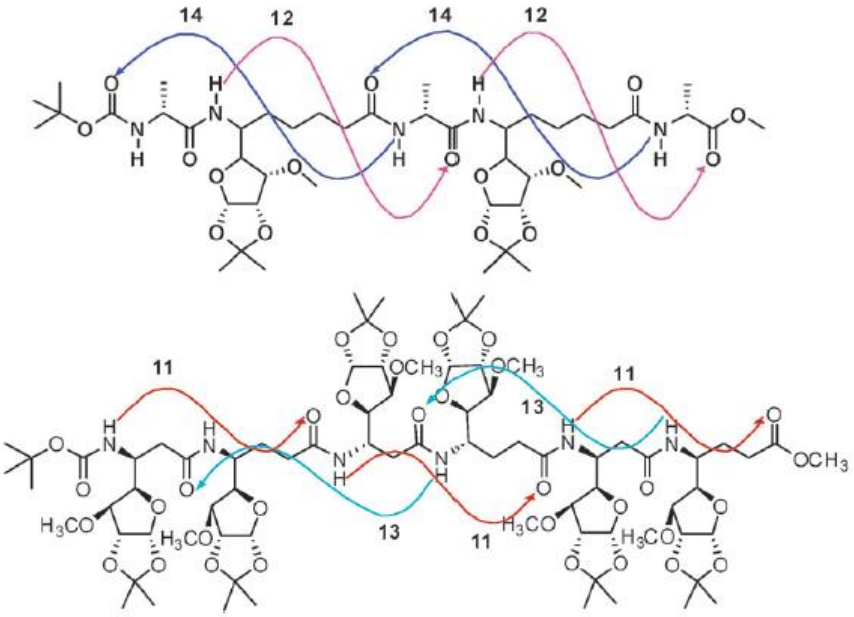

Figure 32: Heterogeneous peptide foldamers from Sharma and Kunwar at al. β/γ-peptide foldamer-11/13-helix (top) and α/ε-peptide foldamer-14/12-helix(below).[57, 56]

On way to construct foldamers is to introduce constrained cyclic amino acids building blocks. Some are presented in Figure 33.

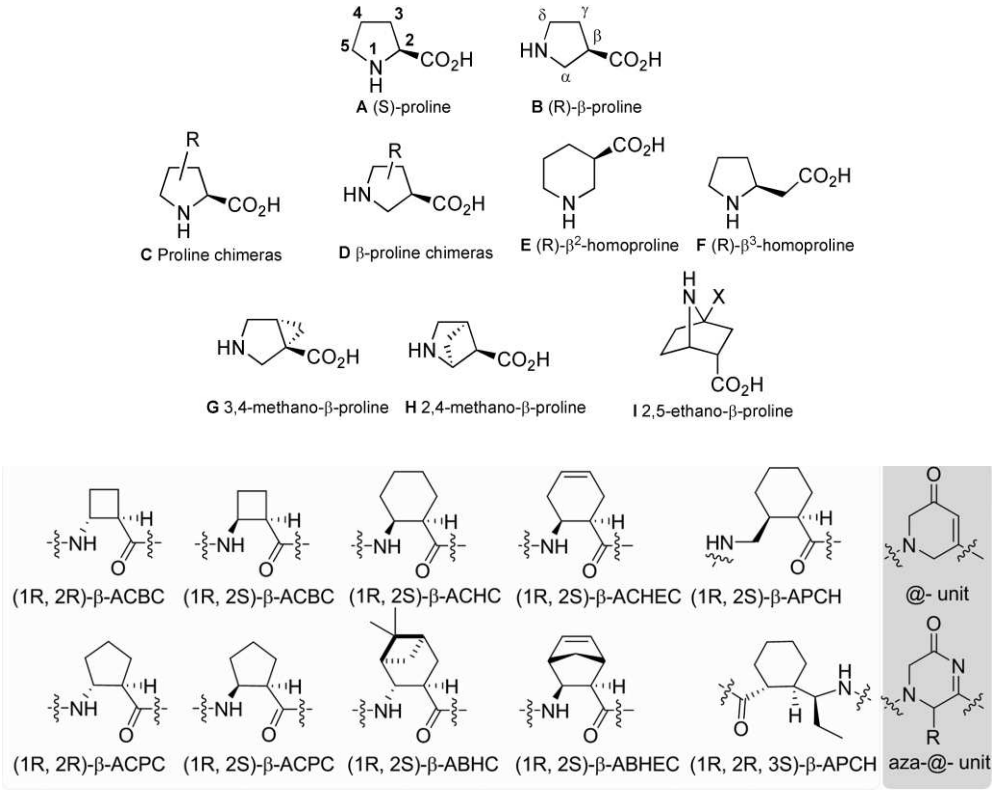

Figure 33: Examples of cyclic amino acid building blocks.

In 2017, Vezenkov *et al.* foldamers alterning cyclic α-amino-γ-lactam motives and α-aminoacids residues having cationic (Arg) and amphipathic (Trp) side-chains, distributed on different faces of the foldamer backbone. They demonstrated that these foldamers adopted a ribbon-like structure (Figure 34) and were able to efficiently deliver a biologically relevant cargo inside the cell.[58] Moreover, they showed a dramatically improved protease resistance.

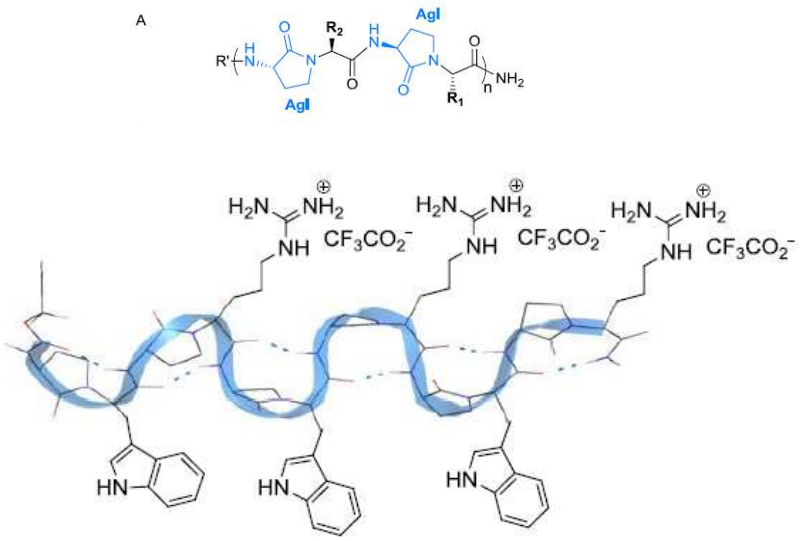

Figure 34: Structure of Agl-AA foldamers and graphical representation of compound 2c. R1 and R2 = Arg or Trp side-chains.[58]

Manish Nepal *et al.* published in 2015 a new type of polyproline (PPII) helical scaffold (Figure 35), designed as CPP displaying an intrinsic antibacterial activity. Their goal was to combine the properties of CPPs and antimicrobial peptides (AMPs) in one agent. As CPP, most AMPs have both cationic hydrophilic and hydrophobic side chains, distributed on different faces on the overall folded conformation and actually, AMPs often display their antimicrobial activity through a membrane-lytic mechanism of action. Their good selectivity allows them to cross the bacterial or mammalian cell membranes.[59] Among the various polyproline foldamers developed by Nepal, one of them $((P_RP_RP_L)_5$ (Figure 36) displayed one of the best properties for cell-penetration and anti-lytic antibacterial activity *in vitro* and *in cellulo*.[60,35]

a)

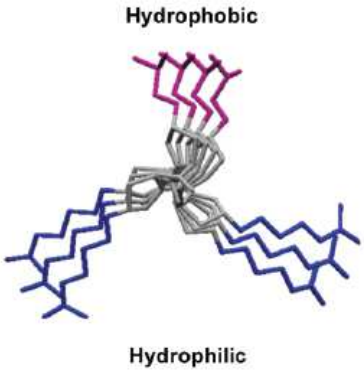

b)

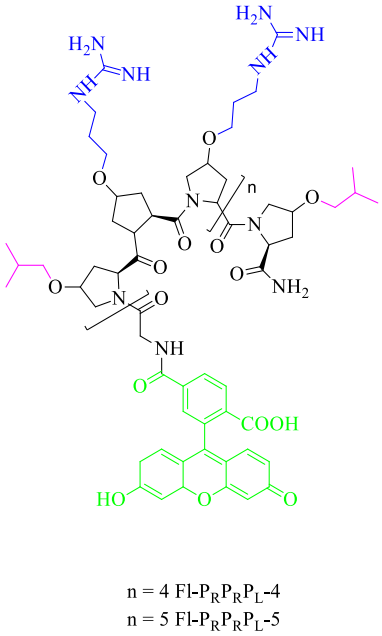

Figure 35: Polyproline foldamers (CAPHs) developed by Manish Nepal et al. a) Top view of the helix model b) Structure of labeled CAPHs incorporating the fluorescein fluorophore (in green).[60]

I.-4.2 Cyclic Peptides secondary structure mimetics

Today, cyclic peptides generate an ongoing interest, notably in the field of PPI inhibition, since they may adopt thermodynamically stable protein-like conformations (helices, strands and turns), mimicking efficiently the stabilized native states of folded proteins.[14,6] As well as foldamers, their conformational rigidity helps to minimize the entropic penalty associated with the target binding. Moreover, these cyclic structures display an increased resistance to degradation by proteases, as compared to their linear counterpart.

I.-4.2.1 α–Helix mimetics

40% of secondary structure motifs are α-helix and more than 60% of all proteins in PDB have an α-helix sequence at their surface. That's the reason for the interest of mimicking helical regions to influence protein-protein interfaces.[61] Many methods for stabilizing a peptide sequence in an α-helix conformation have been published and presented in the review of Pelay-Gimeno *et al.*[6] and Hill *et al.*[14]. The most common method consists in "stapling" -covalently or not - two side-chains of two residues that will be located on the same face of the a-helix. A distinction is made between two techniques of stapling: one- vs two-component stapling. The one-component stapling is the stapling of two side chains while, the two-component stapling uses a bifunctional linker to connect two side chains (Figure 36).[14,62,63]

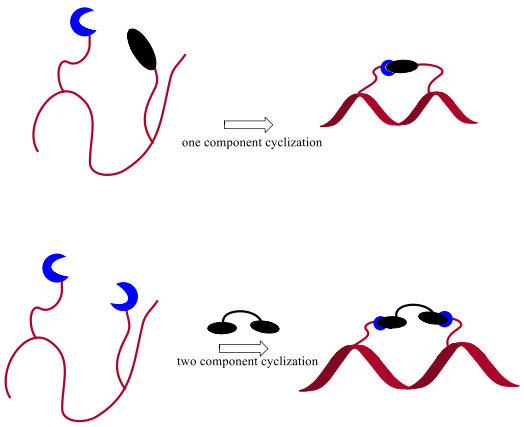

Figure 36: One- vs. two-component cyclization.[61]

Different kind of strategies of stapling are described in the literature, like salt bridges, lactam bonds, disulfide bridges, hydrophobic interactions, metal ligation, triazole stapling, photo controllable macrocycles and hydrocarbon stapling (Figure 37).

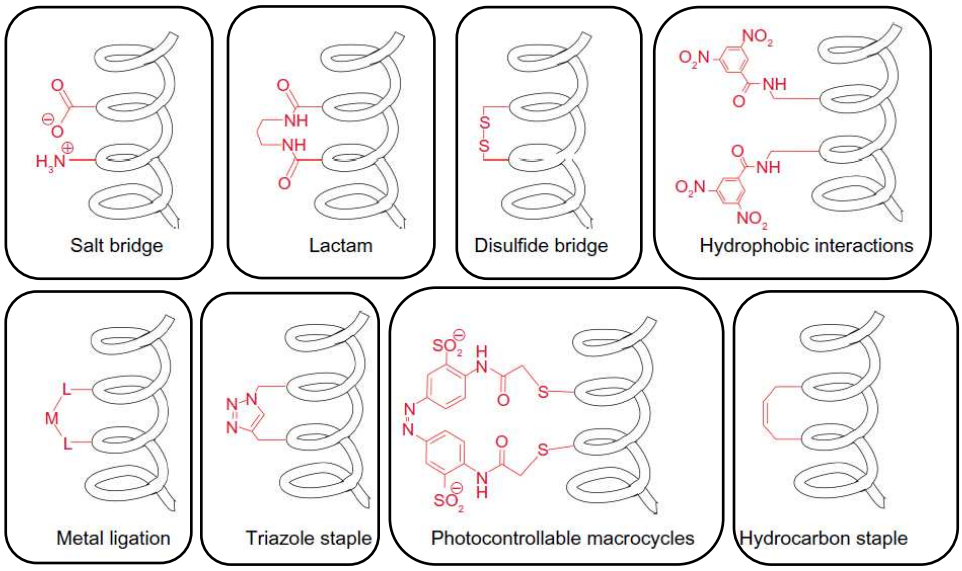

Figure 37: Various stapling techniques.[64]

In the next section, we will focus particularly on lactam bridges peptides and hydrocarbon stapled peptides, which have given the best results as biomedical research tools and prototype therapeutics.[16,61]

a) Lactam bridged peptides

Fujimoto *et al.* followed the two-component cyclization approach using different kinds of cross-linking agents, to stabilize an helical structure conformation in short peptides containing two Lysine residues in positions (*i/i+4), (i/i+7)* or *(i/i+11*) (Figure 38).[65]

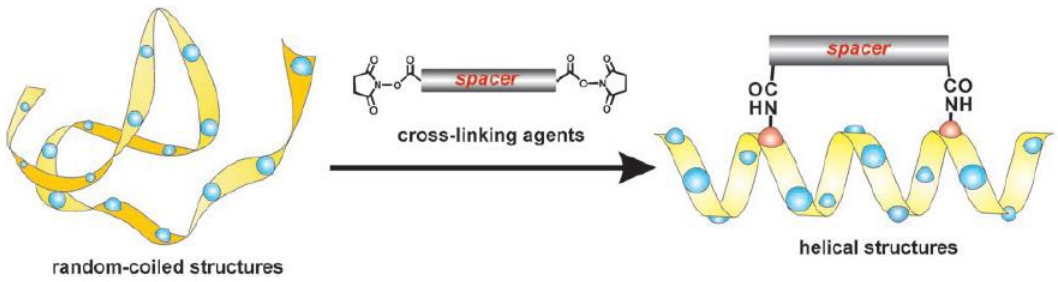

Figure 38: Illustration of cross-linked peptides elaborated by Fujimoto et al..[65]

Lactam-bridged peptides following the two-component approach have also been used to inhibit the HIV entry into host cells. The glycoprotein 41 (gp41) is an HIV transmembrane protein responsible for the fusion of the viral envelope and host cell membrane, making gp41 a valuable therapeutic target (Figure 39).[66] The insertion of the *N*-terminal coiled coil of gp41 into the host cell is followed by a structural rearrangement, leading to a six α-helix bundle. C-terminal heptad repeat (CHR)-derived peptides, stabilized by the introduction of one (HIV C14 Linkmid)[67] or two lactam-linkers (HIV 31) were developed as antiviral therapeutics because of their interaction with the assembly of the helix bundle (Figure 39).[6,66,68]

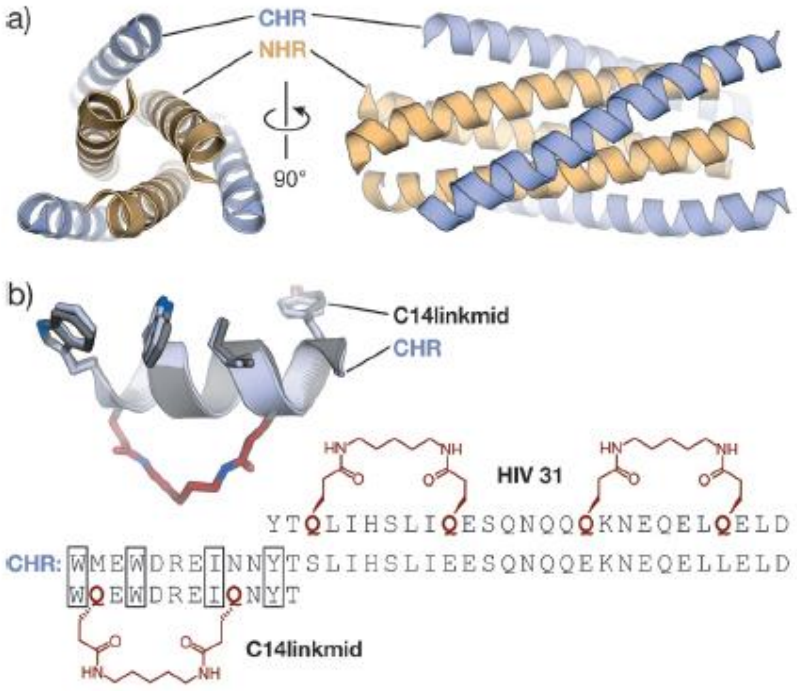

Figure 39:Six-helix bundle of gp-41 C-terminal heptad repeat (CHR) and N-terminal heptad repeat (NHR) helices: a)Crystal structure of six-helix bundle involving three CHR (blue) and three NHR helices (orange) (PDB:1AAlK)[66] b) Two examples of lactam bridged CHR-derived α-helices: HIV 31 and C14Linkmid including superimposed crystal structures of CHR fragment (blue, PDB:1AlK) and C14Linkmid (gray, PDB:1GZL).[6,68,67]

Lactam-bridged peptides for stabilization of the α-helical conformation have been reviewed in 2002 by Taylor *et al.*.[63] In 2005, Shepherd *et al.* found the pentapeptide 15

Lys(*i*) → Asp(*i+4*) to be superior to other lactam bridged macromolecules for the stabilization of α-helices (Figure 40).[14,62]

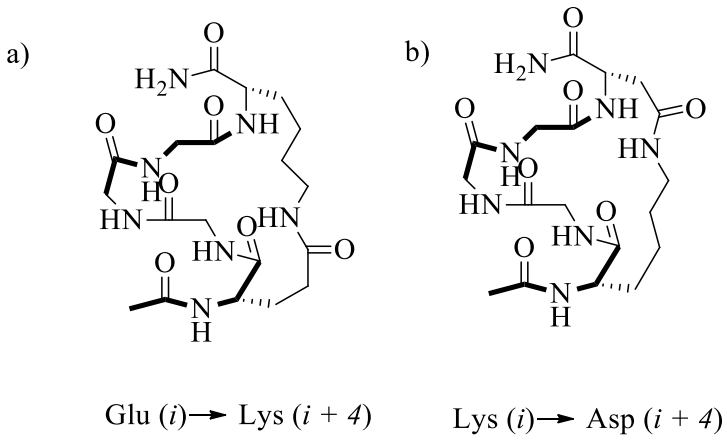

Figure 40: Lactam-bridged peptides (i --> i+4) to stabilize α-helix structures.[14,62]

b) Hydrocarbon stapled peptides

Hydrocarbon-stapled peptides are peptides in which two alkenyl side-chains of two unnatural α-amino acids joined to form a macromolecule, using ruthenium-catalyzed RCM (ring closing metathesis) as the key step in the synthesis. The first stapled peptides were introduced in 2000 by Verdine *et al.* and expanded by Blackwell and Grubbs (Figure 41).[69,70,71,14]

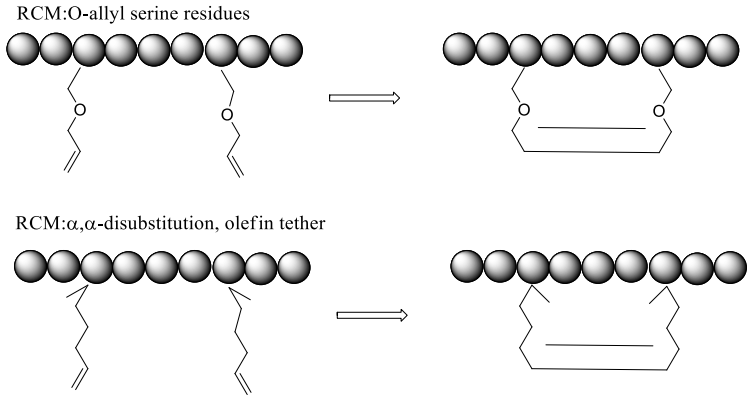

Figure 41: Ruthenium olefin metathesis for crosslinking of macropeptides. Metathesis of Blackwell and Grubbs on O-allylserine residues (top). Metathesis of Schafmeister and Verdine on α,α -disubstituted non-natural amino acids (bottom).[71]

Hydrocarbon linkers are introduced into a polypeptide by incorporating two α-methyl, α-alkenylglycine residues with defined stereochemistry, in chosen position. As illustrated in Figure 42, these two residues are separated by two (*i, i+3)*, three (*i, i+4)* or six *(i, i+7*) amino acids.

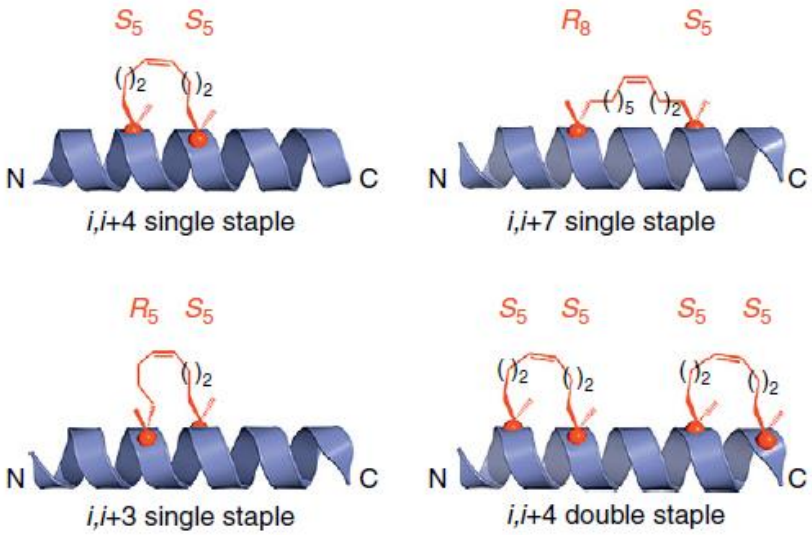

Figure 42: Hydrocarbon stapled peptides. Different α-methyl, α-alkenylglycine amino acids are used to introduce each staple type. These are indicated using the naming convention X_Y, where X is the stereochemistry at the α-carbon (Cahn–Ingold–Prelog designations) and Y is the length, in carbons, of the alkenyl side chain.[72]

Because of their large contact surface area, hydrocarbon stapled peptides are used to

inhibit intra- and extra-cellular protein-protein and protein/nucleic acids interactions. Moreover, they are readily accessible through standard solid-phase peptide synthesis.[72,71] Most stapled peptides display dramatically improved pharmacologic parameters, such as resistance to proteolytic degradation, cell-penetration, and *in vivo* half-life as compared to disulfide and lactam bridges.[72,71]

Today, stapled peptides are largely used to disrupt PPIs involved in human diseases, particularly in cancer. In many types of cancer, proteins MDM2 and MDMX (also called MDM4 and HDM4/HDMX) downregulate the tumor suppressor p53 protein, *via* their binding to the α-helical *N*-terminal transactivation domain of p53. The crystal structure of this complex is illustrated in Figure 43. The known structural information of p53 hot-spot residues (Phe19, Trp23 and Leu26) given par the crystal structure made it possible to develop new PPI inhibitors for anticancer strategies. One of them, targeting the oncogenic interaction p53-MDM2 / MDMX and another, agonist of the hormone GHRH, are currently under clinical trial trials.[6,73]

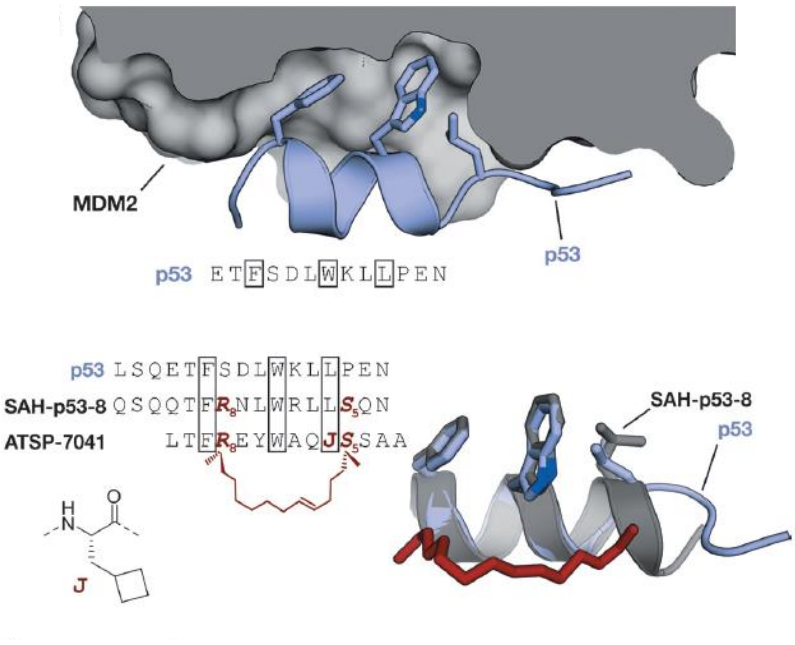

Figure 43: MDM2-p53 interaction. On top: Crystal structure of MDM2 with the N-terminal transactivation domain of p53 (PDB:1YCR). Below: Sequence of stapled peptides and superimposed crystal structures of p53 (blue, PDB: 1YCR) and SAH-p53-8 (gray/red PDB:3V3B). Hydrocarbon-linker is presented in red.[6,74]

Beak *et al.* developed a series of stapled α-helical p53-derived peptides cross-linked at positions *i, i+7* (Figure 43). As compared with the wild-type p53 peptide, they displayed an increased α-helicity, improved the binding affinity for MDM2 and enhanced proteolytic stability. Crystallographic data showed, that the hydrocarbon linker is involved in the binding to MDM2, explaining the affinity increase "Hydrocarbon" stapling has been also used in the context of HIV, to obtain inhibitors of viral replication acting on fusion, viral DNA integration and capsid steps. These molecules proved efficiency in animal models of human disease.[6,74]

I.-4.2.2 Cyclic β-strands/sheets mimics

β-sheets are formed by several β–strands that are stabilized by hydrogen bonding. Peptide β-sheets are usually antiparallel, parallel or barrel β-sheets (Figure 2). These structures constitute important recognition motifs in protein–protein interactions (PPIs), in the case of proteases, amyloids major histocompatibility complex (MHC) proteins, transferases, SH2, and PDZ domain proteins.[14,5] They are also involved in many neurological disorders, characterized by the formation of abnormal aggregates in which proteins tend to adopt a β-sheet structure. Often, tri-and tetrapeptides cyclized via side chains (*i, i+2*) form β-sheet mimetics. In Figure 44, potent and selective HIV proteases inhibitors are presented. They bind to the viral enzyme under a suitable preorganized β-strand conformation.[5]

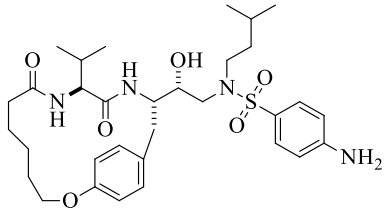

Ki (HIV-1 protease) = 1.7 nM
IC_{50}(HIV-1 infected MT2 cells) = 90 nM

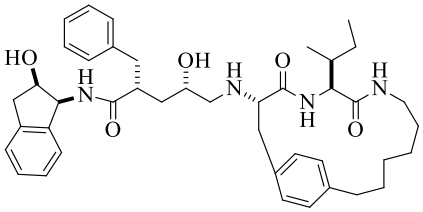

Ki (HIV-1 protease) = 0.6 nM
IC_{50} (HIV-1infected MT2 cells) = 60 nM

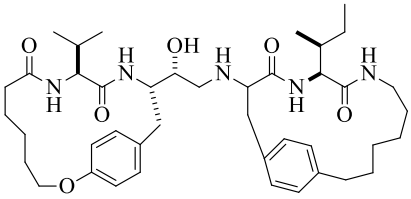

Ki (HIV-1 protease) = 5 nM

Figure 44: Cyclic peptides forming β-strands (PDB:1d41)(PDB:1d4k).[5]

In Figure 45, the binding conformation, in the HIV-1 protease active site, of the cyclic inhibitor 17 (PDB entry: 1d4l, orange) and of the cognate linear peptide substrate (PDB entry: 1mt7, yellow) are compared.[75]

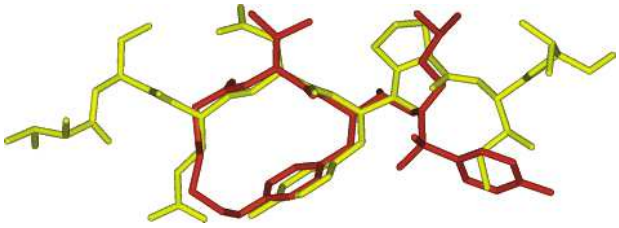

Figure 45: Comparison of the HIV-1 protease active site binding conformation of the cyclic inhibitor 17 (PDB:1d41) in orange and the linear peptidic substrate (PDB:1mt7) in yellow. Illustration by Insight II.[75]

Many cyclic β-strands mimetics have been developed to inhibit proteases, like aspartic proteases and serine proteases, as well as β-secretase and metalloproteases. Many examples are presented in the review of Hill *et al.*.[14]

I.-4.2.3 Turn mimetics

Mimicking the conformation of PPI-relevant turn structures is considered as a promising strategy towards PPI inhibitors. Most examples involve inhibitors of enzymes (e.g. proteases) or of interactions between peptide ligands and proteins (e.g. ligand-activated G-protein-coupled receptors).[14] Introducing Proline, Glycine, *D*-amino acids or *N*-methyl amino acids into linear peptide structures has a turn-inducing effect, which can be enhanced or locked in place by subsequent cyclization. In Figure 46, examples of such structures are presented. In nature, Proline has the highest tendency of all amino acids to form reverse turns. Glycine has the smallest side chain and, because of that, the most conformational freedom.[14]

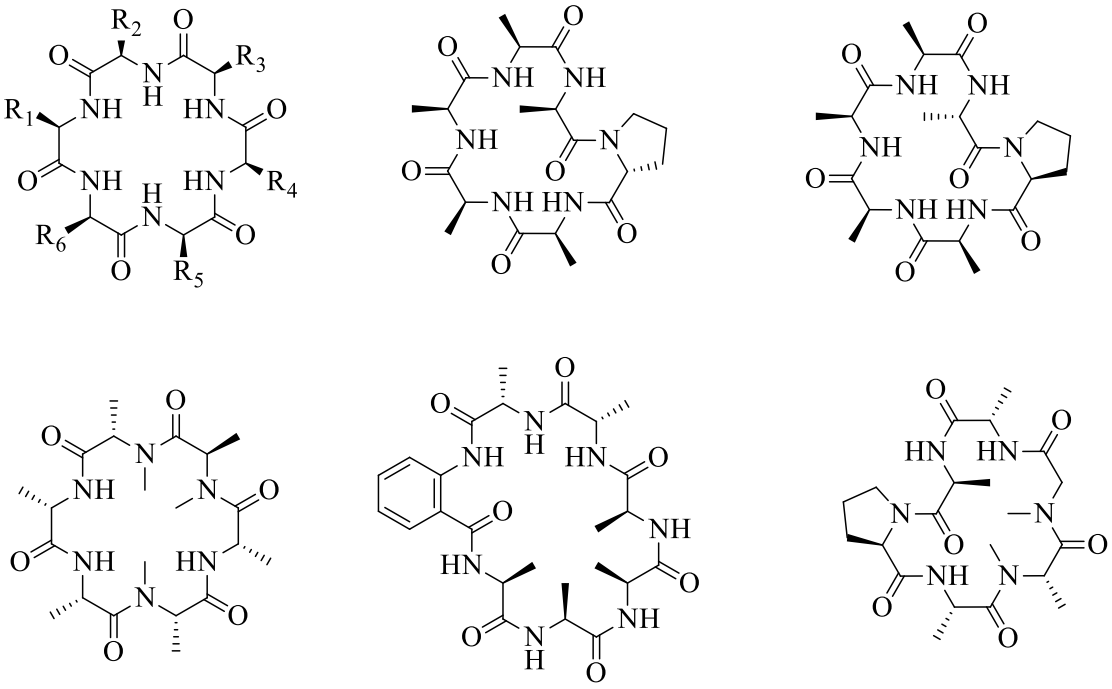

Figure 46: Cyclic peptides inducing turn motives as D-amino acids (14), D-Proline (15), L-Proline (16), N-methylated amino acids(19), aromatic linker (18) or combination of several of them (17).[14]

Somatostatin is a 14-amino acid cyclic peptide expressed in the central nervous system, gastrointestinal tract, and endocrine tissues. It is used in clinical treatment against cancer and acromegaly. However, Somatostatin is limited in its *in vivo* application because its rapid proteolytic degradation. The octapeptide Sandostatin, also used in therapy, represent a potent analogue of somatostatin showing higher metabolic stability. The Somatostatins structure is characterized by a type II´-β-turn structure, while structural studies from Melacini *et al.* and Pohl *et al.* have shown that Sandostatin adopts a type II β-turn or a type II´ β-turn (Figure 7). This structure has been stabilized in hexapeptide and bicyclic compound (Figure 47). These two compounds show similar biological properties as somatostatin and a 10-fold potency enhancement in the inhibition of insulin, glucagon and growth hormone release.[76,77,78]

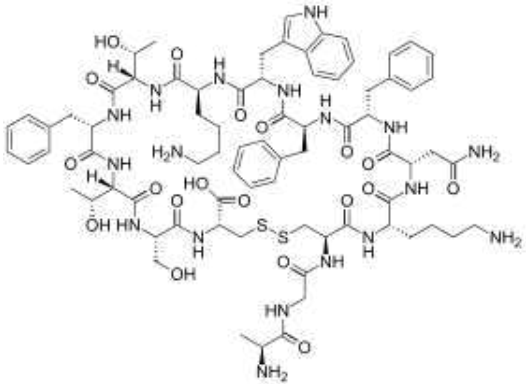

Somostatin

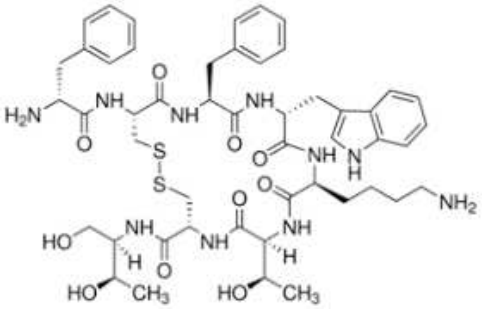

Sandostatin

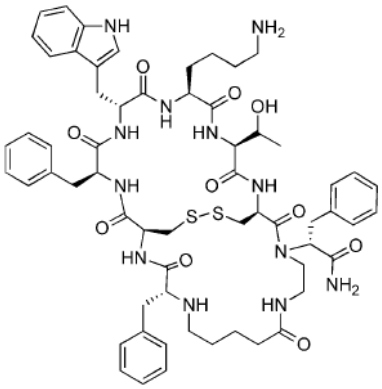

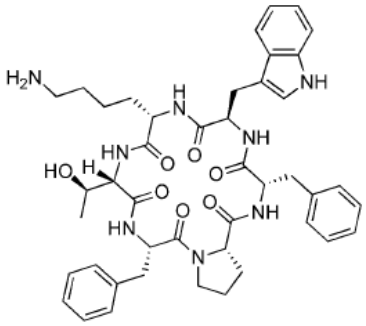

Figure 47: Structures of Somatostatin, Sandostatin, bicyclic compound and hexapeptide.[14]

Several examples of α- and γ-turn structures for PPIs inhibition are published and are presented in the review of Hill *et al.* from 2014.[14] Turns and loops specially exist in β-hairpin structures. Mimetics of such structures, are presented in the following part.

I.-4.2.4 β-Hairpin structure mimetics

Many β-hairpin loops are present on protein surface as recognition motifs. β-hairpin structures mimics have been mostly synthesized for the modulation of protein-/protein and protein/nucleic acids interactions. To introduce stability in these β-hairpin mimetics, several strategies have been developed, mostly head-to-tail cyclization, disulfide-linkage and *D*-Pro-L-Pro turns.[15]

In the literature, one special example of β-hairpin mimetic was applied to inhibit the HIV replication. The interaction between the basic region of the HIV Tat protein and the TAR RNA element of the HIV genome play an essential role in the transcription step of the later, constituting thus an attractive target. Athanassion *et al.* published the design of a β-hairpin structure mimicking the basic region of the viral Tat, in view of inhibiting the natural Tat/TAR complex (Figure 48). The design was based on the known structure of the complex established in solution between TAR RNA and the linear basic region of BIV-Tat. This sequence adopts a *β*-hairpin conformation when it bounds to TAR. [79,80] In BIV-2 the linear sequence is cyclized *via* a *D*-Pro-*L*-Pro dipeptide template, inducing a stable *β*-hairpin conformation, as confirmed by NMR studies.[79]

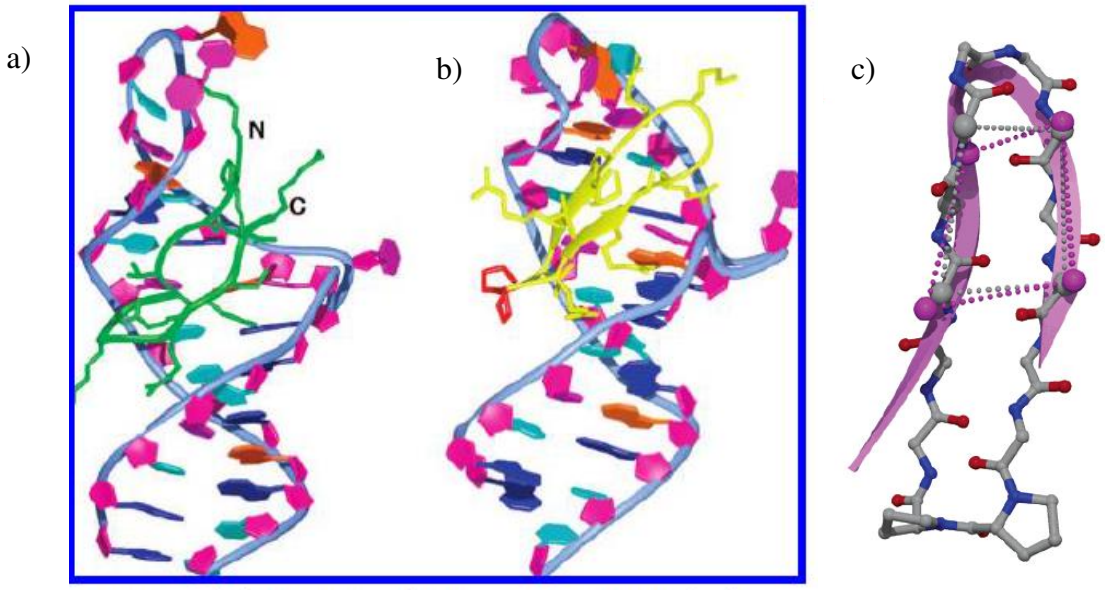

Figure 48: a) 3D Solution structure of BIV Tat-TAR RNA complex (PDB: 1mNB) b) BIV-2-TAR RNA complex (PDB: 2A9X). N- and C-terminal of BIV-Tat are illustrated in green... c) NMR structure of BIV2 as compared to the bound form of BIV Tat peptide. [80,79]

On the other hand, *β*-hairpin stabilized peptides have shown potential to modulate PPIs. Thus, one of them, mimicking an α-helical epitope in the N-terminal segment of the p53 protein, binds with a nanomolar affinity to the cognate p53 partner, i.e. the MDM2 protein (Figure 49).[16,81]

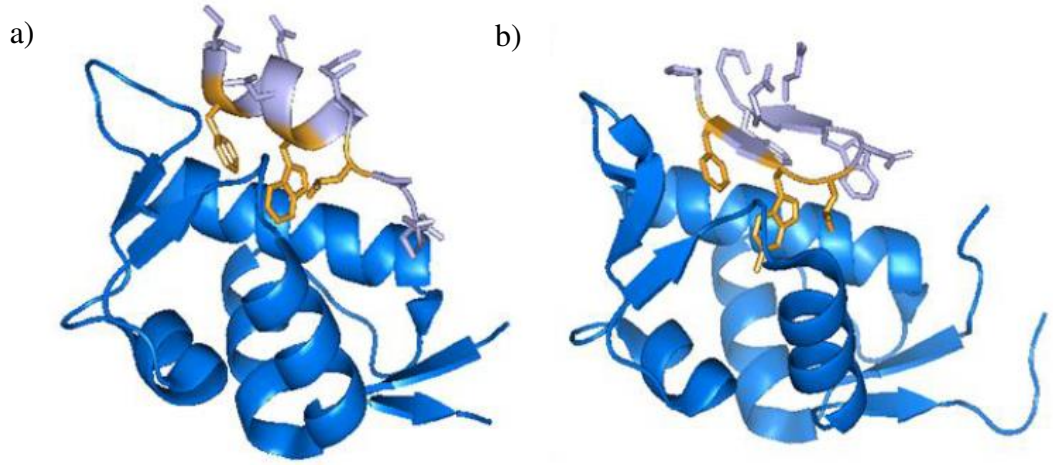

Figure 49: β-hairpins as mimics of α–helices. a) crystal structure of the complex formed between MDM2 and the α-helical epitope located in the N-terminal segment of p53 [PDB 3DAC] b) interaction between MDM2 and the p53 derived β-hairpin structure [PDB 2AXI].[16]

Most β-hairpin mimics have been developed as part of the famous interaction between the Rev peptide and the HIV-1 mRNA region called Rev Response Element (RRE). The RRE/Rev interaction is important in the temporal control of HIV-1 mRNA splicing. The Rev sequence interacting with RRE has an α–helical conformation. In Figure 51b, the X-ray structure shows the binding of Rev in the major groove of the RNA. It is visible that the RNA-interacting side-chains are displayed around almost the entire circumference of the Rev α-helix. Further informations concerning the HIV-1 Rev/RRE complex are in the publication of Battiste *et al.*.[82] In 2007, Robinson *et al*. made calculations showing that the interacting domain of Rev could be mimicked by 12-residues model 2:2-hairpin structures (Figure 50c). They designed several β-hairpin mimetics stabilized by the D-Pro-L-Pro template, in view of inhibiting the Rev/RRE interaction. NMR studies of these mimics revealed that their structures were disordered in solution, since stable hairpin conformations could not be detected. Just one structure, R-27, was stable enough because of the introduction of a disulfide bridge (Figure 50e). This β-hairpin structure was presented as a relative successful Rev peptide mimic for the inhibition of the HIV-1 Rev/RRE complex.[80,83]

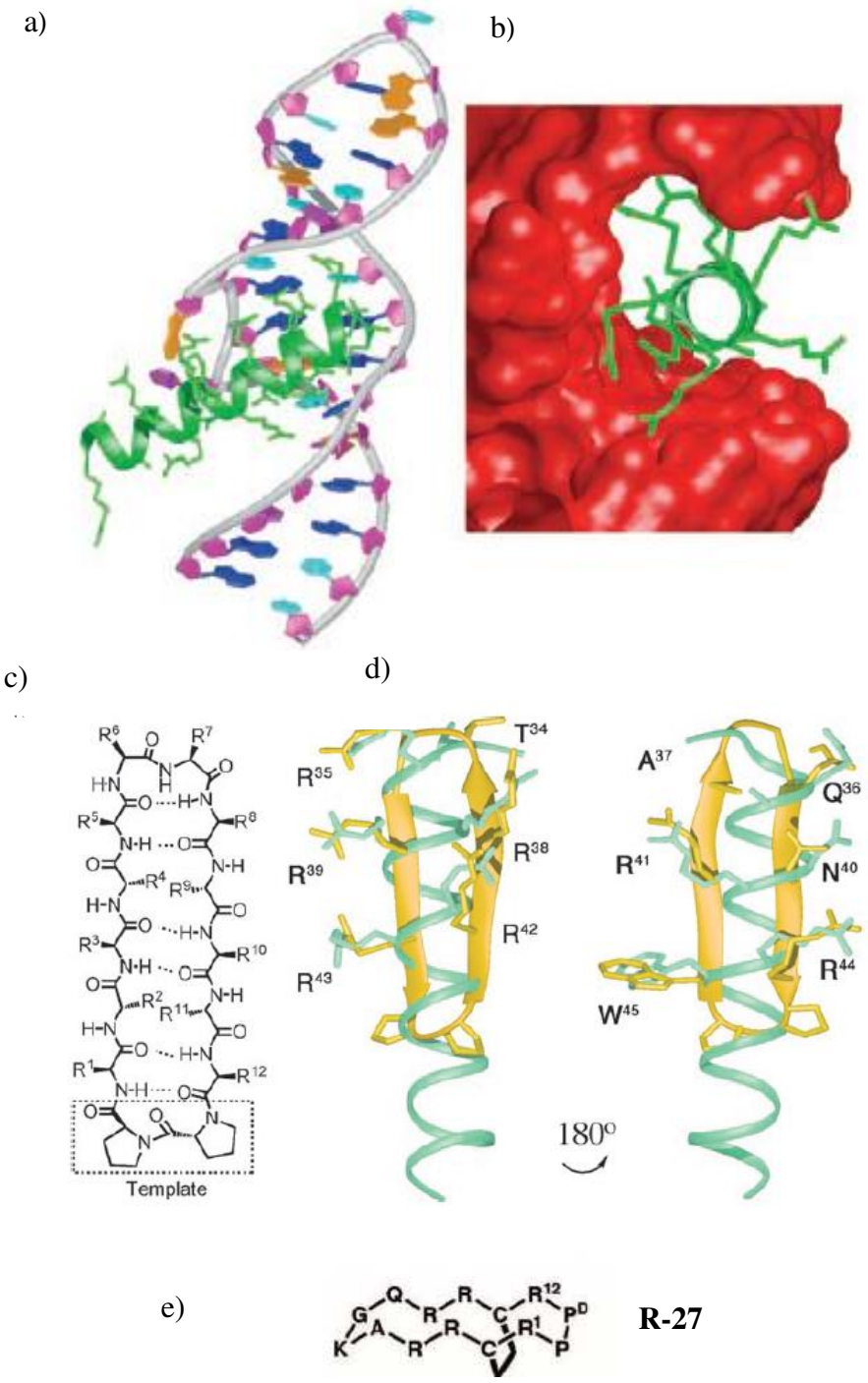

Figure 50: a) X-ray structure of Rev peptide binds (green) to HIV RRE (PDB:1ETF). b) Rev (green) binds to major groove of RRE (red). c) The helical Rev peptide is mimicked by a 2:2 β-hairpin structure (D-Pro-L-Pro template). d) Superimposition show the side chains of the helix (green) of Rev peptide and of the β-hairpin mimic(yellow), which are relatively well overlapping. e) Structure of R-27.[80,83]

II. Aims of our work

The aim of the first part of this thesis was to elaborate and to study new families of peptide foldamers, based on unnatural enantiomerically pure cyclic α-amino acids, *i.e.* 6-substituted 4-oxopipecolic acids (Figure 51), whose the stereoselective synthesis and structures were published by Daly *et al*. in 2012.[84]

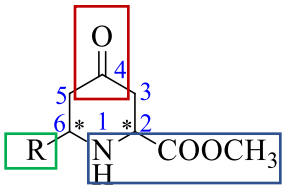

(2S, 6R) majo and (2S, 6S) mino

Figure 51: 6-substitued 4-oxo-pipecolic acid derivatives. α-amino acid function=blue, side chain=green, ketone-group=red. R = Phenyl, Phenylethyl.

Various characteristics of these 6-substituted 4-oxo-pipecolic acid derivatives confer them interesting properties in the area of foldamers:

- The cyclic structure of the 6-substituted 4-oxo-pipecolic acid should introduce rigidity and it has been shown in the previous chapter that various cyclic amino acids containing five and six atoms (*e.g. S*-proline chimeras in Chapter 2.3.1) can lead to foldamers.
- The introduction of different side chains in the cyclic monomer at position 6 could be a possibility to modulate the biological properties of the foldamer.
- On the other hand, the foldameric structures should have an overall dipole moment reflecting the aggregate effect of the individual microdipoles from the carbonyl groups of both the peptide bond and of the ketone functions. This may have importance for an optimal interaction with the target.[85]

We planned to develop two strategies to elaborate homogenous and heterogenous peptide foldamers (Scheme 52). In strategy 1, homogenous foldamers should be obtained via repetitive couplings of substituted 6-substituted 4-oxopipecolic acid units. In strategy 2, cyclic monomers should be alternatively coupled with natural α-amino acids, in order to obtain heterogeneous foldamers. Heterogeneity in foldameric structures has been already published. One of the newest publications are from Amblard *et al*. in 2017.

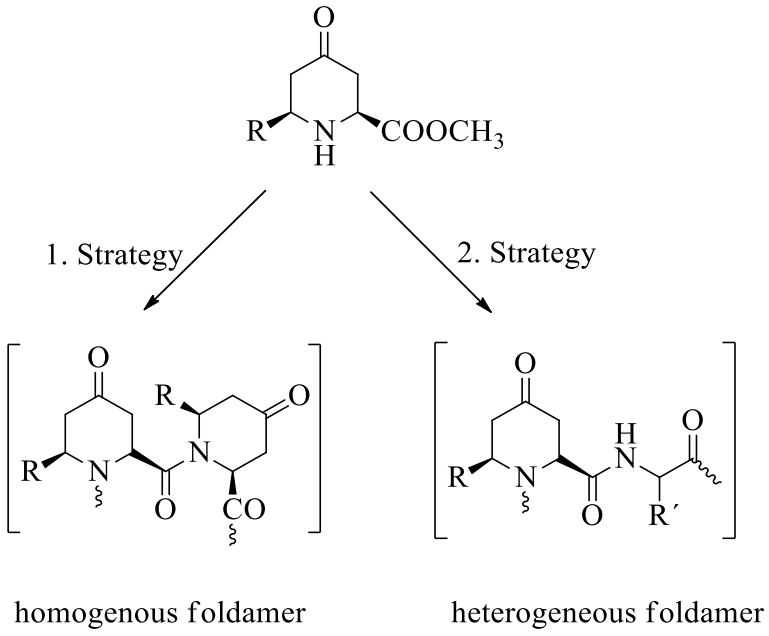

Figure 52: Illustration of both synthetic strategies for peptide foldamers.

Our first goal was to set up synthetic methodologies in liquid-phase to obtain di- and trimeric sequences of homo/hetero foldamers, then to apply them for the solid-phase synthesis of longer oligomers (tetra-, hexa- or decamer). Afterwards, their structure should be studied by NMR, IR and Circular Dichroism.

III. Synthesis of constrained peptidomimetics

In this work, we decided to use the major diastereomer (2S, 6R) of 4-oxo-pipecolic acid incorporating a phenyl substituent at position 6. Two synthons should be first synthetized: the 6-phenyl-4-oxo-pipecolic acid methyl ester and a *N*-protected 6-phenyl-4-oxopipecolic acid residue (Figure 53).

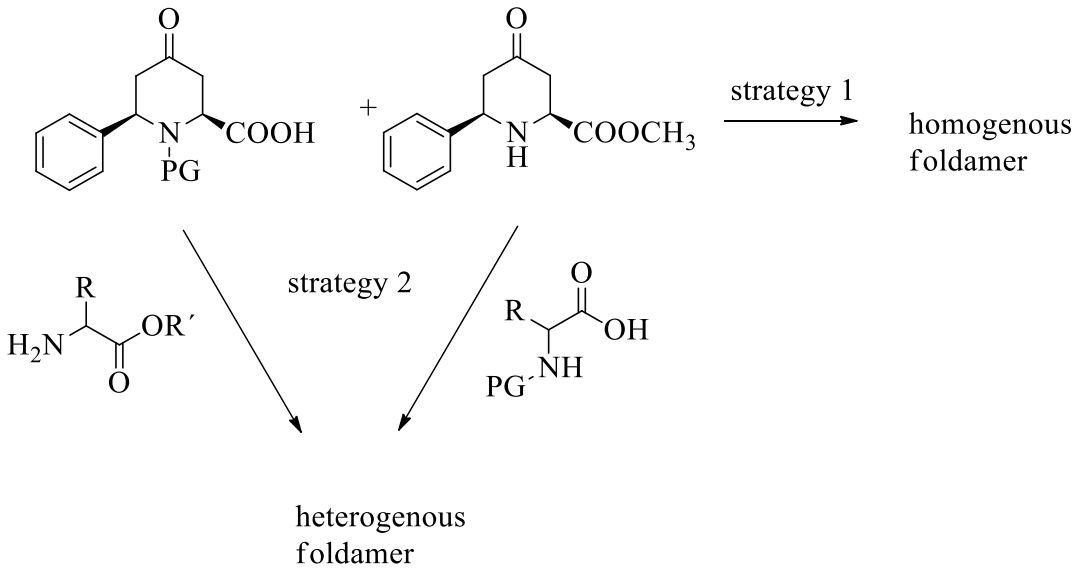

Figure 53: Synthetic strategies for homogeneous and heterogeneous structures.

III.-1 Synthesis of protected (2S, 6R)-6-phenyl-4-oxo-pipecolic acid derivatives

III.-1.1 6-phenyl-4-oxo-pipecolic methyl ester

The synthesis of the phenyl-4-oxo-pipecolic acid methyl ester was performed according to the thesis and publication of Marc Daly *et al.* in 2012.[84,86] This monomer was prepared in five steps in 13 % overall yield (Scheme 1 and 2).

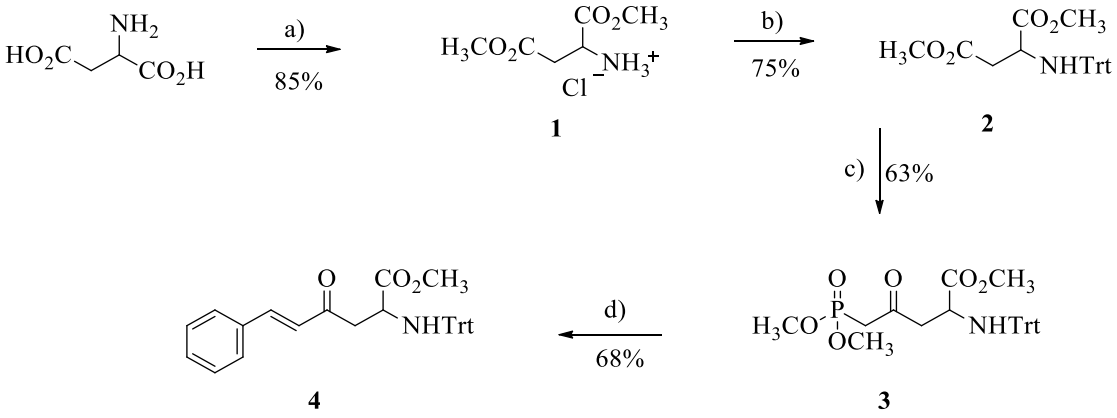

Scheme 1: Synthesis of α,β-unsaturated ketone. A) AcCl, MeOH, 65°C; b) TrtCl, TEA, DCM; c) DMMP, n-BuLi, THF (dry), -78°C d) Benzaldehyde, K_2CO_3, MeCN, reflux.

In the first step, *L*-aspartic acid was esterified with acetyl chloride in MeOH, giving the dimethyl diester hydrochloride salt **1** in 85% yield. In the following step, the amino group on **1** was protected using tritylphenylmethyl chloride in presence of TEA in DCM leading to compound **2** in 75% yield. The reaction of compound **2** with the anion of dimethyl methylphosphonate (DMMP), generated at -78°C using *n*-BuLi, afforded compound **3** in 63% yield. Subsequently, a Horner-Wadsworth-Emmons-reaction was performed with benzaldehyde to generate the α,β-unsaturated ketone **4**. The cyclization leading to the desired 4-oxo-pipecolic acid **69** was performed in two consecutive steps,

without isolation of intermediates (Scheme 2). First, the cleavage of the trityl-protecting group was performed with a 2M HCl solution in MeOH, followed by the cyclization in H_2O with DIPEA at pH = 8. These last steps were poorly reproducible and led to diastereomers **69** and **70** in relatively low yields (47% and 12%, respectively), after Flash Chromatography purification.

Applying another protocol, published by Harkiss *et al.* in 2018, allowed us to improve yields in compounds **6** and **7**.[87] First, the cleavage of the trityl group was realized using TFA in DCM and the TFA salt **5** was isolated in quasi-quantitative yield. In a second step, the cyclization of **5** was carried out by means of DIPEA in MeOH. In this way, diastereomers **6** and **7** were isolated in respectively 60% and 30% yields (Scheme 2).

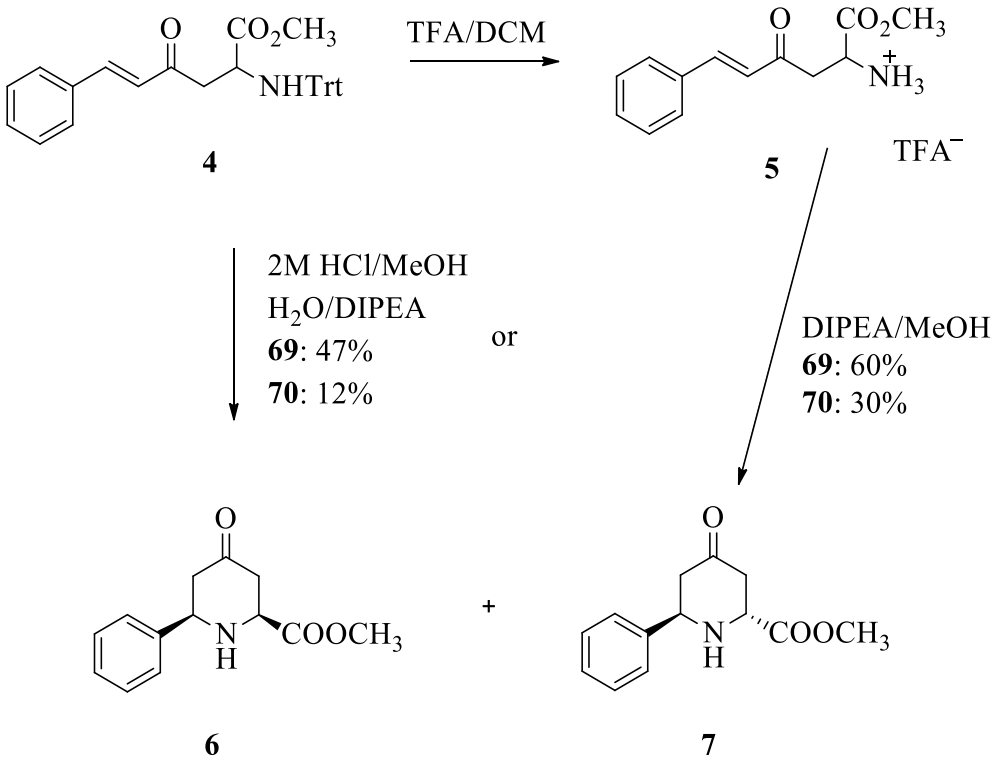

*Scheme 2: Cyclization to 4-oxo-pipecolic acid methyl esters **6** and **7**.*

III.-1.2 N-protected phenyl-4-oxo-pipecolic acid derivatives

We first focused on the synthesis of *N*-protected derivatives **8**, presented in Scheme 3.

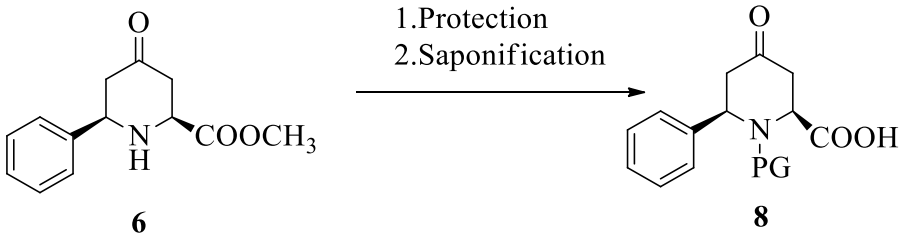

Scheme 3: Synthetic scheme of the synthesis of N-protected 4-oxo-pipecolic acid derivatives.

First, we tried to introduce three protecting-groups on the free secondary amine: the Fmoc, Boc and Alloc ones, *via* Fmoc-Cl, Boc_2O and Alloc-Cl reagents, respectively (Scheme 4). Only the Alloc protection could be performed in 95% yield. In the case of Boc, no reaction occurred while in the case of Fmoc, the only product formed was the dibenzofulvene (DBF), due to the elimination, on Fmoc-Cl reagent, of HCl by the secondary amine of **6**.

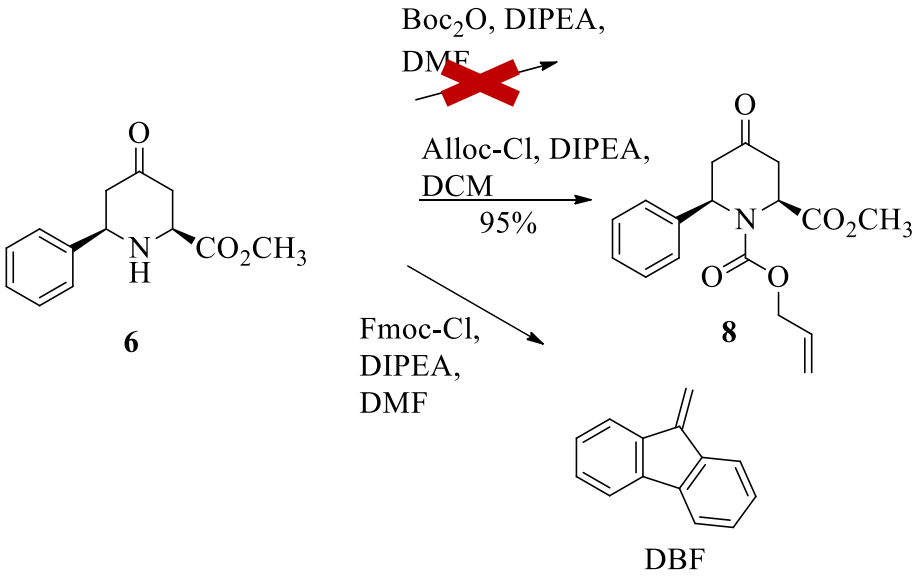

*Scheme 4: Conditions of protection of free secondary amine of cyclic monomer **6**.*

This likely signifies that the strong steric hindrance due to the presence of substituents on 2- and 6-positions of the 4-oxo-pipecolic acid moiety did not allow the protection by the spacious Fmoc- and Boc-protecting-groups.

The second step was the saponification of the methyl ester **8** (Scheme 5). It was carried out under different conditions that are presented in Table 2.

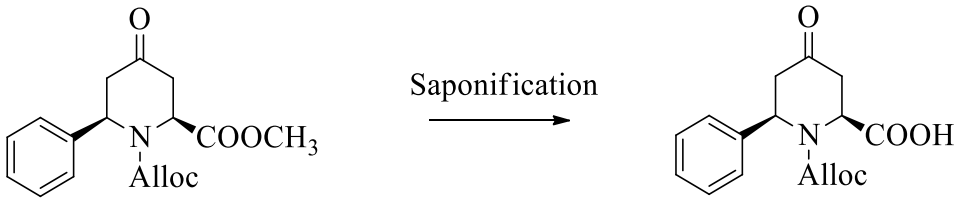

8 **9**

Scheme 5: Saponification of cyclic monomer 8.

The saponification of **8** was assayed in basic and acid media. In acidic conditions, the degradation of the molecule was observed. In basic medium, the best results could be obtained (50% yield of **9**) using the conditions published by Nicolaou *et al., i.e* Me_3SnOH in 1,2-dichlorethane at 80°C (Table 2).[88]

*Table 2: Conditions of saponification of cyclic monomer **8**.*

Conditions	**Yield**
LiOH/Dioxane/H_2O	20%
6M HCl[84]	/
NaOH/$CaCl_2$/*i*PrOH-H_2O(7:3) [89]	/
Me_3SnOH/1,2-DCE/80°C[88]	50%

The two synthons **6** and **9** required for the peptide synthesis were then obtained. However, the synthesis of **6** according to Daly *et al.* is very time-consuming, and the yields are neither satisfying nor really reproducible.[84] Consequently, we tried to synthesize the monomer **6** following a new strategy.

III.-2 Development of a new methodology for the synthesis of 6-phenyl-4-oxo pipecolic acid derivatives via the imino-Diels-Alder-reaction

III.-2.1 Imino Diels Alder reaction

To synthesize a six-membered ring, the Diels-Alder reaction is the most known approach. The publication of Aznar *et al.*[90] in 2006 showed us a new opportunity to synthesize diastereospecifically the protected monomer **9**, *via* a *L*-proline catalyzed imino Diels-Alder reaction (Scheme 6). Starting from the α,β-unsaturated ketone and from *N*-allyl phenylmethanimine, they obtained the product with a high diastereomeric excess.

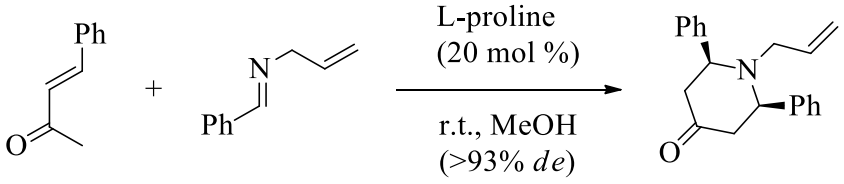

Scheme 6: Imino-Diels-Alder reaction catalyzed with L-proline by Aznar et al..[90]

In our case, we envisaged to prepare *N*-protected 6-phenyl 4-oxo-pipecolic methyl esters starting from methyl (2*E*) 4-oxo pent-2-enoate **10** and from *N*-protected imines **11** and **13**. In this reaction, imines **11** and **13** represent the electrophilic diene components and compound **11** the dienophile (Scheme 7).

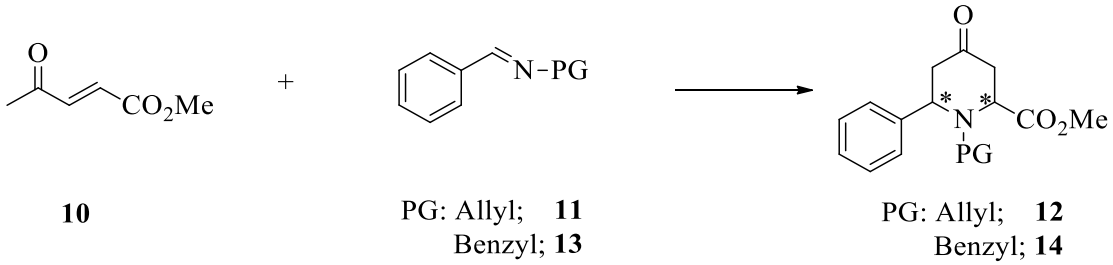

*Scheme 7: Synthesis of N-protected 4-oxo-pipecolic acid methyl esters **12** and **14**.*

Compound **10** was synthesized according to the publication of Zari *et al.* in 2014.[91] Methyl levulinate was first brominated with Br_2 in $CHCl_3$, then *in situ* debrominated in presence of NEt_3, giving the desired product **10** in 34% yield (Scheme 8).

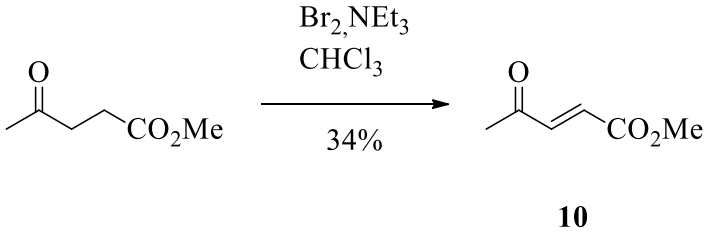

*Scheme 8: Synthesis of methyl (2E) 4-oxo pent-2-enoate **10**.*[91]

Imines **11** and **13** were synthesized in one step, *via* the protocol described by Trost *et al.* in 2015 (Scheme 9). Benzaldehyde reacted with allyl or benzyl amine in DCM, in presence of $MgSO_4$, affording the desired imines **11** and **13** in 95% yield.[92]

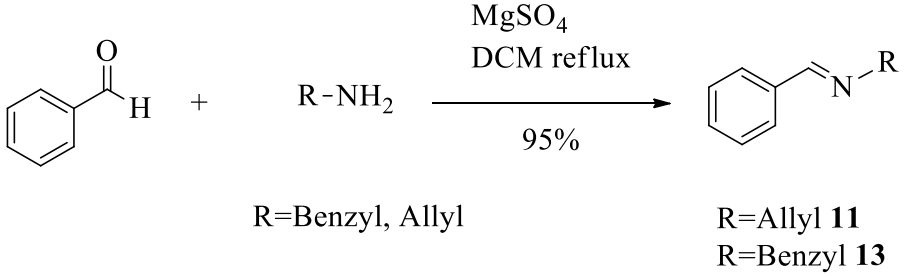

*Scheme 9: Synthesis of imines **11** and **13**.*[92]

Scheme 10 shows the Diels-Alder-reaction between **10** and imines **11** and **13**. 1 eq of the imine **11** or **13** and 4 eq of compound **10** in presence of 20 mol% *L*-proline as catalyst in MeOH formed the desired compounds **12** or **14** in 40% yield. Using only 1 eq of compound **10** decreased the yield from 40 to about 25% in the two cases.

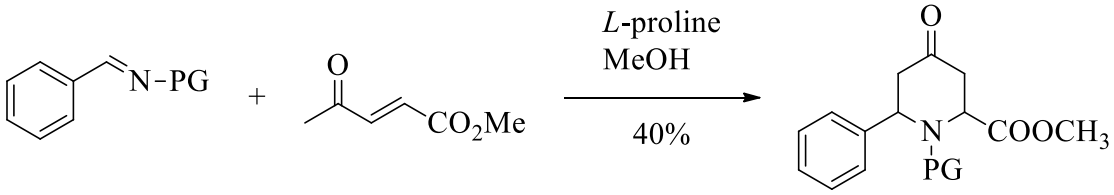

PG: Allyl; **11**
Benzyl; **13**

10

PG: Allyl; **12**
Benzyl; **14**

Scheme 10: Imino-Diels-Alder reactions. PG = Allyl; ***12*** *and PG = Benzyl;* ***14*****.**

Encouraged by this experiment, we investigated different reaction conditions to optimize the yield of the Diels-Alder reaction, taking compound **12** as target. First, we studied the solvent effect. Neither anhydrous solvents nor the use of inert atmosphere conditions were found to be necessary or beneficial. Different solvents were used for the reaction (DCM, DMF, ACN, CH, H_2O, EtOAc, Et_2O, Toluene, DMSO, IPA), but none of them led to higher yields.

As expected, **12** and **14** were obtained as racemic mixtures. Indeed, the optical optical rotation angles of these products, measured by polarimetry, were found to be 0. Moreover, in the ^{1}H-NMR-spectra, adding $Eu(hfc)_3$ induced the doubling of the signal of the methyl groups (Figure 54), confirming this fact.

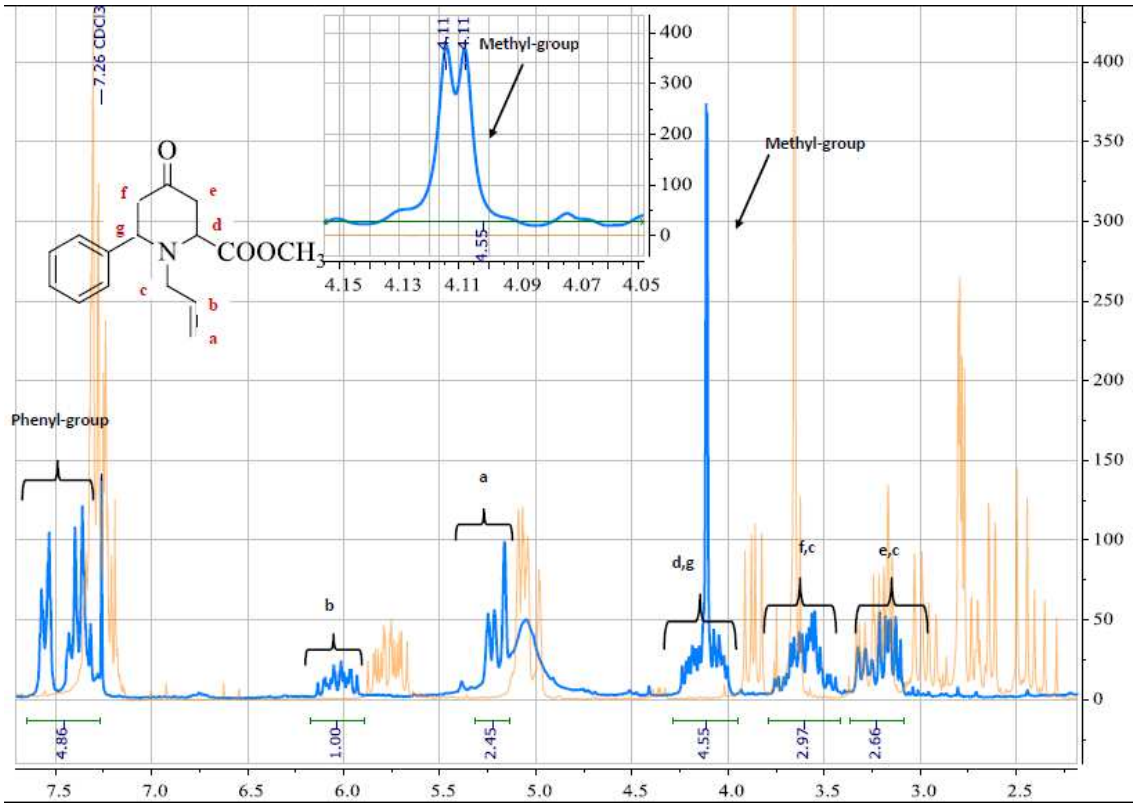

*Figure 54:¹H-NMR-spectrum of **12** in presence of Eu(hfc)3 (blue) compared to ¹H-NMR of compound **12** alone (orange). Doubling of the signal of the methyl group was observed and is shown.*

We tried other catalysts (Quinidine, (R)-(+)-N-Amino-2-methoxymethyl-pyrrolidine and *L*-ProPro) in view of both improving the yield and obtaining some enantioselectivity, but all of them failed to obtain the desired product (LC-MS and TLC).

Even if monomers **12** and **14** were obtained as racemic mixtures, this strategy based on the Diels-Alder reaction remained interesting since coupling with a chiral amino acid should lead to two possibly separable diastereomers. In view of peptide synthesis, we then focused on *i*) deprotection of the *N*-allyl and benzyl group on respectively compounds **12** and **14** *ii*) saponification of compounds **12** and **14**.

III.-2.2 Synthesis of racemic phenyl-4-oxo-pipecolic methyl ester

The allyl cleavage was attempted on **12** using several conditions, illustrated in Table 3 (Scheme 11).

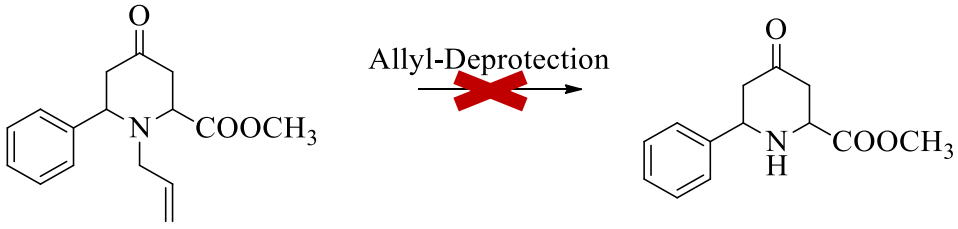

12

Scheme 11: Illustration of allyl-deprotection.

Under conditions 1, the conversion to the desired product occurred. However, the reaction was only partial, even after one week of reaction time (10 %). Using rhodium (conditions 2) or palladium (conditions 3) based-catalysts did not give the deprotected monomer.

Table 3: Conditions of allyl-deprotection.

	Conditions
1	5%mol Grubbs, toluene, argon, 80°C[93,90]
2	$RhCl_3$ hydrate, EtOH/H_2O, 90°C[94]
3	NDDBA, $Pd(PPH_3)_4$, DCM(dry), argon, 35°C[95]

On the other hand, several conditions for the *N*-benzyl deprotection were carried out (Table 4).

Table 4: Conditions of benzyl-deprotection.

	Conditions
1	Pd/C, H_2, MeOH
2	Pd(OH)/C, MeOH, acetic acid[96]
3	H-Cube, 10 bar, 0.5mL/min
4	H-Cube, 10 bar, 0.1mL/min

All conditions allowed conversion into the product. However, as in the case of allyl cleavage, deprotection reactions were incomplete, even after one week. Due to lack of time, further assays could not be achieved.

III.-2.3 Synthesis of N-Allyl-6-phenyl-4-oxo-pipecolic acid

The saponification of the ester-function of compound **12** was carried out using Me_3SnOH in 1,2-DCE at 80°C. The corresponding acid derivative **15** was obtained in 55% yield (Scheme 12).

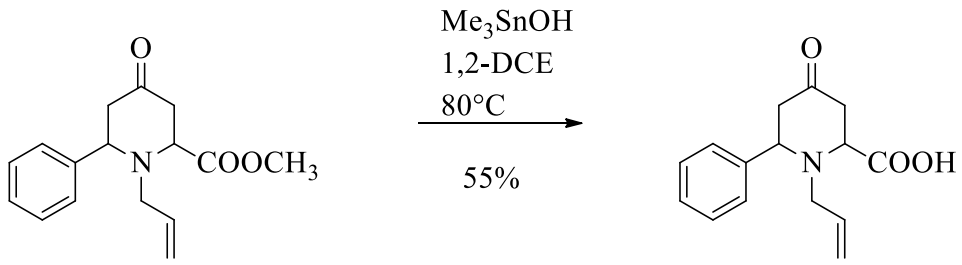

12 **15**

*Scheme 12: Synthesis of N-Allyl-6-phenyl 4-oxo-pipecolic acid **15**.*

In order to elaborate a synthetic strategy applicable to the synthesis of homogeneous and heterogeneous foldamers (Figure 54), we studied coupling conditions starting from enantiomerically pure monomers **6** and **9,** and from racemic derivative **15**.

III.-3 Foldamer synthesis

III.-3.1 Homogeneous foldamer

We tried to obtain the dipeptide by coupling the two enantiomerically pure residues **9** and **6** (Scheme 13).

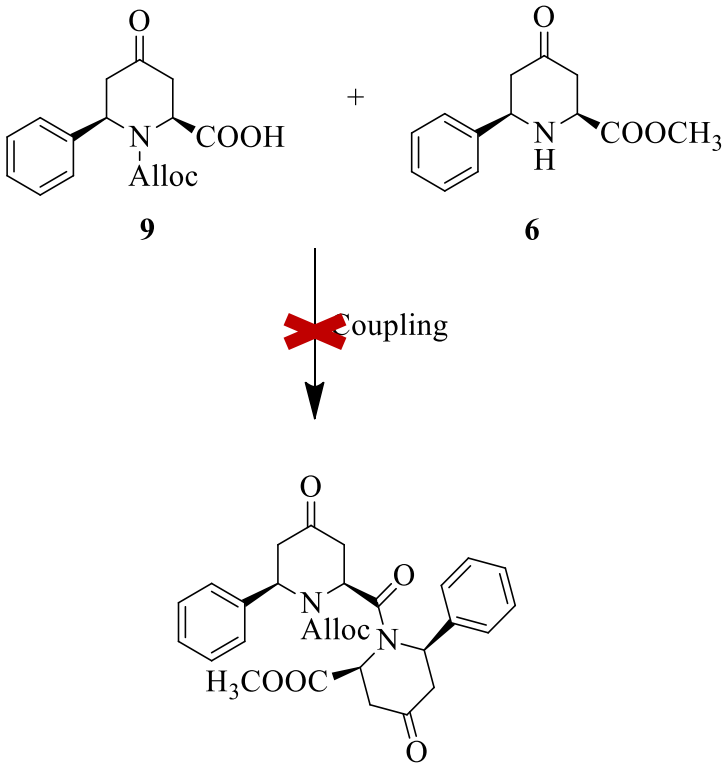

Scheme 13: Coupling between two cyclic monomers.

Different coupling reagents were tried, these are given in Table 5.

*Table 5: Coupling reagents for the condensations of monomers **9** and **6**.*

Coupling conditions
HBTU/DIPEA/DMF
DCC/HOSu/DMF
EDC/DMAP/DMF
CDI/DMAP/DMF
DIC/DMAP/DMF

HBTU/DMAP/DMF
HBTU/HOBt/DMAP/DMF

For each case, the reaction was performed for 48 hours at room temperature, afterwards at 40°C for 3 days and then at 70°C overnight. But in neither case, the formation of the dipeptide could be detected (TLC and LC-MS analyses). The steric hindrance at positions 2 and 6 on residues **6** and **9** likely inhibits their coupling. The coupling between two cyclic units was also attempted from the *trans* diastereomer (*2S*, *6S*) of the 6-phenyl 4-oxo pipecolic acid **7**, but it gave no results.

III.-3.2 Heterogeneous foldamers

The condensation of two cyclic monomers was not possible. Bypassing the steric hindrance, occurring in compound **6**, the coupling of compound **9** with *L*-alanine methyl ester **16**, using HBTU, afforded the desired dipeptide **18** in 90% yield (Scheme 14).

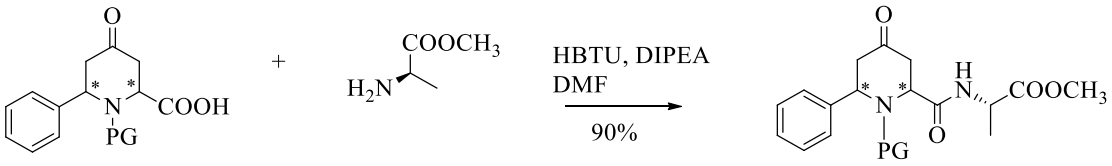

PG=Allyl **12**; *racemic*
PG=Alloc **9**; *(2S, 6R)*

16

PG=Allyl **17**
PG=Alloc **18**

*Scheme 14: Coupling of cyclic monomer **9** and **12** with H-L-Ala-OCH$_3$ **16**.*

On the other hand, to verify if the coupling of the racemic *N*-Allyl monomer **12** with a chiral α-amino acid could lead to two separable diastereomers, we also condensed, in the same way as **9** (Scheme 14).

Dimer **17** dimer was obtained in 90% yield as racemic mixture, as confirmed by ^{1}H-NMR (Figure 81). Unfortunately, the diastereomers were not distinguishable from each other in TLC and HPLC and could not be separated.

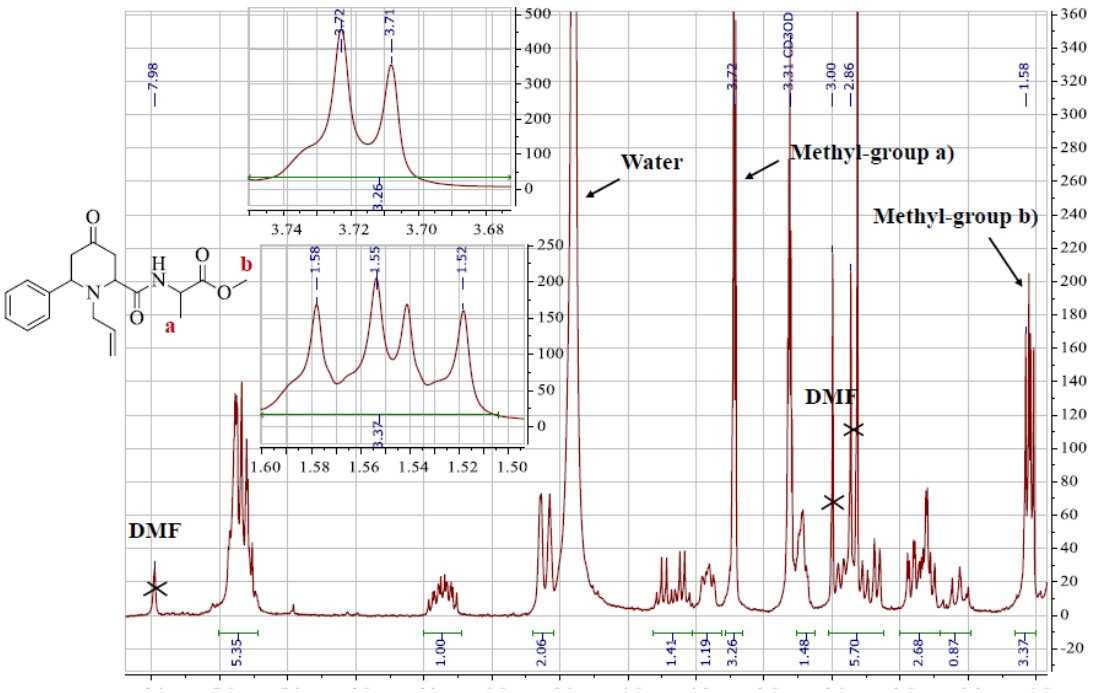

*Figure 81:¹H-NMR-spectra of **17** after coupling with H-L-Ala-OCH$_3$ **16**. The methyl-groups of alanine side-chain and of the ester are duplicated.*

These two coupling reactions demonstrated that the condensation of the carboxylic acid function of the *N*-protected cyclic monomers does not present any difficulties (Scheme 14). By contrast, attempts to condense the *N*-Alloc-*L*-alanine residue on the secondary amine of the cyclic methyl ester monomer **6** failed (Scheme 15).

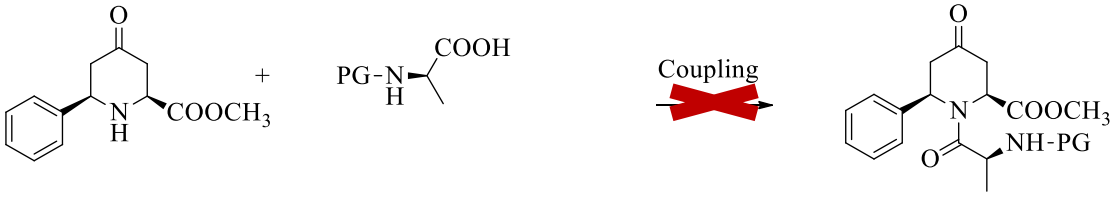

6 PG: Alloc Z PG: Alloc Z

*Scheme 15: Attempts to condense the cyclic monomer **6** with N-protected Alloc-L-Alanine residues **19** and **20**. Z= benzyloxycarbonyl.*

Different coupling reagents traditionally used in peptide synthesis were tested (Table 6).

Table 6: Coupling conditions.

Coupling-conditions
HBTU/DIPEA/DMF
DCC/DhbtOH
PyBOP/DIPEA/DMF

All conditions were performed at room temperature. Any conversion into the dipeptide could be detected on TLC after 3 days. Afterwards, the reactions were performed at 40°C and at 70°C for 3 days, but no product formation could be observed on TLC and in LC-MS. Changing the protecting group Alloc of the alanine residue by a benzyloxycarbonyl one, did not influence the course of the reaction. (Scheme 15).

To decrease the steric hindrance likely occurring during the coupling step, attempts to condense compound **6** with Boc-Gly-OH and Boc-β-Ala-OH residues, using HBTU, were carried out. In the two cases, no conversion into the desired dipeptide could be detected on TLC (Scheme 16), even if the coupling was carried out using 5 eq of the Boc-amino acid.

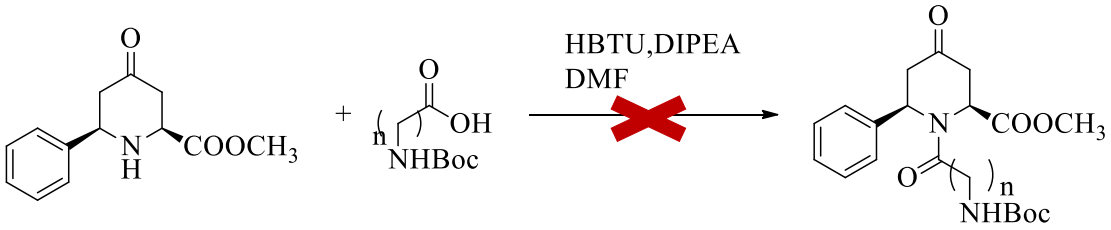

6

*Scheme 16: Attempts to condense the cyclic monomer **6** with amino acids Boc-Gly-OH and Boc–β-Ala-OH.*

The coupling reactions using the uronium family HBTU reagent were unsuccessful, even performed for several days and under heating. We focused on other activation methods using less hindered reagents.

III.-3.2.1 Acid chlorides

The most obvious method to activate an acid compound is to convert it into the corresponding chloride derivative. Acid chlorides can be formed using various chlorinating agents (pivaloyl chloride, phthaloyl dichloride, thionyl chloride and oxalyl chloride). In our case, Alloc-*L*-Ala-OH was chlorinated by means of thionyl chloride in DCM. The mixture was just dried over reduced pressure. Afterwards, the coupling between the crude chloride **19** and the cyclic monomer **6** was directly attempted, in presence of NEt_3 or DIPEA in dry DMF (Scheme 17). As inferred on TLC and by LC-MS analyses, these conditions did not give the desired compound.

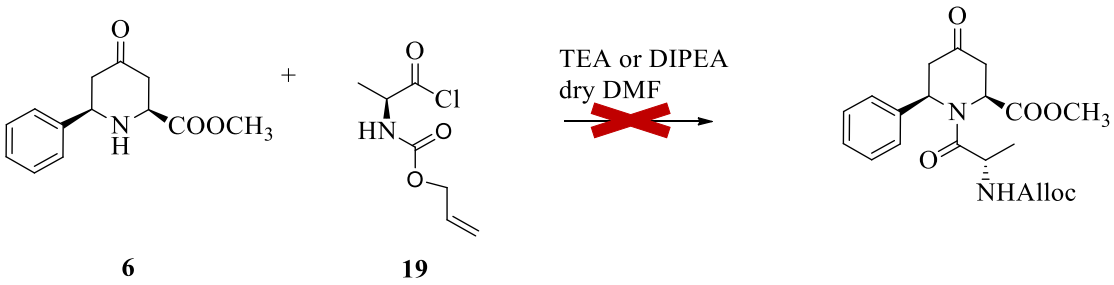

6 **19**

*Scheme 17: Attempts to condense Alloc-L-Ala-Cl **19** and the cyclic monomer **6**.*

Acid chlorides are very sensitive to water. Because of that, new conditions were applied allowing to perform the coupling step *in situ*, without the need to isolate the chloride. Cyanuric chloride makes possible a fast formation of acid chlorides in basic media. During this reaction, cyanuric chloride is converted into an insoluble product: dichlorohydroxy- or chlorohydroxys-triazine (Scheme 18).[97] Triazine-based reagents have been reviewed in 2000 by Kaminski *et al*.[98]

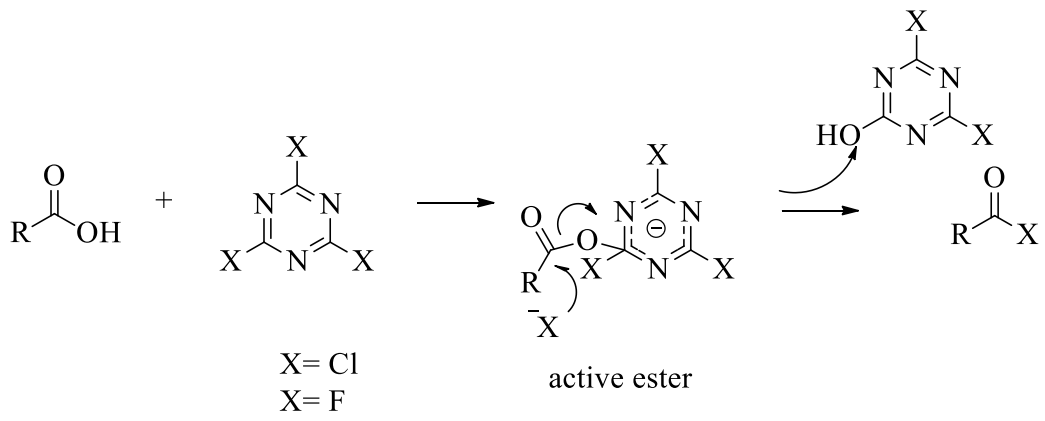

Scheme 18: Mechanism of acetyl chloride (or fluoride) formation with cyanuric chloride (or fluoride).[97]

The acid chloride of *N*-Alloc alanine residue was thus prepared using cyanuric chloride**,** in dry acetone, under argon-atmosphere (Scheme 18). This reaction mixture was dried under reduced pressure. The residue was directly dissolved in dry DCM and then the

cyclic monomer **6** added dropwise in dry DCM at 0°C under argon-atmosphere (Scheme 19).[97] Because no reaction could be observed at ambient temperature, the mixture was afterwards heated, but formation of dipeptide **91** could not be detected on TLC and in LC-MS. (Scheme 19). The steric hindrance of *L*-alanine influencing perhaps the reactivity, we tried to condense the Boc-*β*-alanine residue using cyanuric chloride following the same protocol (Scheme 19). No reaction occurred (TLC and LC-MS), even upon heating.

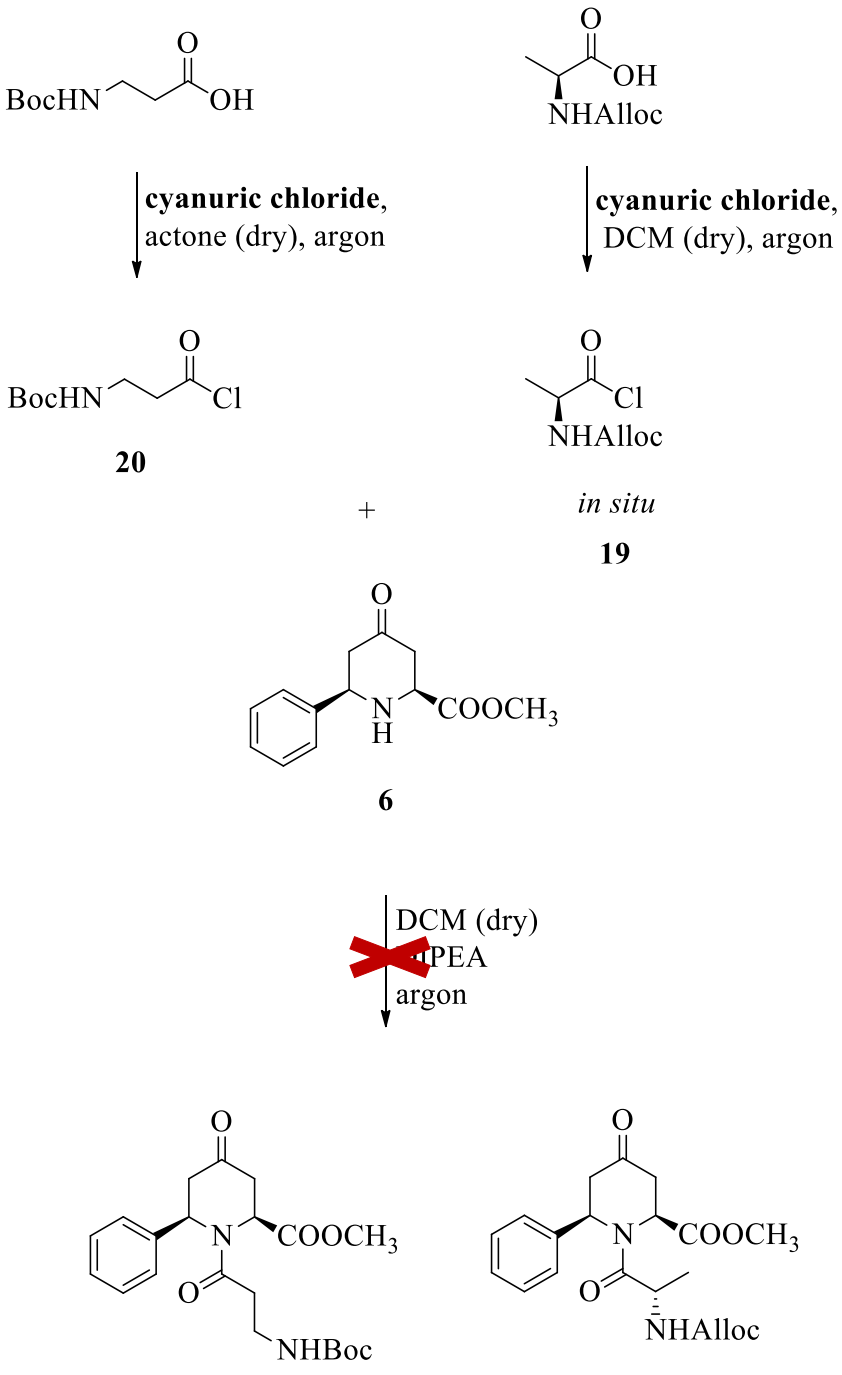

*Scheme 19: Assays to condense in situ monomer **6** to Alloc-Ala **19** and Boc-β-Ala **20** residues via their chloride form.*

III.-3.2.2 Acyl fluorides

It is known that acyl fluorides show lower reactivity towards common nucleophiles compared to acid chlorides. But they are less moisture sensitive, they can be used in solution and solid-phase synthesis and are compatible with most protecting groups. They do not lead to racemization. Because of the small size of the fluorine atom, they are often used in the case of sterically hindered disubstituted amino acid coupling

One way to generate acid fluorides is to use cyanuric fluoride**,** analogous to the chloride. The mechanism of acid fluoride and chloride formation via the corresponding cyanuric derivatives and is the same (Scheme 18).[99] In our case, fluoride derivatives of Alloc-*L*-Ala-OH and of Boc-β-Ala-OH was generated *in situ* in dry DCM, using cyanuric fluoride in presence of pyridine, under argon-atmosphere (Scheme 20).[99] A DCM solution of the cyclic monomer **6** was then added dropwise at 0°C to each of these mixtures (Scheme 20). However, no reaction occurred in these cases also, even under heating.

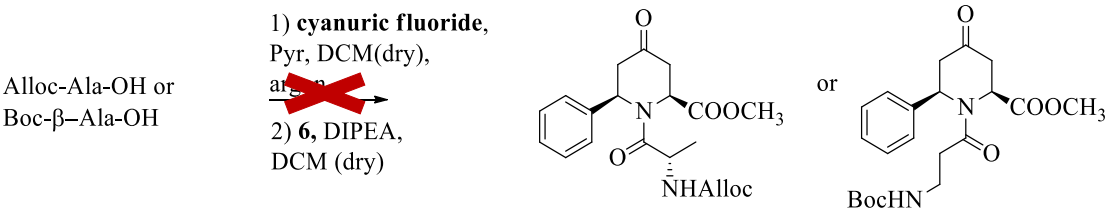

*Scheme 20: Attempts of coupling cyclic monomer **6** in its fluoride form.*

III.-3.3 Synthesis of 6-phenylethyl-4-oxo-pipecolic acid derivatives

We hypothesized that the introduction of a spacer between the phenyl substituent and the carbon at position 6 of the 4-oxo-pipecolic acid should reduce the overall steric hindrance and should allow a coupling between two cyclic monomers or between one monomer and a *N*-protected amino acid. The synthesis of the monomer **22** containing a

phenylethyl chain was carried out as for compound **6** (Chapter 3.1). Simply, the Wittig-Horner reaction was carried out starting from hydrocinnamaldehyde instead of benzaldehyde (Scheme 21). Diastereomers *(2R, 6S)* (**22**) and *(2S, 6S)* (**23**) were obtained in 43% and 17% yields, respectively.

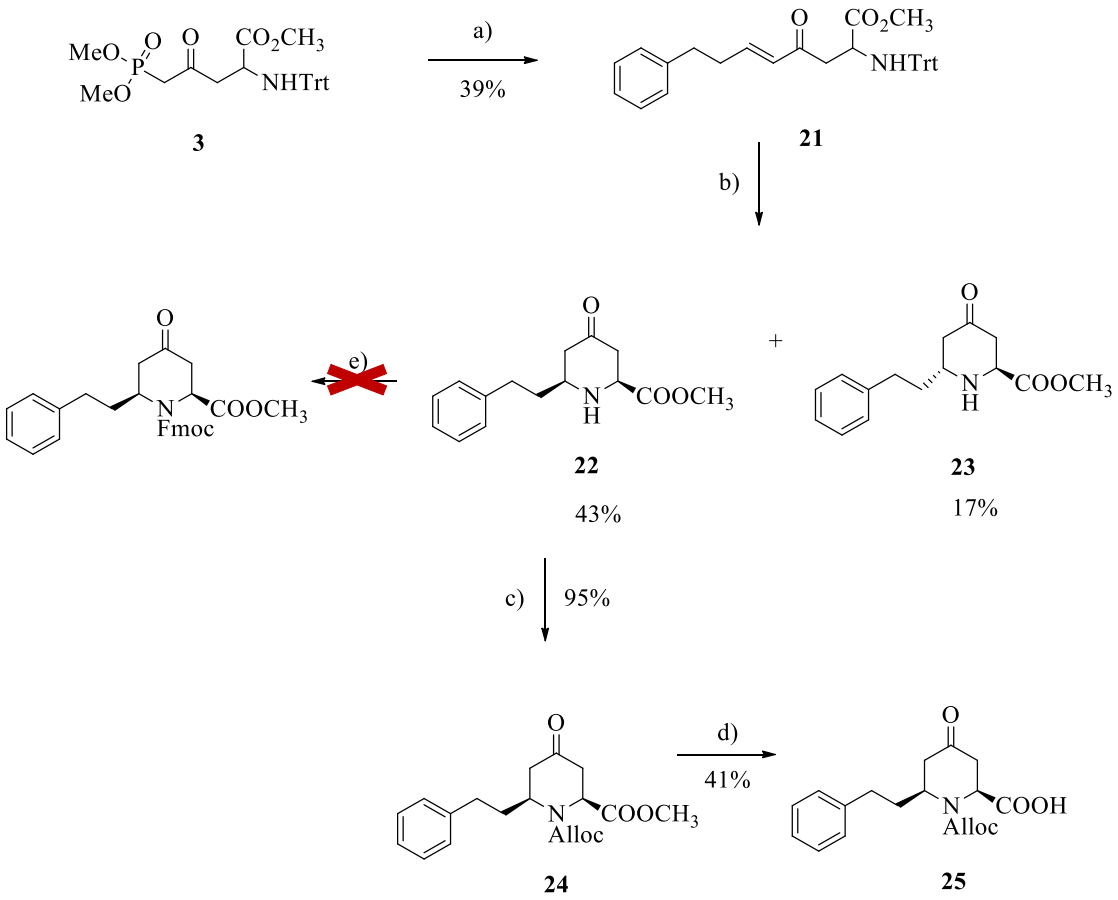

Scheme 21: Synthesis of cyclic monomer **22**. *a) Hydrocinnamaldehyde, K_2CO_3, MeCN, 96h reflux b) 2M HCl/MeOH, DIPEA/H2O c) allyl chloroformate, DIPEA, DCM d) Me_3SnOH, 1,2-DCE, 80°C e) Fmoc-Cl, DIPEA, DMF.*

As in the case of 6-phenyl substituted monomer **6**, the Fmoc protection of compound **23** was unsuccessful but, the Alloc protected derivative **24** was obtained in 95% yield. It was then saponified using Me_3SnOH in 1,2-DCE at 80°C, given compound **25** in 45% yield (Scheme 21). These results demonstrate that the introduction of a hydrocarbon

side-chain at position 6 does not decrease the steric hindrance during the coupling. Further assays were not performed, because of time limitations (Scheme 22).

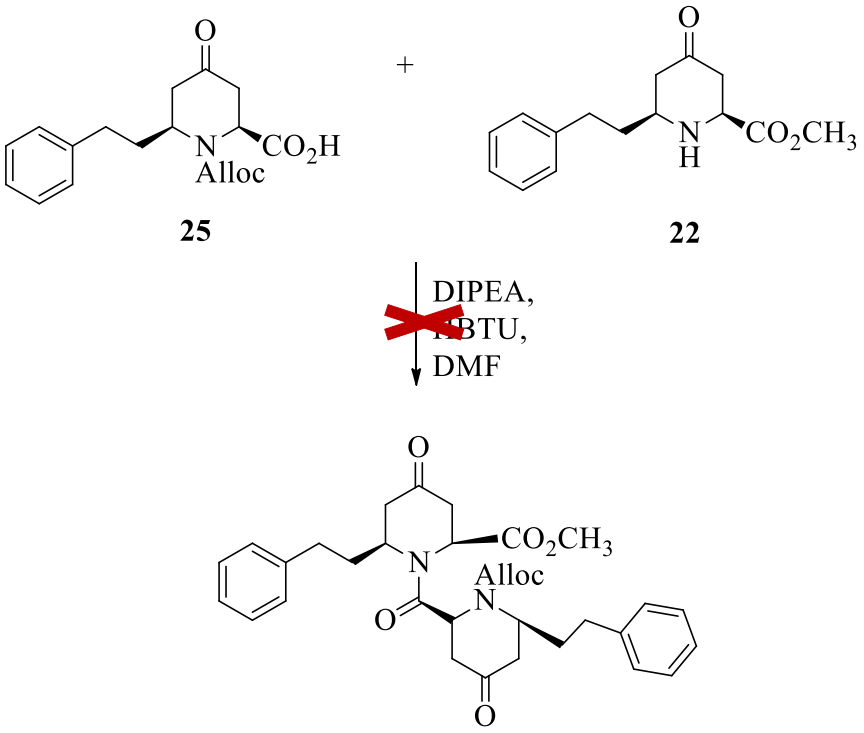

Scheme 22: Attempts to couple 6-phenyl ethyl substituted monomers.

IV. Conclusion and Outlook

Our goal was to evaluate 6-substituted 4-oxo-pipecolic acids as building blocks in peptide synthesis, then to construct homogenous and heterogenous structures by solid-phase synthesis.

Two methyl ester residues containing a phenyl and a phenylpropyl groups in position 6 were synthesized. The protection of the secondary amine of the two cyclic residues could be successfully performed only with the Alloc protecting group, suggesting that this function is highly hindered, due to the proximity of two substituents in *cis*, in position 2 and 6 of the ring. This has been confirmed by the fact that neither the hindered 6-substituted 4-oxo-pipecolic methyl ester residues nor the unhindered *L*-alanine, β-alanine and *L*-glycine ones could be condensed on it. Even acid chloride or fluoride activation was unsuccessful. Otherwise, the peptide coupling from the carboxyl-function of the *N*-Alloc cyclic monomer was easily accessible.

In parallel of these works, a new synthetic way has been developed to form *N*-allyl or *N*-benzyl 6-substituted 4-oxo-pipecolic acid residues, by an imino-Diels-Alder reaction. Unfortunately, this reaction leads to a racemic mixture, which is unsuitable in view of peptide synthesis.

This work opens new research perspectives. Firstly, the unsubstituted and unhindered 4-oxo pipecolic acid residue (Figure 56) should be synthesized, then analyzed for its ability to give homogeneous or heterogeneous foldamers. Further functionalization on them might be achieved *via* the reaction of carbonyl functions with nucleophiles.

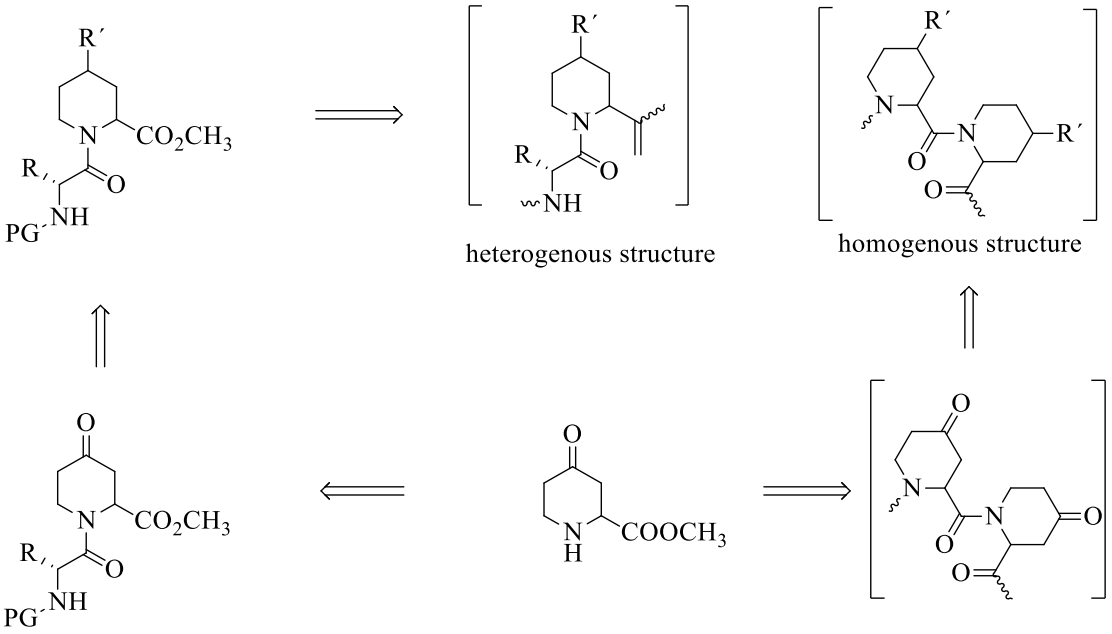

Figure 56: Prospects: coupling of the 6-unsubstituted 4-oxo pipecolic acid residue.

On the other hand, the ketone-function in the ring of 6-substituted 4-oxo pipecolic acids could have a negative influence at the level of their coupling. The reduction of ketone to tetrahedral alcohol function might be performed and the peptide coupling assessed (Figure 57). The reduction from ketone to the alcohol using $NaBH(OAc)_3$, is described in the thesis and publication of Daly *et al.*.[84]

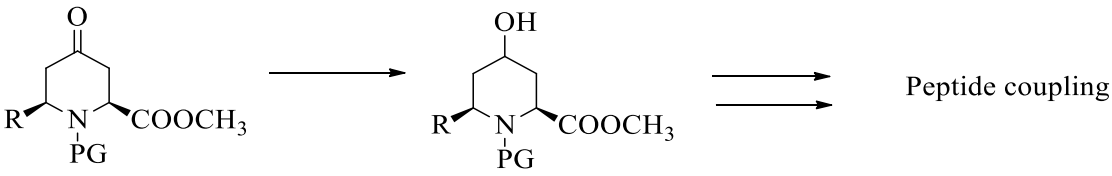

Figure 57: Prospects: coupling of the 6-substituted 4-hydroxy pipecolic acid residues.

Finally, the insertion of a linker at the secondary amine or at the carbonyl function of 6-substituted 4-oxo pipecolic acid derivatives should be tried *via* reductive amination, affording new synthons, which could be useful to induce turns in a structure (Figure 58).

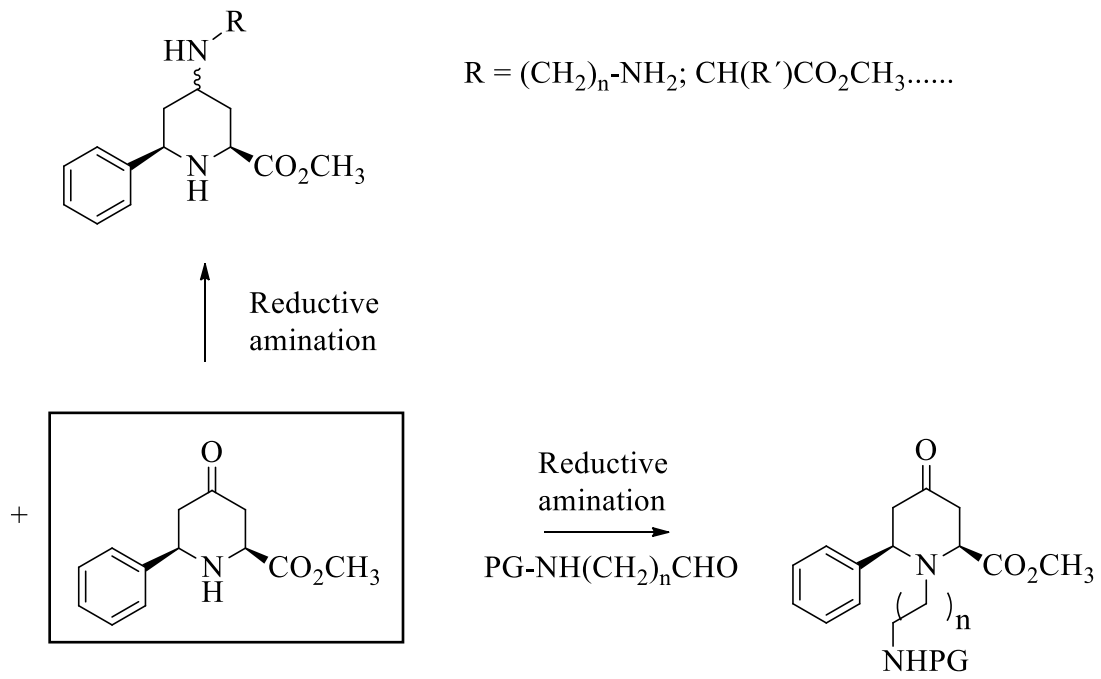

Figure 58: Prospects for reductive amination of the 6-substituted 4-oxo pipecolic ester.

PART II

Stapled *di*-α-PNA as building blocks for the development of constrained Peptide Nucleic Acids

I. Bibliography

I.-1. Nucleic acid mimics for antisense oligonucleotide therapeutics

Short single stranded nucleic acid (or mimic) sequences that bind to complementary RNA targets through antisense mechanism *via* Watson-Crick specific base pairing are called antisense oligonucleotide therapeutics (AONs) and are highly interesting for treatment of many diseases. These sequences have normally 10-30 nucleotides in length and many structural modifications as compared to natural nucleic acids have been done in previous years. These AONs can interrupt protein translation by interacting with complementary mRNA sequences (Figure 59), as well they can have an influence in various biological processes by targeting non-coding RNA.[100]

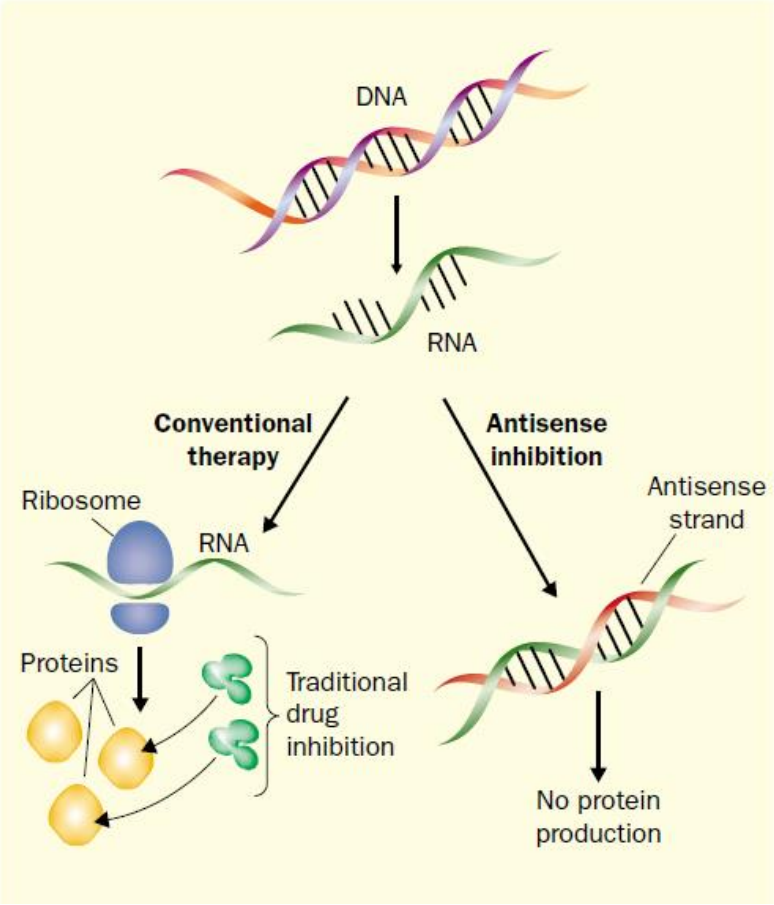

Figure 59: Principle of protein production inhibition of AONs.[100]

Most AONs are applied as gapmers, steric block ONs, antagomirs, small interfering RNAs (siRNAs), micro-RNA mimics, and splice switching ONs.[101] They represent great therapeutic potential for various diseases[102], like cancer, viral and bacterial infections[103], neurological disorders.[104] Those who bind to Toll-like receptors (TLRs) and those forming aptamers represent oligonucleotide therapeutics that interact with their target using a new mechanism. Nowadays, 76 oligonucleotide drug candidates have been tested in clinical trials for treatment of various diseases.[105] Many of them have promising potential and are registered by the FDA.[106]

I.-2. AON modifications

In 1997, Paterson *et al.* introduced for the first time the use of antisense oligonucleotide therapeutics. They reported the application of nucleic acids for the modulation of gene expression. However, the use of natural nucleic acids as antisense agents faces several issues such as nuclease sensitivity, off-target effects and efficient delivery. Thus, the binding affinity, nuclease resistance, biostability and pharmacokinetics have been improved by inserting various chemical modifications in the phosphodiester backbone, heterocyclic nucleobase and sugar moiety. These modifications are illustrated in Figure 60.[105]

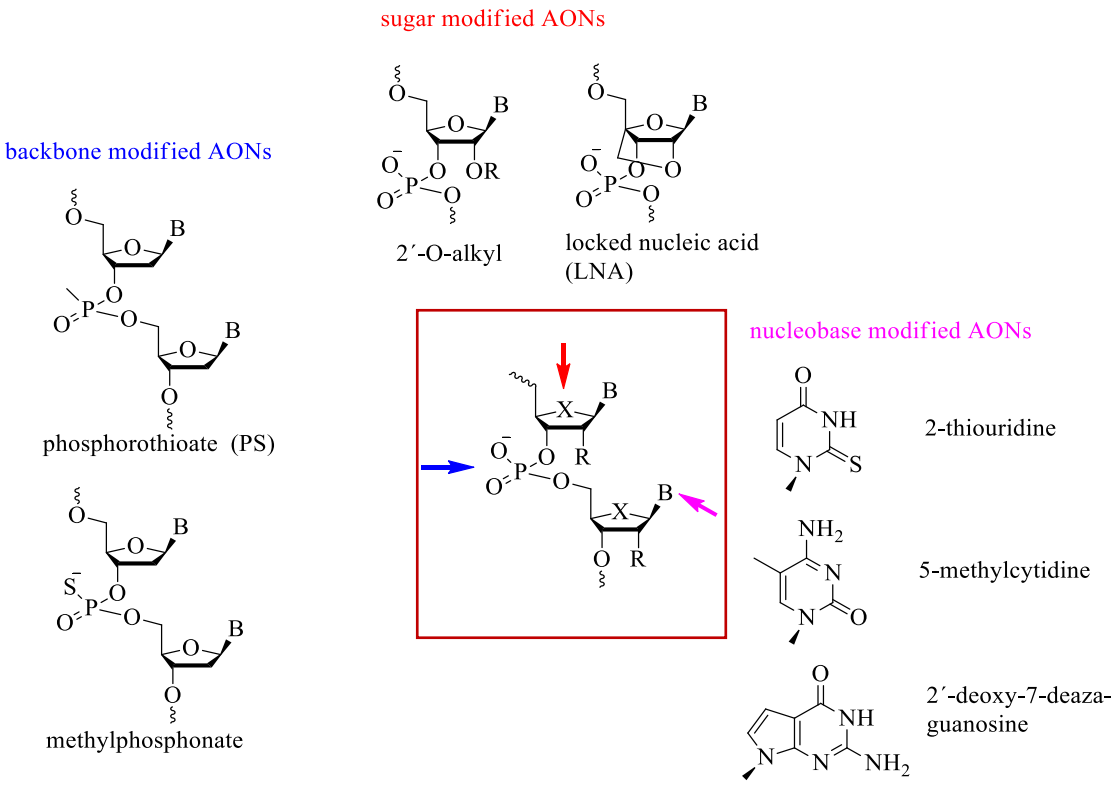

Figure 60: Different modifications of antisense oligonucleotides. B=nucleobase.[105]

Advanced modifications of AONs have been done, which are presented in the following chapters.

I.-2.1 Internucleoside linkage/backbone modified AONs

Fritz Eckstein developed in 1969 the PS-ONs chemistry.[107] Internucleoside linkages are divided in 3 classes: neutral, anionic and cationic internucleoside linkage of AONs and are shown in Figure 61. Internucleoside linkage AONs represent the first generation of modified AONs and were developed to avoid the physical and biological limitations of the natural phosphodiester linkage. The most common ones are the phosphorothioate oligonucleotides (PS-ONs), which are successfully applied in gene silencing.[105,101]

a) neutral internucleoside linkage

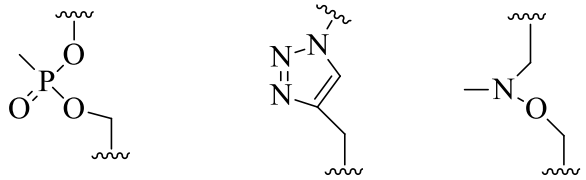

methylphosphonate triazole MMI

b) anionic internucleoside linkage

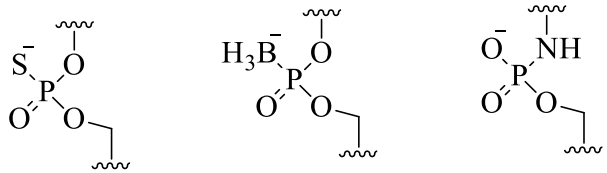

PS boranophosphate NP

c) cationic internucleoside linkage

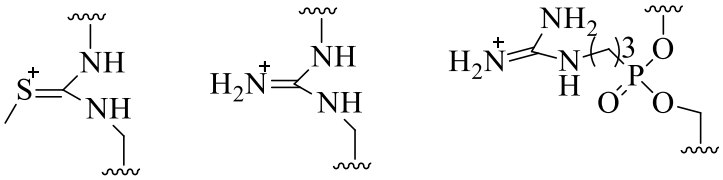

S-methylthiourea guanidinium guanidinopropyl phosphoramidate

Figure 61: Backbone modified internucleoside residues. A)neutral internucleoside linkage b) anionic internucleoside linkage c) cationic internucleoside linkage.[105]

In 1998, the FDA registered the first antisense drug 31 Vitravene, which was described 2002 from Stein and Dias as drug. This AON is a 21-merPS-ONs for the treatment of AIDS-related cytomegalovirus (CMV) retinitis. The mRNA, applied as target, encoded the CMV immediate-early (IE)-2 protein, which is required for viral replication. [105]

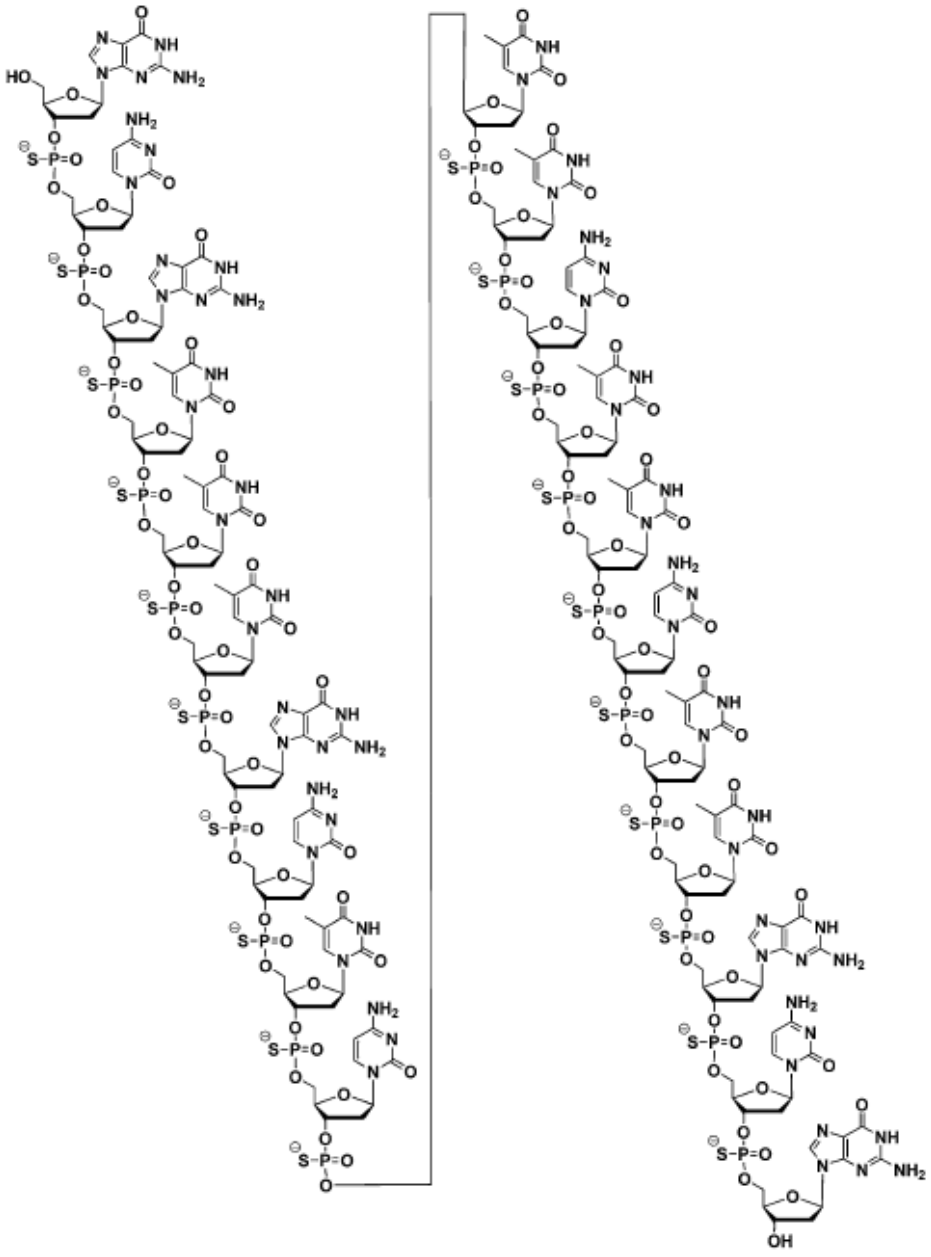

Figure 62: Antisense drug vitravene.[105]

Nevertheless, poor binding affinity to the target RNA, lack of specificity and low cellular uptake represent major drawbacks of PS-ONs.[105]

I.-2.2 Sugar modified AONs

Second-generation AONs are sugar modified constrained AONs, which are illustrated in Figure 63. They are modified with an electronegative atom or substituent at the 2'-position of the sugar, an extra ring fused to the sugar moiety, a modification of the sugar ring structure or an introduction of a spirocyclic ring at different positions of the sugar moiety (Figure 63).

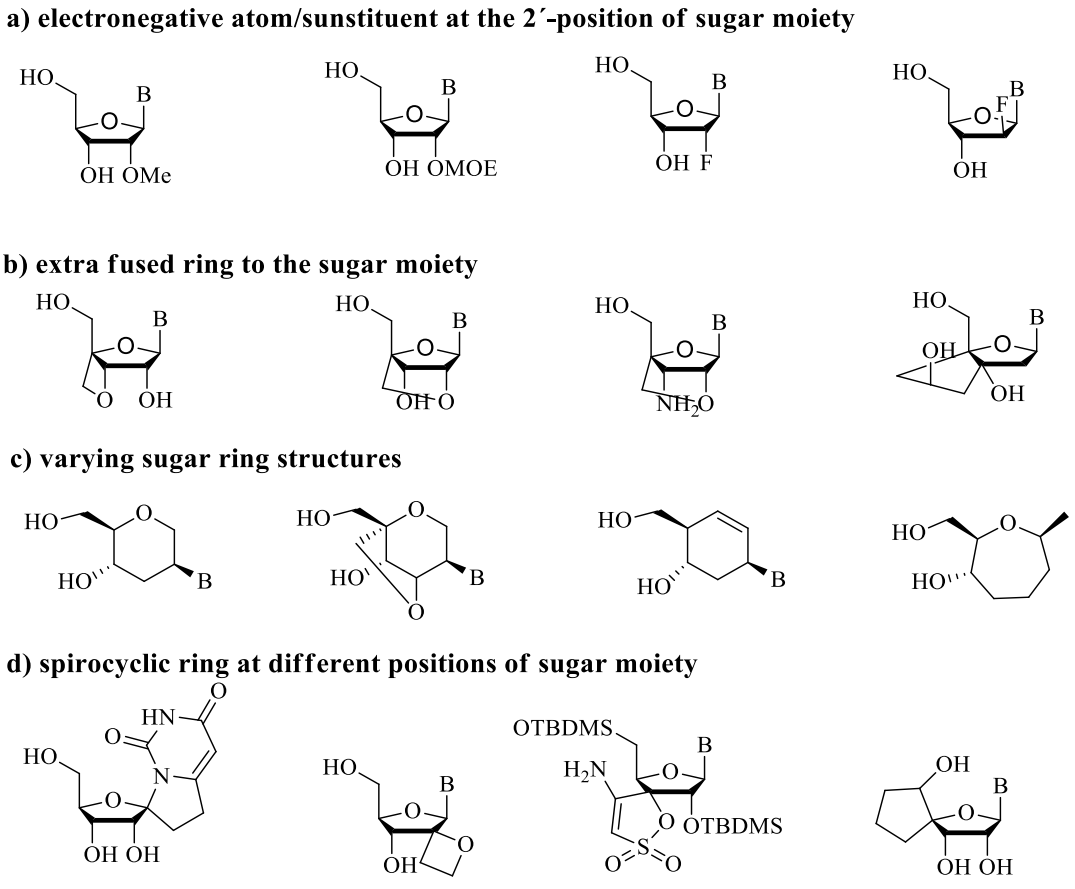

Figure 63: Different types of sugar modified constrained nucleoside analogues.[105]

Various reported 2'-substitutions have shown excellent results in antisense therapeutics, providing high metabolic stability and high affinity for the targeted

mRNA, that was confirmed by Dean and Bennett in 2003.[108] The most important members are 2'-O-Methyl (2'-OMe), 2'-O-methoxyethyl (2'-OMOE) and locked nucleic acid (LNA). In 2004, pegaptanib sodium (Macugen) was permitted for the treatment of all types of neovascular age-related macular degeneration. Macugen is a single-stranded 27-mer containing 2'-F and 2'-OMe substituted sugar moieties (Figure 64), forming a stable three-dimensional structure. It is an aptamer that bind with high affinity and specificity to the anti-vascular endothelial growth factor (anti-VEGF).[105,101]

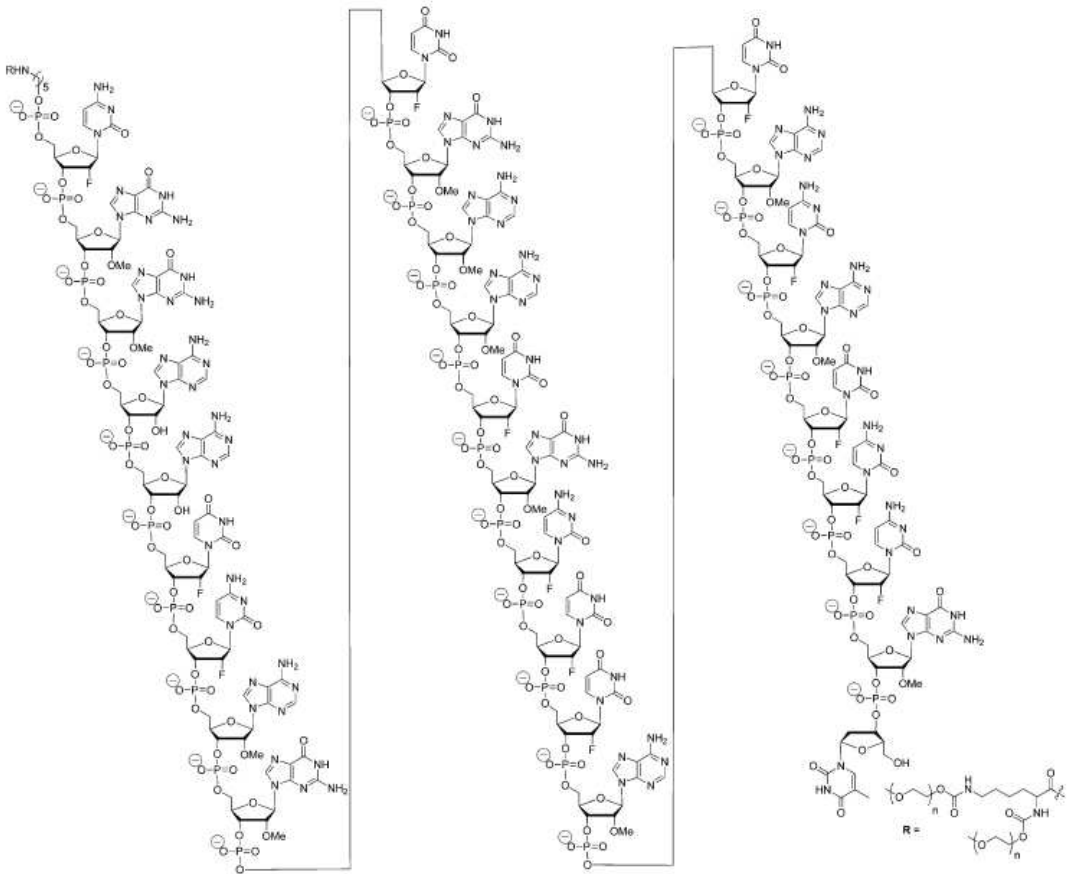

Figure 64: Structure of sugar modified drug Macugen.[105]

I.-2.3 Nucleobase modified AONs

Chemically modified heterocyclic nucleobases are less common than other modified AONs. These modifications can only improve the binding affinity to the complementary nucleic acid, but not the nuclease resistance. Several modified nucleobases are shown in Figure 65, that present modifications on the 4- and 5-position of pyrimidine, 6- and 7-position of purine. Universal bases analogues are also presented. These ones interact only *via* aromatic ring stacking and do not interact *via* hydrogen bonds.[105]

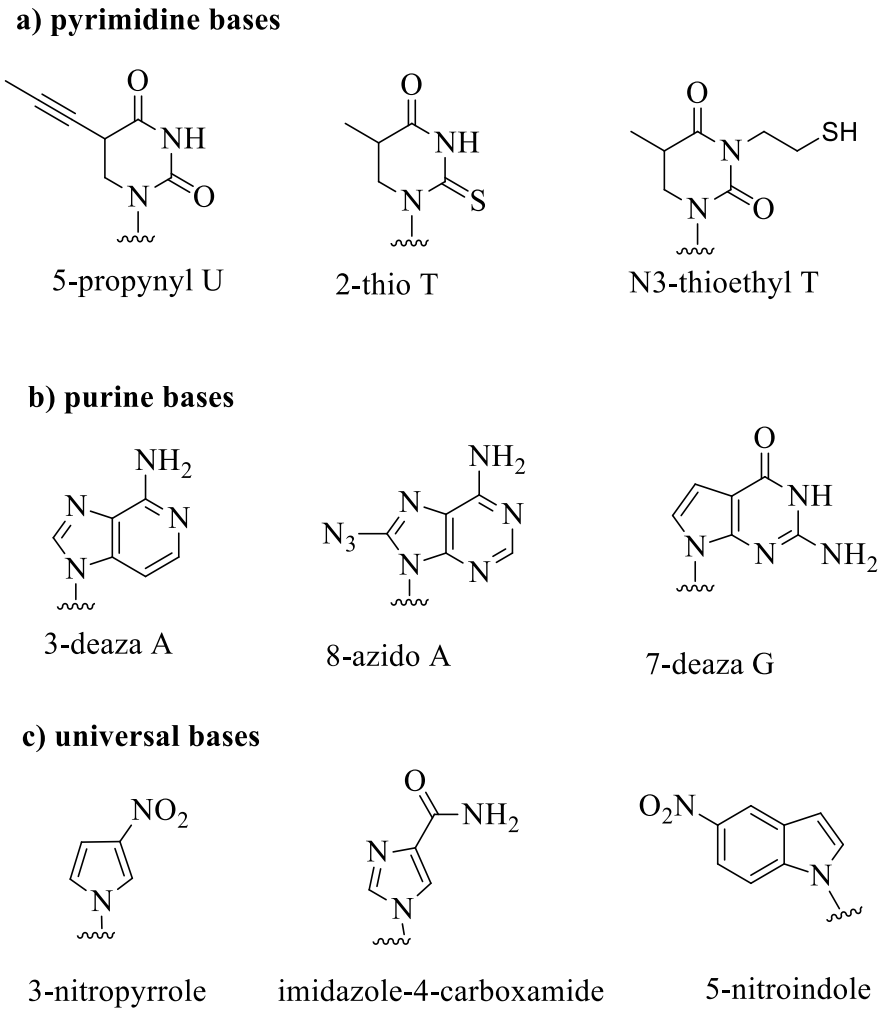

Figure 65: Different types of nucleobase modified nucleoside analogues.[105]

Among them, AONs containing tricyclic phenoxazine, as G-clamp, display dramatically enhanced stability, by maximizing stacking interactions and by recognizing both the Watson–Crick and the Hoogsteen sites of guanine. That is shown in Figure 66.[105]

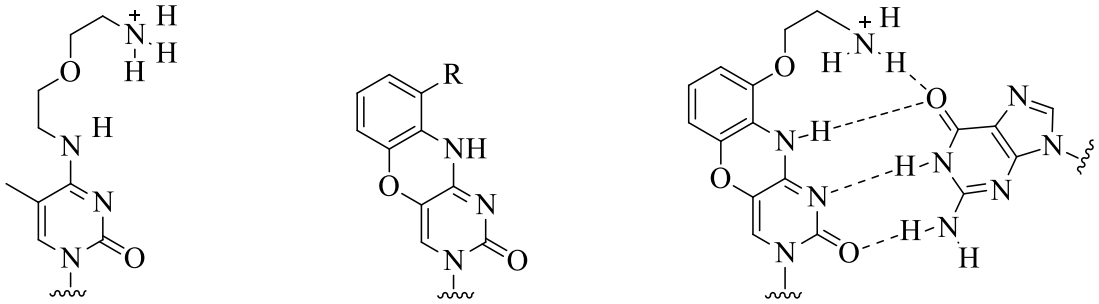

Figure 66: Cytosine modified analogues and interaction with guanosine.[105]

I.–2.4 Other advanced modified AONs

For further improvement of target affinity, nuclease resistance, biostability and pharmacokinetics, an advanced third generation of AONs was developed mainly by modifications of the furanose ring of the nucleotide. A representative is the phosphorodiamidate morpholino family (PMO), which is one of the most well studied third-generation AONs. PMO are non-charged AONs, in which the ribose sugar is replaced by a six-membered morpholino ring and the phosphodiester bond by a phosphoroamidate linkage (Figure 67).[109] In 2016, the FDA approved Eteplirsen, a 30-mer PMO, for the treatment of the Duchenne muscular dystrophy (DMD), a genetic degenerative muscle disease (Figure 68).

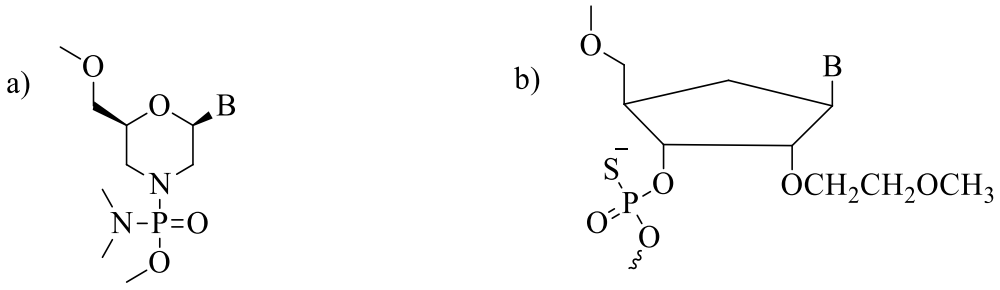

Figure 67: a) phosphorodiamidate morpholino family (PMO) and b) phosphorothioate 2′-O-methoxy (PS-2′-MOE).

Another family is the phosphorothioate 2′-O-methoxyethoxy family (PS-2'-MOE), shown in Figure 67. In 2016, the FDA approved „Nusinersen", a 18-mer PS-2'-MOE, for the treatment of spinal muscular atrophy (SMA) in infants (Figure 68).

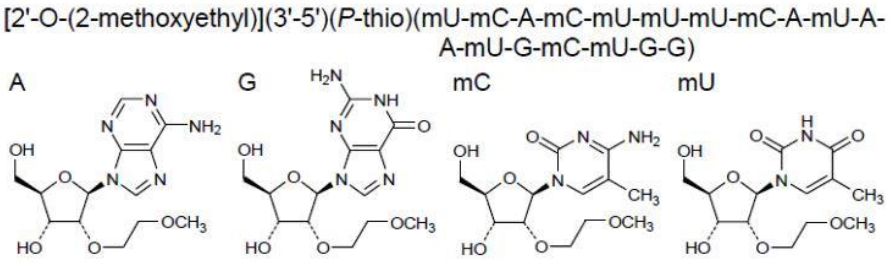

Nusinersen

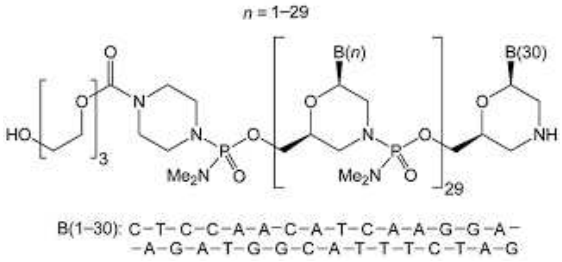

Eteplirsen

Figure 68: Structure of modified antisense ONs, Eteplirsen and Nusinersen.

The best way to inhibit the translation process of a targeted mRNA is to use antisense

ONs (ASO) that are able to hybridize with the target and to induce the cleavage of the mRNA strand by RNase H. Modified AONs do not always allow the recognition of the double strand by RNAse H and to circumvent this problem, chimeric ASO named "gapmers" have been developed. These have a central 'gap' of deoxynucleotides (or mimics) sufficient to induce RNase H cleavage, flanked by modified ON sequences protecting the internal gap from nuclease degradation.[105]

In 2013, FDA approved „Kynamro" for the reduction of the low density of lipoprotein-cholesterol (LDL-C), apolipoprotein-B, total cholesterol and non-high density lipoprotein–cholesterol in patients with homozygous familial hypercholesterolemia (HoFH). Kynamro 35 is a 20-mer oligonucleotide that comprises a central gap of a 10-mer PS-ON, flanked, at its 5' and 3'-ends, by two pentameric 2'-methoxyethoxy (MOE) phosphorothioate sequences (Figure 69). [105]

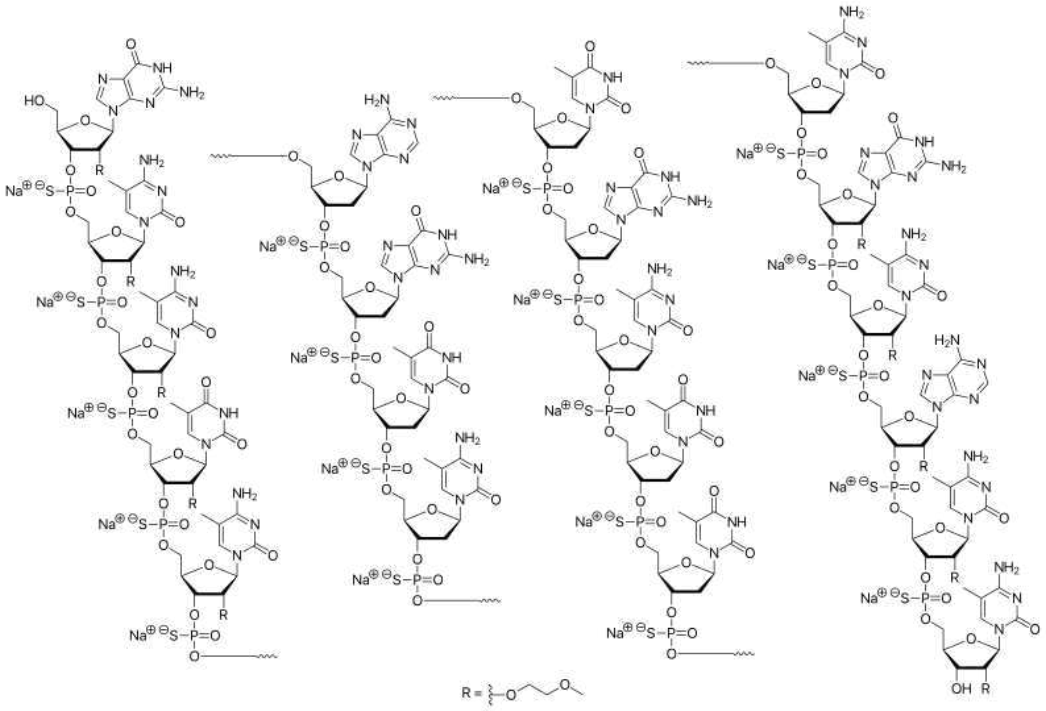

Figure 69: Structure of antisense drug Kynamro.[105]

These later confer to the whole antisense resistance towards exonucleases, strongly

increase the stability of the mRNA/ASO duplex and help to enable cleavage of the mRNA by RNase H.[105]

I.-3. Peptide nucleic acid[110]

Peptide Nucleic Acids (PNAs) are achiral and non-natural nucleic acid mimics, constituted by *N*-(2-aminoethyl)glycine units onto which are condensed nucleic basis. It is reported 1991 by Nielsen *et al*.[111] and developed as a DNA/RNA analogs with therapeutic potential (Figure 70). [112]

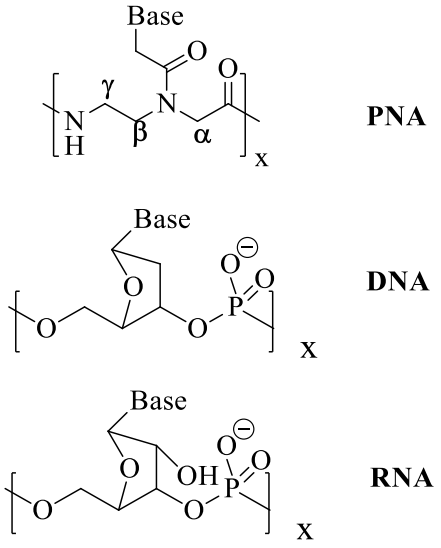

Figure 70: Comparison of PNA, RNA and DNA structure.[112]

Contrary to DNA and RNA, the *aeg*-PNA backbone is uncharged, and due to the absence of electrostatic repulsion, *aeg*-PNAs hybridize with complementary RNA or DNA strands with an unprecedent affinity, giving duplexes more stable than DNA/DNA and RNA/RNA. Moreover, they have a propensity to hybridize to highly structured targets such as DNA duplexes, hairpin structures and guanine quadruplexes, by strand invasion or by forming triplexes. [113]

The *aeg*-PNA backbone presents a good structural mimic of the ribose-phosphate backbone of DNA/RNA. Their remarkable hybridization properties and their high

stability in chemical and biological media make *aeg*-PNA ideal tools in various applications, including laboratory techniques such as PCR, purification of nucleic acids, southern and northern blotting, molecular beacons, microarrays and FISH. From a therapeutic point of view, they have a great potential in various diseases since they are able to inhibit biological processes as DNA replication and transcription, RNA translation, and to modulate the expression of targeted genes *via* their interaction with microRNA and their precursors (pre-miR).[114] However, they present some major drawbacks for their *in vivo* application, and such as low solubility in aqueous media and poor cellular uptake, and various conjugates of PNA and of "cell penetrating moieties" (CPP, R-rich peptide sequences, triphenylphosphonium moiety…) have been elaborated to overcome these problems.[115] Moreover, the flexible backbone of *aeg*-PNA allows them to bind with similar affinities to DNA and RNA strands, forming right-handed helices in respectively B/A and A form, preferentially in antiparallel direction but also in parallel mode (Figure 71).[116]

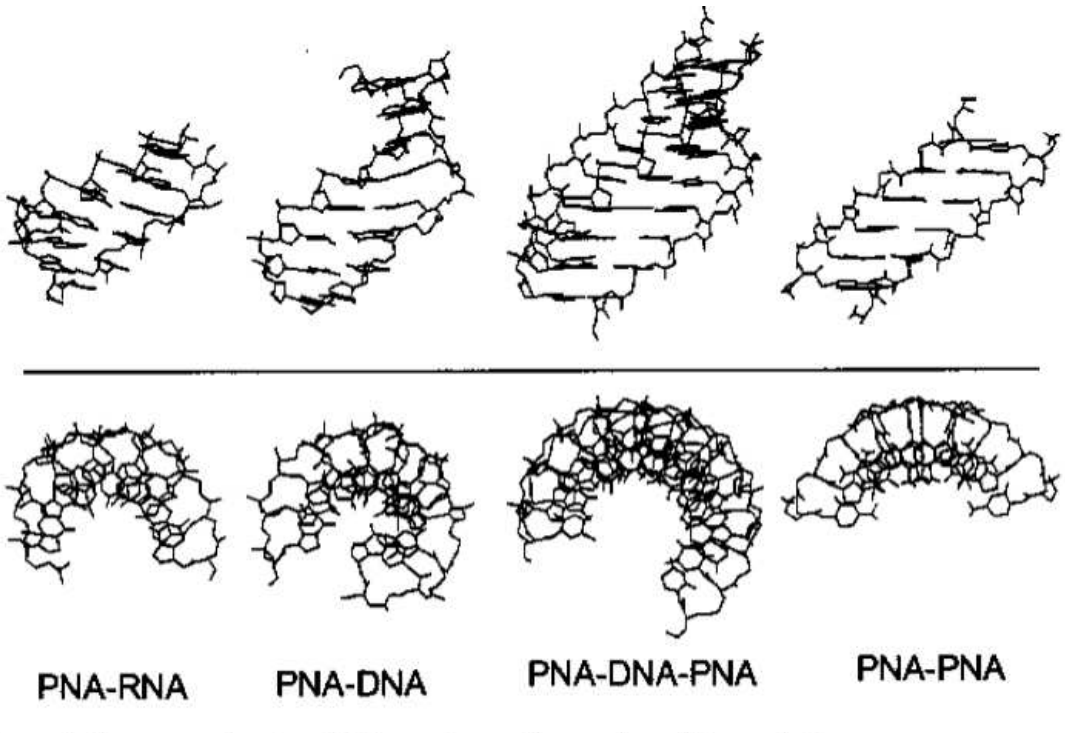

Figure 71: Structures of different aeg-PNA complexes.[117]

This potentially may cause undesirable side effects. To improve the selectivity of PNA and consequently, their antisense and antigene potency, preorganized PNAs structure in a right-handed helical conformation should be designed. This can be achieved by adding substituents to the backbone or by cyclization of the PNA backbone. These two strategies will be presented in the following chapters.[110]

I.-3.1 Chiral α-, β- and γ-PNA

To study the impact of the chirality on PNA hybridization properties, stereogenic centers were introduced in the PNA backbone, giving three different types of chiral PNAs. These chiral PNAs are defined by the position of substituents on the PNA backbone. Several chiral PNAs with substituents at the α-, β-, or γ-positions have been reported. These are illustrated in Figure 72.[112]

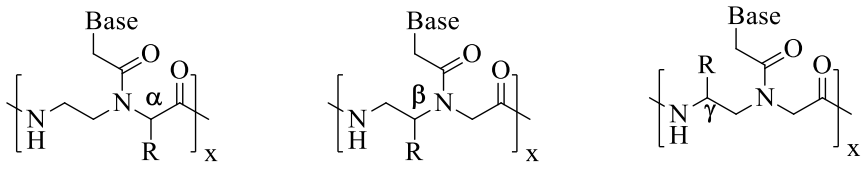

Figure 72: Structure of chiral PNAs (α-, β– and γ-PNA).[112]

I.-3.1.1 α-PNA

In 1996, Nielsen *et al.* reported α-PNA structures, where the glycine moiety was substituted by *D*- or *L*-α-amino acids and thymine was the nucleobase.[118] They studied the thermal stability of duplexes between *deca*-PNA containing three separated chiral α-PNA monomers and DNA or RNA complementary sequences, in parallel and antiparallel directions. It was established that PNAs containing *D*-α-PNA monomers

bind to complementary DNA with a greater stability than PNAs containing *L*-α-PNA ones (Table 7). This has been explained in terms of pre-helical organization of PNA strands. *D*-α-PNA monomers induce preferentially a right-handed helix for the PNA strand, while *L*-α-PNA ones induce a left handed one. As a result, DNA, which is right-handed, interacts preferentially with the right-handed *D*-α-PNAs containing PNA. Moreover, α-PNAs bind preferentially in the antiparallel mode than in the parallel one (Table 7).

Using bulky (Ile) or anionic (Glu, Asp) α-amino acids led to only a moderate loss of stability, while an increase in DNA hybridization potency was visible with the cationic Lysine residue (Table 7).[119] Like *aeg*-PNA, modified α-PNA showed a stronger interaction with RNA than with DNA and the nature of the amino acid constituting the α-PNA backbone has less impact on duplex stability than for DNA binding.

*Table 7: Melting temperatures of DNA and RNA/α-PNA duplex in parallel and anti- parallel modes. A) PNA sequence: H-G**Tx**AGA**Tx**CAC**Tx**-LysNH$_2$. The backbone at the T_x position was constructed with the monomer derived from the indicated amino acid. b) Anti-// DNA sequence : 5'-d(AGTGATCTAC)-3' ; Anti-// RNA sequence : 5'-AGTGATCTAC)-3' ; // DNA sequence : 5'-d(CATCTAGTGA)-3'.*[119,118]

α-PNA sequence [a)]	T_m(DNA, anti-parallel) [b)]	T_m(DNA, parallel) [b)]	T_m(RNA, anti-parallel) [b)]
Gly	52	38	55
L-Lys	49	41	51
D-Lys	55	40	55
L-Ser	49	37	52
D-Ser	50	38	52

D-Glu	42	28	nd
L-Asp	38	33	nd
L-Ile	44	38	46
Chiral box PNA H-GTAG($A_{D\text{-}Lys}$)($T_{D\text{-}Lys}$)($C_{D\text{-}Lys}$) ACT-NH_2	43	No binding	Not determined

In 2000, Sforza *et al.* showed that the position of the three D-α-PNA monomers into the *deca*-PNA sequence had also an influence. They incorporated in the α-PNA a "chiral box" consisting of three following *D*-α-PNA(Lys) monomers (Figure 73). These were introduced in the middle of the strand and the duplex interactions analyzed (Table 8).

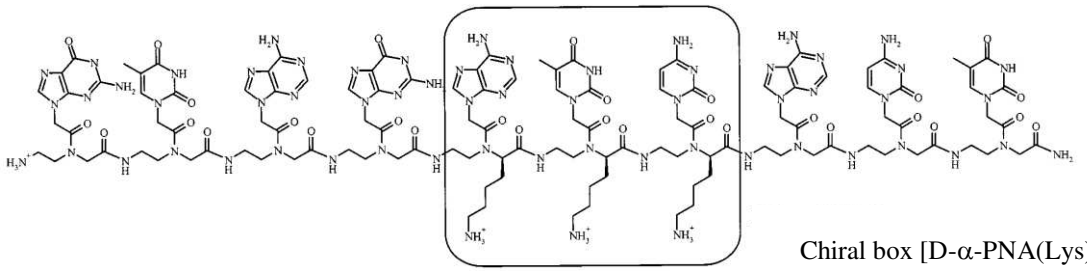

Figure 73: Deca-PNA incorporating three chiral adjacent monomers D-α-PNA(Lys) in the middle of the PNA strand.[119,112]

It can be shown in Table 8, that the presence of the "chiral box" into *deca*-PNA led to a moderate loss of stability, as compared to achiral PNA and to chiral PNA containing three separated α–PNA monomers. However, and in marked contrast with the latter, the "chiral box" PNA interacted with DNA exclusively in antiparallel fashion and showed no affinity for the parallel DNA target. This strong binding selectivity in the

direction control has been attributed to a greater rigidity of the PNA structure, induced by the presence in the middle of the PNA strand, of the chiral box.

As well, the ability of *deca*-PNA containing α-PNA residues to discriminate between mismatched and matched targets was studied (Table 8).[119,112,120]

*Table 8: Melting temperatures Tm (°C) of PNA-DNA and PNA-RNA duplexes with one mismatched base pair, in antiparallel mode. a) T_x PNA sequence: H-G**Tx**AGA**Tx**CAC**Tx**-LysNH₂. The backbone at the T_x position was constructed with the monomer derived from the indicated amino acid. b) mismatched DNA sequence (DNAmis): 5'-d(AGTG**G**TCTAC)-3'; mismatched RNA sequence (RNAmis): 5'-AGTG**G**TCTAC-3'.*[119,118]

T_x α-PNA sequence [(a)]	T_m-(DNAmis)[(b)]	ΔT_m (DNAmis/DNA)	Tm (RNAmis)[(b)]	ΔTm (RNAmis/RNA)
Gly	37	-15	46	-9
L-Lys	35	-14	40	-11
D-Lys	36	-19	43	-12
D-Ser	33	-17	43	-9
D-Glu	28	-20	Not determined	Not determined
L-Ile	28	-16	36	-10
Chiral box PNA H-GTAG($A_{D\text{-}Lys}$)(T_{DLys})($C_{D\text{-}Lys}$) ACT-NH_2	No binding	-	Not determined	Not determined

Globally, PNAs containing *D*- or *L*-amino acids lead to better sequence discrimination against base pair mismatches compared to *aeg*-PNA.[120] On the other hand, α-PNA containing cationic residues (Lys, Arg) present the great advantage, over *aeg*-PNA and

other α-PNAs, to have a significantly improved water solubility. Moreover, in the case of *D*-Arginine based α-PNAs (α-GPNA), guanidinium group does not only increases the PNA solubility, but also significantly enhances the cellular uptake, while improving the discrimination for base pair mismatches in target sequences (Figure 74).[121,122]

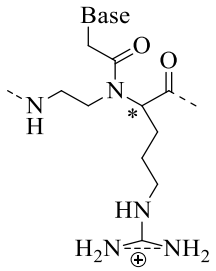

α–GPNA

Figure 74: Structure of D-α-PNA(Arg).[112,122]

Various other α-PNA monomers, like α-PNA monomers with bearing glycosylated side chains or those displaying cyclobutyl-carbonyl-containing or phosphonic ester (pePNA) groups in their side-chains, have been prepared and incorporated into α-PNA sequences. They are shown in Figure 75.[112,123,124,125,126]

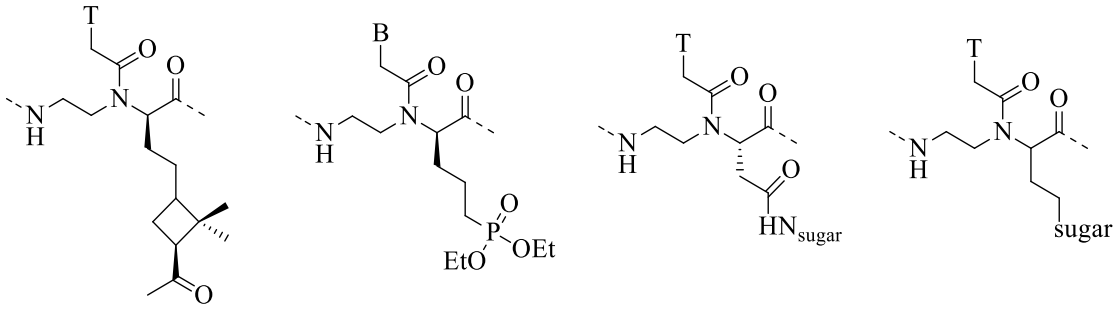

Figure 75: Several examples of different α-PNA monomers.[112,123,124,125,126]

Ganesh *et al.* developed in 2012 a Thymine-PNA monomer having gem-dimethyl substitutions on glycine residue, defined as *dmg*-PNA-T (Figure 76).[127,112]

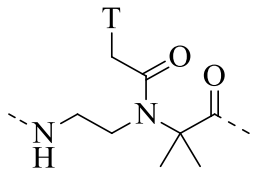

Figure 76: Structure of dmg-PNA-T.[127]

As shown in Table 9, the resulting PNA oligomers hybridized with remarkable affinities with target ssDNA or RNA, preferentially in anti-parallel direction. They showed very substantial higher affinity for DNA than for RNA. This may be a structural consequence of the sterically rigid gem-dimethyl group, imposing a pre-organized conformation favorable for complexation with ssDNA.[127,112]

Table 9:Melting temperatures T_m (°C) of DNA/dmg-PNA and RNA/dmg-PNA duplexes in parallel and anti-parallel directions. Values in parenthesis indicate amount in degrees of stabilization (+) or destabilization (-) over unmodified PNA.[127]

DNA/RNA sequence	*aeg*-PNA H-GTAGATCACT-LysNH$_2$	*dmg*-PNA H-GtAGAtCACt-LysNH$_2$ t: dmg T PNA monomer
5'-d(AGTGATCTAC)-3' anti-parallel	49,8	80,9 (+31,1)
5'-d(CATCTAGTGA)-3' parallel	37,5	56,5 (+19)
5'-AGTGATCTAC-3' anti-parallel	50,1	72,3 (22,2)
5'-CATCTAGTGA-3'	40,5	31,6 (-8,9)

parallel		

I.-3.1.2 β-PNA

In 2011, Sugiyama *et al.* synthesized chiral β-PNA monomers where a methyl group was introduced on the β-position of the PNA backbone (Figure 77).[112,128]

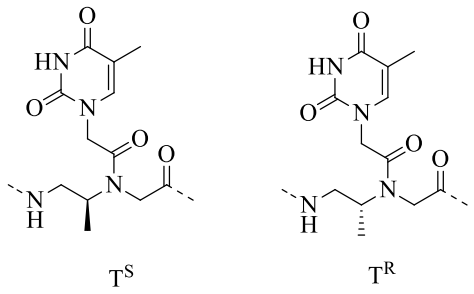

Figure 77: Structure of R- and S-β-Me-PNA.[112,128]

The S- and the R-forms of the β-Me PNA monomers were incorporated individually at positions 2,6 and 10 of a 10-residue PNA sequence (H-GTAGATCACT-lys-NH_2). The melting points of the complexes formed with complementary DNA sequence are given in Table 10. Only the PNA containing the S-forms showed to DNA, with the same affinity than *aeg*-PNA. It has been shown to adopt a right-handed helical structure and to form a right-handed duplex with DNA. By contrast, the PNA containing the R-forms is left-handed and did not bind to DNA. This indicates that the stereochemistry at the β-position is significant for the hybridization stability of PNA and that is strictly limited to the *S*-configuration.[112,128]

Table 10: Melting point of β–Me PNA deca-PNA/DNA complexes.[112]

PNA sequence	**T_m (°C)**
H-GTAGATCACT-L-Lys-NH_2	51.4
H-G**T^S**AGA**T^S**CAC**T^S**- L-Lys-NH_2	51.0
H-G**T^R**AGA**T^R**CAC**T^R**-D-Lys-NH_2	n.d.

Further studies have been done by Sugiyama *et al.* in 2016. They reported also the synthesis of *(S)*-β-Lys PNA monomers, which were incorporated in *deca*-PNA sequences. Compared to *aeg*-PNAs, PNAs containing one and two *β*-Lys PNA units formed less stable hybrid duplexes with DNA (Table 11). This can be explained by the steric hindrance of the side chains of lysine. However, an increase of the sequence selectivity in the *β*-deca-PNA sequences could be observed for the β-*deca*-PNA sequences compared to unmodified *aeg*-PNA.[112,129]

Table 11: Melting point T_m [°C] between PNA sequences containing one or two β-PNA monomers the complementary or mismatched DNA sequences.[112,129]

PNA sequence	**T_m (°C) (DNA)**	**T_m (°C) (DNAmis)**
H-GTAGATCACT-*L*Lys-NH_2	49,7	34,6
H-GTAGA***T***CACT-*L*Lys-NH_2	44,1	24,2
H-G***T***AGA***T***CACT-*L*Lys-NH_2	41,5	Not determined

Comparatively to α and γ-PNAs, β-PNAs do not show significant improvement. Presently, there is not substantial development in this direction.[112]

I.-3.1.3 γ-PNA

The first γ-PNA was reported 1994 by Liang *et al*. and then others appeared starting from 2005.[130] General γ-PNAs are relatively well studied, like α-PNAs. A variety of γ–PNAs bearing side chains derived from amino acids have been studied. Some are illustrated with the references in Figure 78.[112] More information about the γ-PNA monomers are in the references 119-122. [130,131,132,133]

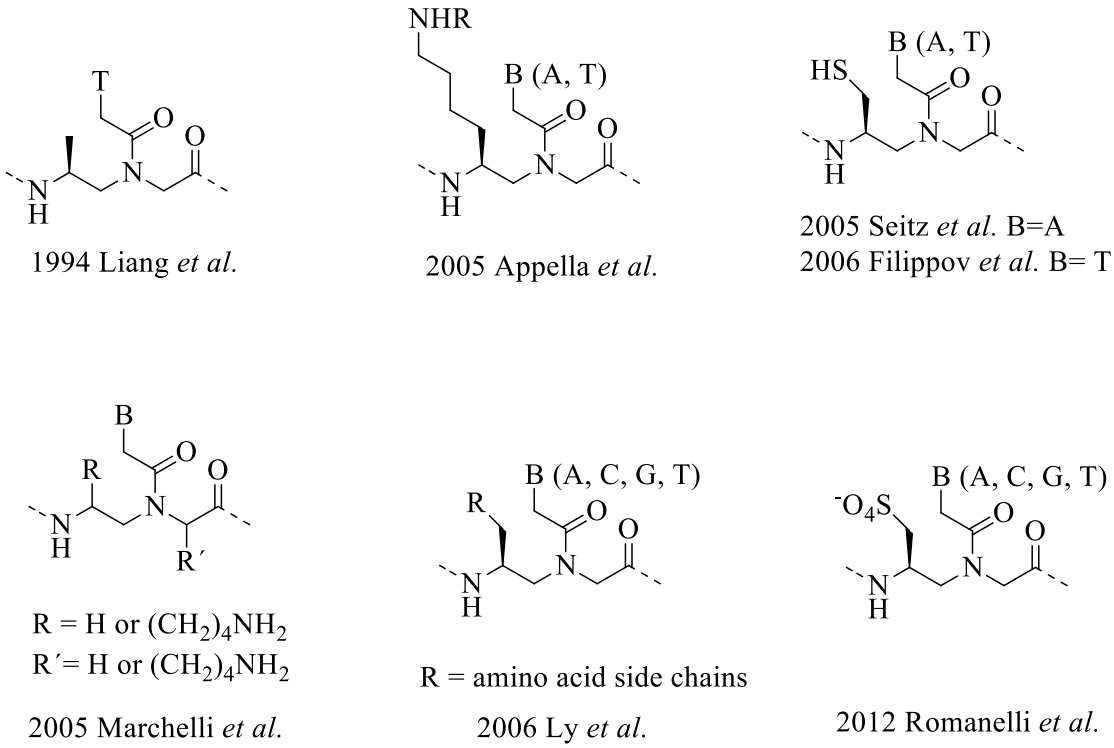

Figure 78:Structures of γ-PNAs and their references.[112]

Ly *et al.* developed a variety of γ-modified PNA structures. They demonstrated that the γ-position can accommodate various hindered L-amino acids side-chains. These have

not negative effects for the hybridization properties of PNAs. Table 12 illustrate the melting points of the duplexes of different γ-PNA sequences and complementary DNA. Marchelli *et al.* compared the thermal stability of α-Lys PNA with γ-Lys PNA. They discover that γ–PNAs react differently to steric hindrance compare to α-PNAs. Additionally, the γ-modification is also more effective, both in DNA binding affinity and sequence selectivity.[134,133] In 2011, Crawford *et al.* showed that γ-PNAs pre-organize into a right-handed or left-handed helical structure, depending of the conformation of the used amino acid. *L*-amino acids in the γ-PNA induce right-handed helices and *D*-amino acids, left-handed helices. This helical induction is sterically driven and stabilized by base-pair stacking.[135]

*Table 12:Melting point [°C] γ-PNA-DNA duplexes. PNA sequences: a) H-GCATG**T**TTGA-^{L}Lys-NH_2 b) H-GTAGA**T**CACT-^{L}Lys-NH_2 c) H-GTAGA**T**CACT-NH_2.*[135,136,134]

Backbone modification	**T_m (°C)**	**PNA sequence**
Gly	47	a
L-Ala	51	a
L-Val	51	a
L-Ile	51	a
L-Phe	51	a
Gly	44	a
L-Ser	48	a
Gly	49.7	b

L-Lys	51.4	b
D-Lys	36.4	b
Gly	50	c
L-Lys	56	c
D-Lys	32	c

In 2012, Bahal *et al.* developed the γ-MiniPEG-PNAs. They are functionalized with a diethylene glycol group and show a high therapeutic potential (Figure 79). This modification has been found to maintain pre-helical organization, to increase affinity and specificity for DNA and RNA, to eliminate nonspecific binding[137], while improving the water solubility.[138] Moreover, due to their helical structure, they display an improved cellular uptake. Also, it has been demonstrated that these γ-MiniPEG-PNAs are able to invade in cell mixed sequence double-helical B-DNA through Watson-Crick base pairing.[137]

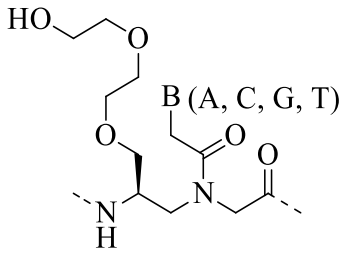

Figure 79:Structure of γ-miniPEG-PNA.[137]

In summary, α–, β– and γ-modified PNAs have an impact in the modulation of the stability and sequence-selectivity of PNA/DNA or PNA/RNA duplexes. These modifications present a simple and effective technique to functionalize the side-chain

residues, with positive charged groups for better solubility, fluorophores for detection, or linkers for surface tethering.[139,140,141,142]

I.-3.2 Conformationally constrained cyclic PNA analogues

2004 Kumar *et al.* introduced five- and six-membered rings in the PNA backbone to maintain the balance between rigidity and flexibility and to highlight interesting effects on the stability of PNA/DNA and PNA/RNA duplexes. The synthesized structures are presented in Figure 80.[143] The cyclization of the PNA backbone monomer should induce conformational preorganization leading to an increase in PNA specificity (DNA *vs* RNA and parallel *vs* antiparallel mode) and additionally the affinity, since it imparts an entropic benefit in the nucleobase recognition process.[112,143]

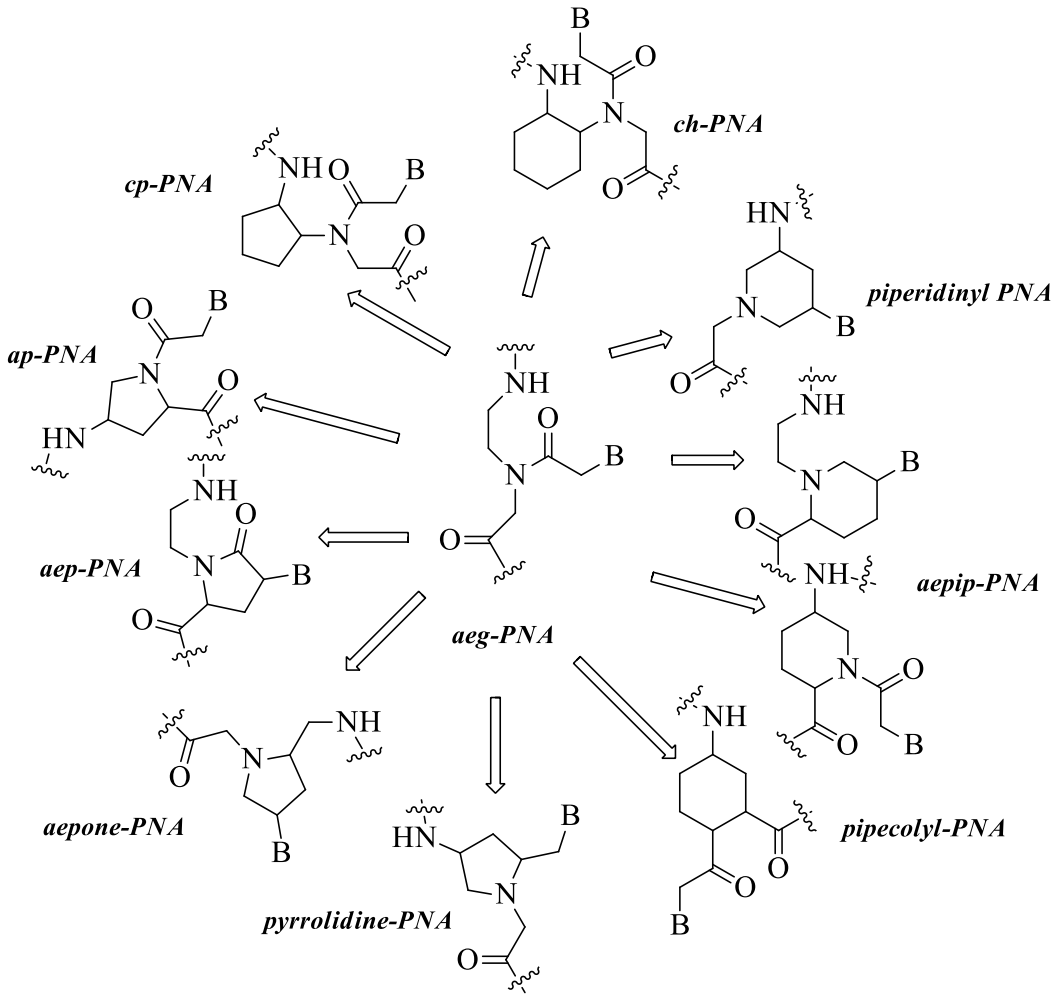

Figure 80: Cyclic PNA structures synthesized by Kumar et al..[143] *ap = aminopropyl-, aep = aminoethylpropyl, aepone = aminoethylpyrrolidinone,- aepip = pipecolic-, ch = cyclohexyl, cp = cyclopentyl-PNA.*[143]

The *ap*- and *aep*-PNA, *aepone*-PNA, pyrrolidinyl-PNA, *aepip*-PNA and piperidinyl-PNA, methylene/ethylene groups are introduced and used to bridge the aminoethylglycyl backbone and the methylene carbonyl side chain, making this structure particularly interesting as constrained structures. General, *aeg*-PNA adopt two conformations (cis and trans) that are in equilibrium and this interferes with hybridization (Figure 81). The high rotation barrier during the interconversion of the rotamers leads to different PNA and DNA/RNA hybridization kinetics in parallel and antiparallel hybrids.[144,145,146,147,148]

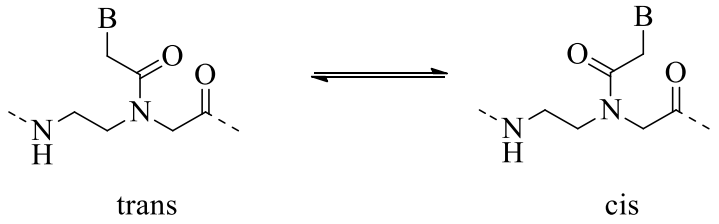

Figure 81: Cis- and trans isomer of aeg-PNA.[146]

In *ap*-, *aepone*-, pyrrolidinyl-, pipecolic- and piperidinyl-PNA, the cyclization achieves a direct attachment of the nucleobases avoiding the rotamer problem of *aeg*-PNA and introducing a chiral center. Moreover, the nucleobase being directly attached to the ring, this defines its orientation.[146] The results of hybridization studies with cyclic-PNA monomers are summarized in Table 13.[143]

Table 13: Results of hybridization studies of cyclic PNA monomers.[143]

PNA	**PNA-modifications and properties**
Propyl-PNA (ap)	No binding of homochiral oligomers, monosubstitution stabilizes PNA/DNA duplexes; stereochemistry-dependent parallel/antiparallel binding preferences
Pyrrolidinone-PNA (aepone)	Mono-, di-, tetra-, and all-modified PNAs stabilize PNA_2:DNA triplexes destabilize triplexes with poly r(A)
Pyrrolidinyl-PNA	(2R, 4S)-T in T_8 stabilize PNA and DNA duplex (2S, 4S)-T in T_8 destabilize PNA and DNA duplex

	(2S, 4S) and (2R, 4R)-T RNA duplex > DNA duplex *ap* duplex is higher binding than parallel duplex
Pipecolic-PNA	Marginal stabilization of PNA_2:DNA triplexes
Piperidinyl-PNA	Stabilization of PNA_2:DNA triplexes

To conclude, constrained cyclic PNA analogues may display interesting features for the hybridization of PNA and DNA/RNA, such as stability, parallel/antiparallel preferences and DNA/RNA hybridization selectivity. In most cases, cyclic PNA monomers show higher affinities without sacrificing their base-pairing specificities. But the mismatched complexes are more destabilized compared to *aeg*-PNA.

II. Aims of our work

One of the drawbacks of *aeg*-PNA is their binding both to complementary DNA and RNA sequences, both in parallel and antiparallel modes. This reduces the target specificity and limits their use as therapeutic agents.

As seen in Figure 82, *aeg*-PNAs give more compact complexes with RNA than with DNA. This implies that the distances between two consecutive amide-bonds in the achiral PNA backbone is shorter in the case of RNA/PNA duplexes than in the case of DNA/PNA ones.

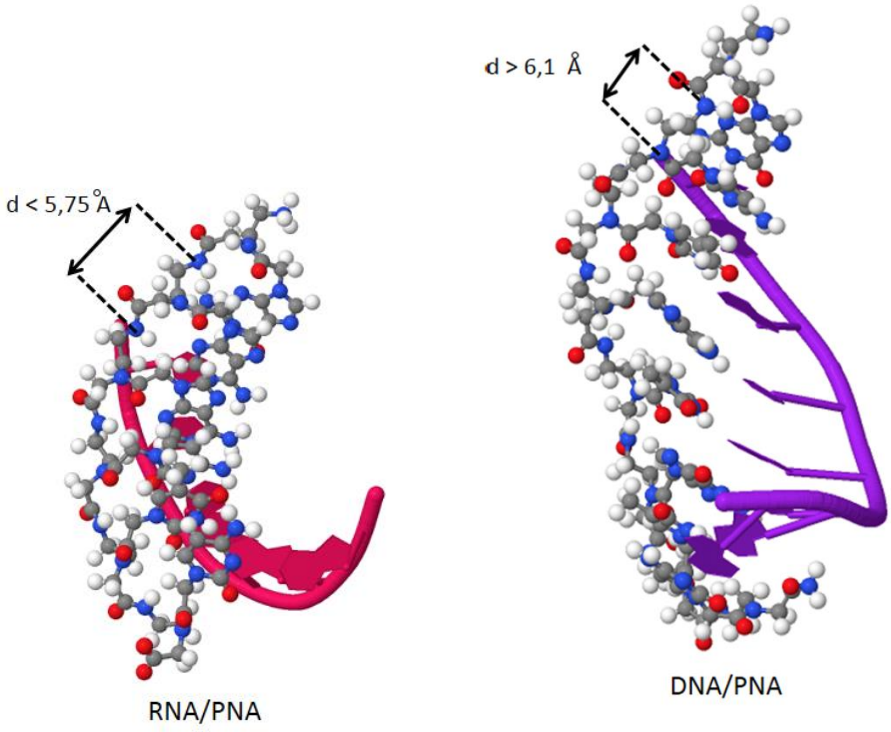

Figure 82: Distances between nitrogen atoms in the backbone in the complexes RNA/aeg-PNA (PDB:176D) and DNA/aeg-PNA(PDB:1RDT).

On the other hand, we have previously reported that the introduction of chiral *D*-amino acids into the PNA backbone induces a right-handed helical conformation. In the case of the "chiral box" *deca*-α-PNA containing three consecutive *D*-α-PNA(lys) (Chapter II.-3.1.1), a strong preference towards the anti-parallel binding mode was demonstrated. Marchelli *et al.* published in 2003 the crystal structure of the duplex

established between DNA and the "chiral box" *deca*–α-PNA. As shown in Figure 83, the three side-chains of the *D*-Lys residues are exteriorized and lie parallel to each other.[120]

Based on these data, we envisaged to rigidify and pre-organize the PNA structure by incorporating one or several "stapled" *di*-*D*-α-PNA blocks, in which the side-chains of two consecutive *D*–α-PNA monomers are linked (Figure 83). According to the length of the linker, these "stapled" *di*-α-PNA blocks should provide the opportunity to modulate the compactness of the PNA structure, favoring either DNA or RNA recognition in an exclusively antiparallel orientation.

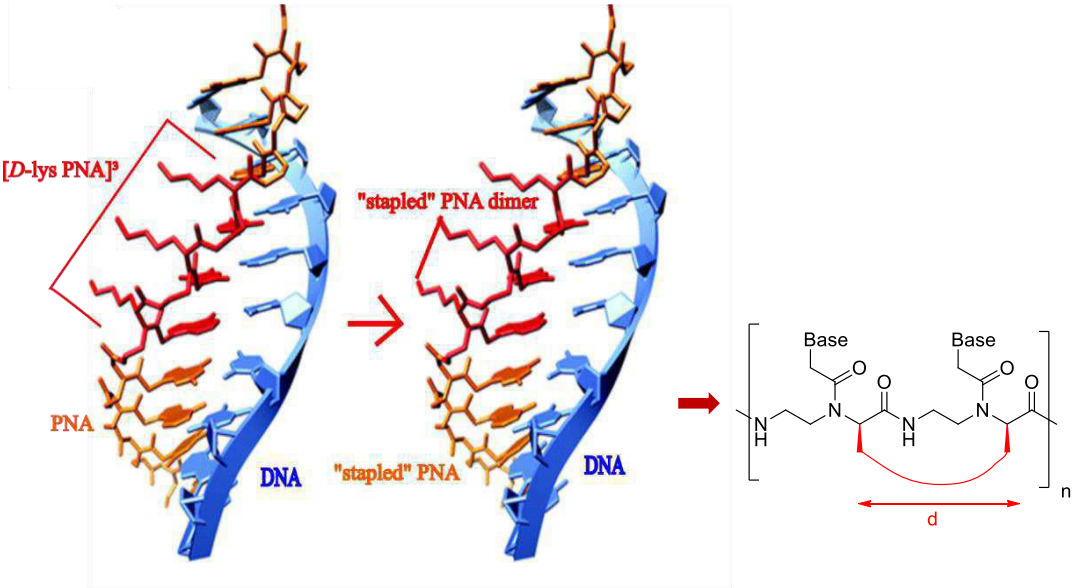

Figure 83: Illustration of stapled PNA-dimers in PNA/DNA duplex.

First, we envisaged to elaborate a general liquid-phase strategy for the synthesis of such "stapled" *di*-*D*-α-PNA blocks, then to apply it for the solid-phase synthesis of tetra-, hexa-, octa- and deca-PNAs incorporating one or several "stapled" blocks. Then, their interaction with complementary DNA and RNA sequences would be studied via

thermal denaturation studies. For comparison, "stapled" *di-L-α*-PNA blocks containing *L*-amino acid residues should be also synthesized and incorporated into poly-PNAs.

III. Liquid phase synthesis of "stapled" PNA-dimers

We first focused on two liquid-phase strategies for the synthesis of "stapled" *di-α*-PNA blocks incorporating thymine nucleobases. According to the first strategy, the stapling would be performed between consecutive lysine (or ornithine) residues, *via* a two-component cyclization step. According to the second strategy, the stapling would be performed in a one component cyclization step, *via* the intra-molecular cyclization of

two consecutive lysine (or ornithine) and glutamic (or aspartic) acid residues (Figure 84):

Strategy 1: two-component reaction

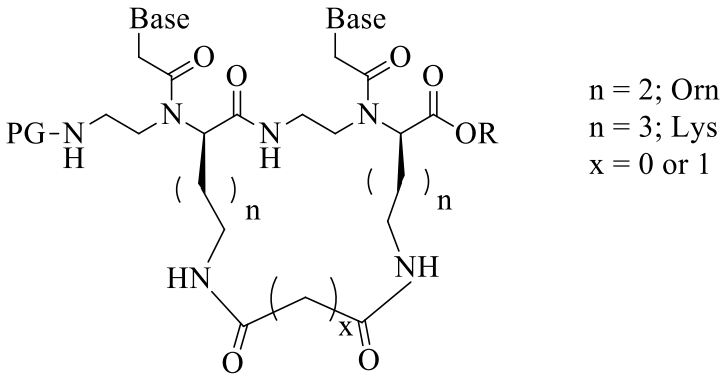

Strategy 2: one-component reaction

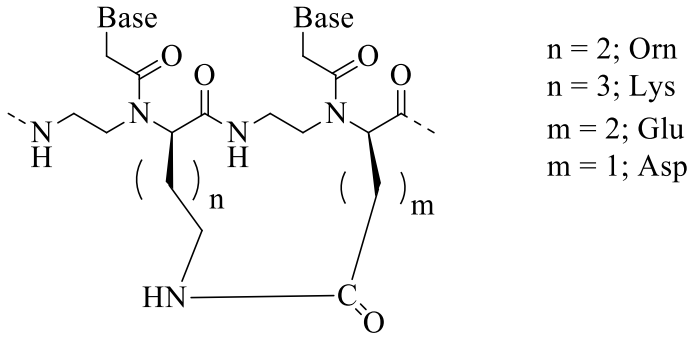

Figure 84: Structures of "stapled" di-α-PNA blocks following the two envisaged strategies.

In all cases, we decided to follow the "Fully Protected Backbone (FPB) Approach" (Figure 85). This strategy has been successfully applied previously, for the liquid- and solid-phase syntheses of linear and cyclic *aeg*-PNAs.[112,149] It consists in building a fully protected PNA backbone, bearing as many different and orthogonal protecting groups as they are different kinds of nucleobases to introduce. After selective and sequential deprotection, the simultaneous condensation of the required number of identical nucleobase acetyl moieties onto the backbone can be performed in one step. This FPB strategy avoids the synthesis of the troublesome PNA monomers and in the case of α-

PNAs, the partial epimerization occurring during the coupling between two α-PNA monomers.

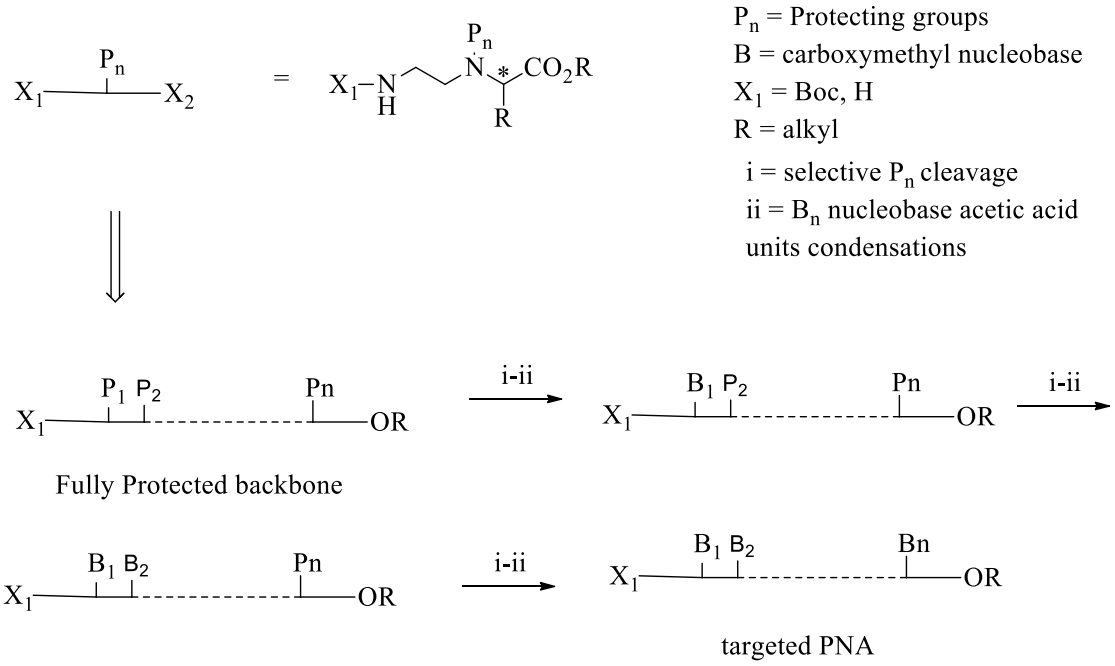

Figure 85: Principle of the liquid-phase FPB strategy.[149]

III.-1. Two-component cyclization based-strategy

We first focused on the synthesis of *di*-α-PNA(*D*-Lys)$_2$ blocks stapled, from the two-Lys side-chains. As shown in Scheme 23, we planned to prepare these compounds starting from two orthogonal protected α-PNA(*D*-Lys) backbone monomers. Coupling between these two monomers would lead to a fully protected dimer. The side-chains of the two Lys residues would be connected *via* bi-carbonyl linkers of different length, using a two-component cyclization strategy, before or after introduction of the thymine nucleobases.

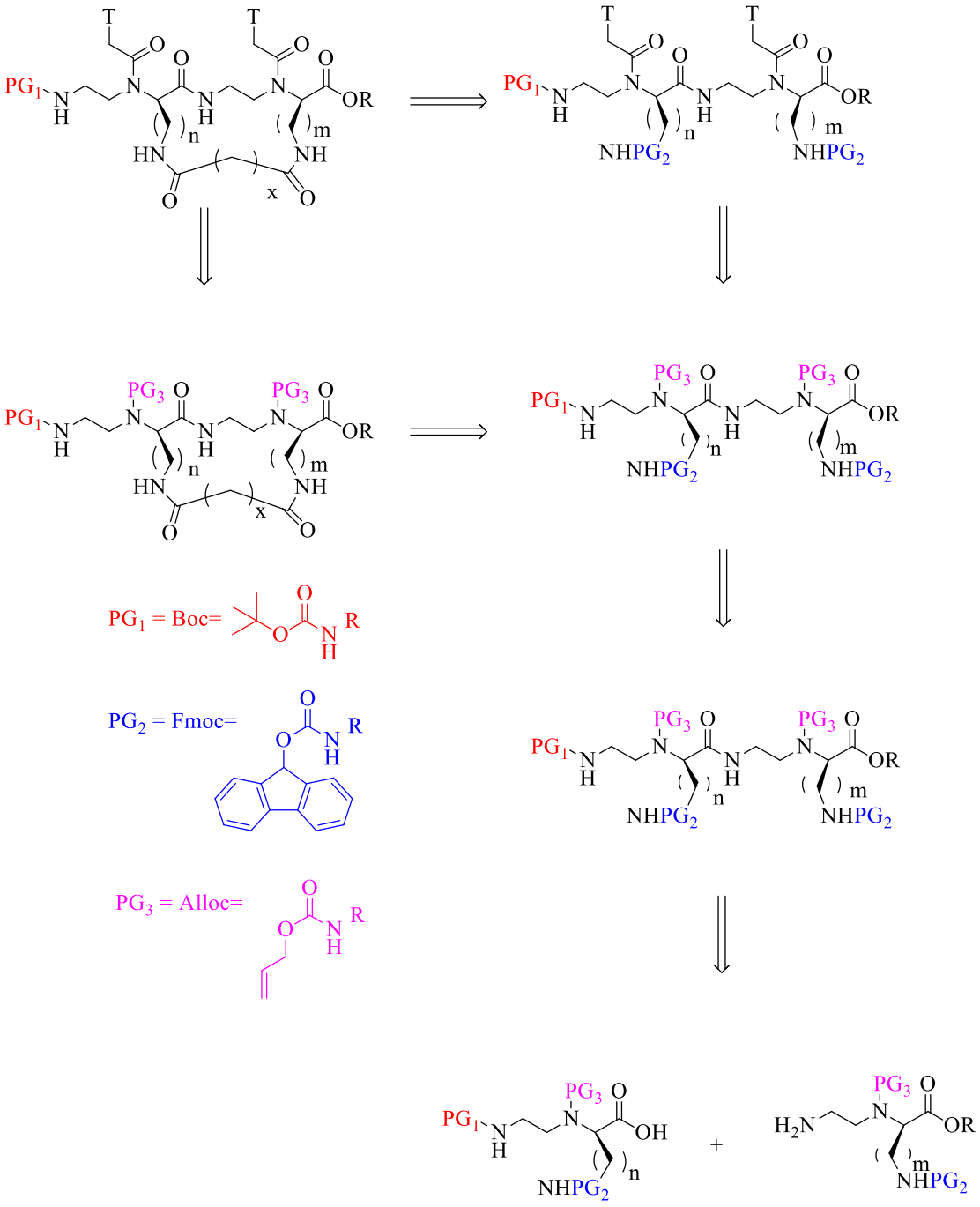

Scheme 23: Retrosynthesis of "stapled" di-α-PNA(D-Lys)₂ blocks.

We have chosen to use the acid-labile *tert*-butoxycarbonyl (Boc) group for protecting the *N*-terminal function of the PNA backbone, the base-labile fluorenylmethyloxycarbonyl group (Fmoc) for the ε-NH_2-groups of the Lys residues

and the allyloxy carbonyl (Alloc) group, removed in presence of Pd(0) catalyst, to protect the secondary amino group of the α-PNA backbone.

III.-1.1 Synthesis of protected α-PNA (*D*-Lys) backbone monomers

The two protected α-PNA(*D*-Lys) backbone monomers **31** and **32** were obtained starting from commercially available Boc-*D*-Lys residue **108**. As presented in Scheme 24, the side-chain of Boc-*D*-Lys-OH was protected in DMF using FmocOSu reagent, giving compound **26** in 95% yield. Then, esterification of **26** with MeI, in DMF, in presence of Cs_2CO_3 led to compound **27** in 95% yield. It is noteworthy that the reaction has to be carried out using only 1 eq of Cs_2CO_3, a bigger amount leading to the Fmoc cleavage and afterwards, to the addition of the dibenzofulvene (DBF) by-product on the free amino group of **27** (Figure 86).

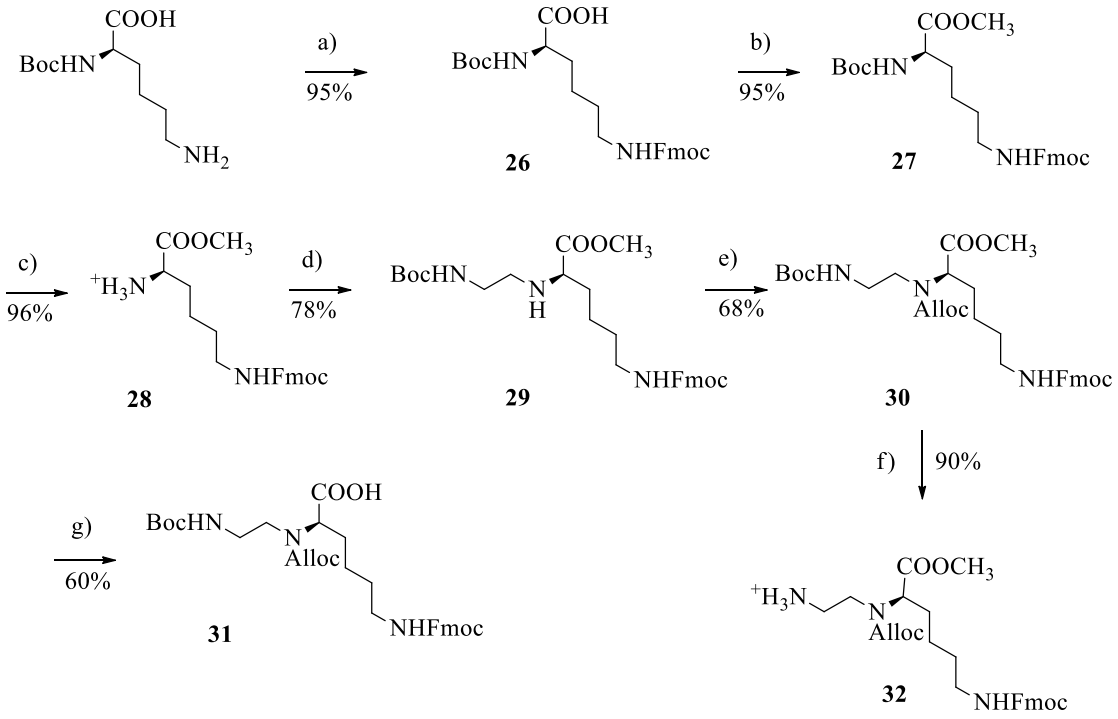

Scheme 24: Synthesis of protected α-PNA (D-Lys) monomers. a) FmocOSu, DIPEA, DMF; b) Cs_2CO_3, MeI, DMF; c) TFA/DCM d) N-Boc-aminoacetalaldehyde, $NaBH_3CN$, CH_3COOH; e) Allyl chloroformate, DIPEA, DCM; f) TFA/DCM; g) LiOH, THF/H_2O.

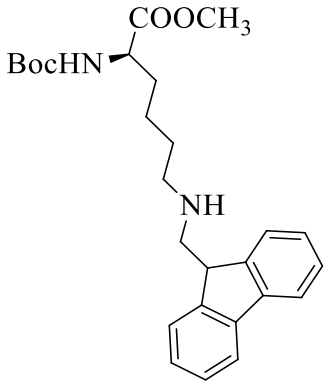

*Figure 86: By-product formed during esterification of compound **27**.*

Cleavage of the Boc group on **27** using TFA afforded the ammonium salt **28**. The next step was a reductive amination with **28,** to form the protected α-PNA(*D*-Lys) backbone. Compound **29** was obtained in 78% yield, using *N*-Boc-aminoacetalaldehyde, $NaBH_3CN$ as hydride donor, MeOH as solvent and acetic acid as catalyst. This step was followed by the Alloc protection of the free secondary amine on **29**, using allyl chloroformate and DIPEA in DCM. Compound **30**, thus obtained in 68% yield, could be either deprotected using TFA to afford the ammonium salt **32** in 90% yield or saponified with a 2M aqueous LiOH solution to obtain the acid-monomer **31** in 60% yield.

III.-1.2 Synthesis of protected di-α-PNA(*D*-Lys) backbone dimers

The two monomers **31** and **32** were coupled using HBTU as reagent, forming successfully the protected dimer **33** in 65% yield (Schema 25).

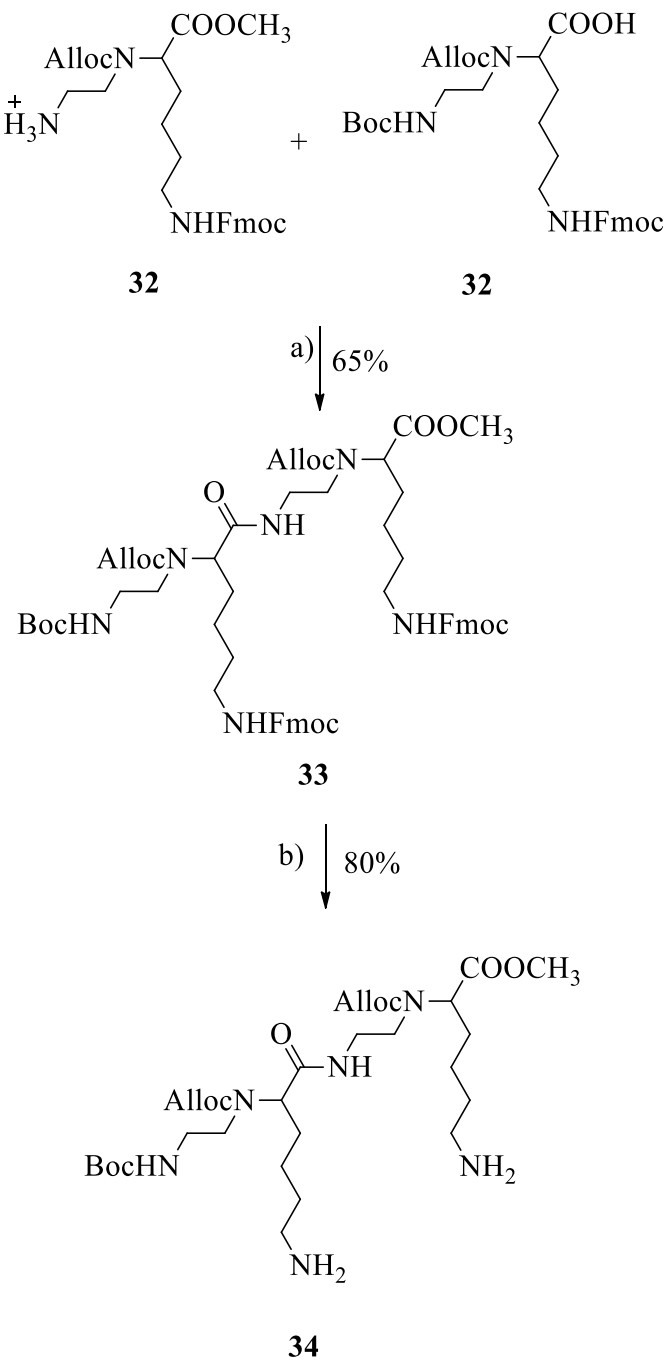

Scheme 25: Synthesis of protected di-α-PNA(D-Lys) backbone. a) HBTU, DIPEA, DMF b) DEA, DMF.

Deprotection of the Lys side-chains was first carried out using piperidine in DCM. However, even if the cleavage of the Fmoc group was effective, these conditions led to problems during the purification of the final product. Indeed, piperidine in DCM formed a salt (Scheme 26), that could not be separated from the final compound.[150,151]

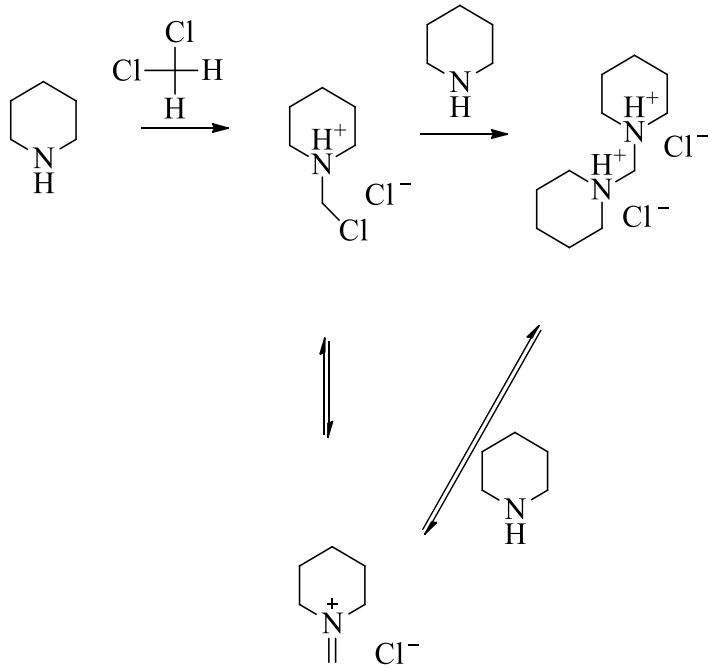

Scheme 26: Reaction between piperidine and DCM.[150]

We overcame this problem by using DEA in DMF. In these conditions, compound **34** was obtained in 80% after Flash Column Chromatography.

III.-1.3 Attempts to "stapled" protected di-α-PNA (*D*-Lys) backbone dimer

After the successful isolation of compound **34**, several attempts have been made to introduce a *di*-carbonyl linker connecting the two amino groups of Lys side-chains. Unfortunately, none of them was successful (Scheme 27).

First, we tried to condense malonic acid (1.1 eq) using HBTU and, DIPEA in DMF (Scheme 27, cond. 1). The reaction was carried out in high dilution conditions to avoid intermolecular reactions. LC-MS analysis did not show any formation of the desired product and only the condensation on one Lys side-chain was detected.

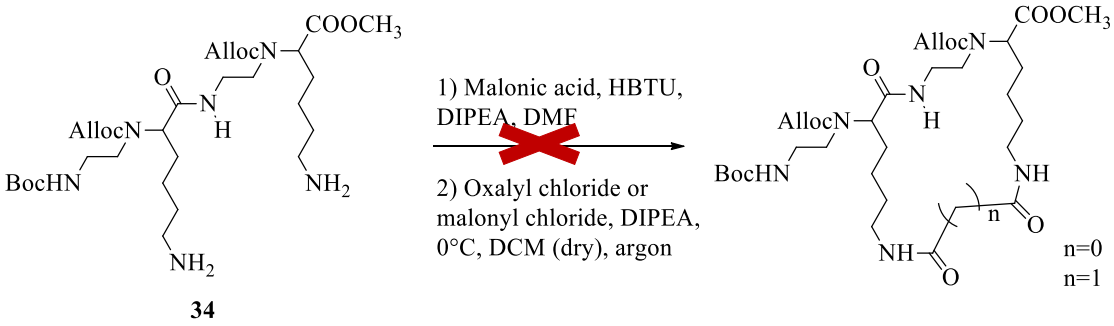

*Scheme 27: Two-component cyclization of dimer **34**.*

To increase the reactivity, the cyclization of **34** was assayed using malonyl chloride and oxalyl chloride, in presence of DIPEA in DCM under dry conditions (Scheme 27, cond. 2). Neither of the two reagents led to the expected products.

Owing to time constraints, further trials related to this two-component cyclization strategy have not been performed and we rather investigated the preparation of "stapled" *di*–*α*-PNA blocks following the second strategy, based on a one-component cyclization step.

III.-2. One-component cyclization based-strategy

The second strategy implies a one-component cyclization to form "stapled" α–PNA dimers. The easiest possibility would be the intra-molecular formation of a lactam bridge connecting the side-chains of two consecutive α-PNA residues: α-

PNA(Lys or Orn)and α-PNA(Glu or Asp). This method has been often used to stabilize α-helix peptides. The cyclization occurs at positions (*i, i+4*) of the peptide sequence, giving a helix motif in which the two residues (*i, i+4*) are about 5.4 Å apart (one helix turn). It is noteworthy that this distance is of the same order than the ones between two consecutive amide-bonds in the *aeg*-PNAs/DNA and RNA duplexes.

We first focused on the synthesis of "stapled" *di-α*-PNAs, containing *L*-lysine, *L*-ornithine and *L*-glutamic acid residues, following two "FPB" approaches (way A and B), starting from orthogonally protected α-PNA backbone monomers **35, 36** and **37**. For this purpose, two protecting group strategies "1" and "2" were developed (Scheme 28):

1) **Strategy 1:** PG_1 = Alloc and PG_2 = Allyl; PG_3 = Fmoc
2) **Strategy 2**: PG_1 = Fmoc and PG_2 = Fm (Fluorenylmethoxycarbonyl); PG_3 = Alloc

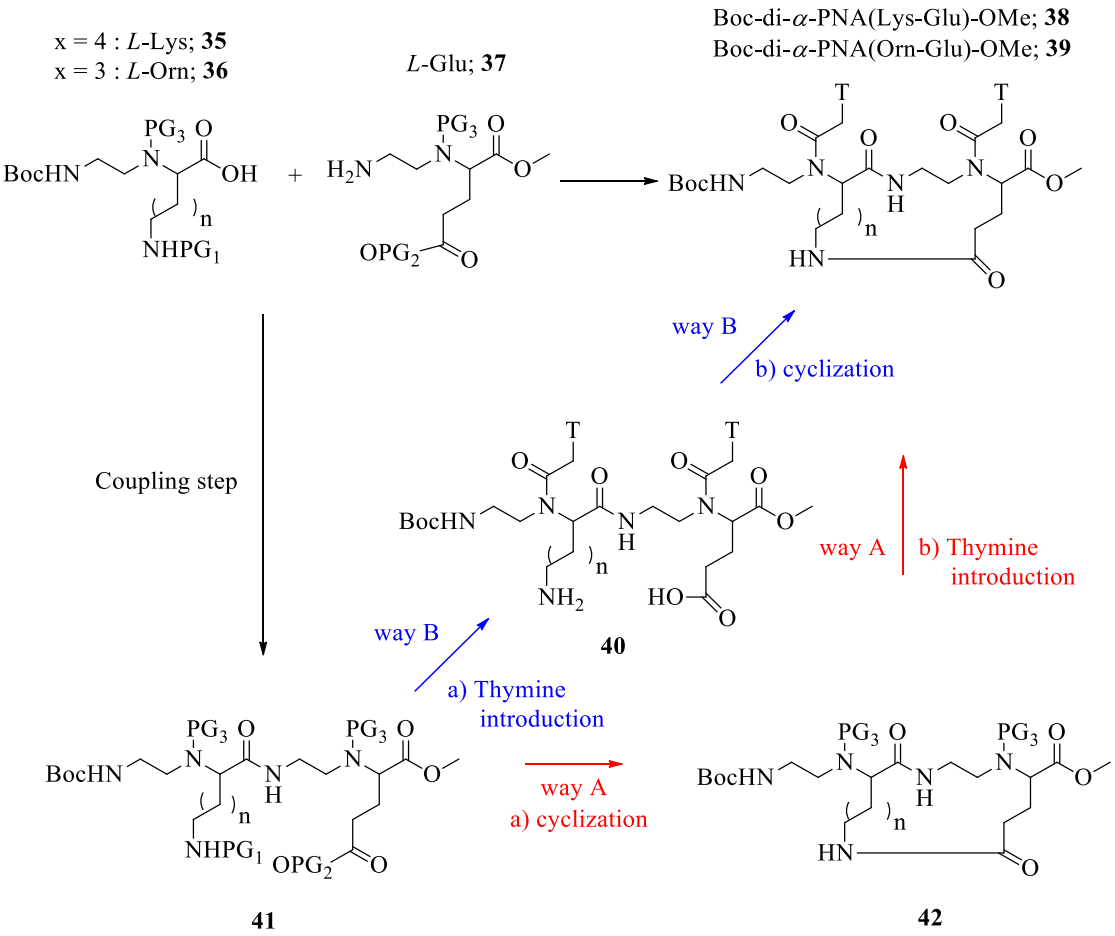

Strategy 1: PG_1= Alloc; PG_2= Allyl ; PG_3= Fmoc
Strategy 2: PG_1= Fmoc; PG_2= Fm; PG_3= Alloc

Scheme 28: Retrosynthetic scheme for the synthesis of "stapled" [di-α–PNA(Lys or Orn)-Glu] dimers. n=2: Ornithine, n=3: Lysine; PG=protecting group.

Following these two orthogonal strategies, PG_1/PG_2 will be cleaved under the same conditions while PG_3 will be removed under orthogonal conditions.

III.-2.1 Synthesis of protected α-PNA backbone monomers

Protected backbones of α-PNA(Glu) **51/52**, and α-PNA(Orn) **69/71** and α-PNA(Lys) **70/72** were synthesized, starting from the corresponding protected α-amino methyl esters **43/44**, **53/55** and **54/56** (Scheme 29).

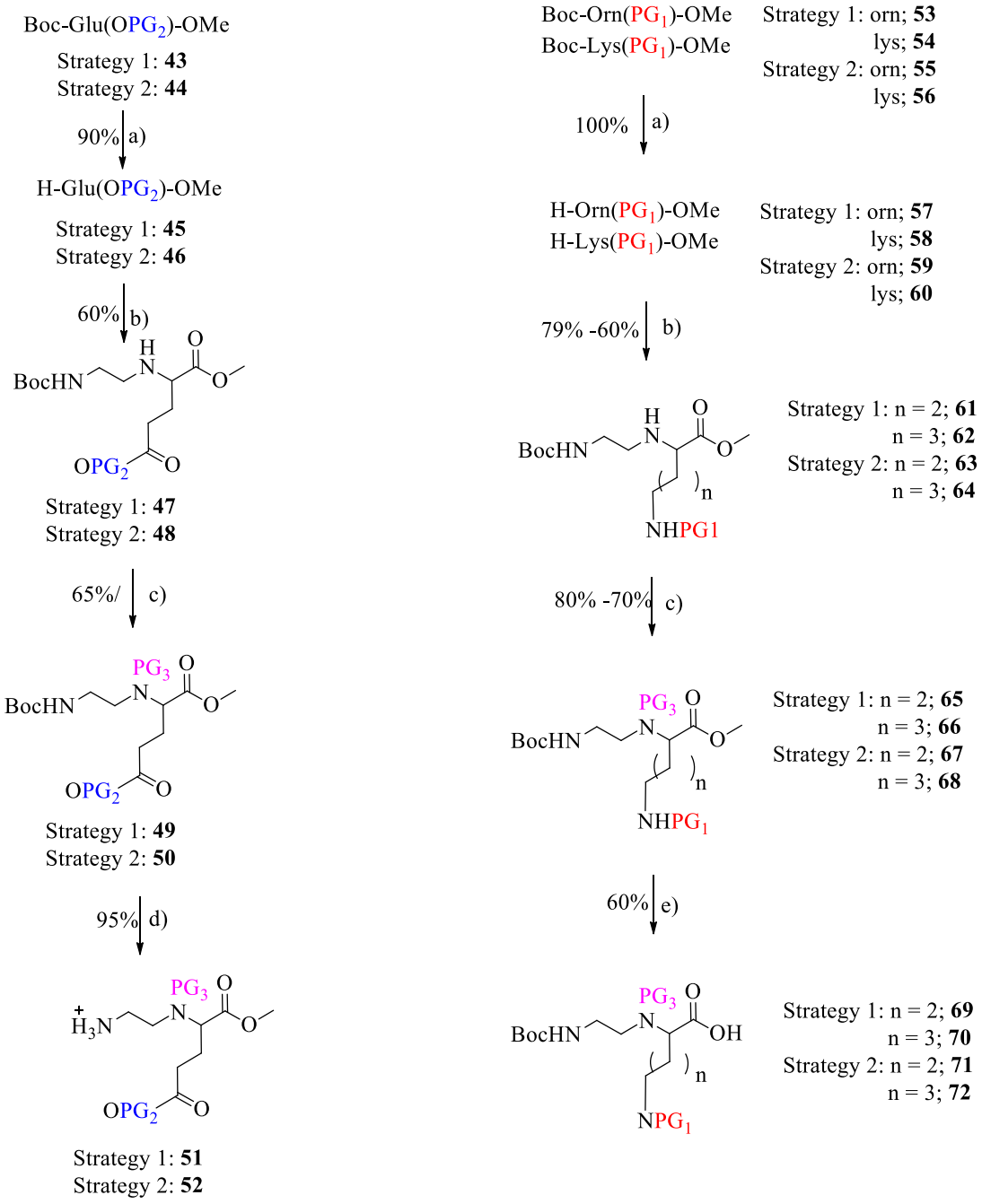

Strategy 1: PG_1 = Alloc; PG_2 = Allyl and PG_3 = Fmoc
Strategy 2: PG_1 = Fmoc; PG_2 = Fm and PG_3 = Alloc

Scheme 29: Synthesis of α-PNA monomers for the stapled di-α-PNA blocks following two orthogonal protecting group strategies a) DCM/TFA b) N-Boc-aminoacetalaldehyde, CH_3COOH, $NaBH_3CN$, MeOH c) Fmoc-Cl or Alloc-Cl, DIPEA, DCM or DMF d) TFA/DCM e) LiOH, Dioxane/H_2O.

The synthesis of these protected α-amino methyl esters are presented in Scheme 29, starting from commercial available compounds Boc-Glu(Bzl)-OH, Boc-Orn(Z)-OH and Boc-Lys-OH. Boc-Glu(Bzl)-OH was esterified with Cs_2CO_3 and MeI in DMF to give compound **73** in 81% yield. After cleavage of the benzyl ester *via* Pd-catalyzed hydrogenation, PG_2-group, Allyl or Fm, was introduced on compound **74** using respectively Allyl-Br or Fmoc-Cl/DMAP reagents, affording respectively **75** and **76** in 95% and 60% yields. Concerning Orn residues **81/82**, the Z-group of the commercially available compound Boc-Orn(Z)-OH was also cleaved by Pd-catalyzed hydrogenation. Introduction of the Alloc or Fmoc group, using their corresponding chloroformate derivative, gave respectively **79/80** in 90-95% yields. Esterification of **79/80** using MeI and Cs_2CO_3 led to compounds **81/82** in quasi-quantitative yields. The introduction of the PG_1-group on Boc-Orn(Z)-OH before esterification is mandatory, since esterification of Boc-Orn(Z)-OH leads to the cyclized product. Concerning Lys derivatives, the synthesis of the Fmoc-protected compound **86** has been already described in Chapter 8.1.1. The Alloc-protected compound **85** was obtained similarly in two steps from Boc-Lys-OH using Alloc-Cl instead of Fmoc-Cl.

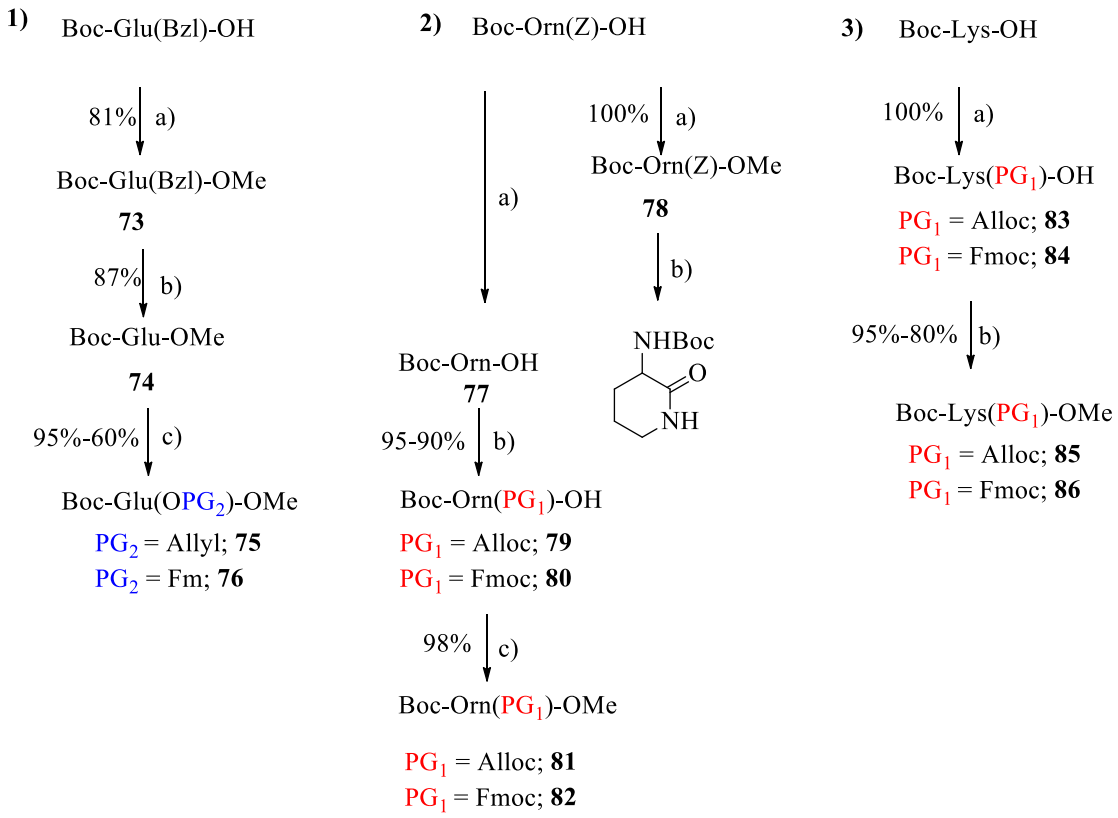

Scheme 30: Synthesis of protected L-amino acid residues.1)a) Cs_2CO_3, MeI, DMF b) Pd/C, H_2, MeOH c) Fmoc-Cl, DIPEA, DMAP, DCM(dry) at o°C or allyl bromide, Cs_2CO_3, DMF.2)a) H_2, Pd/C, MeOH b)Allyl chloroformate, DIPEA, DCM or Fmoc-Cl, DIPEA, DMF c) Cs_2CO_3, MeI, DMF. 3) a) Fmoc-Cl, DIPEA, DMF or allyl chloroformate, DIPEA, DCM b) Cs_2CO_3, MeI, DMF.

The multistep-syntheses of protected α–PNA-monomers backbones deriving from Glu (**51/52),** Orn (**69/71**) and Lys (**70/72),** following the two orthogonal strategies 1 and 2, are presented in Scheme 29. Cleavage of the Boc group on Glu (**75/76**), Orn (**81/82**) and Lys (**85/86**) residues using TFA in DCM (1/1), correspondingly afforded amino-free Glu (**45/46**), Orn (**57/59**) and Lys (**58/60**) methyl esters. Reductive amination of Boc-amino-acetaldehyde with these amino-esters led to Glu -(**47/48**), Orn- (**61/63**) and Lys- (**62/64**) α-PNA backbones in 60%-80% yields. Secondary amines were then protected either with a Fmoc or an Alloc group, using the respective chloroformate reagent. In the case of Glu derivatives, both protections occurred in lower yields (65% yields in **49/50**) than in the case of Orn and Lys derivatives (70%-80% yields in **65/67** or **66/68**). Compounds **65/67** and **66/68** were then saponified using a LiOH 2M solution,

to give respectively **69/71**, and **70/72** in about 60% yields, while the Boc protecting groups of Glu derivatives **49/50** were eliminated using TFA in DCM (1/1), affording **51/52** in 95% yield.

III.-2.2 Synthesis of "stapled" di-α-PNA[(Lys or Orn)-(Glu)] blocks

The two synthetic ways (A and B) developed according to *strategies "1" and "2*" (Scheme 28) are detailed in the following chapters.

III.-2.2.1 Synthesis of stapled PNA dimer:strategy 1-way A

This approach is described in Scheme 31. Condensation of monomers **69/70** with **51** to form the corresponding dimers **87/88** was performed (60% yield) using HBTU, DIPEA in DMF. The Alloc/allyl groups protecting the side-chains of Lys and Glu residues on **87/88** were then cleaved under neutral conditions, using tetrakis(triphenylphosphine)palladium as catalyst and phenylsilane as scavenger.[152] However, these conditions caused the partial cleavage of the Fmoc protecting group, leading to only 50% of the desired products **89/90**. No more attempts were made according this strategy since it could not be applied on solid phase.

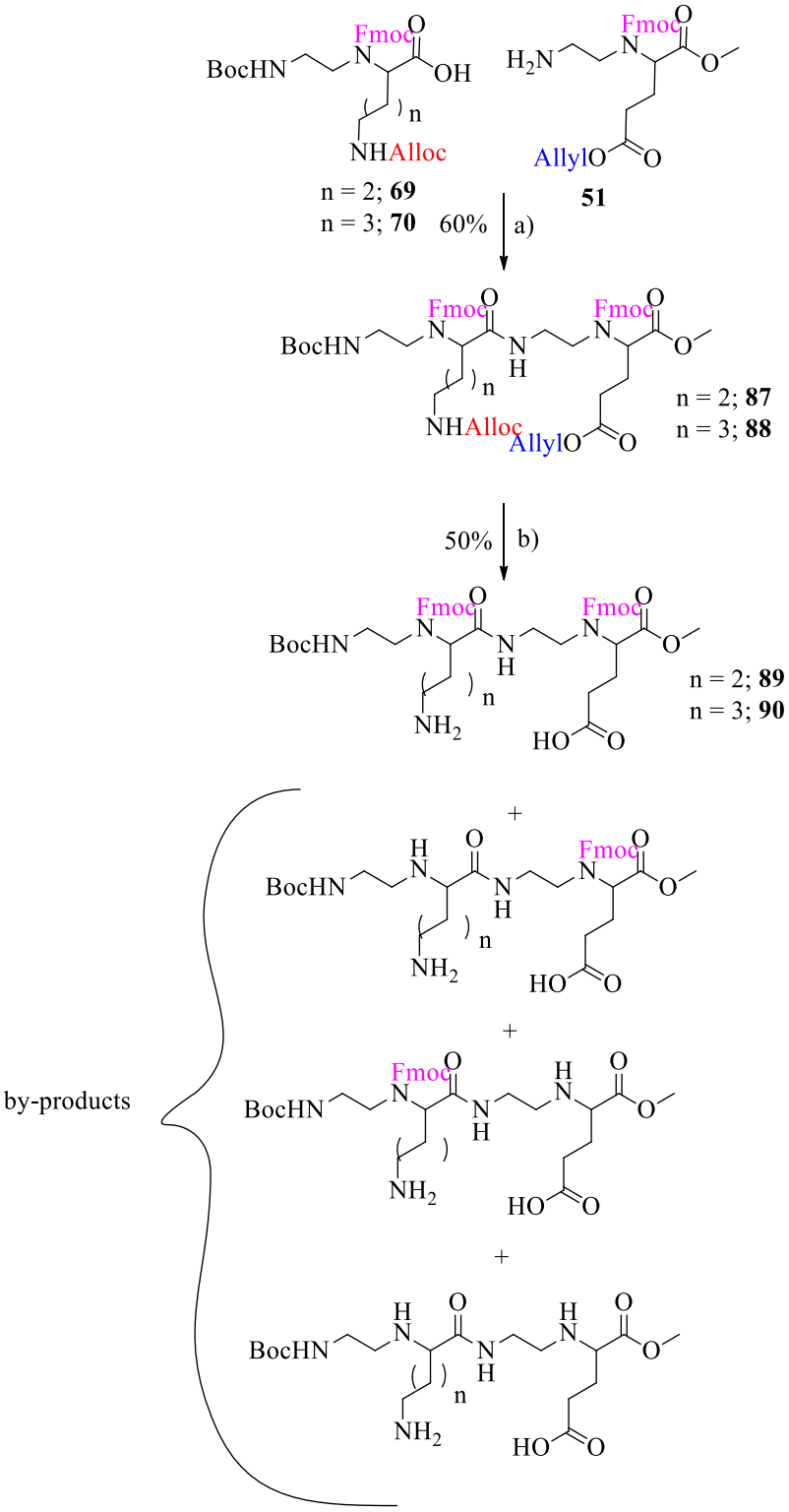

Scheme 31: Synthesis of "stapled" di-α-PNA[(Lys or Orn)-(Glu)] ***Strategy 1- Way*** *A a) HBTU, DIPEA, DMF b) $PhSiH_3$, $Pd(PPh_3)_4$, DCM c) HBTU, DIPEA, DMF d) DEA, DMF e) Thymine-1-acetic acid, HBTU, DIPEA, DMF. n=2 → Ornithine/ n=3 → Lysine*

III.-2.2.1 Synthesis of stapled PNA dimer: strategy 1-way B

We then tried to obtain "stapled" *di–α–*PNAs following way B (Scheme 32). Thus, dimers **87/88** were Fmoc-deprotected using DEA in DMF, giving the desired compounds **91/92** in 80% yields. However, cyclic by-products were also formed, by reaction of the secondary amine of the backbone with the allyl ester function of the Glu residue.

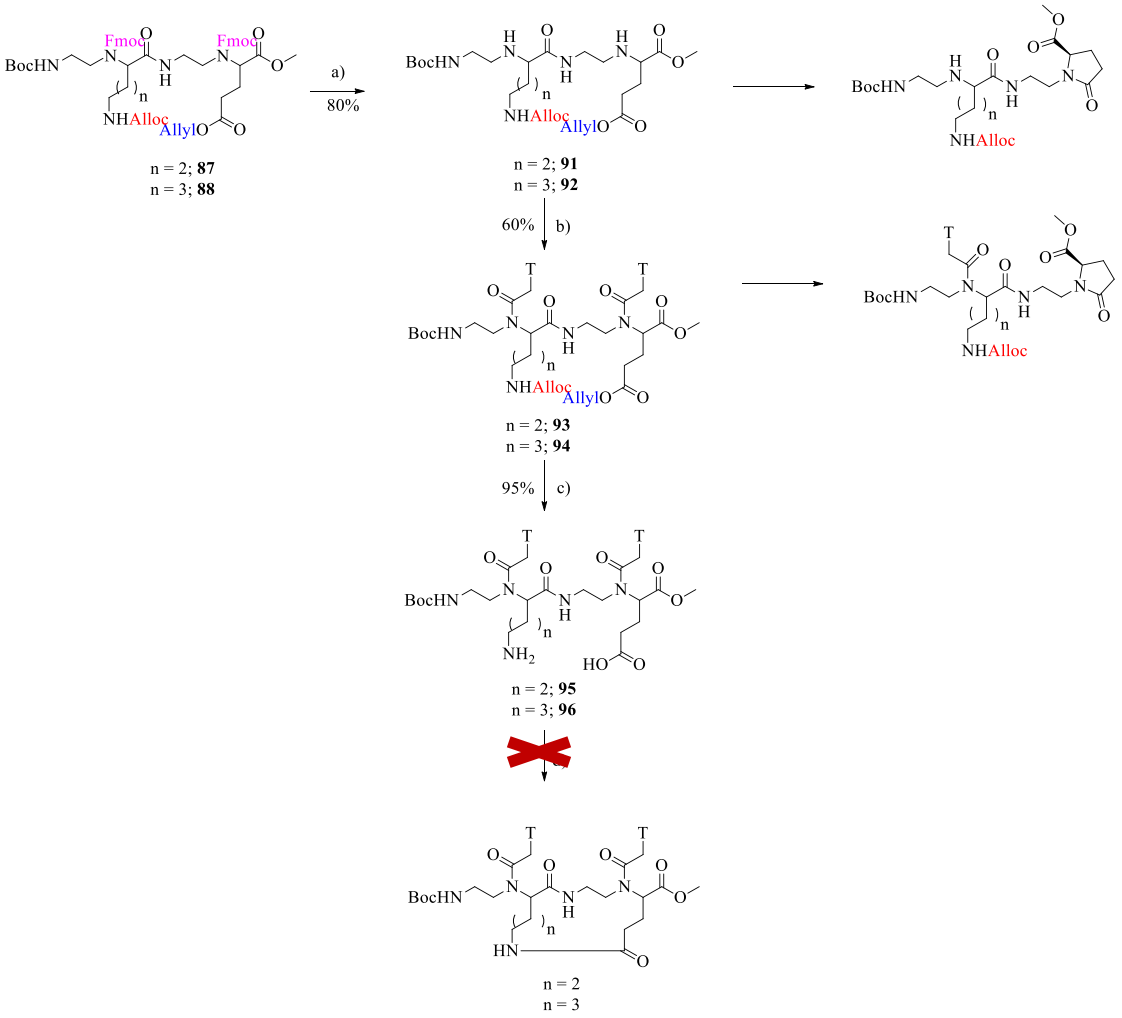

Schema 32: Synthesis of stapled PNA-dimers: strategy 1-Way B a) DEA, DMF; b) DCC, DhbtOH, thymine-1-acetic acid; c) $PhSiH_3$, $Pd(PPh_3)_4DCM$; d)HBTU, DIPEA, DMF.

The next step consisted of introducing the two thymine-1-acetic acid units on **91/92**. However, the use of HBTU as coupling reagent was unsuccessful. The coupling of the thymine-1-acetic acid was consequently analyzed. First, we tried to introduce thymine-1-acetic acid unit onto the protected α-PNA(Lys) backbone **70** (Scheme 33). The use of HBTU did not allow to obtain compound **97** and no conversion was detected. Afterwards, we applied the conditions published by Hunter *et al.,*[118] which use DCC as coupling reagent with DhbtOH as coupling additive in DMF. In this case, compound **97** could be isolated in 65% yield. The main drawback was the formation of DCU during the reaction that complicated the purification.

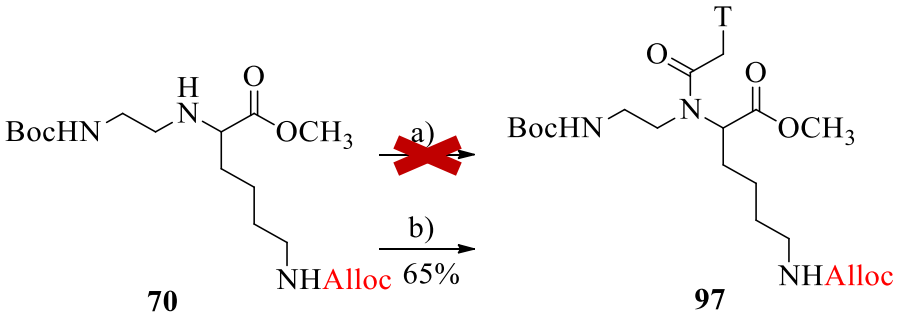

Scheme 33: Coupling of thymine-1-acetic acid on the PNA-monomer. a) HBTU, DIPEA, DMF, thymine-1-acetic-acid b) DCC, DhbtOH, thymine-1-acetic-acid, DMF.

We applied these conditions to condense two thymine-acetic acid units on **91/92**. Respective compounds **93/94** were obtained in 60% yields, together with side-products (Scheme 32) formed, as in the precedent step, by the Glu residue cyclization. This highlights the steric hindrance occurring during the coupling of the second thymine unit. Alloc/Allyl cleavage on side-chains of Lys/Orn and Glu residues of **93/94** was performed using phenylsilane and tetrakis(triphenylphosphine)palladium in DCM, affording compounds **95/96** in quantitative yields. A first assay of cyclization, using HBTU, did not give conclusive results and no more attempts following way B were done.

In conclusion, none of these strategies is applicable to a solid-phase process. The partial deprotection of Fmoc groups during the Alloc/allyl cleavage occurring *via* way A and

the unwanted cyclization of the Glu(OAll) residue occurring *via* way B make *strategy 1* unsuitable for the on-resin synthesis of stapled PNAs.

III.-2.2.1 Synthesis of stapled PNA dimer: strategy 2-way A

This approach is described in Schemes 34 and 35. Protected α-PNA-monomers **71/72** and **52** were first condensed using HBTU, DIPEA in DMF, affording compounds **98/99** in 80% yields. Cleavage of Fmoc/Fm groups with DEA in DMF led to compounds **100/101** in 80% yields after a laborious purification by Column Chromatography, due to the high polarity of these molecules. The cyclization step was carried out in classical high dilution conditions (1 mmol for 10 mL) using HBTU, DIPEA in DMF, to give compounds **102/103** in 65% yields.

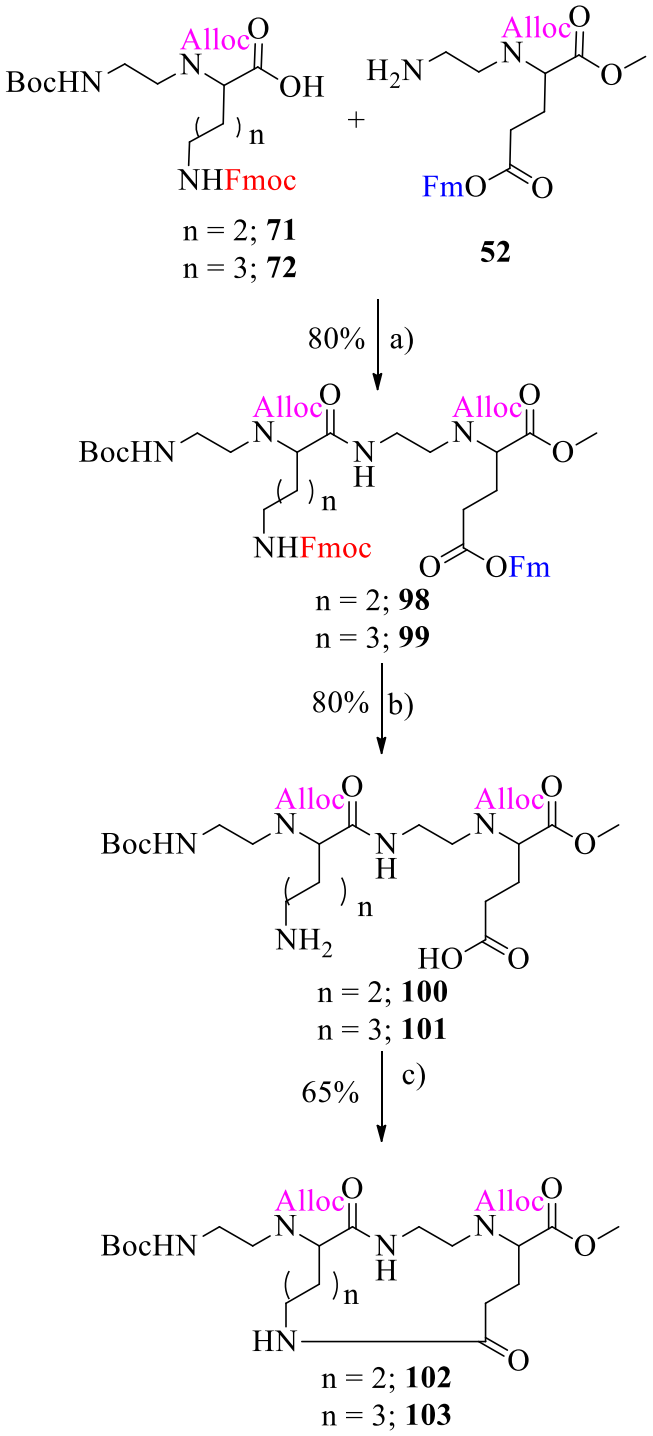

Scheme 34: Synthesis of the "stapled" PNA-dimer: way A strategy 2.a) HBTU, DIPEA, DMF; b) DEA, DMF; c) HBTU, DIPEA, DMF.

The two last steps were assayed on the Lys-based derivative **103** (Scheme 35).

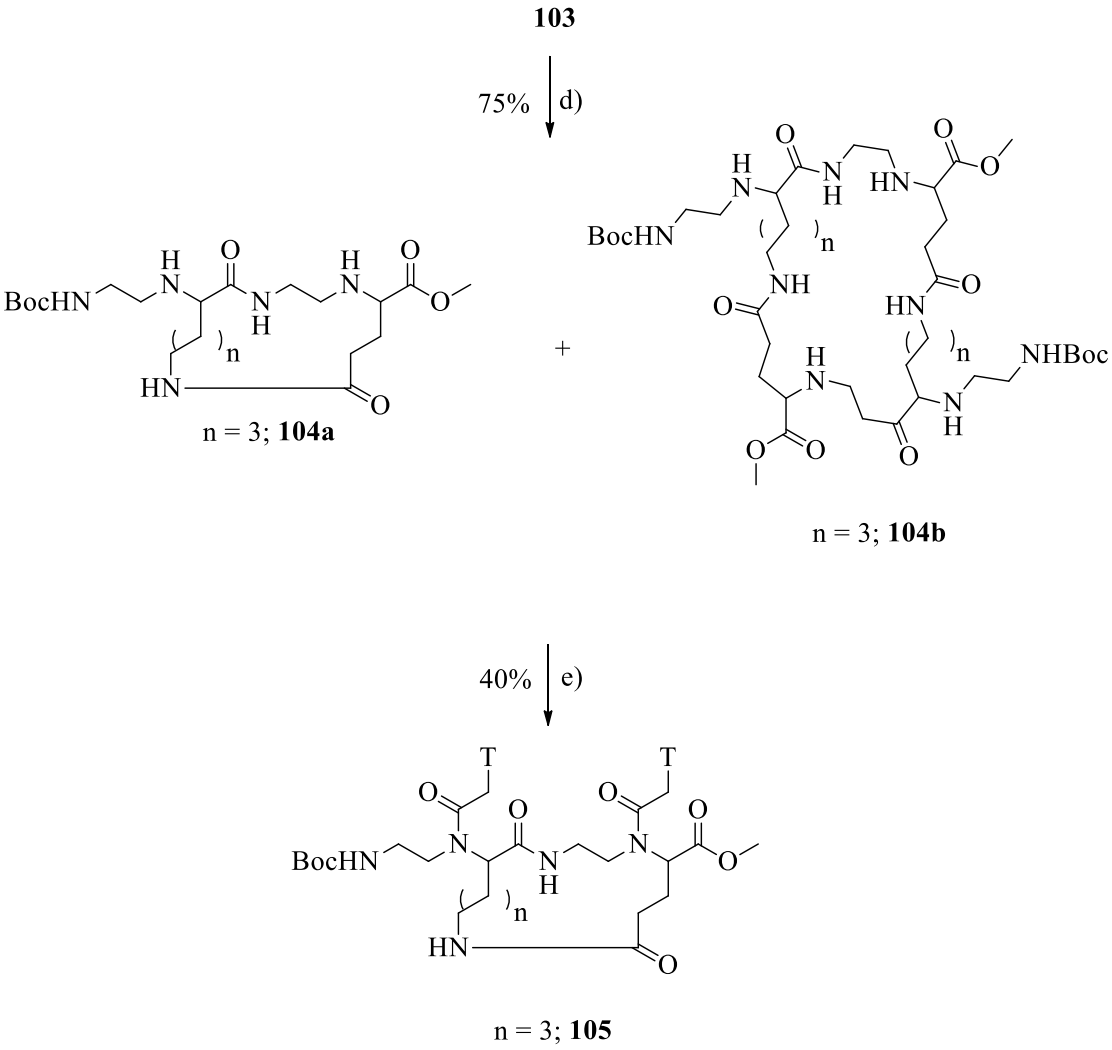

Scheme 35: Synthesis of the "stapled" PNA-dimer: strategy 2- Way A d) $PhSiH_3$, $Pd(PPh_3)_4$, DCM; d) DCC, DhbtOH, thymine-1-acetic-acid, 24h.

Alloc cleavage on **103** resulted in two different products, **104a** (50%) and **104b** (25%) that were hard to distinguish. These two compounds showed the same molecular mass by ESI-MS analyses (Mass = 457.29), but different R_f-values on TLC and different retention times on HPLC. HPLC experiments at variable temperatures demonstrated that **104a** and **104b** were not conformers. ^{1}H-NMR spectra of these two compounds were very complex (see Annex I). For one of them (**104a**), two sets of peaks could be distinguished. In this case, ^{1}H-NMR experiments at different temperatures (25 - 100°C)

were realized in DMSO-d_6 (Figure 87). A change in the amide-bond signals in the region from 8 to 6 ppm could be observed, highlighting the presence, at room temperature, of two stable rotamers. For the other (**104b**), only one series of peaks was observed. Nevertheless, 2D-NMR and ^{13}C-NMR studies demonstrated for both compounds **104a/b** very similar structures. Finally, HRMS experiments allowed us to understand that compound **104a** was the desired stapled *di-α*-PNA while compound **104b** was the corresponding tetramer (Scheme 35). The fact that contrary to tetramer **104b**, the NMR spectrum of the stapled dimer **104b** is doubled, confirms that this compound is constrained and exists preferentially under two conformations, while by contrast, the tetramer is not constrained and may exist under various conformations in fast equilibria.

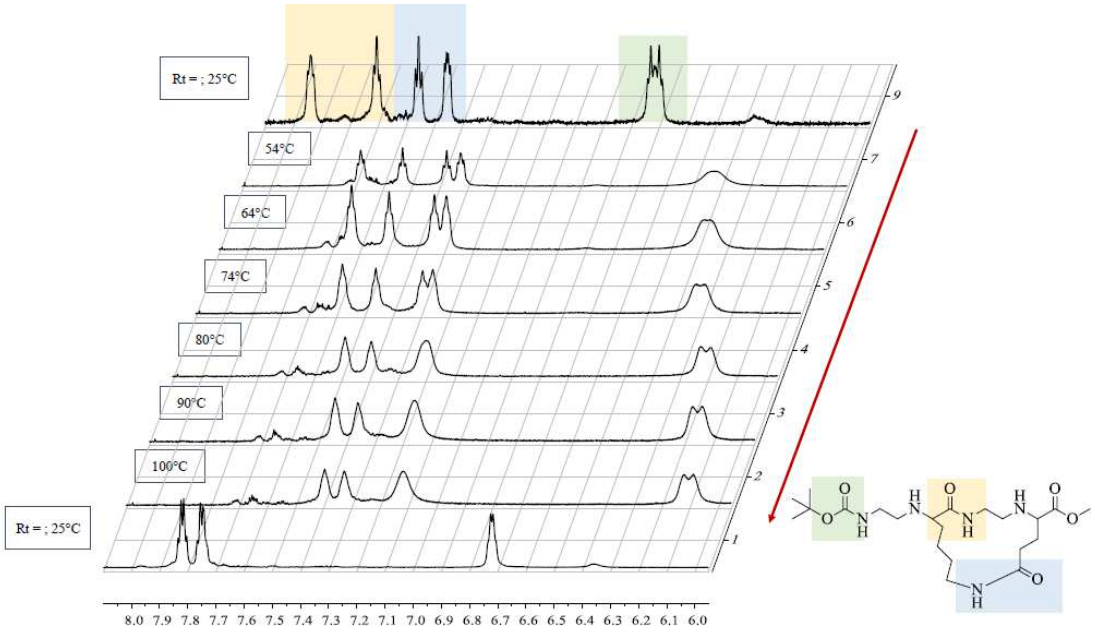

*Figure 87: Temperature dependent ^{1}H-NMR spectra of **104a** in DMSO-d_6. (region from 6 to 8 ppm is shown) and ^{1}H-NMR spectrum of compound **104b**.*

Introduction of the two thymine-1-acetic acid units was realized on compound **104a**, using DCC and DhbtOH in DMF. The polarity and solubility in water of the resulting compound **105** made its isolation highly difficult in liquid-phase. Nevertheless,

purification by semi-preparative RP-HPLC gave stapled *di-α*-PNA[(Lys)-(Glu)] in about 40% yield.

In conclusion, although not perfect, this liquid-phase strategy (strategy 2-way A) allowed us to obtain a first stapled di-α-PNA, fulfilling a part of our aims. Nevertheless, the cyclization step has to be optimized and several parameters should be analyzed, among them the concentration, the coupling reagent, the solvent and the temperature.

At this stage, we wanted to test this synthetic approach on solid-phase, since some problems occurring in liquid-phase could be avoid on-resin (*i.e*. purification of Fmoc-deprotected compounds **100/101**). Moreover, all reactions could be performed using a large excess of reagents, likely leading to higher yields. Finally, a low loading of the resin might mimic the high dilution conditions used in liquid-phase synthesis, to limit/avoid unwanted polymerization reactions.

IV. Solid-phase synthesis of the "stapled" PNA dimers

PNAs are mainly synthesized applying solid-phase strategies, following modified Merrifield methods.[153] According to first one, the first PNA monomer is coupled *via* its carboxylic acid to an insoluble and filtrable resin, and then the polymer is build up from its C-terminal to its N-terminal ends (Figure 88). The second strategy is the submonomeric-approach, starting from protected PNA backbones (Figure 89). This strategy is mostly used for α-PNAs, to avoid the epimerization of the $C^{*}\alpha$ atom of the amino acid residue, occurring during the coupling between two monomers.[149] The third one is the FPB approach, which have been previously described.

Compared to solution-phase syntheses, the synthetic procedure of solid-phase methods is simplified. In solution-phase synthesis, the product is isolated and purified after each reaction. In solid-phase synthesis, by-products are simply removed by washing the insoluble support. Furthermore, the solid-phase is based on repetitive steps (deprotection, washing, coupling, washing), allowing the use of a single reaction vessel and the automation of the PNA synthesis.[154]

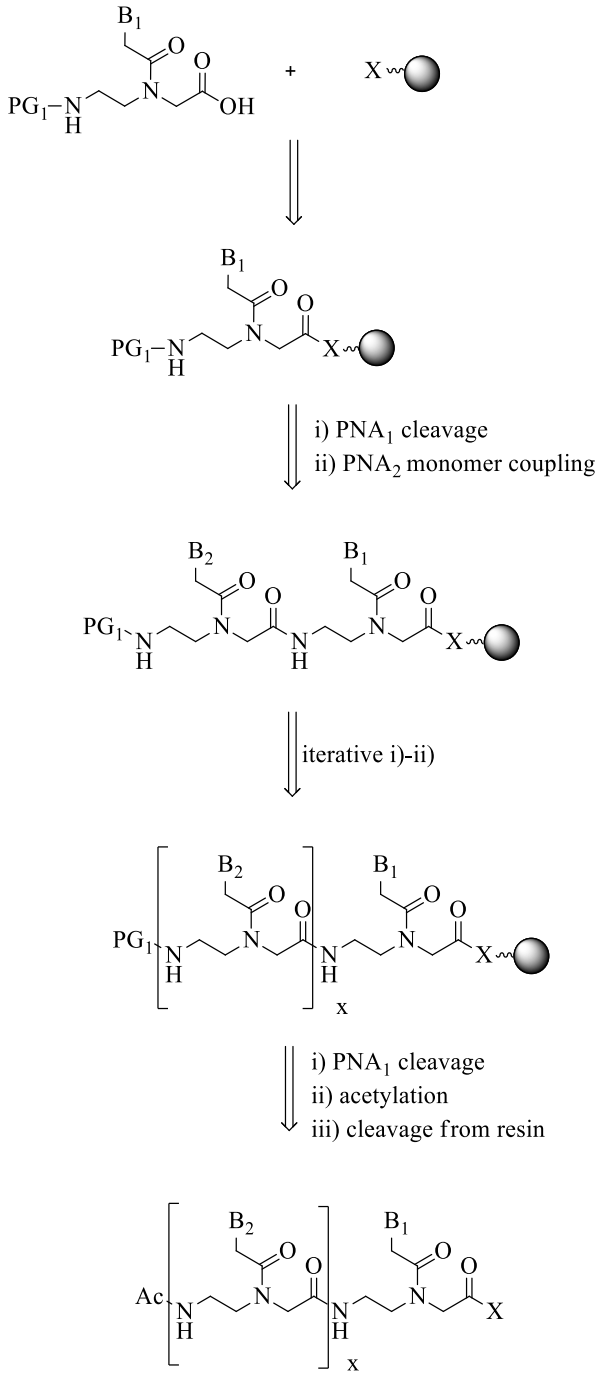

Figure 88: General approach of automated PNA solid-phase synthesis.[154]

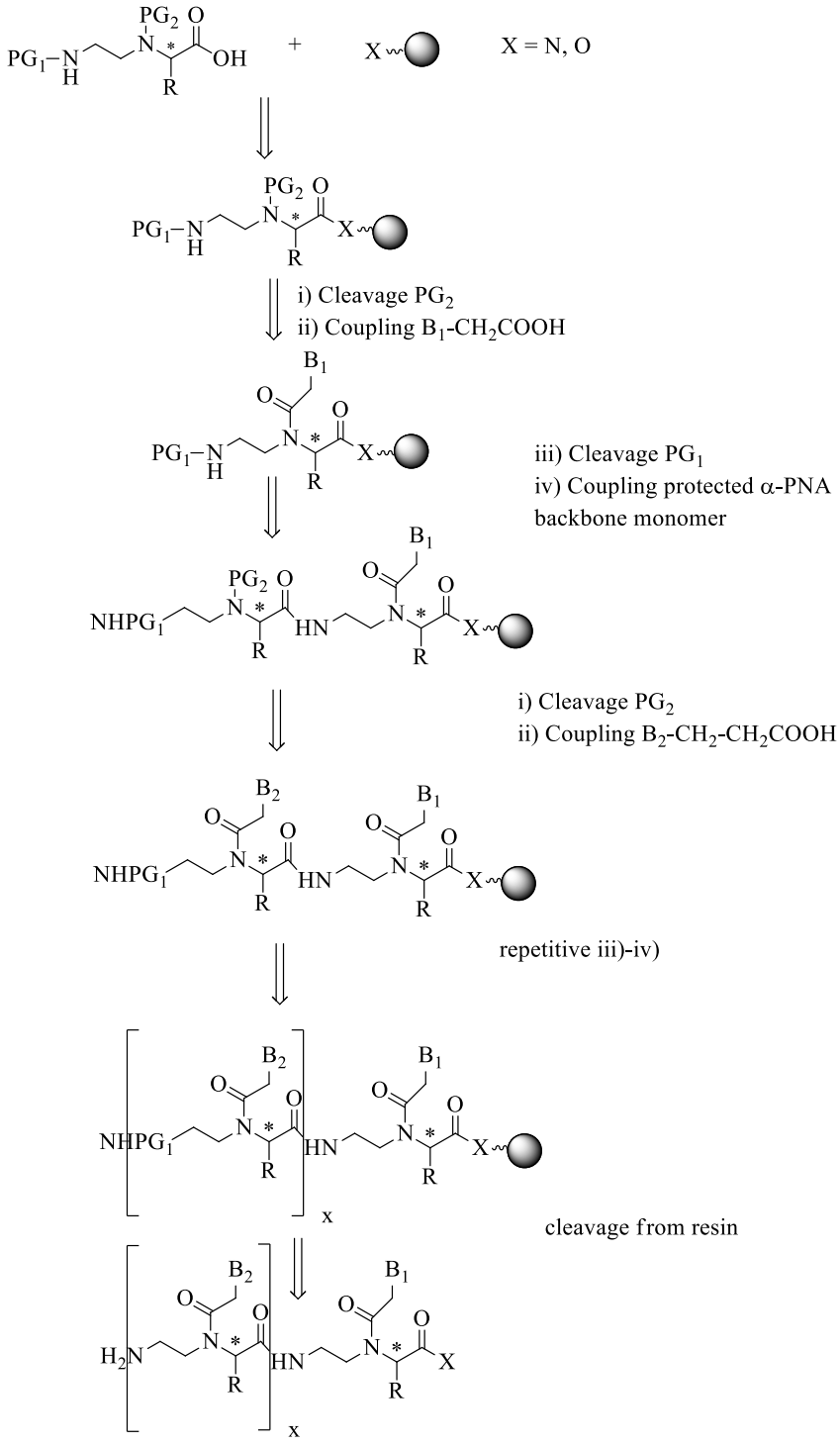

Figure 89: General approach for automated α-PNA solid-phase synthesis following the submonomeric FBP approach.

We have envisioned to synthesis in solid-phase four "stapled" *di*-α–PNA blocks, namely *di*-*α*–PNA[(*L*-Lys or *L*-Orn)-PNA(*L*-Glu)] and their enantiomers *di*-*α*–PNA[(*D*-Lys or *D*-Orn)-PNA(*D*-Glu)]. These syntheses have been performed on MBHA resin starting from six fully protected α-PNA backbone monomers, according to strategy 2, way A (Chapter 3.2.2.1).

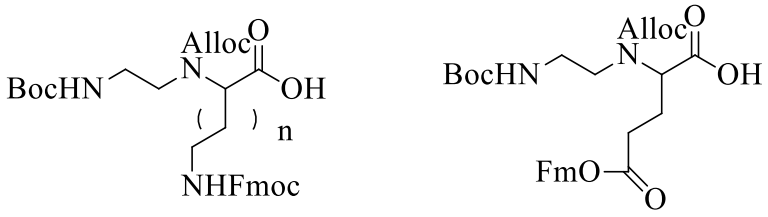

n = 2; *D/L*-Orn; **106/107**
n = 3; *D/L*-Ly**s; 108/109**

D/L-Glu; **116/121**

Figure 90: Illustration of the α-PNA monomers for the solid-phase synthesis.

The synthesis of α-PNA monomers *D/L*-Lys and *D/L*-Orn **106-109** have been previously described in Chapter 3.2.2.1. The syntheses of those deriving from *D*/L-Glu are described in the following paragraph.

IV.-1. Synthesis of protected α-PNA backbones deriving from *D*-Glu and *L*-Glu

The two enantiomers (*L*) **121** and (*D*) **116** of α-PNA backbones deriving respectively from *D*-Glu and *L*-Glu were obtained starting from different commercial synthons and their syntheses were performed according to distinct strategies. The synthesis of protected α-PNA(*D*-Glu) backbone monomer is illustrated in Scheme 36, starting from the commercially available Fmoc-*D*-Glu-OtBu residue. First, the side-chain of Fmoc-*D*-Glu-OtBu was esterified using Cs_2CO_3 and MeI in DMF (95% yield). The Fmoc group was then cleaved using DEA in DMF, giving compound **110** in 90% yield. A reductive amination of *N*-Boc-aminoacetalaldehyde with **111**, using $NaBH_3CN$ and

acetic acid in MeOH led to compound **112** in 45% yield. The free secondary amine on **112** was protected with the Alloc group (65% yield) and the resulting compound **113** was saponified using a 2M aqueous LiOH solution, affording compound **114** in 78% yield. Finally, the Fm-group could be introduced using Fmoc-Cl, DIPEA and DMAP in dry DCM under argon-atmosphere, giving **115** in 60% yield.

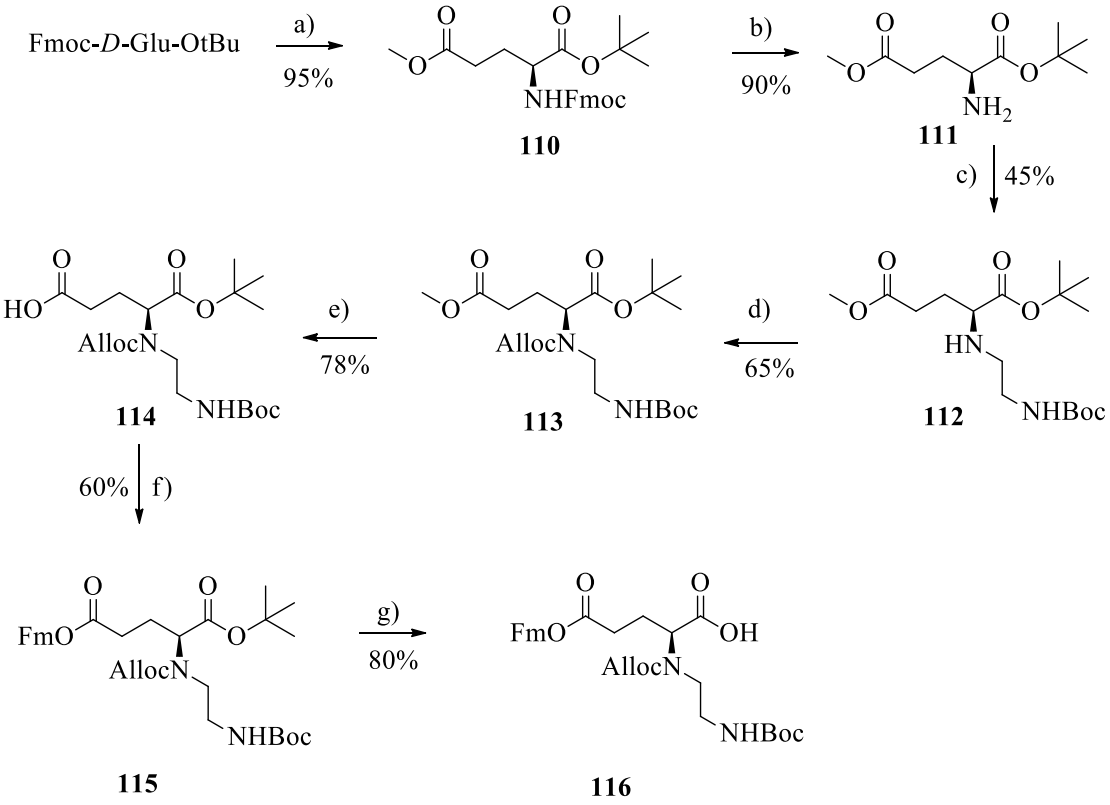

Scheme 36: Synthesis of α-PNA(D-Glu) backbone. a) Cs_2CO_3, MeI, DMF b) DEA, DMF c) N-Boc-aminoacetalaldehyde, $NaBH_3CN$, CH_3COOH, MeOH d) allyl chloroformate, DIPEA, DCM e) LiOH, THF/H_2O g) 1.) TFA/DCM 2.) Boc_2O, NEt_3, Dioxane/H_2O.

For the last step (step g) in Scheme 36, several conditions published in the literature were carried out with the goal to selectively cleave the *tert*-butyl ester group without deprotecting the terminal amino function NH-Boc on compound **115**. These are presented in Table 14.

Table 14: Conditions for selective -tBu deprotection.

Conditions
30 mol% I_2, Acetonitrile, reflux[155]
$ZnBr_2$, DCM/H_2O[156]
$CeCl_3 \cdot H_2O$, KI, Acetonitrile, reflux[157]
5 mol% $Cu(OTf)_2$-trifluoromethanesulfate, DCM[158]

In all cases, the Boc cleavage occurred in parallel. As a result, the reaction was carried out with TFA in DCM (1/1), leading to the cleavage of both protecting groups. Afterwards, the Boc group was reintroduced using Boc_2O and NEt_3 in Dioxane/H_2O to form compound **116** in 80% yield.

The synthesis of the protected α-PNA(*L*-Glu) backbone monomer **121** is illustrated in Scheme 37, starting from the commercially available H-*L*-Glu-OtBu residue**.** The first step consisted in building up the α-PNA backbone **117**, by reductive amination of *N*-Boc-aminoacetalaldehyde with H-*L*-Glu-OtBu, using the same conditions than above (46% yield). The secondary amine on **117** was protected by an Alloc group using allyl chloroformate and DIPEA in DCM. This reaction afforded product **118** in 75% yield. The Benzyl (Bzl) cleavage was then carried out in a 2M aqueous LiOH solution, affording the acid derivative **119** in 64% yield. Side-chain esterification of **119** was performed using Fmoc-Cl, DIPEA and DMAP in dry DCM, to form compound **120** in 48% yield.

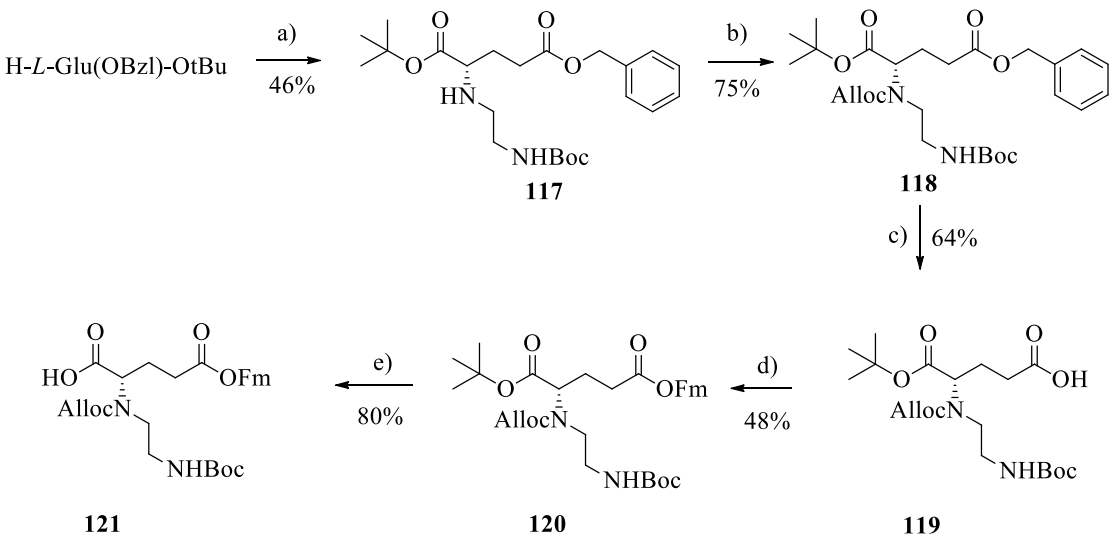

Scheme 37: Synthesis of α-PNA(L-Glu) backbone. a) N-Boc-aminoacetalaldehyde, $NaBH_3CN$, CH_3COOH, MeOH b) allyl chloroformate, DIPEA, DCM c) LiOH, THF/H_2O d) Fmoc-Cl, DIPEA, DMAP, DCM(dry) e) 1.) TFA/DCM 2.) Boc_2O, NEt_3, Dioxane/H_2O.

Finally, compound **121** was obtained in 80% yield after total cleavage of the *tBu* and Boc groups using TFA/DCM, then by re-introducing the Boc one by means of Boc_2O and NEt_3 in DMF.

In the following chapter, the description of the preparation of the four "stapled" PNA dimers on the solid-phase synthesis is presented.

IV.-2. Solid-phase synthesis of "stapled" *di-α*-PNA blocks

The solid-phase synthesis of "stapled" *di-α*-PNA blocks is illustrated in Scheme 38. In order to favorize intra- *vs* inter-molecular reactions, the loading of MBHA resin was fixed at only one-fourth of its capacity. For beginning, we focused on the synthesis of *LL* stereoisomers. Thus, the first on-resin coupling was carried out with α-PNA (*L*-Glu) backbone monomer **121**, using HBTU/DIPEA in NMP. After capping of the free amino groups of the resin using an acetic anhydride/pyridine mixture, the Boc cleavage was

performed using a TFA/DCM (1/1) solution. α-PNA *(L*-Lys) or (*L*-Orn) backbone monomer was then condensed using HBTU/DIPEA, followed by a capping step. Simultaneous cleavage of side-chains protecting groups Fmoc and Fm was performed with a (piperidine/NMP) solution. Cyclization was realized using PyBOP reagent rather than HBTU, to avoid the formation of guadinine side-product occurring with the latter (Figure 91).

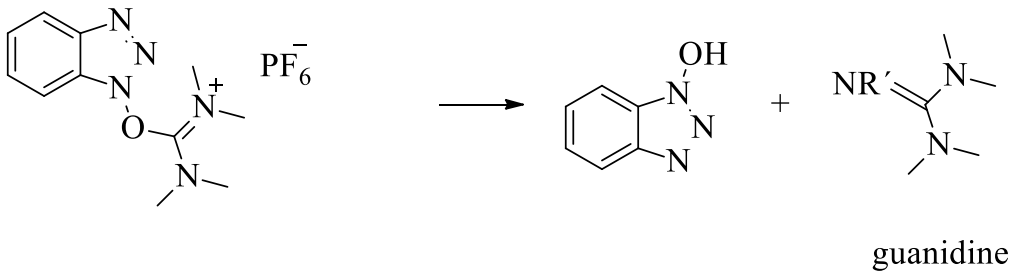

Figure 91: Guanidine by-product using HBTU.

Then, the Alloc cleavage was carried out by means of $Pd(PPh_3)_4$, DIPEA in DCM. Finally, thymine-1-acetic acid units (5 eq) were pre-actived (30 min) using DCC, DhbtOH (5.5 eq) in NMP, then added to the resin. After 24 hours, LC-MS analyses showed an uncompleted reaction. The total conversion to the desired product necessitated to repeat one time the coupling step. After TFA-mediated cleavage of the Boc group, an acetyl group was introduced using the capping solution.

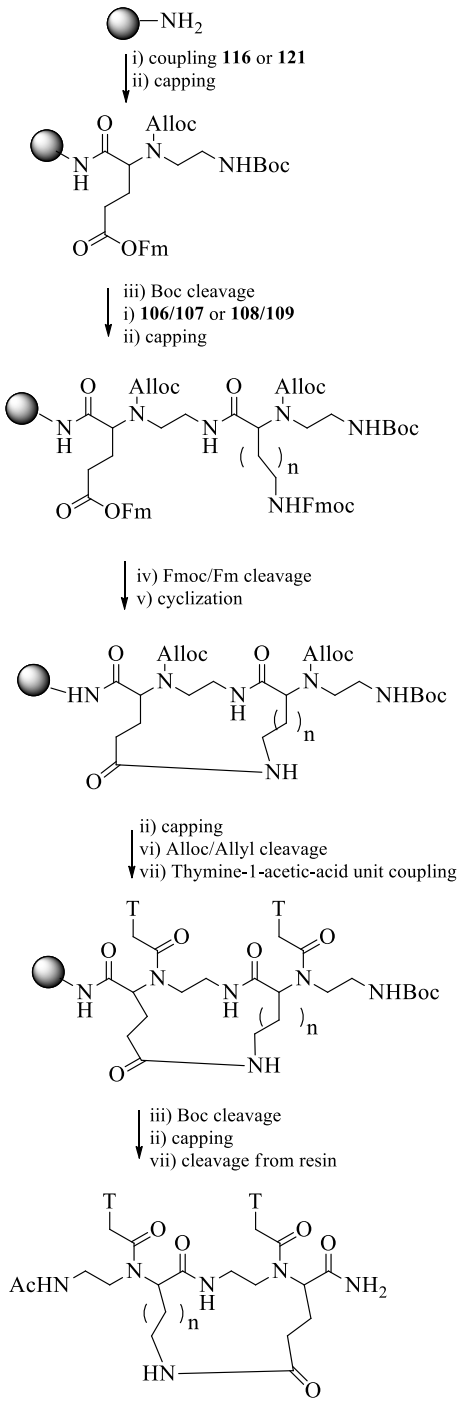

Scheme 38: General procedure for solid-phase synthesis of "stapled" α–PNA dimers. x= 1; L-/D-Ornithine/ x=2; D-/L-Lysine. i) HBTU, DIPEA, NMP; ii) Ac_2O : pyridine(3:2), NMP; iii) TFA/TIPS(9:1), DCM (1/1); iv) piperidine (20%), NMP; v) HBTU, DIPEA, NMP; vi) Phenylsilane, $Pd(PPh_3)_4$, DCM; vii) TFMSA, TFA/TIPS(3:1:1).

The "stapled" α-PNA-dimers were cleaved from the support using a TFA/TFMSA/TIPS solution, then precipitated in cold Et_2O. The precipitate was centrifugated, decantated, washed with Et_2O and analyzed by RP-HPLC.

The chromatograms of the crude products contained a lot of peaks (Figure 92) and varying the column temperature (55°C), the concentration and the flow rate induced few changes in their profiles, showing that these peaks do not represent rotamers.

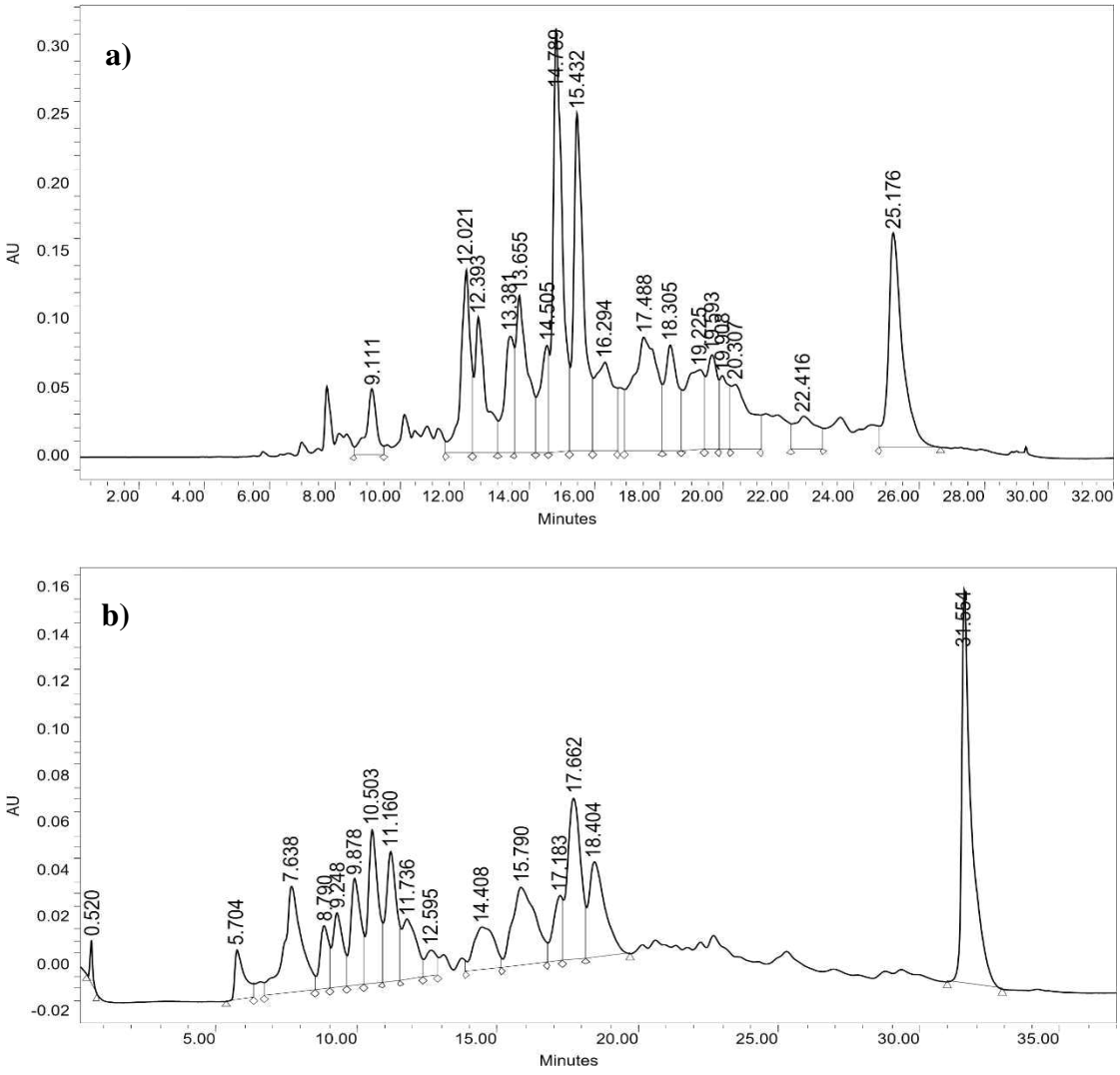

Figure 92: HPLC chromatogram (280 nm) of the "stapled" PNA dimers synthesized by solid-phase synthesis. a) di-α-PNA[(L-Lys)-PNA(L-Glu)] d) di-α-PNA[(L-Orn)-PNA(L-Glu)]. H_2O/ACN+1%TFA: 100/0 → 80/20(5 min → 15 min) → 0/100(20 min) → 100/0(24 min).

In the case of "stapled" dimer [PNA(*L*-Lys)-PNA(*L*-Glu)] the two major peaks (R_t = 14.79 and 15.43 minutes, respectively) could be isolated by RP-HPLC and analyzed by LC-MS and NMR spectroscopy. These analyses demonstrated that the less polar compound was the expected compound while the other was the tetramer [PNA(*L*-Lys)-PNA(*L*-Glu)]$_2$. Because of the complexity of the chromatogram in the case of Ornithine-based α-PNA dimer, no purification by RP-HPLC was realized and no further analyses were attempts.

Since the steric hindrance caused by the proximity of the resin could have an influence on the solid-phase process, we decided to introduce a β-alanine linker on the support before building "stapled" di-α-PNA blocks. Di-α-PNA[(*D/L*-Lys)-(*D/L*-Glu)] and di-α-PNA[(*D/L*-Orn)-(*D/L*-Glu)] were elongated as previously described. After cleavage from the support, the four crude mixtures were analyzed by HPLC. The HPLC (Figure 93).

a) di-α-PNA[(*L*-Orn)-(*L*-Glu)-β-Ala-NH$_2$ **b) di-α-PNA[(*D*-Orn)-(*D*-Glu)-β-Ala-NH$_2$**

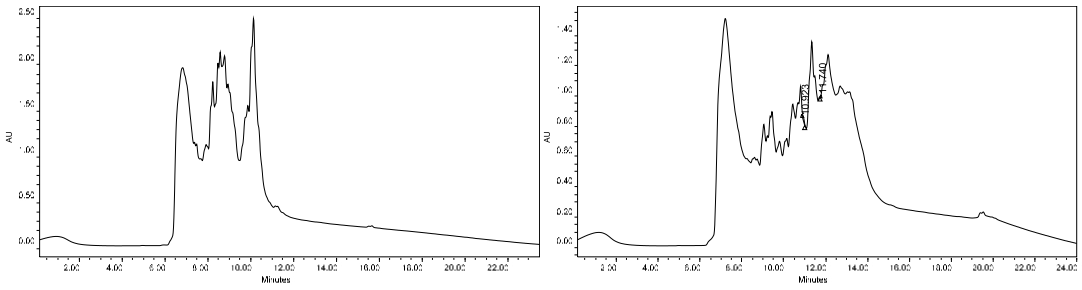

c) di-α-PNA[(*L*-Lys)-(*L*-Glu)-β-Ala-NH$_2$ **d) di-α-PNA[(*D*-Lys)-(*D*-Glu)-β-Ala-NH$_2$**

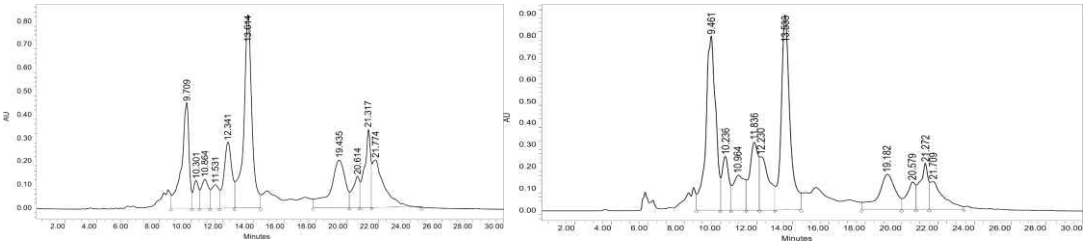

Figure 93: HPLC-chromatograms (280 nm) of the four "stapled" PNA dimers with β-alanine linker. a) and b) H$_2$O/ACN+1%TFA: 100/0 → 50/50 (15 min) → 0/100 (20 min) → 100/0 (24 min). c) and d) H2O/ACN+1%TFA: 100/0 →50/50(20 min) →0/100(22 min) →100/0(30 min).

The presence of the β-Ala linker did not really simplify the HPLC profiles of the crude mixtures. However, as previously (Figure 92), HPLC profiles in the case of stapled *di*-α-PNA[(Lys)-(Glu)] were better resolved than for Orn-based compounds. Moreover, both enantiomers of stapled *di*-α-PNA[(Lys)-(Glu)] displayed very similar HPLC profiles, by contrast with stapled *di*-α-PNA[(Orn)-(Glu)]. The two major products of *DD* and *LL* stapled *di*-α-PNA[(Lys)-(Glu)] were isolated by preparative HPLC and identified by HRMS and NMR experiments. The more polar compounds were shown to be tetramers, while the less polar were the expected dimers.

Because of the complexity of the chromatograms, the crude mixtures corresponding to *LL* and *DD* "stapled" *di*-α-PNA[(Orn)-(Glu)] were not further analyzed.

IV.-3. Conclusion and Outlook

It can be concluded from all these solid-phase experiments that the synthetic strategy that we applied for the "stapled" *di*-α-PNA blocks is not optimal and does not allow the building up of longer stapled PNAs. The major problem is the polymerization occurring during the cyclization step, even when the resin loading is low. In the case of Lys-based compounds, dimers and tetramers are nevertheless the major compounds formed, which is not observed in the case of Orn-based compounds. The Orn side-chain being shorter than the Lys one, it may well be that the cyclization of Orn-based *di*-α-PNAs is disfavored since it would lead to highly constrained molecules. In this context, it would be interesting to study the behavior of linear *di*-α-PNAs containing longer side-chains, since it is possible that from a thermodynamic point of view, dimeric species would be privileged.

To avoid the problem of polymerization occurring during the on-resin cyclization step, the solution would be to use protected "stapled" *di*-*a*-PNA blocks (Figure 94), which can be prepared and purified in liquid-phase in large quantities. These blocks should be

introduced at any position of α-PNA sequence then, after elongation, the nucleic bases could be introduced.

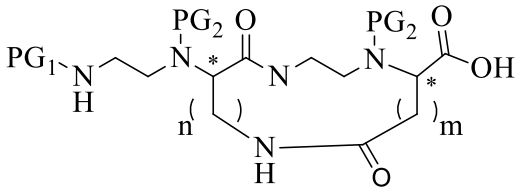

Figure 94: Protected "stapled" di-α-PNA blocks for the solid-phase syntheses of PNA.

General Conclusion

Protein-Protein, Protein-Nucleic Acid (NA) and NA-NA interactions play crucial roles in numerous biological processes, constituting relevant targets in various diseases. Foldamers are sequence-specific oligomers mimicking peptides, proteins and oligonucleotides that fold into well-defined three-dimensional structures. They have emerged as important tools for the modulation of these interactions and the search for new pre-organized structures mimicking the active conformations of proteins or nucleic acids is now an area in full expansion, since advances in the field have demonstrated their potential for the discovery of next generation therapeutics.

The purpose of this thesis concerned the elaboration of two different kinds of constrained foldameric structures, based either on unnatural constrained α-amino acid derivatives or on constrained Peptide Nucleic acid (PNA) analogs, for studying their propensity to adopt pre-organized conformations, to define them and, in the case of PNA analogs, to study their DNA *vs* RNA specificity.

The first part focused on the development of new constrained peptide mimics, starting from unnatural cyclic α-amino-acid residues, namely "6-substituted 4-oxopipecolic acid" residues:

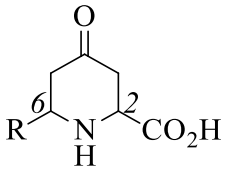

Our goal was to evaluate them as building blocks in peptide synthesis, then to construct homogeneous and heterogeneous structures by solid-phase synthesis. *N*-Alloc 4-oxopipecolic acid and 4-oxopipecolic acid methyl ester residues containing a phenyl and a phenylpropyl groups in position 6 were synthesized. Their couplings between them and with α/β-aminoacids were attempted. No dipeptide formation occurred in the former case. In the latter case, the condensation of the carboxyl-function of the *N*-Alloc

cyclic monomer with α- or β-amino acids was easily performed, whereas attempts to couple *N*-protected α- or β-amino acids with 6-substitued 4-oxopipecolic acid methyl esters failed. This demonstrates that the secondary amino function of the cyclic monomer is highly hindered, due to the proximity of the two substituents at positions 2 and 6. In conclusion, this "6-substituted 4-oxopipecolic acid" residue cannot be used as building blocks for the classical peptide synthesis of homogeneous and heterogeneous structures. In the other hand, in parallel of these works, a new synthetic way has been developed to form *N*-protected 6-substituted 4-oxo-pipecolic acid residues, following an imino-Diels-Alder reaction. Unfortunately, this reaction leads to a racemic mixture, which is unsuitable in view of peptide synthesis. Nevertheless, this work opens new research perspectives that will be developed in the future.

Our second goal was to develop constrained Peptide Nucleic Acids (PNA) analogs. PNA are nucleic acid mimics displaying remarkable properties in the context of antisense technologies and therapies. One of the major drawbacks of PNA is their binding both to complementary DNA and RNA sequences, both in parallel and antiparallel modes. This reduces their target specificity and limits their use as therapeutic agents. In view of increasing the PNA target specificity, we envisaged to rigidify and pre-organize the PNA structure by incorporating, in a given PNA sequence, one or several "stapled" *di*-α-PNA blocks, in which the side-chains of two consecutive α-PNA monomers are linked:

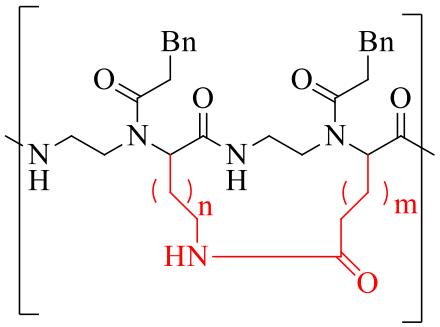

According to the length of the linker, these "stapled" *di*-α-PNA blocks should provide the opportunity to modulate the compactness of the PNA structure, favoring either DNA or RNA recognition in an exclusively antiparallel orientation.

We first focused on a liquid-phase orthogonal strategy allowing to obtain a first stapled *di*-*α*-PNA (*LL di*-*α*-PNA(Lys-Glu)). This methodology was then applied in solid-phase, for the construction of four stapled *di*-*α*-PNA: *LL* and *DD di*-*α*-PNA(Lys-Glu) and *LL* and *DD di*-*α*-PNA(Orn-Glu). In the case of Lys-based *di*-*α*-PNA, two major products could be isolated by semi-preparative HPLC. The first one was the expected stapled dimer while the other was identified to be the corresponding tetramer. In the case of Orn-based compounds, no major product could be isolated among the various polymers formed during the cyclization step. The Orn side-chain being shorter than the Lys one, it is likely that the cyclization of Orn-based *di*-*α*-PNAs is disfavored since it would lead to highly constrained molecules. In this context, it would be interesting to study the cyclization of linear *di*-*α*-PNAs containing longer side-chains, since it is possible that from a thermodynamic point of view, dimeric species would be privileged. To avoid the problem of polymerization occurring during the on-resin cyclization step, the solution would be to use protected "stapled" *di*-*a*-PNA blocks, which can be prepared and purified in liquid-phase in large quantities. These blocks should be introduced at any position of α-PNA sequence then, after elongation, the nucleic bases could be introduced. This will be the subject of a future study.

III. Experimental procedures

a) Apparatus

The characterization of each compound was realized with the following apparatus.

NMR spectra were recorded on a Bruker AC 200, 400 and 500 spectrometers with chemical shift values in ppm relative to tetramethylsilane (TMS) as standard. Assignment of ^{1}H and ^{13}C NMR signals are based on two-dimensional (COSY, TOCSY, HMBC, HSQC) experiments. The NMR samples were mostly dissolved in MeOH-d_4, DMSO-d_6 and CD_3OH. The 1D-NMR spectra of published compounds were just compared with obtained 1D-spectra. The spectra were processed and present with MestreNova 9.0.

Mass spectra were obtained using the Themo Finningan LCQ Mass spectroscopy connected with the HPLC agilent 100 series using the RP-HPLC column 150 x 2.4 mm 5µ Hypurity Elite C18 (solvent : water/0.1% formic acid and ACN/0.1% formic acid).

The chromatograms of each compound were contained with the HPLC Waters 2695 (Separations Module) using the Water 996 Photodiode array detector. The analytical spectra were obtained with the RP-column from Phenomenex "Synergi" Fusion-RP (4µm, 80A, 250x4.60mm), with a flow of 1 mL/min. The purifications were carried out with the RP-column from Thermo Scientific BetaBasic-C18 (5 µm, 250x10 mm) and a flow rate of 3.5 mL/min. The conditions are illustrated under each chromatogram, however it was only used H_2O+0.1% TFA and ACN+0.1%TFA as solvents.

a) Chemicals

All reagents and starting materials were obtained from commercial sources and used as received. The amino acids were exclusively achieved from Sigma Aldrich and FluoroChem. All reactions performed under an atmosphere of argon were mentioned. Purifications were carried out manually and automatically. Manually the Sigma Aldrich Silica gel (60 A, 230-400 mesh, 60-63 μm) and automatically the CombiFlash-Rf from Teledyne ISCO was utilized. In that case, the columns Chromabond Flash from Marcherey-Nagel GmbH were applied. The solvents used for the purifications had a purity of 99% from the suppliers Carlo Erba and Sigma Aldrich. The thin layer chromatography was prepared with Silica gel on AL foils with fluorescence indicator 254 nm from Sigma-Aldrich. The MBHA-resin LL (0.88 mmol/g, 200-400 mesh) was obtained from Novabiochem. The solvents used for the purifications by HPLC were HPLC grade from the suppliers Carlo Erba and Sigma Aldrich. After the solid-phase synthesis all compounds were purified by RP-HPLC.

I. Synthesis of phenyl-4-oxo pipecolic derivatives

I.-1. Following the procedure from Daily et al.

Dimethyl (2*S*)-2-aminobutanedioate hydrochloride (1)

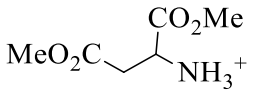

$C_6H_{12}NO_4^+$
MW: 162.16

To a solution of 5.5 g *L*-aspartic acid (1.0 eq, 41 mmol) in 100 mL MeOH was added at 0°C 30 mL acetyl chloride (1.0 eq, 41 mmol). The mixture was heated for 3 h at 65 °C. After the mixture was concentrated under reduced pressure, co-evaporated with toluene and the residue washed with DCM and Et_2O to yield a white solid (6.9 g, 85 %).
R_f (EtOAc/MeOH = 1:1) = 0.73
^{1}H-NMR (200 MHz, $CDCl_3$): δ = 8.61 (s, 2H, NH_2), 4.65 (bs, 1H, CH), 3.83 (s, 3H, CH_3), 3.73 (s, 3H, CH_3), 3.21 – 3.53 (m, 2H, CH_2) ppm.
^{13}C-NMR (50 MHz, $CDCl_3$): δ = 169.5 (C), 168.6 (C), 52.9 (CH_3), 52.0 (CH_3), 48.3 (CH), 33.9 (CH_2) ppm.

Dimethyl (2*S*)-2-(tritylamino)butanedioate (2)

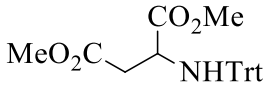

$C_{25}H_{25}NO_4$
MW: 403.47

At 0°C was added to a solution of 5.4 g dimethyl-(2*S*)-2-aminobutanedioate-hydrochloride (1.0 eq, 27 mmol) in 100 mL DCM 7.5 mL TEA (2.0 eq, 54 mmol) and 9 g trityl chloride (1.2 eq, 32 mmol). The mixture was stirred at room temperature for 20 h, concentrated under reduced pressure and re-dissolved in EtOAc. The solution was extracted with H_2O and brine, then dried over anhydrous $MgSO_4$, filtered and concentrated under reduced pressure. The brown oil was purified by Flash Column Chromatography (CH/EtOAc = 10:1 → CH/EtOAc = 2:1), what afforded the product as white solid (8.2 g, 75 %). R_f (CH/EtOAc = 4:1) = 0.54

^{1}H-NMR (400 MHz, $CDCl_3$): δ = 7.45 – 7.38 (m, 6H, CH_{ar}), 7.25 – 7.08 (m, 9H, CH_{ar}). 3.55 - 3.60 (m, 1H, CH), 3.60 (s, 3H, CH_3), 3.19 (s, 3H, CH_3), 2.86 (d, *J* = 8.4 Hz, 1H, NH), 2.58 (dd, *J* = 14.7, 5.4 Hz, 1H, CH_2), 2.50 (dd, *J* = 14.7, 7.1 Hz, 1H, CH_2) ppm.

^{13}C-NMR (101 MHz, $CDCl_3$): δ = 174.0 (C), 171.2 (C), 145.8 (3xC), 128.9 (6 x CH), 128.0 (6 x CH), 126.7 (3 x CH), 71.3 (C), 53.8 (CH), 52.1 (CH_3), 51.9 (CH_3), 40.4 (CH_2) ppm.

Methyl (2*S*)-2-(tritylamino)-5-(dimethoxyphosphoryl)-4-oxopentanoate (3)

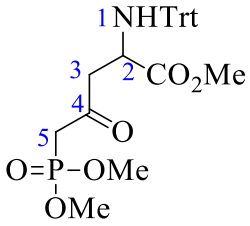

$C_{27}H_{30}NO_6P$
MW: 495.50

Under argon atmosphere, to a solution of 1.04 mL dimethylmethylphosphate (3.2 eq, 15.86 mmol) in 40 mL dry THF was added at -78 °C 9.24 mL 1.6 M *n*-BuLi in hexane (3.0 eq, 14.8 mmol). The reaction mixture was stirred for 1 h and after a solution of 2.0 g dimethyl-(2*S*)-2-(tritylamino)butanedioate (1.0 eq, 4.96 mmol) in 40 mL dry THF at - 78 °C added *via* cannula. The solution was stirred for 4 h at -78 °C. The mixture was warmed for 30 minutes to room-temperature, quenched with sat. NH_4Cl solution and concentrated under reduced pressure. The residue was extracted with EtOAc and the combined organic layers were dried over anhydrous $MgSO_4$, filtered and concentrated under reduced pressure. The Flash Column Chromatography (CH/EtOAc = 10:1) afford the product as yellow solid (1.5 g, 63 %). R_f (EtOAc) = 0.38

^{1}H-NMR (400 MHz, $CDCl_3$): δ = 7.51 – 7.43 (m, 6H, CH_{ar}), 7.32 – 7.14 (m, 9H, CH_{ar}), 3.79 (s, 3H, CH_3), 3.76 (s, 3H, CH_3), 3.72 – 3.66 (m, 1H, CH), 3.29 (s, 3H, CH_3), 3.08 (d, J = 1.7, 1 Hz, 1H, 5-CH_2), 3.03 (d, J = 1.7, 1 Hz, 1H, 5-CH_2), 2.88 (dd, J = 16.7, 4.6 Hz, 2H, 3-CH_2), 2.78 (dd, J = 16.7, 6.9 Hz, 1H, 3-CH_2) ppm.

^{13}C-NMR (101 MHz, $CDCl_3$): δ = 199.4 (d, J = 6.4 Hz), 174.2 (C), 145.8 (3xC), 128.9 (6 x CH), 128.0 (6 x CH), 126.7 (3 x CH), 71.4 (C), 53.4 – 52.9 (m, 3x CH_3+C H), 48.9 (CH_2), 42.7 (CH), 41.4 (CH) ppm.

Methyl (2*S*,5*E*)-2-(tritylamino)-4-oxo-6-phenylhex-5-enoate (4)

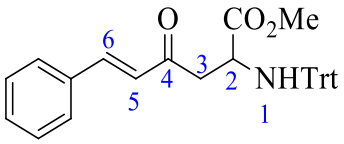

$C_{32}H_{29}NO_3$
MW: 475.58

To a solution of 1.5 g methyl-(2*S*)-2-(tritylamino)-5-(dimethoxyphosphoryl)-4-oxopentanoate (1.0 eq, 3.12 mmol) in 55 mL MeCN was added 0.64 mL benzaldehyde (2.0 eq, 6.24 mmol). The mixture was heated for 40 h at 50 °C. After the mixture was cooled down, sat. NH_4Cl-solution added and concentrated under reduced pressure. The residue was dissolved in EtOAc and washed several times with water. The combined organic layers were dried over anhydrous $MgSO_4$, filtered and concentrated under reduced pressure. The Flash Column Chromatography (CH/EtOAc = 10:1 → CH/EtOAc = 1:1) afforded the product as yellow oil (1.0 g, 68 %). R_f (CH/EtOAc = 4:1) = 0.5

^{1}H- NMR (400 MHz, $CDCl_3$): δ = 7.48 – 7.32 (m, 10H, CH_{ar}), 7.24 – 7.05 (m, 11H, CH_{ar}), 6.61 (d, J = 16.2 Hz, 1H, CH-5), 3.78 - 3.63 (m, 1H, 2-CH), 3.21 (s, 3H, CH_3), 2.84 (dd, J =15.2, 5.2 Hz, 1H, 3-CH_2 and NH), 2.71 (dd, J = 15.2, 7.0 Hz, 1H, 3-CH_2) ppm.

^{13}C- NMR (101 MHz, $CDCl_3$):δ = 197.5 (C), 174.5 (C), 145.8 (3 x C), 143.3 (CH), 134.4 (C), 130.7 (CH), 129.0 (2 x CH), 128.8 (6 x CH), 128.4 (2 x CH), 127.9 (6 x CH), 126.5 (3 x CH),126.4 (CH), 71.3 (C) , 53.8 (CH_3), 52.0 (CH), 45.7 (C H_2) ppm.

Methyl (2*S*,6*R*)-4-oxo-6-phenylpiperidine-2-carboxylate (6) and methyl (2*S*,6*S*)-4-oxo-6phenylpiperidine-2-carboxylate (7)

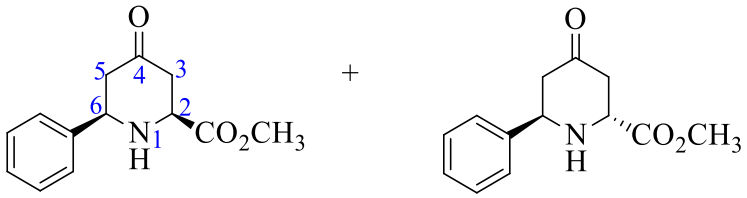

$C_{13}H_{15}NO_3$
MW: 233.26

1. Procedure:

To a solution of 850 mg methyl-(2S,5E)-2-(tritylamino)-4-oxo-6-phenylhex-5-enoate (1.0 eq, 1.84 mmol) in 140 mL MeOH was added 35 mL 2M HCl solution. After 1 h the reaction mixture was diluted with 140 mL H_2O, basified to pH = 8 with DIPEA and stirred for 18h at room temperature. The mixture was after diluted with 250 mL sat. NaCl solution and extracted several times with EtOAc. The combined organic layers were dried over $MgSO_4$, filtered and concentrated under reduced pressure. The Flash Column Chromatography (CH/EtOAc = 2:1→ CH/EtOAc = 0:1) afforded the separation of the diastereomers as colorless oil (200 mg, 47 %) and white solid (5 mg, 12 %). R_f (CH/EtOAc = 1:1) = 0.63 and R_f (CH/EtOAc = 1:1) = 0.43

2. Procedure:

To a solution of 500 mg methyl-(2S,5E)-2-(tritylamino)-4-oxo-6-phenylhex-5-enoate (1.0 eq 1.05 mmol) in 10 mL DCM was added 0.8 mL TFA (10 eq). After 1h of stirring the mixture was concentrated under reduced pressure, co-evaporated with toluene and washed with Et_2O. The white powder was after dissolved in MeOH, the solution cooled down to 0°C, added dropwise DIPEA. The reaction was stirred at room temperature overnight, then concentrate under reduced pressure and purified by Flash Column Chromatography (CH/EtOAc = 2:1). The products were afforded as white solid

(171 mg, 60%) and colorless oil (73 mg, 30%). R_f (CH/EtOAc = 1:1) = 0.63 and R_f (CH/EtOAc = 1:1) = 0.43

1. Diastereomer:

^{1}H-NMR (400 MHz, $CDCl_3$): δ = 7.44 – 7.27 (m, 5H, CH_{ar}), 4.01 – 3.90 (m, 1H, 6-CH), 3.84 - 3.72 (m, 1H, 2-CH), 3.78 (s, 3H, CH_3), 2.87 – 2.74 (m, 1H, 3-CH), 2.67 – 2.50 (m, 2H, 5-CH_2, 3-CH) ppm.

^{13}C-NMR (101 MHz, $CDCl_3$): δ = 206.6 (C), 171.5 (C), 141.8 (C), 128.9 (2 x CH), 128.3 (CH), 126.6 (2 x CH), 60.3 (CH), 58.0 (CH), 52.6 (CH_3), 50.2 (CH_2), 44.0 (CH_2) ppm.

m/z (ESI$^+$) = 233.11; $C_{13}H_{15}NO_3$ requires 233.26

2. Diastereomer:

^{1}H-NMR (400 MHz, $CDCl_3$): δ = 7.44 – 7.27 (m, 5H, CH_{ar}), 4.27-4.07 (m, 2H, 6-CH, 2-CH), 3.76 (s, 3H, CH_3), 2.84 – 2.72 (m, 2H, 3-CH_2), 2.57 (d, *J* = 7.2 Hz, 2H, 5-CH_2) ppm.

^{13}C-NMR (101 MHz, $CDCl_3$): δ = 206.2 (C), 173.0 (C), 142.1 (C), 128.8 (2 x CH), 128.0 (CH), 126.6 (2 x CH), 56.7 (CH), 56.0 (CH), 52.3 (CH_3), 49.2 (CH_2), 41.8 (CH_2) ppm.

m/z (ESI$^+$) = 233.11; $C_{13}H_{15}NO_3$ requires 233.26

(2*S*,6*R*)-1-allyl-2-methyl-4-oxo-6-phenylpiperidine-1,2-dicarboxylate (8)

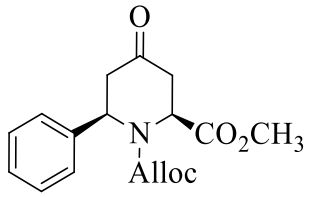

$C_{17}H_{19}NO_5$
MW: 317.34

To a solution of 50 mg (2*S*,6*R*)-methyl4-oxo-6-phenylpiperidine-2-carboxylate in (1.0 eq, 0.21 mmol) in 5 mL DCM was first added at 0°C 0.04 mL DIPEA (1.0 eq, 0.21 mmol) and after 0.03 mL allyl chloroformate (1.2 eq, 0.25 mmol). The reaction mixture was stirred for 2 h at room temperature. Then the mixture was reduced under reduced pressure, the residue was dissolved in EtOAc and extracted with H_2O and Brine. The combined organic layers were dried over $MgSO_4$, filtered and concentrated under reduced pressure. The Flash Column Chromatography afforded the product as a colorless oil (63 mg, 95 %). R_f (CH/EtOAc = 2:1) = 0.6

^{1}H-NMR(200 MHz, $CDCl_3$): δ =7.46 – 7.16 (m, 5H, CH_{ar}), 5.96 – 5.56 (m, 2H, CH_{Alloc} and 6-CH), 5.33 – 4.98 (m, 3H, CH_{2Alloc} and 2-CH), 4.63 (d, *J* = 5.3 Hz, 2H, CH_{2Alloc}), 3.56 (s, 3H, CH_3), 3.19 – 2.58 (m, 4H, 3-CH_2 and 5-CH_2) ppm.
^{13}C-NMR (101 MHz, $CDCl_3$): δ = 132.1, 128.6, 127.6, 126.5, 118.1, 67.1, 54.0, 53.7, 53.5, 52.6, 42.0, 40.4. 18.7, 17.5, 12.1 ppm.

(2*S*,6*R*)-1-allyl-2-methyl-4-oxo-6-phenylpiperidine-1,2-dicarboxylate (9)

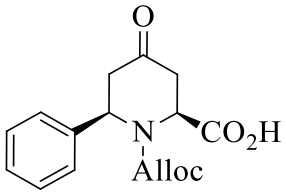

$C_{16}H_{17}NO_5$
MW: 303.31

1. Procedure:

To a solution of 45 mg (2*S*,6*R*)-1-allyl-2-methyl-4-oxo-6-phenylpiperidine-1,2-dicarboxylate (1 eq, 0.142 mmol) in 3 mL 1,2-DCE was added 103 mg Me_3SnOH (4 eq, 0.568 mmol) and the mixture was heated for 12 hours. Then the mixture was reduced under reduced pressure, the residue was dissolved in EtOAc and extracted with 2M HCl solution, H_2O and Brine. The combined organic layers were dried over $MgSO_4$, filtered and concentrated under reduced pressure. The Flash Column Chromatography (CH/EtOAc = 2:1 → CH/EtOAc = 0:1) afforded the product as a colorless oil (22 mg, 50%).

2.Procedure:

To a solution of 70 mg (2*S*,6*R*)-1-allyl-2-methyl-4-oxo-6-phenylpiperidine-1,2-dicarboxylate (1 eq, 0.22 mmol) in 5 mL Dioxane was added 5 mL 2M $LiOH/H_2O$ solution. The reaction mixture was stirred overnight, neutralized with 2M HCl-solution and extracted several times with EtOAc. The combined organic layers were dried over $MgSO_4$, filtered and concentrated under reduced pressure. The Flash Column Chromatography (CH/EtOAc = 2:1 → CH/EtOAc = 0:1) afforded the product as a colorless oil (13 mg, 20%). R_f (EtOAc) = 0.72

^{1}H-NMR (200 MHz, $CDCl_3$): δ = 7.62– 7.16 (m, 5H, CH_{ar}), 5.91 – 5.45 (m, 2H, CH_{Alloc} and 6-CH), 5.16 – 5.01 (m, 3H, CH_{2Alloc} and 2-CH), 4.70 – 4.54 (m, 2H, CH_{2Alloc}), 3.20 – 2.56 (m, 4H, 3-CH_2 and 5-CH_2) ppm.

Dimer 6-phenyl-4-oxo-pipecolic acid and alanine (18)

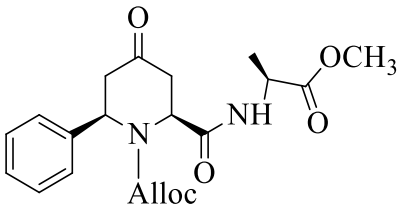

$C_{19}H_{22}N_2O_6$
MW: 374.39

To a solution of 50 mg (2*S*,6*R*)-1-allyl-2-methyl-4-oxo-6-phenylpiperidine-1,2-dicarboxylate (1.0 eq, 0.17 mmol) in 1.0 mL DMF was added 0.1 mL (3.0 eq, 0.5 mmol) DIPEA and 700 mg (1.1 eq, 0.18 mmol) HBTU and the mixture was stirred for 5 minutes at room temperature. After was added to the mixture 17 mg H-*L*-Ala-OCH_3 (1.0 eq, 0.17 mmol) in 1.0 mL DMF and the solution was stirred for 1 hour. The mixture was quenched with H_2O and the aqueous layer was extracted with EtOAc. After the organic layer was dried over $MgSO_4$ and concentrated. The residue was purified by Flash Column Chromatography (CH/EtOAc = 1:1). The product was obtained as a clear foam in 95% yield. R_f (CH/EtOAc = 1:1) = 0.38

^{1}H-NMR(400 MHz, $CDCl_3$): δ = 7.41 – 7.22 (m, 5H, CH_{Phenyl}), 5.65 (s, 1H, CH_{alloc}), 5.33 (s, 1H, 5-CH), 5.22 – 4.98 (m, 3H, CH_{2Alloc} and 5-CH), 4.53 (m, 3H, CH_{2Alloc} and $CH_{alanine}$), 3.76 (s, 3H, -OCH_3), 3.03 (ddd, *J* = 35.1, 17.4, 6.8 Hz, 2H, 3-CH and 5-CH), 2.65 (ddd, *J* = 34.1, 17.4, 5.9 Hz, 2H, 3-CH and 5-CH), 1.39 (s, 3H, $CH_{3alanine}$) ppm.
^{13}C-NMR (101 MHz, $CDCl_3$): δ = 205.4, 170.7, 142.0, 131.8, 128.9, 127.8, 126.0, 118.6, 67.4, 56.2, 55.3, 52.7, 48.3, 45.1, 39.5, 18.2 ppm.

Methyl (2S,5E)-2-(tritylamino)-4-oxo-8-phenyloct-5-enoate (21)

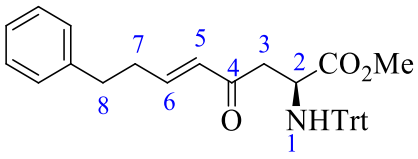

$C_{34}H_{33}NO_3$
MW: 503.63

To a solution of 2.0 g Methyl (2*S*)-2-(tritylamino)-5-(dimethoxyphosphoryl)-4-oxopentanoat (1 eq, 4.15 mmol) in 115 mL MeCN was added 1.07 mL hydrocinnamaldehyde (2.0 eq, 8.3 mmol) and 0.6 g K_2CO_3 (1.1 eq, 4.6 mmol). The reaction mixture was heated for 48 hours at 50 °C. After the mixture was cooled down and concentrated under reduced pressure. The residue was dissolved in EtOAc and extracted several times with H_2O and Brine. The combined organic layers were dried over anhydrous MgSO4, filtered and concentrated under reduced pressure. The Flash Column Chromatography (CH/EtOAc = 10:1 → CH/EtOAc = 1:1) afforded the product as a yellow oil (810 mg, 39 %). R_f (EtOAc) = 0.6

^{1}H-NMR (200 MHz, $CDCl_3$): δ = 7.54-7.43 (m, 5H, CH_{ar}), 7.19-7-08 (m, 9H, CH_{ar}), 6.78 (dt, *J* = 16.0, 6.7 Hz, 1H, 6-CH), 6.06 (d, *J* = 15.9 Hz, 1H, 5-CH), 3.76 - 3.63 (m, 1H, 2-CH), 3.19 (s, 3H, CH_3), 2.81 – 2.37 (m, 7H, 3-CH_2, 7-CH_2, 8-CH_2 and NH) ppm.

^{13}C-NMR (101 MHz, $CDCl_3$): δ = 34.2 (CH_2), 34.4 (CH_2), 45.0 (CH_2), 51.9 (CH_3), 53.7 (CH), 71.3 (C), 126.3 (CH), 126.6 (3 x CH), 127.9 (6 x CH), 128.4 (2 x CH), 128.6 (2 x CH), 128.9 (6 x CH), 131.0 (CH), 140.7 (C), 145.9 (CH), 147.1 (3 x C), 174.5 (C), 197.6 (C) ppm.

Methyl (2S,6S)-4-oxo-6-(2-phenylethyl)piperidine-2-carboxylate (22) and methyl (2S,6R)4-oxo-6-(2-phenylethyl)piperidine-2-carboxylate (23)

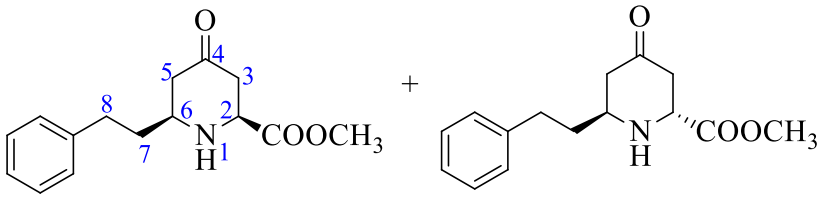

$C_{15}H_{19}NO_3$
MW: 261.32

To a solution of 695 mg (2S,5E)-2-(tritylamino)-4-oxo-8-phenyloct-5-enoate (1 eq, 1.4 mmol) in 50 mL MeOH was added 12 mL 2M HCl solution. The reaction mixture was stirred for 1h at room temperature. After the mixture was diluted with 50 mL H_2O, basified to pH = 8 with DIPEA and stirred for 18h at temperature. Then the mixture was diluted with sat. NaCl solution and extracted several times with EtOAc. The combined organic layers were dried over $MgSO_4$, filtered and concentrated under reduced pressure. The Flash Column Chromatography (CH/EtOAc = 1:1 → 0:1) afforded the products as a white solid (158 mg, 43%) and colorless oil (0.063 mg, 17%). R_f (CH/EtOAc = 4:1) = 0.33 and R_f (CH/EtOAc = 4:1) = 0.11.

1. Diastereomer:

^{1}H-NMR (200 MHz, $CDCl_3$): δ = 7.38 – 7.11 (m, 5H, CH_{ar}), 3.77 (s, 3H, CH_3), 3.59(dd, *J* = 12.1, 3.5 Hz, 1H, 2-CH), 2.96 – 2.61 (m, 4H, 6-CH, 3-CH and 8-CH_2), 2.56 – 2.40 (m, 2H, 3-CH and 5-CH), 2.24 – 1.78 (m, 3H, 5-CH and 7-CH_2) ppm.

^{13}C-NMR (101 MHz, $CDCl_3$): δ = 206.8 (C) 171.8 (C), 141.1 (C), 128.6 (2 x CH), 128.5 (2 x CH), 126.2 (CH), 57.9 (CH), 55.2 (CH), 52.5 (CH_3), 48.4 (CH_2), 44.5 (CH_2), 38.3 (CH_2), 30.3 (CH_2) ppm.

2. Diastereomer:

^{1}H-NMR (200 MHz, $CDCl_3$): δ = 7.43 – 7.04 (m, 5H, CH_{ar}), 4.10 – 4.00 (m, 1H, 2-CH), 3.71 (s, 3H, CH_3), 3.12 (m, 1H, 6-CH), 2.85 – 2.66 (m, 4H, 8-CH_2 and 3-CH_2), 2.54 – 2.38 (m, 1H, 5-CH), 2.35 – 2.00 (m, 1H, 5-CH), 1.95 - 1.68 (m, 2H, 7-CH_2) ppm.
^{13}C-NMR (101 MHz, $CDCl_3$): δ = 206.7 (C), 173.0 (C), 141.1 (C), 128.5 (2 x CH), 128.3 (2 x CH), 126.1 (CH), 55.7 (CH), 52.3 (CH), 52.1 (CH_3), 47.6 (CH_2), 42.3 (CH_2), 37.6 (CH_2), 31.9 (CH_2) ppm.

I.-2. Diels-Alder reaction

***(E)-N*-benzylideneprop-2-en-1-amine (11)**

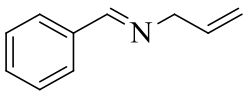

$C_{10}H_{11}N$
MW: 145.20

To a solution of 1 mL Benzaldehyde (1.0 eq, 10 mmol) in 12 mL DCM and 1.0 g $MgSO_4$ (1.5 eq, 15 mmol) was added 628 mg allyl amine (1.1 eq, 11 mmol). The mixture was heated for 3 hours at 50°C. After the $MgSO_4$ was filtered off and the solution concentrated under reduced pressure. Further purifications were not carried out. The product was afforded as colorless oil and directly used for the following reaction (1.38 g, 95%). R_f (CH/EtOAc = 10:2) = 0.57.

^{1}H-NMR (200 MHz, $CDCl_3$): δ = 8.30 (t, *J* = 1.3 Hz, 1H), 7.85 – 7.68 (m, 2H), 7.50 – 7.36 (m, 3H), 6.08 (ddt, *J* = 16.1, 10.5, 5.6 Hz, 1H), 5.32 – 5.08 (m, 1H), 4.27 (dd, *J* = 5.4, 1.7 Hz, 1H), 4.27 (dq, J= 5.7, 1.5 Hz, 2H) ppm.

^{13}C-NMR (50 MHz, $CDCl_3$): δ = 162.1, 136.2, 135.9, 130.8, 128.6, 128.2, 116.1, 63.6 ppm.

***(E)-N*-benzylidene-1-phenylmethanamine (13)**

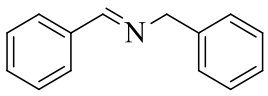

$C_{14}H_{13}N$
MW: 195.26

To a solution of 2 mL (1.0 eq, 19.7 mmol) Benzaldehyde in 20 mL DCM and 2 g $MgSO_4$ (1.5 eq, 29.6 mmol) was added 2.15 mL Benzylamine (1.0 eq, 19.7 mmol). The mixture was heated for 2 hours at 50°C. After the $MgSO_4$ was filtered off and the solution concentrated under reduced pressure. Further purifications were not carried out. The product was afforded as yellow oil and directly used for the next reaction. (3.7 g, 95%). R_f (CH/EtOAc = 2:1) = 0.2

^{1}H-NMR (200 MHz, $CDCl_3$): δ = 8.32 (s, 1H, CH), 7.71 (dd, *J* = 6.7, 3.0 Hz, 2H, 2xCH_{phenyl}), 7.41 – 7.10 (m, 8H, 8xCH_{phenyl}), 4.76 (d, *J* = 1.2 Hz, 2H, CH_2) ppm.

^{13}C-NMR (50 MHz, $CDCl_3$): δ = 162.0, 130.8, 128.64, 128.62, 128.54, 128.52, 127.03, 126.8, 65.0 ppm.

***(E)*-methyl 4-oxopent-2-enoate (10)**

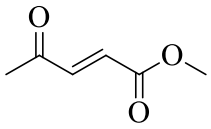

$C_6H_8O_3$
MW: 128.13

To a solution of 2.0 mL Methyl levulinate (1.0 eq, 1.6 mmol) in 10 mL $CHCl_3$ was added 1 hour dropwise 0.9 mL Br_2 (1.1 eq, 1.8 mmol) in $CHCl_3$ under argon atmosphere. After was added 3.0 mL NEt_3 (1.3 eq, 2.0 mmol) during 1 hour at 0°C and stirred for 30 minutes at room temperature. The mixture was extracted with H_2O, 1M HCl and sat. KCO_3 solution. The combined organic layers were dried over $MgSO_4$, filtered and concentrated under reduced pressure. The Flash Column Chromatography (CH/EtOAc = 10:1→5:1) afforded the products as colorless oil (700 mg, 34%). R_f (CH/EtOAc = 1:1) = 0.83

^{1}H-NMR (200 MHz, $CDCl_3$): δ =7.00(d, J = 16.1 Hz, 1H, CH), 6.63 (d, J=16.1Hz, 1H, CH), 3.79(s, 1H, -OCH_3), 2.34(s, 3H, CH_3) ppm.

^{13}C-NMR (101 MHz, $CDCl_3$): δ = 197.6, 140.2, 131.2, 77.6, 52.5, 28.3 ppm.

Methyl 1-allyl-4-oxo-6-phenylpiperidine-2-carboxylate (12)

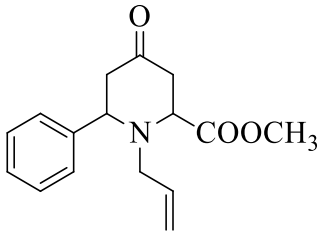

$C_{16}H_{19}NO_3$
MW: 273.33

To a solution of 150 mg *(E)*-methyl 4-oxopent-2-enoate (4 eq, 12 mmol) in 5 mL MeOH was added 20mol% L-Proline and after 40 mg *(E)-N*-benzylideneprop-2-en-1-amine (1 eq, 0.3 mmol). The mixture was stirred at room temperature overnight. Then the mixture was concentrate under reduced pressure, the residue was dissolved in EtOAc and extracted with $NaHCO_3$-solution. The combined organic layers were dried over $MgSO_4$, filtered and concentrated under reduced pressure. The Flash Column Chromatography (CH/EtOAc = 10:1) afforded the products as colorless oil (0.32 g, 40%). R_f (CH/EtOAc = 2:1) = 0.97

^{1}H-NMR (200 MHz, $CDCl_3$): δ = 7.49 – 7.17 (m, 5H, CH_{phenyl}), 5.84 (dddd, *J* = 16.8, 10.4, 7.7, 5.8 Hz, 1H, CH_{allyl}), 5.26 – 4.98 (m, 2H, CH_{2Allyl}), 3.94 (dd, *J* = 10.7, 6.7 Hz, 1H, CH), 3.72 (s, 3H, CH_3), 3.48 – 3.17 (m, 2H, CH_{allyl} and CH), 3.17 – 2.91 (m, 1H, CH_{allyl}), 2.91 – 2.63 (m, 3H, CH_2 and CH), 2.63 – 2.28 (m, 1H, CH) ppm.
^{13}C-NMR (50 MHz, $CDCl_3$): δ = 133.07(CH_{allyl}), 128.67 (CH_{phenyl}), 127.67(CH_{phenyl}), 118.78 (CH_{2allyl}), 65.57(CH), 63.25(CH), 53.19 (CH_{2allyl}), 46.54 (CH_2), 35.74 (CH_2) ppm.
m/z (ESI$^+$) =274.13; $C_{16}H_{19}NO_3$ requires 273.14

1-allyl-4-oxo-6-phenylpiperidine-2-carboxylic acid (15)

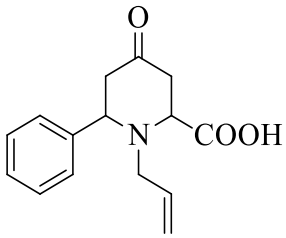

$C_{15}H_{17}NO_3$
MW: 259.30

To a solution of 60 mg (1.0 eq, 0.22 mmol) in 2 mL 1,2-DCE was added 0.2 g Me_3SnOH (4.0 eq, 0.88 mmol). The reaction mixture was heated for 12 hours at 80°C. Then the mixture was concentrate under reduced pressure, the residue was dissolved in EtOAc and extracted with 2M HCl solution, H_2O and Brine. The combined organic layers were dried over $MgSO_4$, filtered and concentrated under reduced pressure. The Flash Column Chromatography (CH/EtOAc = 10:1 → 2:1) afforded the products as colorless oil (31 mg, 55%). R_f (CH/EtOAc = 2:1) = 0.62.

^{1}H-NMR (200 MHz, $CDCl_3$): δ = 7.61 – 7.06 (m, 5H, CH_{phenyl}), 6.00-5.56 (m, 1H, CH_{allyl}), 5.25 – 4.90 (m, 2H, CH_{2Allyl}), 4.11 - 3.67 (m, 1H, CH), 3.43 - 2.12 (m, 7H, 3 x CH_2, CH) ppm.

m/z (ESI$^+$) =260.07; $C_{15}H_{17}NO_3$ requires 259.12

Methyl 1-benzyl-4-oxo-6-phenylpiperidine-2-carboxylate (14)

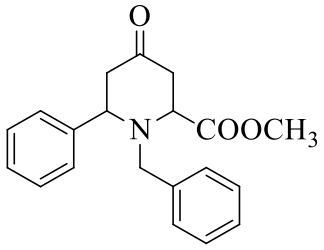

$C_{20}H_{21}NO_3$
MW: 323.39

To a solution of 1.0 g *(E)*-methyl 4-oxopent-2-enoate (4.0 eq, 8 mmol) in 15 mL MeOH was added 20mol% L-Proline and after 40 mg *(E)-N*-benzylideneprop-2-en-1-amine (1.0 eq, 2 mmol). The mixture was stirred at room temperature overnight. Then the mixture was concentrate under reduced pressure, the residue was dissolved in EtOAc and extracted with $NaHCO_3$-solution. The combined organic layers were dried over $MgSO_4$, filtered and concentrated under reduced pressure. The Flash Column Chromatography (CH/EtOAc = 10:1→2:1) afforded the products as colorless oil (1.0 g, 40%). R_f (CH/EtOAc = 2:1) = 0.67.

^{1}H-NMR (400 MHz, $CDCl_3$): δ = 7.57 – 7.09 (m, 10H, CH_{phenyl}), 4.36 (dd, *J* = 9.1, 5.2 Hz, 1H, CH), 3.88 (dd, *J* = 6.4, 2.3 Hz, 1H, CH), 3.74 (s, 4H, CH_3 and CH), 3.22 (d, *J* = 13.8 Hz, 1H, CH), 2.81 – 2.35 (m, 4H, 2 x CH_2) ppm.
^{13}C-NMR (101 MHz, $CDCl_3$): δ = 206.1 (C), 172.06 (C), 143.01 (C), 138.42 (C), 129.16 (CH), 128.62(CH), 128.07(CH), 127.4(CH), 62.78 (CH), 58.67 (CH), 54.31 (CH_2), 51.71(CH_3), 49.28(CH_2), 43.01(CH_2) ppm.

m/z (ESI$^+$) =345.20; $C_{19}H_{24}N_2O_4$ requires 344.17

(2R)-methyl 2-(1-allyl-4-oxo-6-phenylpiperdine-2-carboxamido) propanoate (17)

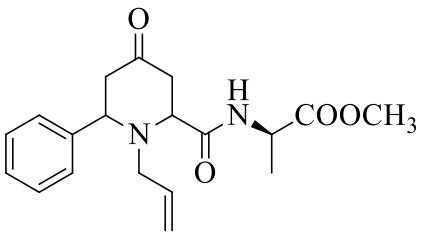

$C_{19}H_{24}N_2O_4$
MW: 344.40

To a solution of 37 mg 1-allyl-4-oxo-6-phenylpiperidine-2-carboxylic acid (1.0 eq, 0.14 mmol) in 1.5 mL DMF was added 0.08 mL (3.0 eq, 0.43 mmol) DIPEA and 57 mg (1.1 eq, 0.16 mmol) HBTU and the mixture was stirred for 5 minutes at room temperature. After was added to the mixture 20 mg H-*L*-Ala-OCH_3 (1.0 eq, 0.14 mmol) in 1.3 mL DMF and the solution was stirred for 1h. The mixture was quenched with H_2O and the aqueous layer was extracted with EtOAc. After the organic layer was dried over $MgSO_4$ and concentrated. The residue was purified by Flash Column Chromatography (CH/EtOAc = 10:1→2:1). The product was obtained as a clear foam in 90 % yield. R_f (CH/EtOAc = 2:1) = 0.58

^{1}H-NMR (400 MHz, MeOD-*d_4*): δ = 9.07 – 8.73 (m, 5H, 5 x CH_{phenyl}), 7.56 – 7.27 (m, 1H, CH_{alloc}), 6.80 – 6.59 (m, 2H, CH_{2Alloc}), 5.92 – 5.58 (m, 1H, CH), 5.58 – 5.40 (m, 1H, CH), 5.28 (d, *J* = 3.0 Hz, 3H, CH_3), 4.82 (m, 1H, CH), 4.60 – 4.14 (m, 2H, CH_2), 4.11 – 3.78 (m, 2H, CH_2), 3.11 (ddd, *J* = 7.1, 4.7, 2.0 Hz, 3H, $CH_{3alanine}$) ppm.

m/z (ESI$^+$) =345.20; $C_{19}H_{24}N_2O_4$ requires 344.17

II. Synthesis of α-PNA-Dimer

II.-1. Liquid phase: strategy 1

Boc-Orn(Alloc)-OH (79)

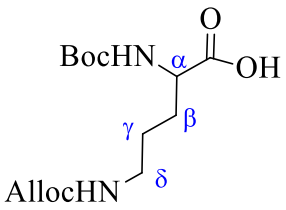

$C_{14}H_{24}N_2O_6$
MW: 316.35

To a solution of 1.0 g (1.0 eq, 4.6 mmol) H-Orn(Alloc)-OH in 50 mL DMF and 0.37 mL (1.0 eq, 4.6 mmol) NEt_3 was added 0.36 g (1.1 eq, 2.5 mol) Boc_2O was and stirred at room temperature overnight. After the reaction mixture was extracted several times with sat. $NaHCO_3$-solution and Brine and the aqueous phase acidified to pH=1 using a 1M HCl solution. The aqueous Phase was extracted several times with EtOAc. After the organic layers were dried over $MgSO_4$ and concentrated under reduced pressure. The product was obtained as a clear oil (1.4 g, 95%).

^{1}H-NMR (200 MHz, $CDCl_3$): δ = 6.02 – 5.75 (m, 1H, CH_{Alloc}), 5.22 – 5.14 (m, 2H, CH_2-*Alloc*), 4.53 – 4.51 (m, 2H, CH_2-*Alloc*), 4.29 – 4.25 (m, 1H, CH_α-*Orn*), 3.27 – 3.03 (m, 2H, $CH_{2\delta}$-*Orn*), 1.95 – 1.57 (m, 4H, $CH_{2\beta}$-*Orn* and $CH_{2\gamma}$-*Orn*), 1.40 (s, 9H, 3 x CH_3-*Boc*) ppm.

m/z (ESI$^+$) = [M+H$^+$]316.07; $C_{28}H_{45}N_5O_{10}$ requires 316.16

Boc-Orn(Alloc)-OCH_3 (81)

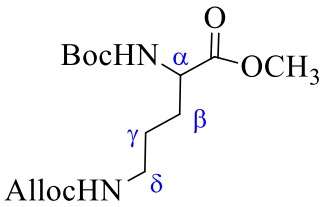

$C_{15}H_{26}N_2O_6$
MW: 330.38

To a solution of 1.0 g (1.0 eq, 3.2 mmol) Boc-Orn(Alloc)-OH in 20 mL DMF was added 1.24 g Cs_2CO_3 (1.0 eq, 3.8 mmol) and 0.3 mL MeI (1.5 eq, 4.7 mmol) at 0°C. The reaction mixture was stirred for 2 h at room temperature. After was added H_2O and Brine and the mixture was extracted several times with EtOAc. The reaction was quenched with sat. NH_4Cl-solution and was again extracted with EtOAc. The combined org. layers were dried over $MgSO_4$, filtered and concentrated under reduced pressure. Following purifications were not necessary. The product Boc-Orn(Alloc)-OMe was obtained as white solid (1.2 g, 95%). R_f (CH/EtOAc = 2:1 = 0.4.

^{1}H-NMR (200 MHz, $CDCl_3$): δ = 6.01 – 5.79 (m, 1H, CH_{Alloc}), 5.37 – 5.01 (m, 2H, CH_2-*Alloc*), 4.53 (d, *J* = 5.1 Hz, 2H, CH_2-*Alloc*), 4.28 – 4.21 (m, 1H, CH_α-*Orn*), 3.72 (s, 3H, CH_3), 3.16 (q, *J* = 6.5 Hz, 2H, $CH_{2\delta}$-*Orn*), 1.88 – 1.48 (m, 4H, $CH_{2\beta}$-*Orn* and $CH_{2\gamma}$-*Orn*), 1.42 (s, 9H, 3 x CH_3-*Boc*) ppm.
^{13}C-NMR (50 MHz, $CDCl_3$): δ = 173.4, 162.7, 156.5, 155.6, 133.1, 117.7, 80.0, 65.6, 53.3, 52.4, 40.7, 36.6, 32.4, 29.5, 28.4, 28.0, 22.5 ppm.
m/z (ESI$^-$) = [M-H$^-$] 329.07; $C_{15}H_{16}N_2O_6$ requires 330.18

H-Orn(Alloc)-OCH$_3$ (57)

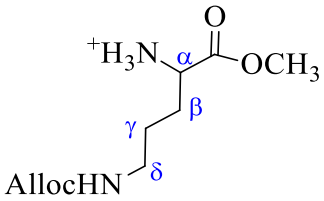

$C_{10}H_{19}N_2O_4^+$
MW: 231.27

1.0 g Boc-Orn(Alloc)-OMe (1.0 eq, 3.0 mmol) was dissolved in 5mL DCM and 5 mL TFA. The mixture was stirred at room temperature overnight. After the reaction mixture was concentrated under reduced pressure and co-evaporated with toluene. The residue was washed with Et_2O to induce the precipitation of the product. The product was obtained as a white solid (0.6 g, 90%).

^{1}H-NMR (200 MHz, $CDCl_3$): δ = 6.00 – 5.80 (m, 1H, CH_{Alloc}), 5.37 – 5.11 (m, 2H, CH_2-*Alloc*), 4.53 (d, *J* = 5.1 Hz, 2H, CH_2-*Alloc*), 3.97 (t, *J* = 6.2 Hz, 1H, CH_α-*Orn*), 3.79 (s, 3H, CH_3), 3.27 – 3.10 (m, 2H, $CH_{2\delta}$-*Orn*), 2.00 – 1.85 (m, 2H, $CH_{2\beta}$-*Orn*), 1.62 – 1.35 (m, 2H, $CH_{2\gamma}$-*Orn*).

m/z (ESI$^-$) = [M-H$^-$] 231.13; $C_{14}H_{16}N_2O_6$ requires 230.13

Product 61

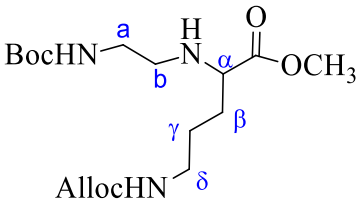

$C_{17}H_{31}N_3O_6$
MW: 373.44

To a solution of 1.2 g (1.0 eq, 5.2 mmol) H-Orn(Alloc)-OMe in 50 mL MeOH was added 0.83 g (1.0 eq, 5.2 mmol) *N*-Boc-aminoacetaldehyde. The mixture was stirred for 30 minutes at room temperature. The solution was cooled to 0°C and 0.33 g (1.0 eq, 5.2 mmol) $NaBH_3CN$ and 0.3 mL (1.0 eq, 5.2 mmol) CH_3COOH were added. The reaction mixture was concentrated under reduced pressure after 2 h and the residue was dissolved in EtOAc and was extracted with sat. $NaHCO_3$-solution and Brine. After the organic layers were dried over $MgSO_4$ and concentrated under reduce pressure. The residue was purified by Flash Column Chromatography (CH/EtOAc = 1:0→4:1→1:1) and the product was obtained as a clear oil (1.2 g, 60%). R_f (EtOAc) = 0.64.

^{1}H-NMR (200 MHz, $CDCl_3$): δ = 6.06 – 5.78 (m, 1H, CH_{Alloc}), 5.39 – 5.14 (m, 2H, CH_2-*Alloc*), 5.14 (bs, 1H, NH), 5.02 (bs, 1H, NH), 4.54 (d, *J* = 5.5 Hz, 2H, CH_2-*Alloc*), 3.71 (s, 3H, CH_3), 3.24 – 3.20 (m, 5H, $CH_{2\varepsilon}$-*Orn* and CH_2-*b* and CH_{α}-*Orn*), 2.85 – 2.60 (m, 1H, CH-*a*), 2.62 – 2.44 (m, 1H, CH-*a*), 1.85 – 1.29 (m, 4H, $CH_{2\beta}$-*Orn* and $CH_{2\gamma}$-*Orn*), 1.43 (s, 9H, CH_3-*Boc*) ppm.
^{13}C-NMR (50 MHz, $CDCl_3$): δ = 175.4, 162.2, 156.3, 156.2, 133.0, 117.7, 65.5, 60.7, 52.0, 47.7, 40.6, 30.5, 28.4, 26.4 ppm.
m/z (ESI$^-$) = [M+H$^+$] 374.13; $C_{17}H_{31}N_3O_6$ requires 373.22

Product 69

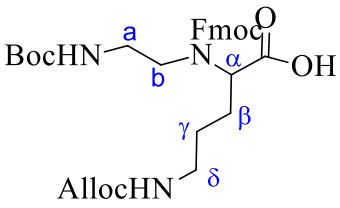

$C_{31}H_{39}N_3O_8$
MW: 581.66

0.3 g (1.0 eq, 0.8 mmol) Product 61 was diluted in 5 mL THF was added 2M $LiOH/H_2O$ (1.2 eq) solution and stirred overnight. After the mixture of 1.0 eq Fmoc-OSu in THF was added and the mixture was stirred for 3h. The end of the reaction was verified by TLC and added sat. $NaHCO_3$ solution. The solution was neutralized with 2M HCl-solution and extracted with EtOAc. The combined organic layers were dried over $MgSO_4$, filtered and concentrated under reduced pressure. The Flash Column Chromatography (CH/EtOAc = 3:1→1:1→0:1) afford the product as a colorless oil (1.3 g, 80%). R_f (CH/EtOAc = 1:1) = 0.78.

^{1}H-NMR (400 MHz, $CDCl_3$): δ = 7.74 (t, *J* = 7.0 Hz, 2H, CH-*Fmoc*), 7.55 (d, *J* = 5.8 Hz, 2H, CH-*Fmoc*), 7.51 – 7.21 (m, 4H, CH-*Fmoc*), 5.89 – 5.91 (m, 1H, CH_{Alloc}), 5.36 – 5.06 (m, 2H, CH_2-*Alloc*), 4.72 – 4.46 (m, 4H, CH_2-*Alloc* and CH_2-*Fmoc*), 4.23 – 4.18 (m, 1H, CH-*Fmoc*), 3.26 – 2.77 (m, 5H, CH_2-*a*, CH_2-*b* and CH_α-*Orn*), 2.08 – 1.88 (m, 1H, CH_δ-*Orn*), 1.88 – 1.66 (m, 1H, CH_δ-*Orn*), 1.39 (s, 9H, 3 x CH_3-*Boc*), 1.44 – 1.30 (m, 4H, $CH_{2\beta}$-*Orn* and $CH_{2\gamma}$-*Orn*) ppm.

^{13}C-NMR (50 MHz, $CDCl_3$): δ = 174.3, 156.5, 143.9, 141.5, 127.6, 124.9, 120.0, 117.7, 65.6, 60.7, 47.4, 40.7, 39.7, 29.5, 28.5 ppm.

Boc-Glu(Allyl)-OMe (75)

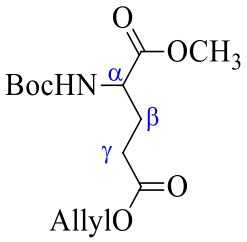

$C_{14}H_{23}NO_6$
MW: 301.34

To a solution of 4.28 g (1.0 eq, 16.4 mmol) Boc-Glu-OMe in 50 mL DMF was added 5.34g Cs_2CO_3(1.0 eq, 16.4 mmol). The solution was cooled to 0°C and 2.9 mL (1.2 eq, 33 mmol) allyl bromide was added. After 1h, H_2O and sat. $NaHCO_3$-solution was added in the reaction mixture. The solution was extracted several times using EtOAc. After the organic layers were dried over $MgSO_4$ and concentrated under reduced pressure. The residue was purified by Flash Column Chromatography (CH/EtOAc = 2:1). The product was obtained as a clear oil (4.7 g, 95%). R_f (EtOAc) = 0.74.

^{1}H-NMR (400 MHz, $CDCl_3$): δ = 6.02 – 5.75 (m, 1H, CH_{Alloc}), 5.34 – 5.07 (m, 3H, CH_2-*Alloc* and NH), 4.56 (d, *J* = 6.8 Hz, 2H, CH_2-*Alloc*), 4.31 (q, *J* = 7.9 Hz, 1H, CH, CH_α-*Glu*), 3.72 (s, 3H, CH_3), 2.43 (d, *J* = 6.9 Hz, 2H, $CH_{2\gamma}$-*Glu*), 2.34 – 2.07 (m, 1H, CH_β-*Glu*), 2.07 – 1.79 (m, 1H, CH_β-*Glu*), 1.41 (s, 9H, 3 x CH_3-*Boc*) ppm.

^{13}C-NMR (101 MHz, $CDCl_3$): δ = 172.8, 172.4, 155.4, 132.1, 118.5, 80.1, 65.5, 53.0, 52.5, 30.3, 28.4, 27.8 ppm.

H-Glu(Allyl)-OMe (45)

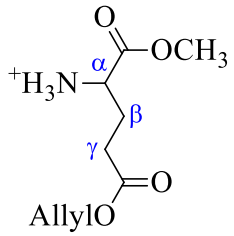

$C_9H_{16}NO_4^+$
MW: 202.23

4.0 g of Boc-Glu(Allyl)-OMe (13.3 mmol) was dissolved in 15mL DCM and 15 mL TFA. The mixture was stirred at room temperature overnight. The reaction mixture was concentrated under reduced pressure and co-evaporated with toluene. The residue was washed with Et_2O to induce the precipitation of the product. The product was obtained as a clear oil (2.4 g, 90%).

^{1}H-NMR (400 MHz, $CDCl_3$): δ = 5.98 – 5.79 (m, 1H, CH_{Alloc}), 5.38 – 5.15 (m, 2H, CH_2-*Alloc*), 4.57 (d, *J* = 5.8, 2H, CH_2-*Alloc*), 3.78 – 3.75 (m, 1H, CH_α-*Glu*), 3.77 (s, 3H, CH_3), 2.58 (d, *J* = 7.1 Hz, 2H, $CH_{2\gamma}$-*Glu*), 2.36 – 2.16 (m, 2H, $CH_{2\beta}$-*Glu*) ppm.
^{13}C-NMR (50 MHz, $CDCl_3$): δ = 172.5, 169.7, 131.8, 128.7, 118.9, 66.0, 53.5, 52.4, 29.7, 25.4 ppm.
m/z (ESI$^+$) = [M+H$^+$]202.13; $C_9H_{15}NO_4$ requires 201.11

Product 47

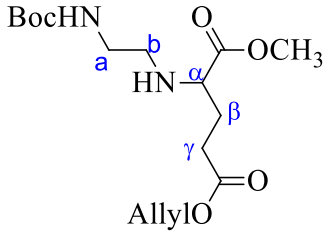

$C_{16}H_{28}N_2O_6$
MW: 344.40

To a solution of 1.0 g (1.0 eq, 5 mmol) H-Glu(Allyl)-OMe in 50 mL MeOH was added 0.8 g (1.0 eq, 5 mmol) *N*-Boc-aminoacetaldehyde. The mixture was stirred for 30 minutes at room temperature. The solution was cooled to 0°C and 0.31 g (1.0 eq, 5 mmol) $NaBH_3CN$ and 0.3 mL (1.0 eq, 5 mmol) CH_3COOH were added. The reaction mixture was concentrated under reduced pressure after 2 h and the residue was dissolved in EtOAc and was extracted with sat. $NaHCO_3$-solution and Brine. After the organic layers were dried over $MgSO_4$ and concentrated under reduce pressure. The residue was purified by Flash Column Chromatography (CH/EtOAc = 10:1→1:1) and the product was obtained as a clear oil (1.0 g, 60%). R_f (DCM/EtOAc = 1:1) = 0.69.

^{1}H-NMR (400 MHz, $CDCl_3$): δ = 6.04 – 5.84 (m, 1H, CH_{Alloc}), 5.39 – 5.17 (m, 2H, CH_2-*Alloc*), 4.58 (dd, *J* = 5.7, 1.6 Hz, 2H, CH_2-*Alloc*), 4.31 (bs, 1H, CH_α-*Glu*)3.72 (s, 3H, CH_3), 3.40 – 3.35 (m, 1H, CH-*a*), 3.21 – 3.04 (m, 3H, CH_2-*b*, CH-*a*), 2.10 – 1.95 (m, 1H, CH_β-*Glu*), 1.90 – 1.80 (m, 1H, CH_β-*Glu*), 1.50 – 1.36 (m, 2H, $CH_{2\gamma}$-*Glu*), 1.44 (s, 9H, 3 x CH_3-*Boc*) ppm.

^{13}C-NMR (101 MHz, $CDCl_3$): δ = 175.3, 172.9, 156.7, 156.2, 132.2, 128.7, 128.4, 118.5, 115.2, 79.3, 65.3, 60.4, 52.6, 52.1, 47.6, 42.3, 40.5, 30.9, 29.5, 28.5, 28.4, 23.3 ppm.

m/z (ESI$^+$) = [M+H$^+$]345.07; $C_{16}H_{28}N_2O_6$ requires 344.19

Product 49

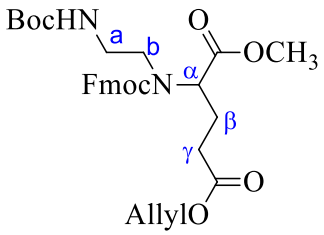

$C_{31}H_{38}N_2O_8$
MW: 566.64

To a solution of 1.34 g (1.0 eq, 4 mmol) Product 47 in 30 mL DMF was added 1.0 g Fmoc-Cl (1.0 eq, 4 mmol) and 1.53 mL DIPEA (2.2 eq, 8.8 mmol) until pH = 9 and stirred for 1h at room temperature. After was added 50 mL sat. $NaHCO_3$-solution and adjusted pH = 5 with 0.5 M HCl. The mixture was extracted with EtOAc and the combined organic layers were dried over $MgSO_4$, filtered and concentrated under reduced pressure. The Flash Column Chromatography (CH/EtOAc = 10:1→1:1) afforded the product as a white solid (1.4 g, 65 %). R_f (CH/EtOAc = 3:1) = 0.51.

^{1}H-NMR (200 MHz, $CDCl_3$): δ = 7.76 (d, *J* = 7.7 Hz, 2H, CH_{ar}-*Fmoc*), 7.56 (d, *J* = 7.4 Hz, 2H, CH_{ar}-*Fmoc*), 7.47 – 7.21 (m, 4H, CH_{ar}-*Fmoc*), 5.99 – 5.80 (m, 1H, CH_{Alloc}), 5.38 – 5.15 (m, 2H, CH_2-*Alloc*), 4.59 – 4.47 (m, 4H, CH_2-*Fmoc* and CH_2-*Alloc*), 4.31 – 4.12 (m, 2H, CH_α-*Glu* and CH-*Fmoc*), 3.70 (s, 3H, CH_3), 3.55 – 3.37 (m, 2H, CH_2-*b*), 3.34 – 3.12 (s, 2H, CH_2-*a*), 2.30 (bs, 1H, CH_β-*Glu*), 2.05 (bs, 1H, CH_β-*Glu*), 1.52 – 1.33 (m, 2H, $CH_{2\gamma}$-*Glu*), 1.44 (s, 9H, 3 x CH_3-*Boc*).

^{13}C-NMR (101 MHz, $CDCl_3$): δ = 172.2, 156.6, 155.8, 143.74, 141.4, 132.0, 127.0, 124.5, 119.9, 118.5, 79.1, 67.0, 65.3, 60.4, 52.5, 47.4, 39.3, 30.6, 28.4, 24.4, 21.0 ppm.

m/z (ESI$^+$) = [M+H$^+$]566.87; $C_9H_{15}NO_4$ requires 566.26

Product 51

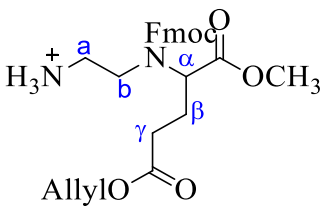

$C_{26}H_{31}N_2O_6^+$
MW: 467.53

1.0 g of Product 49 (1.8 mmol) was dissolved in 5 mL DCM and 5 mL TFA. The mixture was stirred at room temperature overnight. The reaction mixture was concentrated under reduced pressure and co-evaporated with toluene. The residue was washed with Et_2O to induce the precipitation of the product. The product was obtained as a clear oil (0.8 g, 95%).

^{1}H-NMR (200 MHz, MeOD-d_4): δ = 7.82 (d, *J* = 7.2 Hz, 2H, CH-*Fmoc*), 7.59 (d, *J* = 7.5 Hz, 2H, CH-*Fmoc*), 7.39 (d, *J* = 8.7 Hz, 4H, CH-*Fmoc*), 6.06 – 5.84 (m, 1H, CH_{Alloc}), 5.47 – 5.17 (m, 2H, CH_2-*Alloc*), 4.78 – 4.46 (m, 4H, CH_2-*Alloc* and CH_2-*Fmoc*), 4.32 – 4.19 (m, 1H, CH-*Fmoc*), 4.06 – 3.96 (m, 1H, CH_α-*Glu*), 3.92 – 3.53 (m, 2H, CH_2-*a*), 3.45 (s, 3H, CH_3), 3.10 – 2.96 (m, 2H, CH_2-*b*), 1.98 (d, *J* = 7.1 Hz, 2H, $CH_{2\gamma}$-*Glu*), 1.80 (dd, *J* = 14.0, 7.4 Hz, 1H, CH_β-*Glu*), 1.41 (s, 1H, CH_β-*Glu*) ppm.
^{13}C-NMR (101 MHz, DMSO-d_6): δ = 164.9, 163.6, 148.7, 135.7, 133.35, 124.1, 119.36, 118.7, 115.98, 111.65, 58.9, 56.9, 51.5, 43.8, 29.7, 21.7, 16.4 ppm.

Boc-Lys(Alloc)-OH (83)

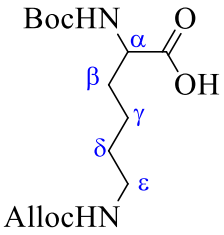

$C_{15}H_{26}N_2O_6$
MW: 330.38

To a solution of 5.0 g (1.0 eq, 20 mmol) Boc-Lys-OH in 50 mL DCM was added 3.54 mL (1.0 eq, 20 mmol) DIPEA. The solution was cooled to 0°C and 2.55 mL (1.2 eq, 24 mmol) allyl chloroformate was added. After 1 h the reaction mixture was concentrated under reduced pressure and the residue was dissolved in EtOAc. The solution was extracted several times with sat. $NaHCO_3$-solution and Brine. After the organic layers were dried over $MgSO_4$ and concentrated under reduced pressure. Further purifications were not necessary. The product was obtained as a clear oil (820 mg, 60%).6.6 g, quantitative). R_f (EtOAc) = 0.47.

^{1}H-NMR (200 MHz, $CDCl_3$): δ = 7.55 (bs, 1H, OH), 6.01 – 5.81 (m, 1H, CH_{Alloc}), 5.33 – 5.17 (m, 2H, CH_2-*Alloc*), 4.68 – 4.53 (m, 3H, CH_2-*Alloc*), 4.29 (bs, 1H, CH_α-*Lys*), 3.17 (q, *J* = 6.9, 6.4 Hz, 2H, $CH_{2\varepsilon}$-*Lys*), 1.97 – 1.63 (m, 4H, $CH_{2\beta}$-*Lys* and $CH_{2\delta}$-*Lys*), 1.43 (s, 9H, 3 x CH_3-*Boc*), 1.49 – 1.40 (m, 2H, $CH_{2\gamma}$-*Lys*) ppm.
^{13}C-NMR (50 MHz, $CDCl_3$): δ = 176.0, 163.4, 156.7, 155.9, 133.0, 117.8, 80.1, 65.6, 53.3, 40.6, 36.9, 32.1, 31.8, 29.4, 28.4, 22.4 ppm.
m/z (ESI$^+$) = [M-H$^-$]329.00; $C_{15}H_{26}N_2O_6$ requires 330.13

Boc-Lys(Alloc)-OMe (85)

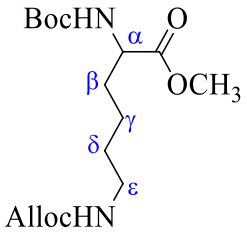

$C_{16}H_{28}N_2O_6$
MW: 344.40

To a solution of 5.34 g (1.0 eq, 16 mmol) Boc-Lys(Alloc)-OH in 50 mL DMF was added 6.26 g (1.0 eq, 16 mmol) Cs_2CO_3. The solution was cooled to 0°C and 1.5 mL (1.2 eq, 14 mmol) MeI was added. After 1h the reaction mixture was concentrated under reduced pressure and the residue was dissolved in EtOAc. The solution was extracted several times with sat. $NaHCO_3$-solution and Brine. After the organic layers were dried over $MgSO_4$ and concentrated under reduced pressure. Further purifications were not necessary. The product was obtained as a clear oil (5.2 g, 95%). R_f (CH/EtOAc = 1:1) = 0.51.

^{1}H-NMR (200 MHz, $CDCl_3$): δ = 5.99 – 5.80 (m, 1H, CH_{Alloc}), 5.37 – 5.01 (m, 2H, CH_2-*Alloc*), 4.87 (bs, 1H, NH), 4.53 (d, *J* = 5.4 Hz, 2H, CH_2-*Alloc*), 4.32 – 4.21 (m, 1H, CH_α-*Lys*), 3.72 (s, 3H, CH_3), 3.16 (q, *J* = 6.5 Hz, 2H, $CH_{2\varepsilon}$-*Lys*), 1.88 – 1.48 (m, 4H, $CH_{2\beta}$-*Lys* and $CH_{2\delta}$-*Lys*), 1.42 (s, 9H, 3 x CH_3-*Boc*), 1.41 – 1.21 (m, 2H, $CH_{2\gamma}$-*Lys*) ppm.

^{13}C-NMR (50 MHz, $CDCl_3$): δ = 173.4, 162.7, 156.5, 155.6, 133.1, 117.7, 80.0, 65.6, 53.3, 52.4, 40.7, 36.6, 32.4, 31.6, 29.5, 28.4, 28.0, 22.49 ppm.

m/z (ESI$^+$) = [M+H$^+$]344.93; $C_{16}H_{28}N_2O_6$ requires 344.19

H-Lys(Alloc)-OMe (58)

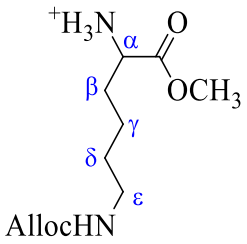

$C_{11}H_{21}N_2O_4^+$
MW: 245.29

1.0 g of Boc-Lys(Alloc)-OMe (2.9 mmol) was dissolved in 5mL DCM and 5 mL TFA. The mixture was stirred at room temperature overnight. The reaction mixture was concentrated under reduced pressure and co-evaporated with toluene. The residue was washed with Et_2O to induce the precipitation of the product. The product was obtained as a white solid (1.0 g, 95%). R_f (EtOAc) = 0.12.

^{1}H NMR (200 MHz, $CDCl_3$): δ = 6.00 – 5.80 (m, 1H, CH_{Alloc}), 5.37 – 5.11 (m, 2H, CH_2-*Alloc*), 4.53 (d, *J* = 5.1 Hz, 2H, CH_2-*Alloc*), 3.97 (t, *J* = 6.2 Hz, 1H, CH_α-*Lys*), 3.79 (s, 3H, CH_3), 3.27 – 3.10 (m, 2H, $CH_{2\varepsilon}$-*Lys*), 2.00 – 1.85 (m, 2H, $CH_{2\beta}$-*Lys*), 1.62 – 1.35 (m, 4H, $CH_{2\delta}$-*Lys* and $CH_{2\gamma}$-*Lys*) ppm.
m/z (ESI$^+$) = [M+H$^+$]245.20; $C_{11}H_{21}N_2O_4^+$ requires 245.15

Product 62

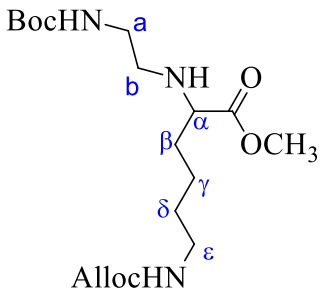

$C_{18}H_{33}N_3O_6$
MW: 387.47

To a solution of 1.0 g (1.0 eq, 4.3 mmol) H-Lys(Alloc)-OMe in 50 mL MeOH was added 0.68 g (1.0 eq, 4.3 mmol) *N*-Boc-aminoacetaldehyde. The mixture was stirred for 30 minutes at room temperature. The solution was cooled to 0°C and 0.27 g (1.0 eq, 4.3 mmol) $NaBH_3CN$ and 0.25 mL (1.0 eq, 4.3 mol) CH_3COOH were added. The reaction mixture was concentrated under reduced pressure after 2 h and the residue was dissolved in EtOAc and was extracted with sat. $NaHCO_3$-solution and Brine. After the organic layers were dried over $MgSO_4$ and concentrated under reduce pressure. The residue was purified by Flash Column Chromatography (CH/EtOAc = 10:1→1:1) and the product was obtained as a clear oil (1.2 g, 70%). R_f (CH/EtOAc = 1:1) = 0.27.

^{1}H-NMR (200 MHz, $CDCl_3$): δ = 6.06 – 5.78 (m, 1H, CH_{Alloc}), 5.39 – 5.14 (m, 2H, CH_2-*Alloc*), 4.96 (bs, 1H, NH-*Boc*), 4.54 (d, *J* = 5.5 Hz, 2H, CH_2-*Alloc*), 3.71 (s, 3H, CH_3), 3.19 (dq, *J* = 12.5, 6.5 Hz, 4H, CH_2-*b*, CH_α-*Lys* and $CH_{2\varepsilon}$-Lys), 2.85 – 2.60 (m, 1H, CH-*a*), 2.62 – 2.44 (m, 1H, CH-*a*), 1.66 – 1.16 (m, 6H, $CH_{2\beta}$-*Lys*, $CH_{2\gamma}$-*Lys* and $CH_{2\delta}$-*Lys*), 1.43 (s, 9H, 3 x CH_3-*Boc*) ppm.

^{13}C-NMR (50 MHz, $CDCl_3$): δ = 175.9, 156.2, 133.1, 117.7, 111.8, 79.4, 65.6, 61.0, 58.5, 51.9, 47.6, 40.8, 33.1, 29.8, 28.5, 23.0, 18.5 ppm.

m/z (ESI$^+$) = [M+H$^+$]388.13; $C_{18}H_{33}N_3O_6$ requires 387.24

Product 70

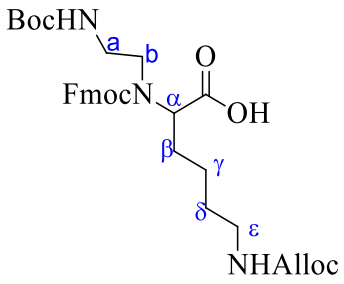

$C_{32}H_{41}N_3O_8$
MW: 595.68

2.6 g BocNH-C_2H_4-Lys(Alloc)-OCH_3 (1.0 eq, 6.7 mmol) was dissolved in 15 mL Dioxane and was added 2M $LiOH/H_2O$ (1.2 eq) solution was added at 0°C and stirred overnight. After, a mixture of 1.7 g Fmoc-Cl (1.0 eq, 6.7 mmol) in THF was added and the mixture was stirred for 3h. The end of the reaction was verified by TLC and after sat. $NaHCO_3$ solution added. The reaction mixture was neutralized with 2M HCl-solution and extracted with EtOAc. The combined organic layers were dried over $MgSO_4$, filtered and concentrated under reduced pressure. The Flash Column Chromatography (CH/EtOAc = 10:1→1:1→0:1) afford the product as a colorless oil (2.4 g, 60%). R_f (EtOAc) = 0.31.

^{1}H NMR (200 MHz, $CDCl_3$): δ = 7.77 – 7.72 (m, 2H, CH-*Fmoc*), 7.55 (d, *J* = 5.8 Hz, 2H, CH-*Fmoc*), 7.51 – 7.21 (m, 4H, CH-*Fmoc*), 5.90 (d, *J* = 9.9 Hz, 1H, CH_{Alloc}), 5.36 – 5.06 (m, 2H, CH_2-*Alloc*), 4.98 (bs, 1H, NH-*Boc*), 4.72 – 4.46 (m, 4H, CH_2-*Alloc* and CH_2-*Fmoc*), 4.30 – 4.09 (m, 1H, CH-*Fmoc*), 3.19 (dt, *J* = 28.7, 6.1 Hz, 5H, $CH_{2\varepsilon}$-Lys, CH_2-*b* and CH_α-*Lys*), 2.86 (bs, 2H, $CH_{2\beta}$-*Lys*), 2.04 – 1.13 (m, 4H, $CH_{2\gamma}$-*Lys* and $CH_{2\delta}$-*Lys*), 1.44 (s, 9H, 3 x CH_3-*Boc*) ppm.

^{13}C NMR (50 MHz, $CDCl_3$): δ = 174.3, 156.52, 144.0, 141.5, 133.1, 127.9, 127.4, 127.2, 124.9, 120.0, 117.7, 79.6, 65.6, 60.7, 55.4, 47.5, 40.8, 39.7, 29.4, 28.5, 23.7 ppm.

m/z (ESI$^+$) = [M+H$^+$]596.00; $C_{32}H_{41}N_3O_8$ requires 595.29

Product 97

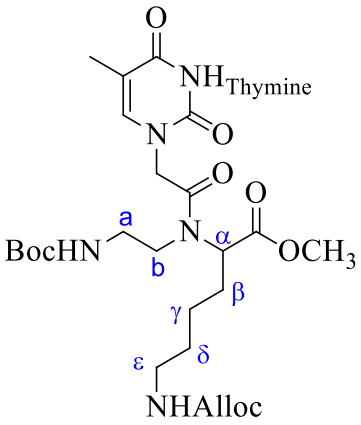

$C_{25}H_{39}N_5O_9$
MW: 553.61

To a solution of 12 mg Thymine-1-acetic acid (1.0 eq, 0.062 mmol) and 11 mg DhbtOH (1.1 eq, 0.07 mmol) in dry DMF was added 13 mg DCC (1.0 eq, 0.062 mmol) and stirred for 30 minutes at room temperature. After BocNH-C_2H_4-Lys(Alloc)-OMe was added to the solution and the reaction mixture was stirred for 6h. After, the reaction mixture was filtered off and the solution was concentrated under reduced pressure. The residue was purified by Flash Column Chromatography (CH/EtOAc = 1:1→0:1) and afford the product as a colorless oil (22 mg, 65%). R_f (EtOAc) = 0.31.

^{1}H-NMR (200 MHz, $CDCl_3$): δ = 6.97 (s, 1H, $CH_{Thymine}$), 6.07 – 5.79 (m, 1H, CH_{Alloc}), 5.61 – 5.30 (m, 3H, CH_2-*Alloc* and NH), 5.29 - 5.16 (m, 2H, CH_2-*Alloc*), 4.39 – 4.22 (m, 2H, CH_2), 4.17 – 4.06 (m, 1H, CH_{α}-*Lys*), 3.73 (s, 3H, CH_3), 3.57 – 3.03 (m, 5H, CH_2-*b*, $CH_{2\varepsilon}$-*Lys*), 2.11 – 1.76 (m, 2H, $CH_{2\beta}$-*Lys*), 1.76 (s, 3H, CH_3-*Thymine*), 1.44 (s, 9H, CH_3-*Boc*), 1.66 – 1.18 (m, 4H, $CH_{2\gamma}$-*Lys* and $CH_{2\delta}$-*Lys*) ppm.

Product 87

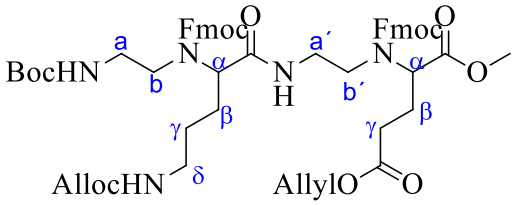

$C_{57}H_{67}N_5O_{13}$
MW: 1030.17

To a solution of 538 mg (1.0 eq, 1.0 mmol) Product 69 in 1.0 mL DMF was added 0.52 mL (3.0 eq, 3.0 mmol) DIPEA and 260 mg (1.1 eq, 1.1 mmol) HBTU and the mixture was stirred for 5 minutes at room temperature. After was added to the mixture 540 mg (1.0 eq, 1.0 mmol) Product 51 in 1.0 mL DMF and the solution was stirred for 1h. The mixture was quenched with H_2O and the aqueous layer was extracted with EtOAc. After the organic layer was dried over $MgSO_4$ and concentrated. The residue was purified by Flash Column Chromatography (CH/EtOAc = 10:1→2:1). The product was obtained as a clear foam (620 mg, 60%).

^{1}H-NMR (500 MHz, DMSO-*d_6*): δ = 7.89 – 7.84 (m, 4H, CH-*Fmoc*), 7.79 – 7.57 (m, 6H, CH-*Fmoc* + 2 x NH, 7.47 – 7.28 (m, 8H, CH-*Fmoc*), 7.21 – 7.16 (m, 1H, NH), 5.92 – 5.84 (m, 2H, 2 x CH_{Alloc}), 5.29 – 5.13 (m, 4H, 2 x CH_2-*Alloc*), 4.52 – 4.18 (m, 12H, 2 x CH_2-*Alloc*, 2 x CH_2-*Fmoc*, 2 x CH-*Fmoc,* $CH_α$-*Glu* and $CH_α$-*Orn*), 3.56 (s, 3H, CH_3), 3.27 – 2.96 (m, 8H, CH_2-*b,* CH_2-*b´*, CH_2-*a* and CH_2-*a´*), 2.20 – 1.97 (m, 2H, $CH_{2γ}$-*Glu*), 1.90 – 1.72 (m, 2H, $CH_δ$-*Orn* and $CH_β$-Glu), 1.05 – 1.45 (m, 2H, $CH_δ$-*Orn* and $CH_β$-Glu), 1.34 (s, 9H, 3 x CH_3-*Boc*), 1.39 – 1.27 (m, 4H, $CH_{2β}$-*Orn* and $CH_{2γ}$-*Orn*) ppm.

^{13}C-NMR (125 MHz, $CDCl_3$): δ = 155.9 (C), 143.8 (C), 140.7, 133.8 (CH_{Alloc}), 132.6, 127.7 (CH-*Fmoc*), 127.1 (CH-*Fmoc*), 127.0 (CH-*Fmoc*), 125.1 (CH-*Fmoc*), 124.6, 120.1, 117.8 (CH_2-*Alloc*), 116.9, 64.5 (CH_2-*Alloc*), 64.1 (CH_2-*Alloc*), 67.5 (CH_2-Fmoc), 60.3 ($CH_α$-Orn), 58.9 ($CH_α$-Glu), 53.01 (CH_3), 47.4 (CH), 47.3 (CH), 46.7

(CH_2), 40.1 (CH), 38.4 (CH), 30.9 (CH-*Glu*), 29.1 (CH_2-*Orn*), 29.9 (CH_3-*Boc*), 27.4 (CH_2-*Orn*), 27.1 (CH-*Glu*), 25.1 (CH-*Glu*), 25.3 (CH-*Glu*) ppm.

R_t (H_2O + 0.1 % TFA / ACN + 0.1% :5 0/50 → 0/100) = 10.3 min

m/z (ESI$^+$) = [M+H$^+$]1044.27; $C_{58}H_{69}N_5O_{13}$ requires 1043.49

Product 92

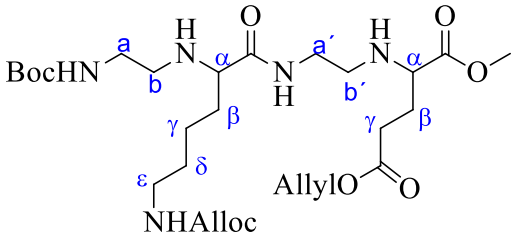

$C_{28}H_{49}N_5O_9$
MW: 599.72

To a solution of 250 mg (0.24 mmol) Product 88 in 5 mL DMF was 0.5 mL DEA added. The reaction mixture was stirred overnight. After The reaction mixture was concentrated under reduced pressure. The residue was purified by Flash Column Chromatography (DCM/MeOH = 20:1). The product was obtained as a clear oil (115 mg, 80%).

^{1}H-NMR (400 MHz, $CDCl_3$): δ = 5.89 – 5.78 (m, 2H, 2 x CH_{Alloc}), 5.27 – 5.02 (m, 4H, 2 x CH_2-*Alloc*), 4.44 (ddt, *J* = 27.3, 5.3, 1.5 Hz, 4H, 2 x CH_2-*Alloc*), 3.62 (s, 3H, CH_3), 3.27 – 3.16 (m, 4H, 2 x CH_2-*b*), 3.11 – 2.89 (m, 4H, CH_α-*Glu*, $CH_{2\varepsilon}$-*Lys* and CH_α-*Lys*), 2.67 – 2.61 (m, 1H, CH_β-*Glu*), 2.57 – 2.34 (m, 5H, CH_β-*Glu*, $CH_{2\gamma}$-*Glu* and CH_2-*a*), 1.93 – 1.73 (m, 2H, CH_2-*a*), 1.52 (tdd, *J* = 15.8, 11.4, 6.8 Hz, 2H, $CH_{2\beta}$-*Lys*), 1.45 – 1.38 (m, 2H, $CH_{2\gamma}$-*Lys*), 1.34 (s, 9H, 3 x CH_3-*Boc*), 1.30 – 1.20 (m, 2H, $CH_{2\delta}$-*Lys*) ppm.

^{13}C-NMR (101 MHz, $CDCl_3$): δ = 176.81, 173.92, 172.68, 156.67, 137.49, 133.13, 117.67, 115.31, 79.58, 77.36, 65.60, 64.08, 61.99, 59.93, 52.82, 48.39, 42.12, 40.59, 40.41, 37.21, 30.12, 29.62, 28.57, 26.08, 23.36 ppm.

m/z (ESI$^+$) = [M+H$^+$]600.13; $C_{32}H_{41}N_3O_8$ requires 599.35

Product 94

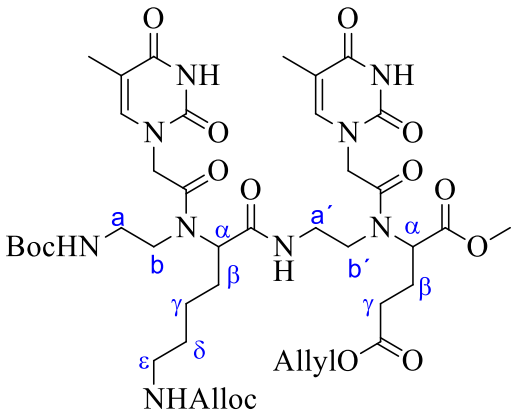

$C_{43}H_{63}N_9O_{14}$
MW: 930.01

To a solution of 43 mg (2.0 eq, 0.23 mmol) thymine-1-acetic acid in 3 mL DMF was 42 mg (2.2 eq, 0.25 mmol) DhbtOH and 48 mg (2.0 eq, 0.23 mmol) DCC added and stirred for 30 minutes at room temperature. After, 97 mg (1.0 eq, 0.16 mmol) Product 92 were added to the reaction mixture and stirred for 1h. The reaction mixture was filtered off and the solution was quenched with H_2O. The aqueous layer was extracted several times with EtOAc. After the organic layer was dried over $MgSO_4$ and concentrated. The residue was purified by Flash Column Chromatography (CH/EtOAc = 5:2). The product was obtained as a clear foam (140 mg, 65%).

^{1}H-NMR (400 MHz, MeOD-d_4): δ = 7.43 – 7.23 (m, 2H, 2 x $CH_{Thymine}$), 5.99 – 5.88 (m, 2H, 2 x CH_{Alloc}), 5.39 – 5.08 (m, 4H, 2 x CH_2-*Alloc*), 4.79 – 4.36 (m, 9H, 2 x CH_2-*Alloc,* 2 x CH_2-*Thymine* and CH_α-*Lys*), 4.31 – 4.17 (m, 1H, CH_α-*Glu*), 3.83 – 2.99 (m, 13H, CH_2-*a*, CH_2-*a´*, CH_2-*b* and CH_2-*b´*,CH_3 and $CH_{2\varepsilon}$-*Lys*), 2.59 – 2.16 (m, 4H, $CH_{2\gamma}$-

Glu and 2 x CH_{β}-*Glu*), 2.10 – 1.92 (m, 2H, $CH_{2\beta}$-*Lys*), 1.90 – 1.69 (m, 6H, 2 x CH_3-*Thymine*), 1.69 – 1.52 (m, 2H, $CH_{2\delta}$-*Lys*), 1.44 (m, 9H, 3 x CH_3-*Boc*), 1.41 – 1.20 (m, 2H, $CH_{2\gamma}$-*Lys*) ppm.

m/z (ESI^+) = $[M+H^+]$931.80; $C_{43}H_{63}N_9O_{14}$ requires 931.80

Product 91

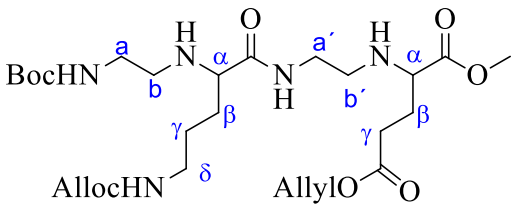

$C_{27}H_{47}N_5O_9$
MW: 585.34

To a solution of 250 mg (0.24 mmol) Product 87 in 5 mL DMF was 0.5 mL DEA added. The reaction mixture was stirred overnight. After The reaction mixture was concentrated under reduced pressure. The residue was purified by Flash Column Chromatography (DCM/MeOH = 20:1). The product was obtained as a clear oil (112 mg, 80%).

^{1}H-NMR (400 MHz, $CDCl_3$): δ = 7.60 (s, 1H, NH), 6.06 – 5.77 (m, 2H, 2 x CH_{Alloc}), 5.37 – 5.06 (m, 6H, 2 x CH_2-*Alloc* and 2 x NH), 4.61 – 4.43 (m, 2H, CH_2-*Alloc*), 4.41 – 4.27 (m, 1H, CH_{α}-*Glu*), 4.17 – 4.06 (m, 2H, CH_2-*Alloc*), 3.80 – 3.56 (m, 4H, CH_3 and CH-*a*), 3.54 – 3.42 (m, 1H, CH-*a*), 3.32 – 3.12 (m, 7H, CH_2-*b*, CH_2-*b´*, CH_2-*a´*, CH_{α}-*Orn*), 2.85 – 1.91 (m, 6H, $CH_{2\beta}$-*Glu,* $CH_{2\gamma}$-*Glu* and $CH_{2\delta}$-*Orn*), 1.70 – 1.46 (m, 4H, $CH_{2\beta}$-*Orn* and $CH_{2\gamma}$-*Orn*), 1.37 (s, 9H, 3 x CH_3-*Boc*) ppm.

^{13}C-NMR (101 MHz, $CDCl_3$): δ = 133.2, 13.3, 117.0, 116.0, 64.8, 62.4, 59.9, 51.0, 47.6, 46.8, 40.1, 38.6, 32.9, 30.0, 29.4, 27.7, 27.4, 22.7 ppm.

Product 93

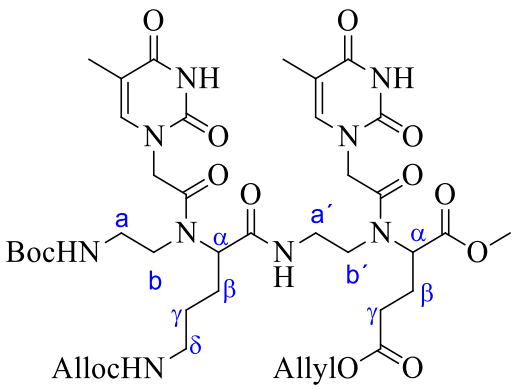

$C_{42}H_{61}N_9O_{14}$
MW: 917.96

To a solution of 43 mg (2.0 eq, 0.23 mmol) thymine-1-acetic acid in 3 mL DMF was 42 mg (2.2 eq, 0.25 mmol) DhbtOH and 48 mg (2.0 eq, 0.23 mmol) DCC added and stirred for 30 minutes at room temperature. After, 97 mg (1.0 eq, 0.16 mmol) Product 91 were added to the reaction mixture and stirred for 1h. The reaction mixture was filtered off and the solution was quenched with H_2O. The aqueous layer was extracted several times with EtOAc. After the organic layer was dried over $MgSO_4$ and concentrated. The residue was purified by Flash Column Chromatography (CH/EtOAc = 5:2). The product was obtained as a clear foam (138 mg, 65%).

^{1}H-NMR (400 MHz, $CDCl_3$): δ = 7.24 (s, 1H, NH), 7.22 – 6.88 (m, 2H, 2 x $NH_{Thymine}$), 5.93 – 5.83 (m, 2H, 2 x CH_{Alloc}), 5.57 (bs, 1H, NH), 5.45 (bs, 1H, NH), 5.41 – 5.10 (m, 4H, 2 x CH_2-*Alloc*), 4.88 – 4.28 (m, 9H, 2 x CH_2-*Alloc*, 2 x CH_2-*Thymine* and CH_α-*Glu*), 3.86 – 3.72 (m, 3H, CH_3), 3.67 – 3.04 (m, 9H, CH_2-*a*, CH_2-*a´*, CH_2-*b*, CH_2-*b´* and CH_α-*Orn)*, 2.15 – 1.93 (m, 6H, $CH_{2\beta}$-*Glu,* $CH_{2\gamma}$-*Glu* and $CH_{2\delta}$-*Orn*), 1.94 – 1.65 (m, 6H, 2 x CH_3-*Thymine*), 1.42 (s, 9H, 3 x CH_3-*Boc*), 1.63 – 1.41 (m, 4H, $CH_{2\beta}$-*Orn* and $CH_{2\gamma}$-*Orn*) ppm.

^{13}C-NMR (101 MHz, $CDCl_3$): δ = 176.8, 173.1, 172.7, 171.8, 171.5, 170.7, 168.7, 168.8, 164.41, 156.6, 151.4, 142.0, 141.5, 133.1, 132.0, 129.2, 128.4, 125.4, 118.9,

117.7, 110.5, 100.1, 80.0, 65.6, 60.0, 59.53.53.1, 52.8, 49.3, 40.5, 37.5, 33.9, 32.0, 30.5, 29.6, 28.6, 26.8, 25.5, 25.0, 24.1, 23.5, 22.8 ppm.

m/z (ESI^+) = [M-H^-]916.20; $C_{42}H_{61}N_9O_{14}$ requires 917.14

II.-2. Liquid phase: strategy 2

Boc-Lys(Fmoc)-OCH_3 (27)

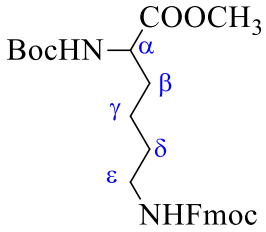

$C_{27}H_{34}N_2O_6$
MW: 482.57

To a solution of 5.0 g Boc-Lys(Fmoc)-OH (1.0 eq, 11 mmol) in 30 mL DMF was added at 0°C 3.5 g Cs_2CO_3 (1.0 eq, 11 mmol) and 1.0 mL MeI (1.5 eq, 17 mmol). The reaction mixture was stirred for 2 hours at room temperature. After was added H_2O and sat. Brine and the mixture was extracted with EtOAc. The reaction was quenched with sat. NH_4Cl-solution and extract with EtOAc. The combined org. layers were dried over $MgSO_4$, filtered and concentrated under reduced pressure. Following purifications were not necessary. The product Boc-Lys(Fmoc)-OMe was obtained as white solid (4.8 g, 95 %). R_f (EtOAc) = 0.88.

^{1}H-NMR (200 MHz, $CDCl_3$): δ = 7.84 – 7.68 (m, 2H, CH_{ar}-*Fmoc*), 7.59 (d, *J* = 7.1 Hz, 2H, CH_{ar} - *Fmoc*), 7.45 – 7.16 (m, 4H, CH_{ar} -*Fmoc*), 5.02 (d, *J* = 8.5 Hz, 1H, NH_{Boc}), 4.89 - 4.68 (m, 1H, NH_{Fmoc}), 4.47 – 4.07 (m, 4H, CH_2, CH_α-*Lys*, CH), 3.66 (s, 3H,

CH_3), 3.23 – 3.00 (m, 2H, $CH_{2\varepsilon}$-*Lys*), 1.86 – 1.44 (m, 4H, $CH_{2\delta}$-*Lys* and $CH_{2\beta}$-*Lys*), 1.37 (s, 10H, 3xCH_3-*Boc*), 1.32 – 1.14 (m, 2H, $CH_{2\gamma}$-*Lys*) ppm.

^{13}C-NMR (50 MHz, $CDCl_3$): δ = 176.0, 156.7, 127.6, 127.0, 125.0, 119.9 ,66.5 ,53.1 ,52.3 ,47.2 ,40.6 ,32.4 ,29.4 ,28.3 ,22.4 ppm.

H-Lys(Fmoc)-OCH$_3$ (28)

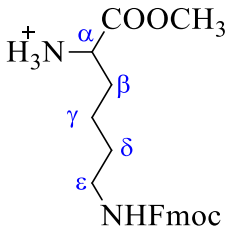

$C_{22}H_{27}N_2O_4^+$
MW:: 383.46

1.4 g Boc-Lys(Fmoc)-OCH_3 (2.9 mmol) was diluted in a 50/50 solution of DCM/TFA and stirred overnight at room temperature. Afterwards the mixture was concentrated under reduced pressure and several times co-evaporated with toluene. The TFA-salt was precipitated with Et_2O, filtrated and washed several times with Et_2O. The white solid was dried on high vacuum. (1.063 g, 96 %). R_f (EtOAc) = 0.15.

^{1}H-NMR(400 MHz, MeOH-d_4): δ = 7.66 (d, *J* = 7.3 Hz, 2H, CH_{ar}-*Fmoc*), 7.48 (d, *J* = 7.0 Hz, 2H, CH_{ar}-*Fmoc*), 7.37 – 7.13 (m, 4H, CH_{ar}-*Fmoc*), 4.37 – 4.19 (m, 2H, CH_2-*Fmoc*), 4.19 – 4.02 (m, 1H, CH-*Fmoc*), 3.70 (s, 3H, CH_3), 3.43 (bs, 1H, CH_α-*Lys*), 3.14 – 2.95 (m, 2H, $CH_{2\varepsilon}$-*Lys*), 1.75-1.54 (m, 2H, $CH_{2\beta}$-*Lys*), 1.53 – 1.35 (m, 4H, $CH_{2\delta}$-*Lys* and $CH_{2\gamma}$-*Lys*) ppm.

^{13}C-NMR (101 MHz, MeOH-d_4): δ = 170.95, 145.28, 142.57, 128.76, 128.11, 126.08, 120.92, 67.60, 53.83, 53.59, 48.45, 41.08, 31.17, 30.36, 23.13 ppm.

m/z (ESI$^+$) = [M+H$^+$]383.20; $C_{22}H_{26}N_2O_4$ requires 382.20

Product 29

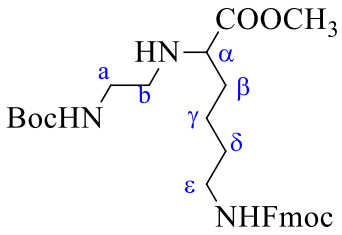

$C_{29}H_{39}N_3O_6$
MW: 525.64

1.06 g H-Lys(Fmoc)-OMe (1.0 eq, 2.78 mmol) and 0.33 g *N*-Boc-aminoacetaldehyd (1.0 eq, 2.78 mmol) were dissolved in 60 mL MeOH and stirred for 30 minutes at room temperature. Then the solution was cooled to 0 °C and 0.14 g $NaBH_3CN$ (1.0 eq, 2.78 mmol) and CH_3COOH (1.1 eq, 2.78 mmol) were added. After the mixture was stirred again for 3 hours, until the TLC showed the end of the reaction. The mixture was concentrated under reduced pressure and the residue was dissolved in DCM and washed with sat. $NaHCO_3$ solution. The combined organic layers were dried over $MgSO_4$, filtered and concentrated under reduced pressure. The Flash Column Chromatography (CH/EtAOc=10:1→0:1) afforded the product as a colorless oil (1.14 g, 78 %). R_f (CH/EtOAc = 1:1) = 0.29.

^{1}H-NMR(200 MHz, $CDCl_3$): δ = δ 7.89-7.71 (m, 2H, CH_{ar}-*Fmoc*), 7.59 (d, *J* = 7.3 Hz, 2H, CH_{ar}-*Fmoc*), 7.52 – 7.20 (m, 4H, CH_{ar}-*Fmoc*), 4.55 -4.52 (bs, 1H, NH), 4.34 - 4.30 (m, 2H, CH_2-*Fmoc*), 4.17 – 4.13 (m, 1H, CH-*Fmoc*), 3.74 (s, 3H, CH_3), 3.40-2.97 (m, 5H, CH_2-*b,* $CH_{2\varepsilon}$-*Lys,* CH_{α}-*Lys*), 2.75 (m, 1H, CH-*a*), 2.68 – 2.41 (m, 1H, CH-*a*), 1.75 – 1.12 (m, 6H, $CH_{2\beta}$-*Lys,* $CH_{2\gamma}$-*Lys* and $CH_{2\delta}$-*Lys*), 1.44 (s, 9H, 3 x CH_3-*Boc*) ppm.

^{13}C-NMR (50 MHz, $CDCl_3$): δ = 175.8, 156.5, 156.1, 144.0, 141.3, 127.6, 127.0, 125.1, 120.0, 66.5, 60.9, 51.8, 47.4, 47.7, 40.3, 40.4, 32.9, 29.6, 28.4, 22.9 ppm.
m/z (ESI$^+$) = [M+H$^+$] 526.27; $C_{29}H_{39}N_3O_6$ requires 525.28.

Product 30

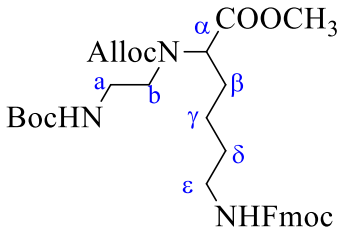

$C_{33}H_{43}N_3O_8$
MW: 609.71

To a solution of 0.7 g Product 29 (1.0 eq, 1.33 mmol) in 10 mL DCM was added 0.23 mL DIPEA (1.0 eq, 1.33 mmol) at 0 °C and dropwise 0.17 mL allyl chloroformate (1.2 eq, 1.6 mmol) and the mixture stirred for 2 h at room temperature. Afterwards the mixture was concentrated under reduced pressure and the residue dissolved in EtOAc. The solution was extracted several times with water and Brine. The combined organic layers were dried over $MgSO_4$, filtered and concentrated under reduced pressure. The Flash Column Chromatography (CH/EtOAc = 7:1→3:1) afford the product as a colorless oil (0.56 g, 68 %). R_f (CH/EtOAc = 1:1) = 0.53.

^{1}H-NMR(200 MHz, $CDCl_3$): δ = 7.85 – 7.67 (m, 2H, CH_{ar}-*Fmoc*), 7.59 (d, *J* = 7.2 Hz, 2H, CH_{ar}-*Fmoc*), 7.48 – 7.18 (m, 4H, CH_{ar}-*Fmoc*), 6.09 – 5.74 (m, 1H, CH_{Alloc}), 5.33-5.18 (m, 2H, CH_2-*Alloc*), 4.60 (d, *J* = 4.5 Hz, 2H, CH_2-*Alloc*), 4.38 (d, *J* = 6.9 Hz, 2H, CH_2-*Fmoc*), 4.34 – 4.14 (m, 1H, CH-*Fmoc*), 3.72 (s, 3H, CH_3), 3.66 – 3.42 (m, 1H, CH-*a*), 3.42 – 2.97 (m, 4H, CH_2-*b,* CH-*a,* CH_{α}-*Lys*), 2.09 – 1.93 (m, 2H, $CH_{2\varepsilon}$-*Lys*), 1.70-1.22 (m, 6H, $CH_{2\beta}$-*Lys,* $CH_{2\gamma}$-*Lys* and $CH_{2\delta}$-*Lys*), 1.44 (s, 9H, 3 x CH_3-*Boc*) ppm.

^{13}C-NMR (50 MHz, $CDCl_3$): δ = 172.25(C), 156.45 (C), 144.13(C) , 141.43 (C) , 132.62 (C), 127.6 (CH_{ar}), 127.0 (CH_{ar}), 125.0 (CH_{ar}),, 119.9 (CH_{ar}), 99.97(CH) , 66.5(CH_2), 60.5 (CH), 52.4 (CH_3), 47.3 (CH), 40.6 (CH_2), 39.7 (CH_2), 29.43 (CH_2), 26.9 (CH_2),23.6 (CH_2) ppm.
m/z (ESI$^+$) = [M+H$^+$] 609.93; $C_{33}H_{43}N_3O_8$ requires 609.31.

Product 32

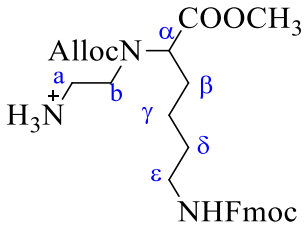

$C_{28}H_{36}N_3O_6^+$
MW: 510.60

260 mg Product 30 (0.43 mmol) was diluted in a 50/50 solution of DCM and TFA (3mL/3mL) and stirred overnight at room temperature. Afterwards the mixture was concentrated under reduced pressure and several times co-evaporated with toluene. The TFA-salt was precipitated with Et_2O, filtrated and washed several times with Et_2O. The white solid was dried on high vacuum (200 mg, 90 %).

^{1}H-NMR(200 MHz, $CDCl_3$): δ = 7.78 - 7.74 (m, 2H, CH-*Fmoc*), 7.35 – 7.09 (m, 2H, CH-*Fmoc*), 7.43 - 7.29 (m, 4H, CH-*Fmoc*), 5.86 – 5.56 (m, 1H, CH_{Alloc}), 5.30 - 5.20 (m, 3H, CH, CH_2-*Alloc*), 5.04 (bs, 1H, NH), 4.61-4.55 (m, 2H, CH_2-*Alloc*), 4.40 - 4.32 (m, 2H, CH_2-*Fmoc*), 4.23-4.16 (m, 1H, CH-*Fmoc*), 3.72 (s, 3H, CH_3), 3.53 – 3.43 (m, 1H, CH-*a*), 3.25 - 3.15 (m, 6H, CH_2-*b*, CH-*a*, CH_α-*Lys* and $CH_{2\varepsilon}$-*Lys*), 1.65 - 1.42 (m, 2H, $CH_{2\beta}$-*Lys*), 1.41 – 1.17 (m, 4H, $CH_{2\gamma}$-*Lys* and $CH_{2\delta}$-*Lys*) ppm.
m/z (ESI$^+$) = [M+H$^+$] 510.27; $C_{28}H_{35}N_3O_6$ requires 510.26

Product 31

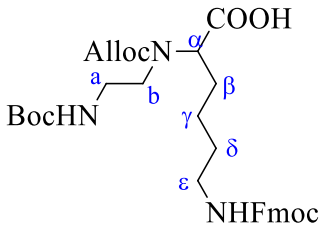

$C_{32}H_{41}N_3O_8$
MW: 595.68

572 mg Product 30 (1.0 eq, 0.94 mmol) was diluted in 5 mL THF and a 2M $LiOH/H_2O$ (1.2 eq) solution added. The mixture was stirred overnight. After a solution of FmocOSu in THF was slowly added and the mixture was stirred for 3h. The end of the reaction was verified by TLC. It was added sat. $NaHCO_3$ solution and the mixture was neutralized with 2M HCl-solution and extracted with EtOAc. The combined organic layers were dried over $MgSO_4$, filtered and concentrated under reduced pressure. The Flash Column Chromatography (CH/EtOAc = 1:1 → 0:1) afford the product as a colorless oil (34 mg, 60%). R_f (CH/EtOAc = 1:1) = 0.14.

^{1}H-NMR (400 MHz, $CDCl_3$): δ = 7.78 - 7.74 (m, 2H, CH-*Fmoc*), 7.63 – 7.54 (m, 2H, CH-*Fmoc*), 7.42 – 7.28 (m, 4H, CH-*Fmoc*), 5.95 - 5.82 (m, 1H, CH_{Alloc}), 5.43 - 5.03 (m, 2H, CH_2-*Alloc*), 4.59 (t, *J* = 6.7 Hz, 2H, CH_2-*Alloc*), 4.44 (bs, 1H, NH), 4.38 - 4.37 (d, *J* = 7.1 Hz, 2H, CH_2-*Fmoc*), 4.13 – 4.10 (m, 1H, CH-*Fmoc*), 3.53 (bs,1H, CH-*a*), 3.46 - 2.95 (m, 6H, CH_α-*Lys,*CH_2-*b,* CH-*a* and $CH_2\varepsilon$-*Lys*), 2.05 (m, 1H, CH_β-*Lys*), 1.92-1.73 (m, 1H, CH_β-*Lys*), 1.64-1.20 (m, 4H, $CH_{2\gamma}$-*Lys* and $CH_{2\delta}$-*Lys),* 1.42 (s, 9H, 3 x CH_3-*Boc*) ppm.

^{13}C-NMR (101 MHz, $CDCl_3$): δ = 156.70 (C), 144.49 (C), 144.11 (C), 141.41 (C), 132.54 (CH_{Alloc}), 127.73 (CH_{ar}), 127.68 (CH_{ar}), 127.16(CH_{ar}), 127.14 (CH_{ar}), 125.03(CH_{ar}), 120.11 (CH_{ar}), 120. 06 (CH_{ar}), 117.99 (CH_2-*Alloc*), 66.68 (2 x CH_2-*Alloc*), 60.75 (CH-*Fmoc*), 50.44 (CH-*Fmoc*), 47.38 (2 x CH-*a,* CH-*Fmoc*), 40.74 (CH_2-

b, CH_{α}-*Lys*), 39.81 (CH_2-*Lys*), 29.23 (2 x CH_2-*Lys*), 28.53 (3 x CH_3-*Boc*), 23.84 (CH_2-*Lys*) ppm.

m/z (ESI^+) = $[M+H^+]$ 596.07; $C_{32}H_{41}N_3O_8$ requires 595.29.

Product 33

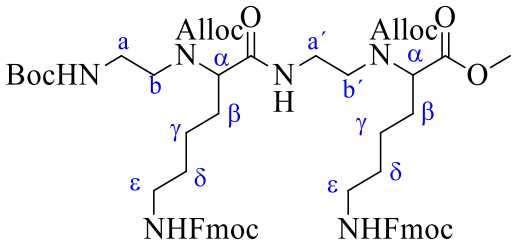

$C_{60}H_{74}N_6O_{13}$
MW: 1087.26

To a solution of 376 mg Product 31 (1.0 eq, 0.063 mmol) in 1.3 mL DMF was added 0.33 mL (3.0 eq, 1.9 mmol) DIPEA and 260 mg (1.1 eq, 0.7 mmol) HBTU and the mixture was stirred for 5 minutes at room temperature. After was added to the mixture 295 mg Product 32 (1.0 eq, 0.063 mmol) in 1.3 mL DMF and the solution was stirred for 1h. The mixture was quenched with H_2O and the aqueous layer was extracted with EtOAc. After the organic layer was dried over $MgSO_4$ and concentrated. The residue was purified by Flash Column Chromatography (CH/EtOAc = 5:2 → 0:1). The product was obtained as a clear foam (44 mg, 65%). R_f (CH/EtOAc = 1:1) = 0.82.

^{1}H-NMR(500 MHz, $CDCl_3$): δ = 7.75 (d, *J* = 7.5 Hz, 4H, CH-*Fmoc*), 7.58 (d, *J* = 7.5 Hz, 4H, CH-*Fmoc*), 7.38 – 7.28 (m, 8H CH-*Fmoc*), 5.97 – 5.81 (m, 2H, 2 x CH_{Alloc}), 5.31– 5.18 (m, 4H, 2 x CH_2-*Alloc*), 5.07 (bs, 2H, NH-*Fmoc*), 4.59 (dt, *J* = 11.7, 5.4 Hz, 4H, CH_2-*Alloc*), 4.37 (dd, *J* = 7.1, 4.1 Hz, 4H, 2 x CH_2-*Fmoc*), 4.21 (d, *J* = 5.8 Hz, 2H, 2 x CH-*Fmoc*), 3.72 (s, 3H, CH_3), 3.52 – 3.07 (m, 10H, 2 x CH_2-*b*, 2 x CH_2-*a*, 2 x CH_{α}-

Lys), 2.07 – 1.66 (m, 6H, 3 x CH_2-Lys), 1.64 – 1.16 (m, 10H, 5 x CH_2-*Lys*), 1.41 (s, 9H, 3 x CH_3-Boc) ppm.

^{13}C-NMR (101 MHz, $CDCl_3$): δ = 132.7 (CH-*Alloc*), 120.4 (CH_{ar}), 125.4 (CH_{ar}), 128.0 (CH_{ar}), 127.3 (CH_{ar}), 132.7 (CH_{Alloc}), 118.2 (CH_2-*Alloc*), 67.0 (CH_2-*Fmoc* and CH_2-*Alloc*), 61.2 (CH-*Fmoc*), 47.8 (CH_2-*a*), 53.0 (CH_3), 41.1 (CH_2-*b,* CH_α-*Lys*), 29.9 (6 x CH_2-Lys), 28.9 (CH_3-*Boc*), 24.2 (2 x CH_2-Lys) ppm.

m/z (ESI$^+$) = [M + Na$^+$] 1109.53; $C_{60}H_{74}N_6O_{13}$ requires 1087.53

Boc-Glu(OBzl)-OCH_3 (73)

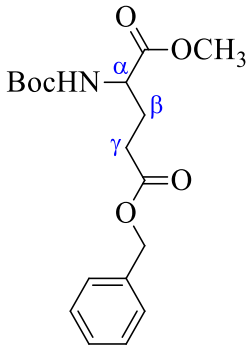

$C_{18}H_{25}NO_6$
MW: 351.39

To a solution of 5.3 g (1.0 eq, 16 mmol) Boc-Glu(Bzl)-OH in 60 mL DMF was added 6.77 g (1.2 eq, 19 mmol) Cs_2CO_3 at 0°C.The mixture was stirred for 10 minutes and dropwise added 1.47 mL (1.5 eq, 24 mmol) MeI. The reaction was stirred for two hours at room temperature. Afterwards quenched with sat. NH_4Cl-solution and extract with EtOAc. The organic layers were dried over $MgSO_4$ and concentrated under reduced pressure. The product Boc-Glu(Bzl)-OMe was obtained as a clear oil (4.0 g, 71%) yield. R_f (CH/EtOAc = 1:1) = 0.89.

^{1}H-NMR (200 MHz, $CDCl_3$): δ = 7.38 - 7.30 (m, 5H, CH_{ar}), 5.11 (s, 2H, OCH_2), 4.43-4.22 (m, 1H, CH_{α}-*Glu*), 3.63 (s, 3H, CH_3), 2.54 – 2.36 (m, 2H, $CH_{2\gamma}$-*Glu*), 2.28 – 2.11 (m, 1H, CH_{β}-*Glu*), 2.04 – 1.86 (m, 1H, CH_{β}-*Glu*), 1.42 (s, 9H,3 x CH_3-*Boc*) ppm.
^{13}C-NMR (50 MHz, $CDCl_3$): δ = 128.6 (CH_{ar}),128.2 (CH_{ar}), 66.5 (CH_2), 52.9 (CH), 52.4(CH_3) ,30.2 (CH_2), 28.3 (CH_3), 27.8 (CH_2) ppm.
m/z (ESI$^+$) = [M+Na$^+$] 374.13; $C_{18}H_{25}NO_6$ requires 351.39

Boc-Glu(Fm)-OCH$_3$ (76)

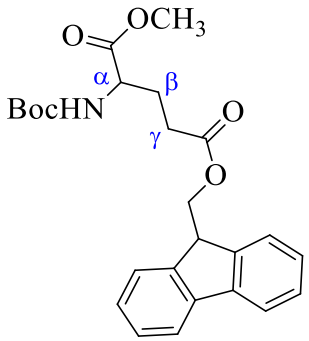

$C_{25}H_{29}NO_6$
MW: 439.50

To a solution of 1.7 g (1.0 eq, 6.7 mmol) Boc-Glu-OMe in 100 mL dry DCM was added 1.16 mL (1.0 eq, 6.7 mmol) DIPEA at argon-atmosphere. The reaction mixture was cooled down to 0 °C and a solution of 1.9 g (1.1 eq, 7.4 mmol) 9-fuorenylmethylchloroformate in 50 mL dry DCM was added. The reaction mixture was stirred for 5 minutes and following was added 0.08 g (0.1-0.15 eq, 6.7 mol) DMAP to the solution. The mixture was after stirred for around 30 minutes at 0 °C. The reaction mixture was diluted with DCM and extracted with sat. NH_4Cl-solution. The organic layers were again extracted with sat. $NaHCO_3$-solution. The organic layers were after dried over $MgSO_4$ and concentrated under reduced pressure. The residue was purified

by Flash Column Chromatography (CH/EtOAc = 10:2). The product Boc-Glu(Fm)-OMe was obtained as a clear oil (2.0 g, 60%). R_f (CH/EtOAc = 1:1) = 0.5.

^{1}H-NMR (200 MHz, $CDCl_3$): δ = 7.83 – 7.72 (m, 2H, CH-*Fmoc*), 7.66 – 7.53 (m, 2H, CH-*Fmoc*), 7.48 – 7.25 (m, 4H, CH-*Fmoc*), 5.12 (d, *J* = 8.0 Hz, 1H, CH_{α}-*Glu*), 4.38 (d, *J* = 6.6 Hz, 2H, CH_2-*Fmoc*), 4.25-4.03 (m, 1H, CH-*Fmoc*), 3.75 (s, 3H, CH_3), 2.59 – 2.35 (m, 2H, $CH_{2\gamma}$-*Glu*), 2.29 - 2.12 (m, 1H, CH_{β}-*Glu*), 2.05 - 1.84 (m,1H, CH_{β}-*Glu*), 1.44 (s, 9H, 3 x CH_3-*Boc*) ppm.

^{13}C-NMR (50 MHz, $CDCl_3$): δ = 172.75 (C), 144.47 (C), 143.86 (C), 141.43 (C), 127.95(CH_{ar}), 127.72 (CH_{ar}), 127.26(CH_{ar}), 127.21(CH_{ar}), 125.15(CH_{ar}), 124.84(CH_{ar}), 120.18 (CH), 80.25, 66.74 (CH_2), 65.49 (CH_2), 52.61 (CH), 50.50 (CH), 46.90 (CH_3) , 30.41 (CH_2), 28.43 (CH_3), 27.90 (CH_2), 27.06 ppm.

H-Glu(Fm)-OCH$_3$ (46)

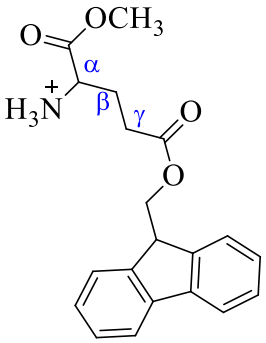

$C_{20}H_{22}NO_4^+$
MW: 340.39

To a solution of 2 g (1.0 eq, 4.8 mmol) Boc-Glu(Fm)-OMe in 50 mL DCM was added 3 mL TFA. The mixture was stirred at room temperature overnight. The reaction mixture was concentrated under reduced pressure. The residue was washed with toluene for an azeotropic mixture and the solution was concentrated under reduced pressure. After the residue was washed with Et_2O to induce the precipitation of the product. The

product H-Glu(Fm)-OMe was obtained as a white solid (1.8 g, 90%). R_f (CH/EtOAc = 10:1) = 0.29.

^{1}H-NMR (200 MHz, $CDCl_3$): δ = 7.80 - 7.76 (m, 2H, CH_{ar}-*Fmoc*), 7.54 (d, *J* = 7.3 Hz, 2H, CH_{ar}-*Fmoc*), 7.47 – 7.25 (m, 4H, CH_{ar}-*Fmoc*), 4.41 – 4.23 (m, 2H, CH_2-*Fmoc*), 4.24 – 4.02 (m, 1H, CH-*Fmoc*), 3.74 (s, 3H, CH_3), 2.76 – 2.54 (m, 2H, $CH_{2\gamma}$-*Glu*), 2.33 – 2.15 (m, 2H, $CH_{2\beta}$-*Glu*) ppm.

Product 48

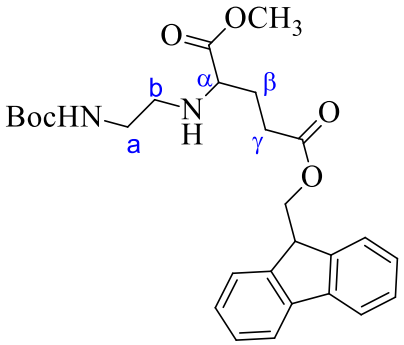

$C_{27}H_{34}N_2O_6$
MW: 482.57

To a solution of 1.31 g (1.0 eq, 3.8 mmol) H-Glu(Fm)-OMe in 100 mL MeOH was added 0.61 g (1.0 eq, 3.8 mmol) *N*-Boc-aminoacetaldehyde. The mixture was stirred for 30 minutes at room temperature. The solution was cooled to 0°C and 0.24 g (1.0 eq, 3.8 mmol) $NaBH_3CN$ and 0.22 mL (1.0 eq, 3.8 mmol) CH_3COOH were added. The reaction mixture was concentrated under reduced pressure after 2 h and the residue was dissolved in EtOAc and was extracted with sat. $NaHCO_3$-solution and Brine. After the organic layers were dried over $MgSO_4$ and concentrated under reduce pressure. The residue was purified by Flash Column Chromatography (CH/EtOAc = 10:2) and the product was obtained as a clear oil (1.3 g, 60%). R_f (CH/EtOAc = 1:1) = 0.55.

^{1}H-NMR (200 MHz, $CDCl_3$): δ = 7.82 – 7.69 (m, 2H, CH-*Fmoc*), 7.65 – 7.51 (m, 2H,CH-*Fmoc*), 7.48 – 7.25 (m, 4H, CH-*Fmoc*), 5.03 (bs, 1H, NH), 4.46 – 4.33 (m, 2H, CH_2-*Fmoc*), 4.19 (t, *J* = 6.9 Hz, 1H, CH-*Fmoc*), 3.70 (s, 3H, CH_3), 3.29 – 3.03 (m, 3H, CH_2-*b* and CH_{α}-*Glu*), 2.79-2.67 (m, 1H, CH-*a*), 2.58 – 2.37 (m, 3H, $CH_{2\gamma}$-*Glu* and CH-*a*), 2.00 – 1.71 (m, 2H, $CH_{2\beta}$-*Glu*), 1.41(s, 9H, 3 x CH_3-*Boc*) ppm.

^{13}C-NMR (50 MHz, $CDCl_3$): δ = 175.3 (C), 173.2 (C), 143.9 (C), 141.4 (C), 127.9 (CH_{ar}), 127.2 (CH_{ar}), 125.2 (CH_{ar}), 125.1 (CH_{ar}), 120.2 (CH_{ar}), 79.3 , 66.5 (CH_2), 60.4 (CH), 52.1 (CH), 47.2 (CH_2) , 46.9 (CH), 31.01 (CH_2), 28.5 (CH_3), 28.4 (CH_2), 27.1 (CH_2) ppm.

Product 50

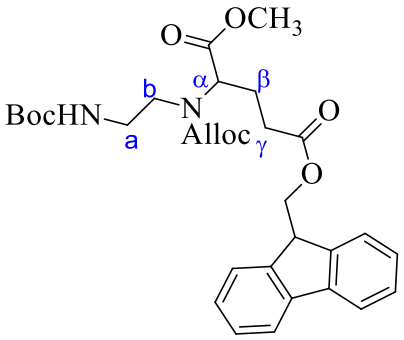

$C_{31}H_{38}N_2O_8$
MW: 566.64

To a solution of 1.0 g (1.0 eq, 2.1 mmol) Product 48 in 50 mL DCM was added 0.37 mL (1.0 eq, 2.1 mmol) DIPEA. The solution was cooled to 0°C and 0.27 mL (1.2 eq, 2.5 mmol) allyl chloroformate was added. After 1 h the reaction mixture was concentrated under reduced pressure and the residue was dissolved in EtOAc. The solution was extracted several times with sat. $NaHCO_3$-solution and Brine. After the organic layers were dried over $MgSO_4$ and concentrated under reduced pressure. The residue was purified by Flash Column Chromatography

(CH/EtOAc = 5:1→1:1). The product was obtained as a clear oil (770 mg, 65%). R_f (CH/EtOAc = 1:1) = 0.71.

^{1}H-NMR (200 MHz, $CDCl_3$): δ = 7.83 – 7.70 (m, 2H, CH_{ar}-F*moc*), 7.70 – 7.46 (m, 2H, CH_{ar}-*Fmoc*), 7.49 – 7.27 (m, 4H, CH_{ar}-*Fmoc*), 6.02 - 5.76 (m, 1H, CH_{Alloc}), 5.33 - 5.15 (m, 2H, CH_2-*Alloc*), 4.53 - 4.50 (m, 2H, CH_2-*Alloc*), 4.45 (d, *J* = 6.7 Hz, 2H, CH_2-*Fmoc*), 4.20 (t, *J* = 6.7 Hz, 1H, CH-*Fmoc*), 4.13 - 3.96 (m, 1H, CH_{α}-*Glu*), 3.69 (s, 3H, CH_3), 3.62 - 3.49 (m, 1H, CH-*a*),3.32 - 3.13 (m, 2H, CH_2-*b*), 3.09 - 2.93 (m, 1H, CH-*a*), 3.16-2.43 – 2.10 (m, 4H, $CH_{2\beta}$-*Glu* and $CH_{2\gamma}$-*Glu*), 1.36 (s, 9H, 3 x CH_3-*Boc*) ppm.
^{13}C-NMR (50 MHz, $CDCl_3$): δ = 172.2 (C), 172.0 (C), 156.1 (C), 155.5 (C), 143.1 (C), 140.8 (C), 131.9 (CH), 127.3(CH_{ar}), 126.6 (CH_{ar}), 124.4 (CH_{ar}), 119.5 (CH_{ar}), 117.4 (CH_2), 78.7 , 66.0 (CH_2), 65.9 (CH_2), 59.5 (CH), 52.0 (CH), 46.3 (CH), 39.0 (CH_2), 30.02 (CH_2), 27.91 (CH_3), 26.41 (CH_2) ppm.

Product 52

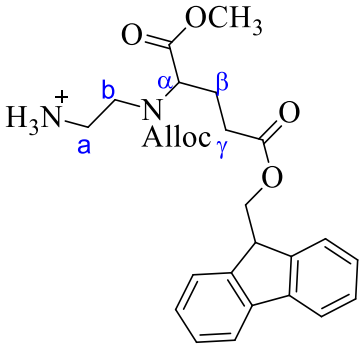

$C_{26}H_{31}N_2O_6^+$
MW: 467.53

820 mg of Product 50 (1.3 mmol) was dissolved in 5mL DCM and 5 mL TFA. The mixture was stirred at room temperature overnight. The reaction mixture was concentrated under reduced pressure and co-evaporated with toluene. The residue was washed with Et_2O to induce the precipitation of the product. The product was obtained as a white solid (510 mg, 85%). R_f (EtOAc) = 0.48.

^{1}H-NMR (200 MHz, $CDCl_3$): δ = 7.74 (d, *J* = 7.3 Hz, 2H, CH_{ar}-*Fmoc*), 7.59 (d, *J* = 6.3 Hz, 2H, CH_{ar}-*Fmoc*), 7.45 – 7.27 (m, 4H, CH_{ar}-*Fmoc*), 5.99 – 5.66 (m, 1H, CH_{Alloc}), 5.33 – 5.10 (m, 2H, CH_2-*Alloc*), 4.64 – 4.35 (m, 4H, CH_2-*Alloc* and CH_2-*Fmoc*), 4.11 (d, *J* = 10.6 Hz, 1H, CH-*Fmoc*), 3.74 (s, 3H, CH_3), 3.51 – 3.04 (m, 6H, CH_2-*a*, CH_2-*b* and $CH_{2\gamma}$-*Glu*), 2.47 – 2.20 (m, 2H, $CH_{2\beta}$-*Glu*) ppm.

^{13}C-NMR (50 MHz, $CDCl_3$): δ = 143.7, 141.4, 128.0, 125.1, 120.2, 66.4, 49.6, 39.3 ppm.

Product 99

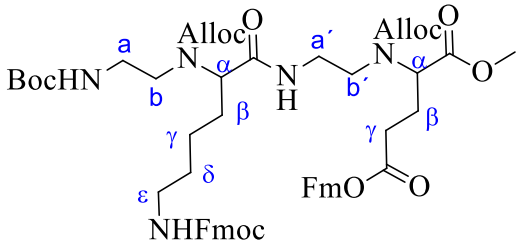

$CH_{58}H_{69}N_5O_{13}$
MW: 1044.19

To a solution of 376 mg (1.0 eq, 0.63 mmol) Product 72 in 1.3 mL DMF was added 0.33 mL (3.0 eq, 1.9 mmol) DIPEA and 260 mg (1.1 eq, 0.07 mmol) HBTU and the mixture was stirred for 5 minutes at room temperature. After was added to the mixture 295 mg (1.0 eq, 0.63 mmol) Product 52 in 1.3 mL DMF and the solution was stirred for 1h. The mixture was quenched with H_2O and the aqueous layer was extracted with EtOAc. After the organic layer was dried over $MgSO_4$ and concentrated. The residue was purified by Flash Column Chromatography (CH/EtOAc = 5:3). The product was obtained as a clear foam (0.5 mg, 80%). R_f (EtOAc) = 0.75.

^{1}H-NMR (500 MHz, DMSO-d_6): δ = 7.92 – 7.81 (m, 4H, CH_{ar}-*Fmoc*), 7.65 (dd, *J* = 17.6, 7.5 Hz, 4H, CH_{ar}-*Fmoc*), 7.44 – 7.28 (m, 8H, CH_{ar}-*Fmoc*), , 5.94 -5.76 (m, 2H, 2 x CH-*Alloc*), 5.41 – 4.99 (m, 4H, 2 x CH_2-*Alloc*), 4.64 – 4.05 (m, 10H, 2 x CH_2-*Alloc*,

2 x CH_2-*Fmoc* and 2 x CH–*Fmoc*), 3.63 (s, 3H, CH_3), 3.47 – 2.88 (m, 10H, CH_{α}-*Lys*, CH_{α}-*Glu,* CH_2-*a*, CH_2-*b,* CH_2-*a´*and CH_2-*b´*), 2.40 (bs, 2H, $CH_{2\gamma}$-*Glu*), 2.14 (q, *J* = 6.6 Hz, 1H, CH_{β}-*Glu*), 2.04 – 1.92 (m, 1H, CH_{β}-*Glu*), 1.81 (bs, 1H, CH_{δ}-*Lys*), 1.61 (bs, 1H, CH_{δ}-*Lys*), 1.41 -1 36 (m, 4H, $CH_{2\gamma}$-*Lys* and $CH_{2\varepsilon}$-*Lys*), 1.34 (s, 9H, 3 x CH_3-*Boc*), 1.18 (bs, 2H, $CH_{2\beta}$-*Lys*) ppm.

^{13}C-NMR (126 MHz, DMSO-d_6): δ = 172.2 (C), 171.0 (C), 170.6 (C), 164.6 (C), 156.0 (C), 155.6 (C), 155.1 (C), 143.9(C), 143.7(C), 143.6 (C), 140.7(C), 133.1 (d, CH_{Alloc}), 127.6 (d, CH_{ar}), 127.0 (d, CH_{ar}), 125.1 (d, CH_{ar}), 120.1 (d, CH_{ar}), 117.0, 116.7 (CH_2-*Alloc*), 65.3 (d, CH_2-*Alloc*), 59.5 (d, CH_2-*Alloc*), 46.8 (CH_2-*Alloc*, CH-*a*, CH-*b*, CH-*a´*and CH-*b´*), 46.3(CH_{α}), 44.3(CH_{α}), 38.24 (CH_3), 30.16 ($CH_{2\gamma}$-*Glu*), 29.1 ($CH_{2\gamma}$-*Lys,* $CH_{2\varepsilon}$-*Lys* and $CH_{2\beta}$-*Lys*), 28.2 (CH_3-*Boc*), 25.0, 24.2, 23.4 (CH_{β}-*Glu*), 23.1 ($CH_{2\delta}$-*Lys*) ppm.

m/z (ESI$^+$) = [M+H$^+$] 1044.00; $C_{58}H_{69}N_5O_{13}$ requires 1044.19

Product 101

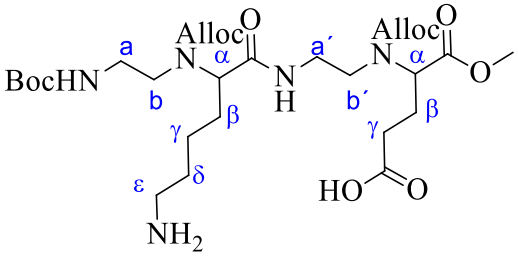

$C_{29}H_{49}N_5O_{11}$
MW: 643.73

To a solution of 386 mg (1.0 eq, 0.37 mmol) Product 99 in 5 mL DMF was added 0.5 mL DEA and the mixture was stirred overnight. The reaction mixture was concentrated

under reduced pressure. The residue was purified by Flash Column Chromatography (CH/EtOAc = 10:2). The product was obtained as a clear oil (0.17 mg, 75%).

^{1}H-NMR (500 MHz, DMSO-d_6): δ = 7.90 (bs, 1H, NH-*amide*), 7.68 (bs, 2H, NH_2-*Lys*), 6.88 (bs, 1H, NH-*amide*), 6.54 (bs, 1H, OH), 5.98 – 5.87 (m 2H, 2 x CH_{Alloc}), 5.42 – 5.06 (m, 4H, 2 x CH_2-*Alloc*), 4.52 (d, *J* = 21.9 Hz, 4H, 2 x CH_2-*Alloc*), 4.33 (bs, 1H, CH_α-*Glu*), 3.11 (td, *J* = 55.7, 55.1, 7.6 Hz, 7H, CH-*a*, CH-*b*,CH-*a´*and CH-*b´*), 2.78 (q, *J* = 7.1, 6.7 Hz, 2H, $CH_{2\varepsilon}$-*Lys*), 2.28 (t, *J* = 8.0 Hz, 2H, CH_{2y}-*Glu*), 2.17 (s, 1H, CH_β-*Glu*), 2.08 – 1.94 (m, 1H, , CH_β-*Glu*), 1.86 (s, 1H, CH_α-*Lys*), 1.69 – 1.48 (m, 2H, $CH_{2\delta}$-*Lys* and $CH_{2\gamma}$-*Lys*), 1.36 (s, 9H, 3 x CH_3-Boc), 1.32-1.21 (m, 2H, $CH_{2\beta}$-*Lys*) ppm.
^{13}C-NMR (126 MHz, DMSO-d_6): δ = 173.8, 171.2, 170.4, 158.0, 157.8, 155.2, 133.2, 133.1, 132.8, 118.2, 116.1, 116.8, 115.81, 77.7, 65.6, 59.2 52.1, 41.5, 38.7, 37.8, 37.4, 30.3, 28.2, 26.9, 25.1, 24.2, 23.0, 22.4 ppm.

m/z (ESI$^+$) = [M+H$^+$] 644.20; $C_{58}H_{69}N_5O_{13}$ requires 643.73

Product 103

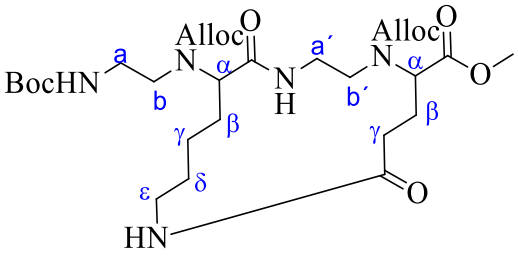

$C_{29}H_{47}N_5O_{10}$
MW: 625.71

To a solution of 48 mg Product 101 (1.0 eq, 0.075 mmol) in 0.75 mL DMF was added 0.04 mL (3.0 eq, 0.22 mmol) DIPEA and 31 mg HBTU (1.1 eq, 0.082 mmol). The mixture was stirred for 1 hour, after quenched with H_2O. The aqueous layer was

extracted several times with EtOAc. After the organic layer was dried over $MgSO_4$ and concentrated under reduced pressure. The residue was purified by Flash Column Chromatography (CH/EtOAc = 5:2). The product was obtained as a clear foam (0.17 mg, 75%).

^{1}H-NMR (500 MHz, DMSO-d_6): δ = 5.89 - 5.79 (s, 2H, 2 x CH_{Alloc}), 5.41 – 5.09 (m, 4H, 2 x CH_2-*Alloc*), 4.56 - 4.48 (m, 4H, 2 x CH_2-*Alloc*), 4.42 - 4.12 (m, 1H, CH_α-*Lys*), 4.04 (s, 3H, CH_3), 3.94 - 3.79 (m, 1H, CH_α-Glu), 3.65 – 2.87 (m, 10H, $CH_{2\varepsilon}$-*Lys,* CH_2-*a,* CH_2-*b,* CH_2-*a´,* CH_2-*b´*), 2.40 - 2.20 (m, 2H, $CH_{2\gamma}$-*Glu*), 2.1 - 1.90 (bs, 2H, $CH_{2\beta}$-*Glu*), 1.80 – 1.60 (m, 2H, $CH_{2\beta}$-*Lys*), 1.6 - 1.45 (m, 4H, $CH_{2\delta}$-*Lys* and $CH_{2\gamma}$-*Lys*), 1.36 (s, 9H, 3 x CH_3-Boc) ppm.

^{13}C-NMR (126 MHz, DMSO-d_6): δ = 135.3, 117.4, 67.8, 56.6, 50.0, 43.9, 42.3, 41.6, 38.5, 32.1, 29.4, 28.8, 25.4, 24.1 ppm.

m/z (ESI$^+$) = [M+H$^+$] 625.99; $C_{29}H_{47}N_5O_{10}$ requires 625.33

Product 104a (Annex I)

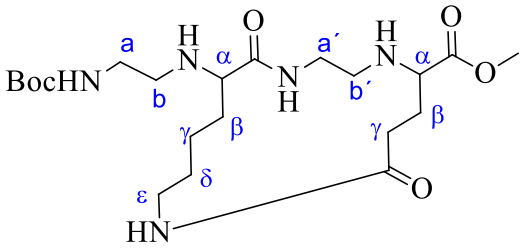

$C_{21}H_{39}N_5O_6$
MW: 457.56

To a solution of 64 mg (1.0 eq, 0.016 mmol) 103 in 5 mL DCM and 0.12 mL (10 eq, 7.2 mmol) Triphenylsilane was added 12 mg (0.1 eq, 0.01 mmol) $Pd(PPh_3)_4$ and the mixture was stirred for 1h. The reaction mixture was concentrated under reduced

pressure. The residue was purified by Flash Column Chromatography (DCM/MeOH= 1:0→50:1). The product was obtained as a clear oil (0.55 mg, 75%).

^{1}H NMR (500 MHz, DMSO-d_6): δ = 7.95 - 7.93 (m, 0.5 H, NH), 7.70 (t, J = 5.6 Hz, 0.5 H, NH), 7.55 (t, J = 5.8 Hz, 0.5 H, NH), 7.45 (dd, J = 7.2, 3.7 Hz, 0.5 H, NH), 6.74 - 6.69 (m, 1H, NH-*Boc*), 3.52 (d, J = 4.9 Hz, 3H, CH_3), 3.50 - 3.43 (m, 1H, CH-*a*), 3.28 – 3.04 (m, 4H, CH-*a,* CH_{α}-*Lys* and $CH_{2\varepsilon}$-*Lys*), 3.03 – 2.89 (m, 5H, CH_2-*b*, CH_2-*b´*and CH-*a´*), 2.80 – 2.68 (m, 1H, CH-*a*), 2.68 – 2.61 (m, 1H), 2.47 – 2.32 (m, 3H, CH_{α}-*Glu*), 2.28 – 2.12 (m, 1H), 2.12 – 1.96 (m, 2H, $CH_{2\gamma}$-*Glu*), 1.94 – 1.84 (m, 1H, CH_{β}-*Glu*), 1.76 – 1.59 (m, 1H, CH_{β}-*Glu*), 1.53 – 1.39 (m, 2H, $CH_{2\delta}$-*Lys*), 1.37 (d, J = 1.3 Hz, 9H, 3 x CH_3-Boc), 1.23 – 1.09 (m, 4H, $CH_{2\gamma}$-*Lys* and $CH_{2\beta}$-*Lys*) ppm.

^{13}C NMR (126 MHz, DMSO-d_6): δ = 175.2(d), 173.9 (d), 171.4 (d), 171.3, 155.6 (d), 77.5, 62.2, 60.5 (d) ,60.4, 59.8, 51.3 (d), 47.4, 46.5, 38.0, 37.5, 32.7 (d), 31.6, 31.4, 28.9, 28.2, 28.1, 27.8, 27.4, 21.7, 21.5 ppm.

m/z (ESI^+) = $[M+H^+]$ 458.13; $C_{21}H_{39}N_5O_6$ requires 457.29

Product 105

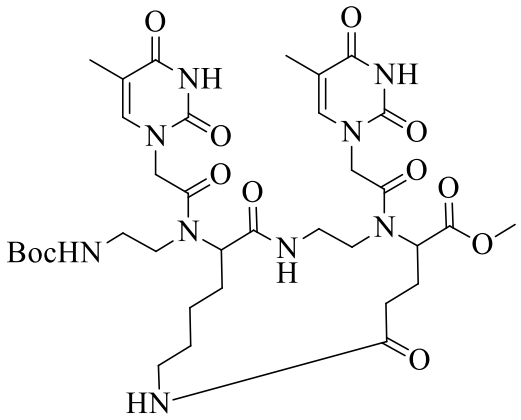

$C_{35}H_{51}N_9O_{12}$
MW: 789.83

To a solution of 64 mg (1.0 eq, 0.016 mmol) Product 104a in 5 mL DCM and 0.12 mL (10 eq, 7.2 mmol) Triphenylsilane was added 12 mg (0.1 eq, 0.01 mmol) $Pd(PPh_3)_4$ and the mixture was stirred for 1h. The reaction mixture was concentrated under reduced pressure. The residue was purified by RP-HPLC (ACN + 0.1% TFA/H_2O + 0.1% TFA). The product was obtained as a clear oil (5 mg, 40%).

R_t (H_2O/ACN + 1%TFA: 100/0 → 50/50(20 min) → 0/100(22 min) → 100/0(30 min)) = 9.34 min

m/z (ESI$^+$) = [M+H$^+$] 789.87; $C_{35}H_{51}N_9O_{12}$ requires 789.37

Boc-Orn(Fmoc)-OH (80)

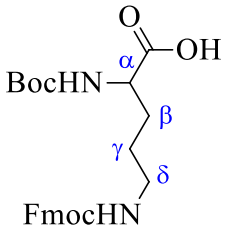

$C_{25}H_{30}N_2O_6$
MW: 454.52

To a solution of 1.71 g Boc-Orn-OH (1.0 eq, 7.4 mmol) in 50 mL DMF and 2 mL H_2O was added Fmoc-OSu and 2.8 mL (2.2 eq, 16 mmol) DIPEA until pH = 9 and stirred for 1h at room temperature. After was added 50 mL sat. $NaHCO_3$-solution and adjusted to pH = 5 with 0.5 M HCl. The mixture was extracted with EtOAc and the combined organic layers were dried over $MgSO_4$, filtered and concentrated under reduced pressure. The Flash Column Chromatography (CH/EtAOc = 2:1 → 0:1) afforded the product as a white solid (3.1 g, 95%).

^{1}H-NMR (400 MHz, $CDCl_3$): δ = δ 7.75 (d, *J* = 7.3 Hz, 2H, CH-*Fmoc*), 7.58 (d, *J* = 7.3 Hz, 2H, CH-*Fmoc*), 7.34 (dt, *J* = 18.1, 7.2 Hz, 4H, CH-*Fmoc*),5.29-5.14 (m, 2H, CH_{δ}-*Orn* and CH_{α}-*Orn*), 4.39 – 4.24 (m, 2H, CH_2-*Fmoc*), 4.20 – 4.12 (m, 1H, CH-*Fmoc*), 3.23-3.05 (m, 1H, CH_{δ}-*Orn*), 2.02-1.52(m, 4H, $CH_{2\beta}$-*Orn and* $CH_{2\gamma}$-*Orn*), 1.44 (s, 9H, 3 x CH_3-*Boc*) ppm.

^{13}C-NMR (101 MHz, $CDCl_3$): δ = 175.4, 163.1, 144.0, 141.4, 127.7, 127.1, 125.3, 120.1, 79.8, 66.8, 53.1, 47.4, 40.7, 36.7, 31.6, 28.5, 25.9 ppm.

m/z (ESI$^-$) = [M-H$^-$] 453.07; $C_{10}H_{20}N_2O_4$ requires 454.31

Boc-Orn(Fmoc)-OMe (55)

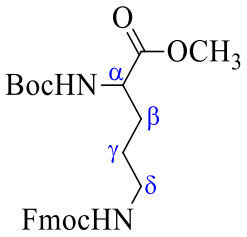

$C_{26}H_{32}N_2O_6$
MW: 468.54

To a solution of 9.7 g Boc-Orn(Fmoc)-OH (1.0 eq, 21 mmol) in 80 mL DMF was added 7.65 g Cs_2CO_3 (1.0 eq, 24 mmol) and 1.0 mL MeI (1.5 eq, 32.5 mmol) at 0°C. The reaction mixture was stirred for 2 h at room temperature. After was added H_2O and Brine. The mixture was extracted with EtOAc. The reaction was quenched with sat. NH_4Cl-solution and extract several times with EtOAc. The combined organic layers were dried over $MgSO_4$, filtered and concentrated under reduced pressure. Following purifications were not necessary. The product Boc-Orn(Fmoc)-OMe was obtained as white solid (9.6 g, 98%). R_f (CH/EtOAc) = 0.55.

^{1}H-NMR (400 MHz, $CDCl_3$): δ = 7.76 (d, *J* = 7.5 Hz, 2H, CH-*Fmoc*), 7.59 (d, *J* = 7.5 Hz, 2H, CH-*Fmoc*), 7.44 – 7.35 (m, 2H, CH-*Fmoc*), 7.31 (td, *J* = 7.4, 1.2 Hz, 2H, CH-*Fmoc*), 5.12(bs, 1H, NH-*Boc*), 4.99 (bs, 1H, NH-*Fmoc*), 4.39 (d, *J* = 6.9 Hz, 2H, CH_2-*Fmoc*), 4.34 – 4.29 (m, 1H, CH-*Fmoc*), 4.25 – 4.16 (m, 1H, CH_{α}-*Orn*), 3.73 (s, 3H, CH_3), 3.27 – 3.17 (m, 2H, $CH_{2\delta}$-*Orn*), 1.90 - 1.73 (m, 1H, CH_{β}-*Orn*), 1.71 - 1.52 (m, 3H, CH_{β}-*Orn* and $CH_{2\gamma}$-*Orn*), 1.45 (s, 9H, 3 x CH_3-*Boc*) ppm.

^{13}C-NMR (101 MHz, $CDCl_3$): δ = 173.1, 156.6, 155.5, 144.1, 141.4, 127.8, 127.2, 125.1, 120.1, 80.2 ,66.7, 53.2, 52.5, 47.4, 40.6, 30.3, 28.5, 26.1 ppm.

m/z (ESI$^+$) = 468.87; $C_{26}H_{32}N_2O_6$ requires 468.23

H-Orn(Fmoc)-OMe (59)

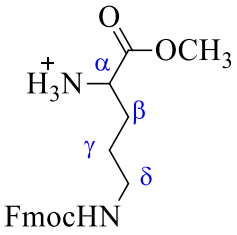

$C_{21}H_{25}N_2O_4^+$
MW: 369.43

1.0 g of Boc-Orn(Fmoc)-OCH_3 (2.2 mmol) was dissolved in 5mL DCM and 5 mL TFA. The mixture was stirred at room temperature overnight. The reaction mixture was concentrated under reduced pressure and co-evaporated with toluene. The residue was washed with Et_2O to induce the precipitation of the product. The product was obtained as a white solid (0.73 g, 90%).

^{1}H-NMR (400 MHz, MeOD-*d*$_4$): δ = δ 7.80 (d, *J* = 7.5 Hz, 2H, CH-*Fmoc*), 7.64 (d, *J* = 7.4 Hz, 2H, CH-*Fmoc*), 7.35 (dt, *J* = 33.8, 7.4 Hz, 4H, CH-*Fmoc*), 4.41 - 4.33 (m, 2H, CH_2-*Fmoc*), 4.22 - 4.19 (m, 1H, CH-*Fmoc*), 4.06 (t, *J* = 6.4 Hz, 1H, CH_{α}-*Orn*), 3.82 (s, 3H, CH_3), 3.16 (t, *J* = 6.6 Hz, 2H, $CH_{2\delta}$-*Orn*), 2.05 – 1.75 (m, 2H, $CH_{2\beta}$-*Orn*), 1.7 - 1.53 (m, 2H, $CH_{2\gamma}$-*Orn*) ppm.

^{13}C-NMR (101 MHz, MeOD -*d*$_4$) δ 170.44, 158.47, 144.87, 142.21, 128.36, 127.70, 125.6, 120.52, 67.29, 53.25, 48.06, 40.36, 28.32, 26.09 .66.37, 65.48, 52.27, 47.07, 39.38, 27.35, 25.11 ppm.

m/z (ESI$^+$) = [M+H$^+$]369.13; $C_{21}H_{24}N_2O_4$ requires 368.18

Product 63

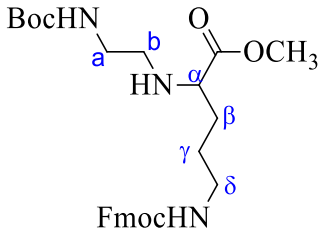

$C_{28}H_{37}N_3O_6$
MW: 511.61

To a solution of 1.31 g (1.0 eq, 3.8 mmol) H-Orn(Fmoc)-OMe in 100 mL MeOH was added 0.61 g (1.0 eq, 3.8 mmol) *N*-Boc-aminoacetaldehyde. The mixture was stirred for 30 minutes at room temperature. The solution was cooled to 0°C and 0.24 g (1.0 eq, 3.8 mmol) $NaBH_3CN$ and 0.22 mL (1.0 eq, 0.0038 mol) CH_3COOH were added. The reaction mixture was concentrated under reduced pressure after 2 h and the residue was dissolved in EtOAc and was extracted with sat. $NaHCO_3$-solution and Brine. After the organic layers were dried over $MgSO_4$ and concentrated under reduce pressure. The residue was purified by Flash Column Chromatography (CH/EtOAc = 5:1→1:1) and the product was obtained as a clear oil (1.3 g, 60%). R_f (EtOAc = 1:1) = 0.47.

^{1}H-NMR (200 MHz, $CDCl_3$): δ = 7.75 (d, *J* = 6.9 Hz, 2H, CH-*Fmoc*), 7.60 (d, *J* = 7.1 Hz, 2H, CH-*Fmoc*), 7.46 – 7.22 (m, 4H, CH-*Fmoc*), 5.34 (bs, 1H, NH-Boc), 5.18 (bs, 1H, NH-Fmoc), 4.40 (d, *J* = 6.7 Hz, 2H. CH_2-*Fmoc*), 4.22 (d, *J* = 6.6 Hz, 1H, CH-*Fmoc*), 3.71 (s, 3H, CH_3), 3.21 – 3.10 (m, 5H, CH_α-*Orn*, $CH_{2\delta}$-Orn, CH_2-*b*), 2.78 – 2.66 (m, 1H, CH-*a*), 2.49 – 2.43 (m, 1H, CH-*a*), 1.94 – 1.46 (m, 4H, $CH_{2\beta}$-*Orn* and $CH_{2\gamma}$-*Orn*), 1.42 (s, 9H, CH_3-*Boc*) ppm.

^{13}C-NMR (101 MHz, $CDCl_3$): δ = 175.66 (C), 156.54 (C), 156.21 (C), 144.11 (C), 141.43 (C), 127.77 (CH_{ar}), 127.15 (CH_{ar}), 125.10 (CH_{ar}), 120.06 (CH_{ar}), 79.31 (CH_2), 66.44 (CH_2), 60.82 (CH), 52.01 (CH_3), 47.65 (CH_2), 47.44 (CH), 40.62 (CH_2), 30.84 (CH), 28.53 (CH_3), 26.52 (CH_2) ppm.

m/z (ESI$^+$) = [M+H$^+$]512.20; $C_{28}H_{37}N_2O_6$ requires 511.27

Product 67

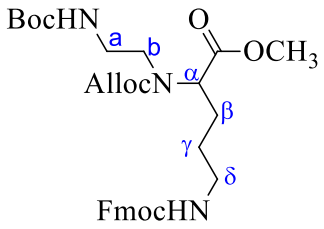

$C_{32}H_{41}N_3O_8$
MW: 595.68

To a solution of 570 mg (1.0 eq, 1.1 mmol) BocNH-C_2H_4-Orn(Fmoc)-OMe in 50 mL DCM was added 0.19 mL (1.0 eq, 1.1 mmol) DIPEA. The solution was cooled to 0°C and 0.14 mL (1.2 eq, 1.3 mmol) allyl chloroformate was added. After 1 h the reaction mixture was concentrated under reduced pressure and the residue was dissolved in EtOAc. The solution was extracted several times with sat. $NaHCO_3$-solution and Brine. After the organic layers were dried over $MgSO_4$ and concentrated under reduced pressure. The residue was purified by Flash Column Chromatography (CH/EtOAc = 6:4 → 1:1). The product was obtained as a clear oil (400 mg, 60%). R_f (CH/EtOAc = 1:1) = 0.69.

^{1}H-NMR (400 MHz, $CDCl_3$): δ = 7.76 (d, *J* = 7.5 Hz, 2H, CH-*Fmoc*), 7.60 (d, *J* = 7.5 Hz, 2H, CH-*Fmoc*), 7.39 (t, *J* = 7.4 Hz, 2H, CH-*Fmoc*), 7.30 (t, *J* = 7.4 Hz, 2H, CH-*Fmoc*), 6.0-5.8 (m, 1H, CH_{Alloc}), 5.36 – 5.09 (m, 3H, CH_2-*Alloc*), 4.60 (t, *J* = 8.0 Hz, 2H, CH_2-*Alloc*), 4.39 (d, *J* = 7.0 Hz, 2H, CH_2-*Fmoc*), 4.25 – 4.19 (m, 1H, CH-*Fmoc*), 3.73 (s, 3H, CH_3), 3.37-3.07 (m, 5H, CH_2-*a* and CH_2-*b*, CH_α-*Orn*), 1.94 (d, *J* = 53.3 Hz, 1H, CH_δ-*Orn*), 2.04-1.77 (m, 1H, CH_δ-*Orn*), 1.64-1.53 (m, 4H, $CH_{2\beta}$-*Orn* and $CH_{2\gamma}$-*Orn*), 1.44 (s, 9H, 3 x CH_3-*Boc*) ppm.

^{13}C-NMR (101 MHz, $CDCl_3$): δ = 172.1, 156.7, 156.3, 144.2, 141.5, 132.6, 127.8, 127.2, 125.2, 120.1, 118.1, 79.5, 66.7, 60.5, 52.6, 47.5, 40.7, 40.0, 28.6, 27.1, 26.7 ppm.

m/z (ESI$^+$) = 595.93; $C_{32}H_{41}N_3O_8$ requires 595.29

Product 71

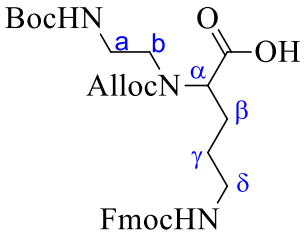

$C_{31}H_{39}N_3O_8$
MW: 581.66

50 mg (1.0 eq, 0.084 mmol) BocN-C_2H_4-Alloc-Lys(Fmoc)-OCH_3 was diluted in 5 mL THF was added 2M LiOH/H_2O (1.2 eq) solution and stirred overnight. After the mixture of Fmoc-OSu (1.0 eq, 0.084 mmol) in THF was added and the mixture was stirred for 3h. The end of the reaction was verified by TLC and added sat. $NaHCO_3$ solution. The solution was neutralized with 2M HCl-solution and extracted with EtOAc. The combined organic layers were dried over $MgSO_4$, filtered and concentrated under reduced pressure. The Flash Column Chromatography (CH/EtOAc = 1:1 → 0:1) afford the product as a colorless oil (50 mg, 60%). R_f (CH/EtOAc = 1:1) = 0.69.

^{1}H NMR (400 MHz, $CDCl_3$): δ = 7.72 (d, *J* = 7.4 Hz, 2H, CH-*Fmoc*), 7.57 (d, *J* = 7.5 Hz, 2H, CH-*Fmoc*), 7.41 – 7.28 (m, 4H, CH-*Fmoc*), 5.85 (bs, 1H, CH_{Alloc}), 5.30 – 5.15 (m, 3H, CH_2-*Alloc*), 4.56 (bs, 2H, CH_2-*Alloc*), 4.46 – 4.25 (m, 3H, CH_2-*Fmoc*), 4.16 (bs, 1H, CH-*Fmoc*), 3.29 – 3.17 (m, 5H, CH_2-*a*, CH_2-*b,* CH_α-*Orn*), 2.11-1.92 (m, 1H, CH_ε-*Orn*), 1.93 – 1.68 (m, 1H, CH_ε-*Orn*), 1.38 - 1.34 (m, 4H, $CH_{2\beta}$-*Orn* and $CH_{2\gamma}$-*Orn*), 1.40 (s, 9H, 3 x CH_3-*Boc*) ppm.

^{13}C NMR (101 MHz, $CDCl_3$): δ = 156.8 (C), 144.2 (C), 141.4 (C), 132.8 (CH_{Alloc}), 127.7 (CH_{Fmoc}), 127.1 (CH_{Fmoc}), 125.3 (CH_{Fmoc}), 120.0 (CH_{Fmoc}), 117.8 (CH_2-*Alloc*), 66.75 (CH_2-*Alloc* + CH_2-*Fmoc*), 53.6, 47.4 (CH-*Fmoc*), 40.8 (CH_2-*a* +CH_2-*b*) 28.6 (CH_3-Boc), 26.8 (3 x CH_2-*Orn*) ppm.

m/z (ESI$^+$) = 595.93; $C_{32}H_{41}N_3O_8$ requires 595.29

Product 100

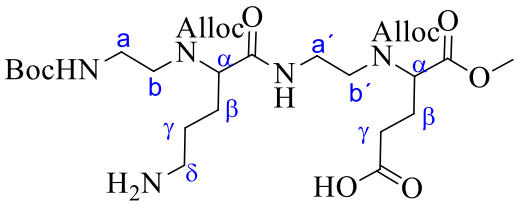

$C_{28}H_{47}N_5O_{11}$
MW: 629.70

To a solution of 150 mg (0.15 mmol) Product 98 in 5 mL DMF was added 1 mL DEA and the mixture was stirred overnight. The reaction mixture was concentrated under reduced pressure and the residue dissolved in EtOAc. The residue was directly purified by Flash Column Chromatography (DCM/MeOH = 10:2). The product was obtained as a clear oil (75 mg, 80 %).

^{1}H-NMR (500 MHz, $CDCl_3$): δ = δ 5.94 – 5.89 (m, 2H, CH-*Alloc*), 5.32 – 5.18 (m, 4H-CH_2-*Alloc*), 4.59 – 4.31 (m, 4H, CH-*Alloc*), 4.43 – 4.24 (m, 2H, CH_α-*Orn* and CH_α-*Glu*), 3.74 (s, 3H, CH_3), 3.70 – 3.55 (m, 2H, CH_2-*a*) 3.44 – 3.19 (m, 6H, CH_2-*b*, CH_2-*b´* and CH_2-*a´*), 3.01 - 2.89 (m, 2H, $CH_{2\delta}$-*Orn*), 2.32 – 1.90 (m, 6H, $CH_{2\gamma}$-*Glu,* $CH_{2\beta}$-*Glu* and $CH_{2\beta}$-*Orn*), 1.73 – 1.54 (m, 2H, $CH_{2\gamma}$-*Orn*), 1.41 (s, 9H, 3 x CH_3-*Boc*) ppm.

^{13}C-NMR (101 MHz, $CDCl_3$): δ = 132.7 (2 x CH_{Alloc}), 118.2 (2 x CH_2-*Alloc*), 67.1 (2 x CH_2-*Alloc*), 61.2 (CH_α-*Glu* and CH_α-*Orn*), 53.0 (CH_3), 48.7 (2 x CH-*a*), 48.9 (CH_2-*b´ and* CH_2-*b*), 40.1 (CH_2-*a´*), 33.8(CH_β-*Glu*), 26.5 (CH_β-*Glu*), 25.5 (3 x CH_2-*Orn*), 29.2 (CH_3-*Boc*) ppm.

m/z (ESI$^+$) = [M+H$^+$]629.33; $C_{57}H_{67}N_5O_{13}$ requires 629.33

Product 102

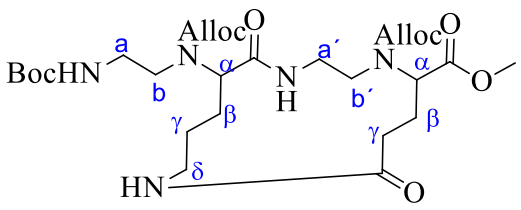

$C_{28}H_{45}N_5O_{10}$
MW: 611.68

To a solution of 48 mg (1.0 eq, 0.075 mmol) Product 100 in 0.75 mL DMF was added 0.04 mL (3.0 eq, 0.22 mmol) DIPEA and 31 mg (1.1 eq, 0.082 mmol) HBTU and the mixture was stirred for 1h. The mixture was quenched with H_2O and the aqueous layer was extracted with EtOAc. After the organic layer was dried over $MgSO_4$ and concentrated. The residue was purified by Flash Column Chromatography (CH/EtOAc = 5:2). The product was obtained as a clear foam (30 mg, 65%).

^{1}H NMR (500 MHz, $CDCl_3$): δ = 5.81 (bs, 2H, 2 x CH-*Alloc*), 5.39 – 5.15 (m, 4H, 2 x CH_2-*Alloc*), 4.77 – 4.43 (m, 5H, 2 x CH_2-*Alloc* and CH_α-*Glu*), 4.19 – 3.89 (m, 2H, CH_α-*Orn* and CH-*a´*), 3.73 (s, 3H, CH_3), 3.57 (bs, 1H, CH-*a´*), 3.31 (s, 4H, CH_2-*b* and CH_2-*b´*), 3.08 (bs, 1H, CH-*a*), 2.93 (bs, 1H, CH-*a*), 2.80 (bs, 1H, CH_γ-*Glu*), 2.51 – 2.38 (m, 1H, CH_γ-*Glu*), 2.29 (bs, 1H, CH_β-*Glu*), 2.00 – 1.81 (m, 3H, CH_β-*Glu* and $CH_{2\delta}$-*Orn*), 1.70 -1.48 (m, 4H, $CH_{2\beta}$-*Orn* and $CH_{2\gamma}$-*Orn*), 1.42 (s, 9H, 3 x CH_3-*Boc*) ppm.

^{13}C-NMR (101 MHz, $CDCl_3$): δ = 172.2 (C), 157.3(C), 156.4 (C), 132.8 (2 x CH_{Alloc}), 132.5, 118.0(2 x CH_2-*Alloc*), 88.0, 66.5 (2 x CH_2-*Alloc*), 52.6 (CH_α-*Orn* and CH-*a*), 51.4 (CH_3), 40.6 (2 x CH-*a´* and CH_2-*b*), 35.6 (CH-*a*), 35.7 (2 x CH_γ-*Glu*), 30.2 (2 x CH_β-*Glu*), 29.9 (CH_3-*Boc*), 28.6 (2 x CH_δ-*Orn*), 26.4 ($CH_{2\beta}$-*Orn* and $CH_{2\gamma}$-*Orn*) ppm.

m/z (ESI$^+$) = [M+H$^+$]612.07; $C_{28}H_{45}N_5O_{10}$ requires 611.32

II.-3. Synthesis of Monomers for Solid-Phase synthesis

Product 117

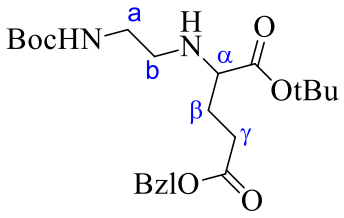

$C_{23}H_{36}N_2O_6$
MW: 436.54

To a solution of 0.5 g H-Glu(OBzl)-OtBu (1.0 eq, 1.5 mmol) in 30 mL MeOH was added 0.24 g *N*-Boc-aminoacetaldehyde (1.0 eq, 1.5 mmol). The mixture was stirred for 30 minutes at room temperature. After the solution was cooled down to 0 °C and 94 mg $NaBH_3CN$ (1.0 eq1.5 mmol) and CH_3COOH (1.0 eq, 1.5 mmol) were added. The mixture was stirred for 2h at room temperature. The reaction mixture was concentrated under reduced pressure, the residue dissolved in EtOAc and washed with sat. $NaHCO_3$-solution. The combined organic layers were dried over $MgSO_4$, filtered and concentrated under reduced pressure. The Flash Column Chromatography (CH/EtOAc=5:1) afforded the product as colorless oil (0.3 g, 46 %). R_f (CH/EtOAc = 1:1) = 0.71

^{1}H-NMR (400 MHz, $CDCl_3$): δ = 7.39-7.27(m, 5H, CH_{ar}), 5.12 (s, 2H, CH_2-*Bzl*), 3.17 (bs, 1H, CH_α-*Glu),* 3.11 – 2.99 (m, 2H, CH_2-*b*), 2.78 – 2.68 (m, 1H, CH-*a*), 2.47 (t, *J* = 7.3 Hz, 3H, $CH_{2\gamma}$-*Glu* and CH-*a*), 2.00 – 1.92 (m, 1H, CH_β-*Glu*), 1.87 – 1.77 (m, 1H, CH_β-*Glu*), 1.44 (d, *J* = 6.2 Hz, 18H, 3 x CH_3 and 3 x CH_3-*t*Bu) ppm.

^{13}C-NMR (101 MHz, $CDCl_3$): δ = 174.3 (C), 173.2 (C), 156.2 (C), 136.1 (C), 128.7 (CH_{ar}), 128.4 (CH_{ar}), 128.4 (CH_{ar}), 66.4 (CH_2), 61.2 (CH), 47.5 (CH_2), 40.5 (CH_2), 31.2 (CH_2), 28.6 (CH_3), 28.2 (CH_3) ppm.

m/z (ESI$^+$) = [M+H$^+$]437.0; $C_{23}H_{36}N_2O_6$ requires 436.5

Fmoc-*D*-Glu(OMe)-OtBu (110)

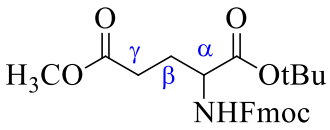

$C_{25}H_{29}NO_6$
MW: 439.50

To a solution of 0.52 g (1.0 eq, 1.22 mmol) Fmoc-*D*-Glu-OtBu in 40 mL DMF was added 0.44 g (1.1 eq, 1.34 mmol) Cs_2CO_3 at 0°C. The mixture was stirred for 2 minutes and added dropwise 0.114 mL (1.5 eq, 1.83 mmol) MeI. The reaction was stirred for 2h at room temperature. The reaction was quenched with sat. NH_4Cl-solution and extracted with EtOAc. The organic layers were dried over $MgSO_4$ and concentrated under reduced pressure. Following purifications were not necessary. The product Fmoc-*D*-Glu(OMe)-OtBu was obtained as a clear oil (100%). R_f (CH/EtOAc = 1:1) = 0.76

^{1}H-NMR (400 MHz, $CDCl_3$): δ = 7.71 (d, *J* = 7.5 Hz, 2H, CH_{ar}-*Fmoc*), 7.54 (d, *J* = 7.4 Hz, 2H, , CH_{ar}-*Fmoc*), 7.34 (t, *J* = 7.5 Hz, 2H, , CH_{ar}-*Fmoc*), 7.30 – 7.22 (m, 2H, , CH_{ar}-*Fmoc*), 5.36 (d, *J* = 8.0 Hz, 1H, NH_{Fmoc}), 4.33 (d, *J* = 7.0 Hz, 2H, CH_2-*Fmoc*), 4.24 (q, *J* = 7.9 Hz, 1H, CH_α-*Glu*), 4.16 (t, *J* = 7.0 Hz, 1H, CH-*Fmoc*), 3.62 (s, 3H, CH_3), 2.45 – 2.26 (m, 2H, $CH_{2\gamma}$-*Glu*), 2.20 – 2.10 (m, 1H, CH_β-*Glu*), 1.96 – 1.86 (m, 1H, CH_β-*Glu*), 1.42 (s, 9H, 3 x CH_3-*t*Bu) ppm.
^{13}C-NMR (101 MHz, $CDCl_3$): δ = 173.40, 171.13, 156.07, 144.0, 143.9, 141.4, 129.2, 128.4, 127.8, 127.2, 125.2, 120.1, 67.2, 53.9, 52.0, 47.3, 30.2, 28.1 ppm.
m/z (ESI$^+$) = 439.73; $C_{25}H_{29}NO_6$ requires 439.20

Product 118

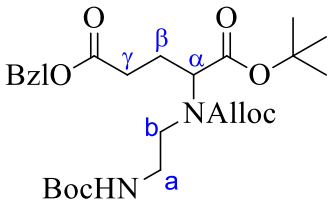

$C_{27}H_{40}N_2O_8$
MW: 520.62

To a solution of 0.19 g (1.0 eq, 0.44 mmol) Product 117 in 10 mL DCM was added 0.056 mL (1.0 eq, 0.44 mmol) DIPEA and 0.076 mL (1.2 eq, 0.528 mmol) Allyl chloroformate at 0°C. After 1h the reaction mixture was concentrated under reduced pressure and the residue dissolved in EtOAc. The solution was extracted several times with sat. $NaHCO_3$-solution and Brine. After the organic layer was dried over $MgSO_4$ and concentrated under reduced pressure. The residue was purified by flash column chromatography (CH/EtOAc = 7:1→1:1) and the product was obtained as clear oil (0.17 g, 75%). R_f (CH/EtOAc = 4:1) = 0.60

^{1}H-NMR (400 MHz, $CDCl_3$): δ = 7.43 – 7.28 (m, 5H, CH_{ar}), 5.94 – 5.79 (m, 1H, CH_{Alloc}), 5.37 (bs, 1H, NH), 5.21-5.07 (m, 2H, CH_2-*Alloc*), 5.07 (s, 2H, CH_2-*Bzl*), 4.71 – 4.43 (m, 2H, CH_2-*Alloc*), 3.93 (bs, 1H, CH_α-*Glu*), 3.64 (dt, *J* = 18.4, 10.1 Hz, 1H, CH-*a*), 3.34 – 3.19 (m, 2H, CH_2-*b*), 3.00 (dt, *J* = 12.1, 5.9 Hz, 1H, CH-*a*), 2.50 – 2.31 (m, 3H, $CH_{2\gamma}$-Glu and CH_β-*Glu*), 2.26 – 2.06 (m, 1H, CH_β-*Glu*), 1.45 (d, *J* = 5.5 Hz, 18H, 3 x CH_3-*Boc* and 3 x CH_3-*t*Bu) ppm.

^{13}C-NMR (101 MHz, $CDCl_3$): δ = 172.8, 172.7, 170.1, 170.0, 156.03, 135.84, 132.70, 132.28, 128.7, 128.4, 118.0, 117.9 82.4, 79.2, 66.5, 61.3, 49.2, 48.5, 39.6, 30.9, 28.5, 28.0, 25.5, 24.7 ppm.

m/z (ESI$^+$) = 520.73; $C_{27}H_{40}N_2O_8$ requires 520.28

Product 119

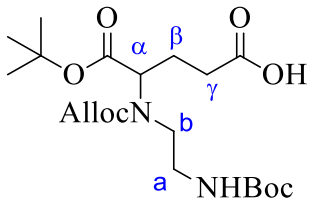

$C_{20}H_{34}N_2O_8$
MW: 430.49

To a solution of 0.17 g (1.0 eq, 0.33 mmol) Product 118 in 10 mL THF was added 1M aqueous solution of LiOH (1.5 eq) at 0°C and stirred at room temperature overnight. The mixture was quenched with H_2O and acidified with 2M HCl solution to pH = 5. The aqueous solution was extracted several times with EtOAc. The organic layers dried over $MgSO_4$ and concentrated under reduced pressure. The residue was purified by flash column chromatography (CH/EtOAc = 10:1 → 1:1) and the product obtained as clear oil (0.09 g, 64%). R_f (CH/EtOAc = 3:1) = 0.70

^{1}H-NMR (400 MHz, $CDCl_3$): δ = 76.71 – 6.40 (m, 1H, OH), 5.87 (m, 1H, CH_{Alloc}), 5.46 (d, *J* = 6.1 Hz, 1H, NH), 5.28 – 5.15(m, 2H, CH_2-*Alloc*), 4.62 – 4.44 (m, 2H, CH_2-Alloc), 3.98 – 3.96 (m, 1H, CH_α-*Glu*), 3.69 – 3.63 (m, 1H, CH-*a*), 3.29 – 3.27 (m, 2H, CH_2-*b*), 3.09 (dt, *J* = 13.0, 6.2 Hz, 1H, CH-*a*), 2.46 – 2.23 (m, 3H, $CH_{2\gamma}$-*Glu* and CH_β-*Glu*), 2.19 – 2.08 (m, 1H, CH_β-*Glu*), 1.43 (d, *J* = 4.9 Hz, 19H, 3 x CH_3-Boc and 3 x CH_3-*t*Bu) ppm.

^{13}C-NMR (101 MHz, $CDCl_3$): δ = 170.2, 156.2, 132.7, 132.3, 118.2, 118.0, 82.5, 79.5, 66.8, 66.5, 61.4, 39.8, 30.7, 28.3, 28.1 ppm.

m/z (ESI$^-$) = [M-H$^-$]429.07; $C_{20}H_{34}N_2O_8$ requires 430.23

Product 112

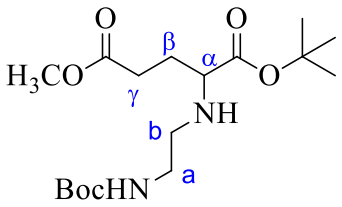

$C_{17}H_{32}N_2O_6$
MW: 360.45

To a solution of 0.19 g (1.0 eq, 0.88 mmol) H-*D*-Glu(OMe)-OtBu in 10 mL MeOH was added 0.14 g (1.0 eq, 0.88 mmol) *N*-Boc-aminoacetaldehyde. The reaction mixture was stirred for 30 minutes at room temperature. The solution was cooled to 0°C and 0.055 g (1.0 eq, 0.88 mmol) $NaBH_3CN$ and 0.05 mL (1.0 eq, 0.88 mmol) CH_3COOH were added. The reaction mixture was stirred at room temperature for 2h and after concentrated under reduced pressure. The residue was after dissolved in EtOAc and washed several times with sat. $NaHCO_3$-solution and Brine. After the organic layer was dried over $MgSO_4$ and concentrated under reduced pressure. The residue was purified by flash column chromatography (CH/EtOAc = 3:1 → 1:1) and the product was obtained as clear oil (0.14 g, 45%).R_f (CH/EtOAc = 1:1) = 0.41

^{1}H-NMR (400 MHz, $CDCl_3$): δ = 5.02 (s, 1H), 3.68 (s, 3H, CH_3), 3.20 (bs, 1H, CH_α-*Glu*), 3.15 – 3.02 (m, 2H, CH_2-*b*), 2.80 - 2.74 (m, 1H, CH-*a*), 2.54 – 2.47 (m, 1H, CH-*a*), 2.42 (td, *J* = 7.4, 3.0 Hz, 2H, $CH_{2\gamma}$-*Glu*), 1.98 – 1.91 (m, 1H, CH_β-*Glu*), 1.87 – 1.77 (m, 1H, CH_β-*Glu*), 1.45 (d, *J* = 6.9 Hz, 21H, 3 x CH_3-Boc and 3 x CH_3-*t*Bu) ppm.
^{13}C-NMR (101 MHz, $CDCl_3$): δ = 176.4, 174.3, 173.9, 156.2, 81.6, 79.2, 61.2, 51.8, 47.5, 40.5, 30.9, 28.6, 28.5, 28.2, 28.1, 23.4 ppm.
m/z (ESI$^-$) = [M+H$^+$]361.0; $C_{17}H_{32}N_2O_6$ requires 360.23

Product 120

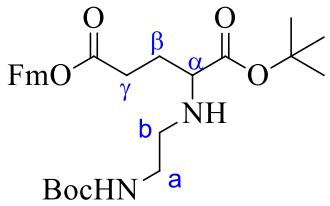

$C_{34}H_{44}N_2O_8$
MW: 608.72

To a solution of 0.74 g (1.0 eq, 1.72 mmol) Product 119 in 20 mL dry DCM at 0°C was added 0.3 mL (1.0 eq, 1.72 mmol) DIPEA at argon-atmosphere. To the reaction mixture was added a solution of 0.49 g (1.1 eq, 1.89 mmol) Fmoc-Cl in 5 mL dry DCM. The mixture was stirred for 5 minutes and 0.025 g (0.1-0.15 eq, 0.2 mmol) DMAP was added. The reaction mixture was after stirred for around 45 minutes at 0 °C and argon-atmosphere, after diluted with DCM and extracted several times with sat. NH_4Cl-solution and sat. $NaHCO_3$-solution. The organic layer was dried over $MgSO_4$ and concentrated under reduced pressure. The residue was purified by flash column chromatography (CH/EtOAc = 3:1) and the product was obtained as white solid (0.5 g, 48 %). R_f (DCM) = 0.3

^{1}H-NMR (400 MHz, $CDCl_3$): δ = 7.77 (d, *J* = 7.5 Hz, 2H, CH_{ar}-*Fm*), 7.58 (d, *J* = 7.4 Hz, 2H, CH_{ar}-*Fm*), 7.41 (t, *J* = 7.4 Hz, 2H, CH_{ar}-*Fm*), 7.32 (t, *J* = 7.4 Hz, 2H, CH_{ar}-*Fm*), 5.96 – 5.80 (m, 1H, CH_{Alloc}), 5.42 – 5.14 (m, 3H, CH_2-*Alloc* and NH), 4.64 – 4.50 (m, 2H, CH_2-*Alloc*), 4.42 (dd, *J* = 6.8, 1.9 Hz, 2H, CH_2-*Fm*), 4.21 (t, *J* = 7.0 Hz, 1H, CH-*Fm*), 3.93 (bs, 1H, $CH_α$-*Glu*), 3.64 (bs, 1H, CH-*a*), 3.30 (bs, 2H, CH_2-*b*), 3.09 – 3.01 (m, 1H, CH-*a*), 2.52 – 2.29 (m, 3H, $CH_{2γ}$-*Glu* and $CH_β$-*Glu*), 2.23 – 2.06 (m, 1H, $CH_β$-*Glu*), 1.52 – 1.38 (m, 18H, 3 x CH_3-Boc and 3 x CH_3- *t*Bu) ppm.

^{13}C-NMR (101 MHz, $CDCl_3$): δ = 144.5 143.8, 141.7, 141.3, 141.0, 128.6, 128.4, 128.0, 127.8, 127.7, 127.3, 127.2, 127.1, 125.0 ,124.7, 120.1, 82.5, 79.3, 66.6, 66.5, 65.4, 65.2, 61.2, 50.4, 46.9, 39.6, 30.9, 28.4, 28.0 ppm.

m/z (ESI$^-$) = [M+H$^+$]608.80; $C_{34}H_{44}N_2O_8$ requires 608.31

Product 121

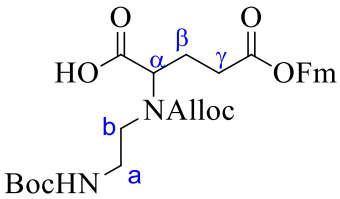

$C_{30}H_{36}N_2O_8$
MW: 552.62

To a solution of 0.5 g (1.0 eq, 0.82 mmol) Product 120 in 5 mL DCM was added 5 mL TFA. The mixture was stirred at room temperature overnight. The reaction mixture was concentrated under reduced pressure, co-evaporate with toluene, washed with Et_2O and the residue was solubilized in dioxane/H_2O. After 0.17 mL NEt_3 (1.1 eq, 0.90 mmol) and 0.26 g Boc_2O (1.1 eq, 0.90 mmol) were added and the reaction mixture stirred for 2h at room temperature. After the reaction mixture was quenched with H_2O and acidified with 2M HCl solution to pH = 1. The aqueous solution was extracted several times with EtOAc. The organic layers were dried over $MgSO_4$ and concentrated under reduced pressure. The residue was purified by flash column chromatography (CH/EtOAc = 1:1 → 0:1) and the product obtained as clear oil (100%). R_f (EtOAc/MeOH = 10:1) = 0.5

^{1}H-NMR (400 MHz, $CDCl_3$): δ = 7.76 (d, *J* = 7.5 Hz, 2H, CH_{ar}-*Fm*), 7.58 (d, *J* = 7.5 Hz, 2H, CH_{ar}-*Fm*), 7.45 – 7.28 (m, 4H, CH_{ar}-*Fm*), 5.96 – 5.79 (m, 1H, CH_{Alloc}), 5.20 (d, *J* = 74.9 Hz, 2H, CH_2-*Alloc*), 4.66 – 4.51 (m, 2H, CH_2-*Alloc*), 4.42 (bs, 2H, CH_2-*Fm*), 4.20 (t, *J* = 6.9 Hz, 1H, CH-*Fm*), 3.67 (bs, 1H, CH-*a*), 3.28 (bs, 2H, CH_2-*b*), 3.08 (bs, 1H, CH-*a*), 2.56 – 2.29 (m, 3H, $CH_{2\gamma}$-*Glu* and CH_β-*Glu*), 2.27 – 2.04 (m, 1H, CH_β-*Glu*), 1.43 (s, 9H, 3 x CH_3-*Boc*) ppm.

^{13}C-NMR (101 MHz, $CDCl_3$): δ = 172.9, 143.8, 141.4, 128.8, 128.5, 128.0, 127.3, 125.1, 120.2, 77.4, 66.8, 53.6, 47.0, 30.8, 28.5 ppm.

m/z (ESI$^+$) = [M+H$^+$]552.8; $C_{30}H_{36}N_2O_8$ requires 552.25

Product 113

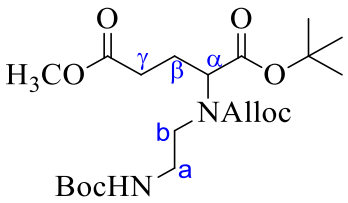

$C_{21}H_{36}N_2O_8$
MW: 444.52

To a solution of 1.25 g (1.0 eq, 3.47 mmol) Product 112 in 50 mL DCM was added 0.60 mL (1.0 eq, 3.47 mmol) DIPEA and 0.44 mL (1.2 eq, 4.16 mmol) allyl chloroformate at 0°C. After 1h the reaction mixture was concentrated under reduced pressure and the residue dissolved in EtOAc. The solution was extracted with sat. $NaHCO_3$-solution and Brine. After the organic layer was dried over $MgSO_4$ and concentrated under reduced pressure. The residue was purified by flash column chromatography (CH/EtOAc = 2:1→ 1:1) and the product was obtained as clear oil (0.93 g, 60%). R_f (CH/EtOAc = 1:1) = 0.77

^{1}H-NMR (400 MHz, $CDCl_3$): δ = 5.93 – 5.75 (m, 1H, CH_{Alloc}), 5.42 – 5.09 (m, 3H, CH_2-*Alloc* and NH), 4.61 – 4.38 (m, 2H, CH_2-*Alloc*), 3.90 (bs, 1H, CH_α-*Glu*), 3.61 (s, 4H, CH_3 and CH-*a*), 3.25 (bs, 2H, CH_2-*b*), 3.06 – 3.01 (m, 1H, CH-*a*), 2.39 – 2.24 (m, 3H, $CH_{2\gamma}$-*Glu* and CH_β-*Glu*), 2.12 – 2.04 (m, 1H, CH_β-*Glu*), 1.38 (d, *J* = 17.1 Hz, 21H, 3 x CH_3-Boc and 3 x CH_3-*t*Bu) ppm.
^{13}C-NMR (101 MHz, $CDCl_3$): δ = 173.4, 170.1, 156.1, 132.5, 118.0, 82.4, 79.3, 66.7, 66.4, 61.4, 51.9, 49.3, 48.5, 39.7, 30.8, 28.5, 28.1, 25.5, 24.8 ppm.

m/z (ESI$^+$) = [M+H$^+$]444.73; $C_{21}H_{36}N_2O_8$ requires 444.25

Product 114

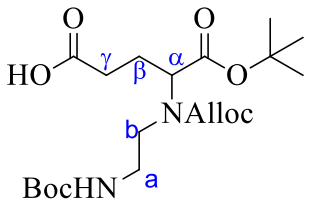

$C_{20}H_{34}N_2O_8$
MW: 430.49

To a solution of 0.85 g (1.0 eq, 1.91 mmol) Product 113 in 50 mL THF was added 1M aqueous solution of LiOH (1.5 eq) at 0°C and stirred at room temperature overnight. The mixture was quenched with H_2O and acidified with 2M HCl solution to pH = 5. The aqueous solution was extracted several times with EtOAc. The organic layers dried over $MgSO_4$ and concentrated under reduced pressure. The residue was purified by flash column chromatography (CH/EtOAc = 3:1 → 1:1) and the product obtained as clear oil (0.64 g, 78%).R_f (CH/EtOAc = 1:1) = 0.51

^{1}H-NMR (400 MHz, $CDCl_3$): δ = 5.97 – 5.83 (m, 1H, CH_{Alloc}), 5.41 (bs, 1H, NH), 5.37 – 5.15 (m, 2H, CH_2-*Alloc*), 4.65 – 4.48 (m, 2H, CH_2-*Alloc*), 3.99 (t, *J* = 7.3 Hz, 1H, CH_α-*Glu*), 3.67 (bs, 1H, CH-*a*), 3.32 (p, *J* = 6.9, 6.1 Hz, 2H, CH_2-*b*), 3.12 (dt, *J* = 12.9, 6.2 Hz, 1H, CH-*a*), 2.52 – 2.27 (m, 3H, $CH_{2\gamma}$-*Glu* and CH_β-*Glu*), 2.26 – 2.06 (m, 1H, CH_β-*Glu*), 1.45 (d, 18H, 3 x CH_3-*Boc* and 3 x CH_3-*t*Bu) ppm.

^{13}C-NMR (101 MHz, $CDCl_3$): δ = 177.0, 156.2, 132.5, 118.1, 82.5, 79.5, 66.6, 61.4, 39.7, 30.7, 28.5, 28.1, 25.5, 24.6 ppm.

m/z (ESI$^-$) = [M-H$^-$]429.0; $C_{20}H_{34}N_2O_8$ requires 430.23

Product 115

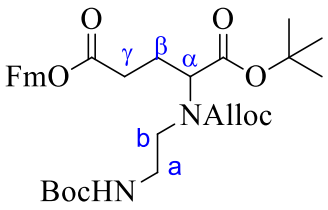

$C_{34}H_{44}N_2O_8$
MW: 608.72

To a solution of 0.64 g (1.0 eq, 1.49 mmol) Product 114 in 20 mL dry DCM at 0°C was added 0.26 mL (1.0 eq, 1.49 mmol) DIPEA at argon-atmosphere. To the reaction mixture was added a solution of 0.43 g (1.1 eq, 1.64 mmol) Fmoc-Cl in 5 mL dry DCM. The mixture was stirred for 5 minutes and 0.018 g (0.1-0.15 eq, 0.15 mmol) DMAP was added. The reaction mixture was after stirred for around 45 minutes at 0 °C and argon-atmosphere, after diluted with DCM and extracted several times with sat. NH_4Cl-solution and sat. $NaHCO_3$-solution. The organic layer was dried over $MgSO_4$ and concentrated under reduced pressure. The residue was purified by flash column chromatography (CH/EtOAc = 3:1) and the product was obtained as white solid (0.45 g, 48%).R_f (DCM) = 0.2

^{1}H-NMR (400 MHz, $CDCl_3$): δ = 7.77 (d, *J* = 7.5 Hz, 2H, CH_{ar}-*Fm*), 7.58 (d, *J* = 7.5 Hz, 2H, CH_{ar}-*Fm*), 7.41 (t, *J* = 7.4 Hz, 2H, CH_{ar}-*Fm*), 7.33 (dd, *J* = 7.5, 1.1 Hz, 2H, CH_{ar}-*Fm*), 6.03 – 5.81 (m, 1H, CH_{Alloc}), 5.42 – 5.15 (m, 3H, NH and CH_2-*Alloc*), 4.68 – 4.38 (m, 4H, CH_2-*Alloc* and CH_2-*Fm*), 4.21 (t, *J* = 6.9 Hz, 1H, CH-*Fm*), 3.92 (bs, 1H, CH_α-*Glu*), 3.65 (bs, 1H, CH-*a*), 3.30 (bs, 2H, CH_2-*b*), 3.10 – 2.98 (m, 1H, CH-*a*), 2.53 – 2.20 (m, 3H, $CH_{2\gamma}$-*Glu* and CH_β-*Glu*), 2.24 – 2.07 (m, 1H, CH_β-*Glu*), 1.52 – 1.37 (m, 18H, 3 x CH_3-*Boc* and 3 x CH_3-*t*Bu) ppm.
^{13}C-NMR (101 MHz, $CDCl_3$): δ = 143.8, 141.4, 128.0, 127.3, 125.1, 120.2, 82.5, 66.7, 46.1, 28.6, 28.1 ppm.

m/z (ESI$^+$) = [M+H$^+$]608.8; $C_{34}H_{44}N_2O_8$ requires 608.31

Product 116

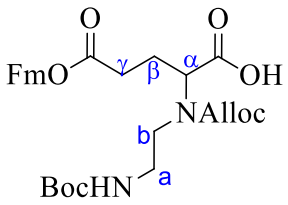

$C_{30}H_{36}N_2O_8$
MW: 552.62

To a solution of 0.5 g (1.0 eq, 0.82 mmol) Product 115 in 5 mL DCM was added 5 mL TFA. The mixture was stirred at room temperature overnight. The reaction mixture was concentrated under reduced pressure and solubilized in dioxane/H_2O. After 0.17 mL NEt_3 (1.1 eq, 0.90 mmol) and 0.26 g Boc_2O (1.1 eq, 0.90 mmol) were added and the reaction mixture stirred for 2h at room temperature. After the reaction mixture was quenched with H_2O and acidified with 2M HCl solution to pH = 1. The aqueous solution was extracted several times with EtOAc. The organic layers were dried over $MgSO_4$ and concentrated under reduced pressure. The residue was purified by Flash Column Chromatography (CH/EtOAc = 1:1 → 0:1) and the product obtained as clear oil (100%). R_f (EtOAc/MeOH = 10:1) = 0.5

^{1}H-NMR (400 MHz, $CDCl_3$): δ = 7.76 (d, *J* = 7.5 Hz, 2H, CH_{ar}-*Fm*), 7.58 (d, *J* = 7.5 Hz, 2H, CH_{ar}-*Fm*), 7.46 – 7.28 (m, 6H, CH_{ar}-*Fm*), 6.95 – 5.78 (m, 1H, CH_{Alloc}), 5.36 – 5.07 (m, 2H, CH_2-*Alloc*), 4.60 – 4.55 (m, 2H, CH_2-*Alloc*), 4.43 (t, *J* = 6.0 Hz, 2H, CH_2-*Fm*), 4.25 – 3.86 (m, 1H, CH-*Fm*), 4.02 – 3.83 (m, 1H, CH_α-*Glu*), 3.68 – 3.54 (m, 1H, CH-*a*), 3.30 – 2.82 (m, 3H, CH_2-*b* and CH-*a*), 2.56 – 2.34 (m, 2H, $CH_{2\gamma}$-*Glu*), 2.22 – 1.95 (m, 2H, 2 x CH_β-*Glu*), 1.43 (s, 9H, 3 x CH_3-*Boc*) ppm.

^{13}C-NMR (101 MHz, $CDCl_3$): δ = 172.8, 143.8, 141.4, 128.8, 128.5, 127.3, 125.1, 120.2, 66.7, 66.3, 47.0, 30.9, 28.54 ppm.

m/z (ESI$^+$) = [M+H$^+$]552.73; $C_{30}H_{36}N_2O_8$ requires 552.25

Thymine-1-acetic acid

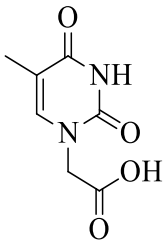

$C_7H_8N_2O_4$
MW: 184.15

1.0 g of Thymine-tBu (4.1 mmol) was dissolved in 10 mL DCM and 5 mL TFA. The mixture was stirred at room temperature overnight. The reaction mixture was concentrated under reduced pressure and co-evaporated with toluene. The residue was washed with Et_2O to induce the precipitation of the product. The product was obtained as a white solid (0.75 g, 95%).

^{1}H-NMR (400 MHz, DMSO-d_6): δ = 11.35 (s, 1H, NH), 7.51 (s, 1H, CH), 4.37 (s, 2H, CH_2), 1.75 (s, 3H, CH_3).
^{13}C-NMR (100 MHz, DMSO-d_6): δ = 170.15, 164.84, 151.45, 142.22, 108.87, 48.89, 12.31.

II.-4. Synthesis on Solid-Phase: General procedure

The solid phase synthesis of the dimers was carried out manually, at room temperature, in frits. Each synthesis was carried out in 0.08 mmol scale, using MBHA resin LL 100-200 mesh HCl (500 mg, 0.88 mmol/g). Before each synthesis, the resin was swelled in NMP overnight. Each step was followed by the Kaiser- and/or Chloranil-test.

- Neutralization of resin

The resin was stirred for 30 minutes in a solution of DIPEA/NMP (2:1). After, the resin was washed several times with NMP.

- Coupling steps

The first coupling reactions were carried out starting from 0.08 mM of α-PNA(Glu) backbone monomer **116** or **121** from 0.08 mM of Boc-β-Ala. They were first pre-activated using 1eq of HBTU, 3.0 eq. DIEA in 1 mL of NMP. After stirring for 5 minutes, the pre-activated mixtures were added to the resin. The resin was stirred 12h then washed 3 times with NMP. The second coupling reactions were performed similarly, using 4.0 eq of α-PNA (Orn or Lys) backbone monomers **106/107** or **108/109**, 4.4 eq HBTU and 12 eq DIPEA.

- Washing steps

After each coupling and deprotection steps, the resin was washed 3 times with NMP. Before Boc-deprotection, the resin was carefully washed 3 times with DCM and after Boc-deprotection, it was washed 5 times with DCM then 3 times with NMP.

- Capping-Acetylation

A solution of acetic anhydride/pyridine (3:2) was prepared, and after each coupling step, 1 mL was added to the resin with 1 mL NMP and stirred for 30 minutes. After, the resin was washed five times with NMP.

- Boc deprotection

The resin was carefully washed 5 times with DCM. Then, 5mL of a solution of TFA/TIPS(10%)-DCM (50:50) was added to the resin and stirred for 5 minutes. The procedure was repeated with a fresh solution for 45 minutes. The resin was cautiously washed with DCM until the pH was neutral then washed again 3 times with NMP.

- Fmoc Deprotection

The Fmoc deprotection on the solid support was carried out using a 20% solution of piperidine in DMF. The resin was stirred 45 minutes at room temperature. The resin was washed after several times with NMP until the pH was neutral.

- Alloc deprotection

A solution of 6 eq $PhSiH_3$ and 0.1 eq $Pd(PPh_3)_4$ in DCM (5 mL) was prepared and stirred for 2 minutes. The mixture was then added to the resin and stirred for one hour at room temperature. After, the resin was washed 3 times with DCM, 3 times with NMP, two times with a solution of 5% natriumdiethyldithiocarbamate in NMP (5 mL) then three times with NMP.

- Cyclization

A solution of 5 eq PyBOP and 5 eq DIPEA in 1mL NMP was prepared and stirred for 3 minutes. The mixture was added to the resin and stirred mechanically overnight.

- Thymine coupling

A solution of Thymine-1-acetic acid (5 eq/amine), 5.5 eq DhBtOH and 5 eq DCC in NMP was prepared and stirred for 40 minutes. After the reaction mixture was added on the solid support and the resin was stirred for 48 hours at room temperature. The

procedure was repeated with a fresh reaction mixture for 48 hours again. Then, the resin was washed 3 times with NMP.

- Cleavage of resin

The dimers were cleaved from the resin using 10 mL of a solution of TFA/TIS/TFMSA (3:1:1). After 4 hours of stirring, the dimer was precipitated in Et_2O at 0°C, then centrifugated for 5 minutes (1200 rpm) at 0°C. The procedure was repeated 2 times and the solid was dried on high vacuum.

- Dimer purification

Crude dimers were purified by reverse phase semi-preparative HPLC, using (H_2O + 0.1% TFA) and (ACN + 0.1%TFA) as elution solvents. The fractions were collected, evaporated under reduced pressure and analyzed by LC-MS. The fractions with the pure product were freeze dried.

“stapled” Dimer: *DD*-Glu-Lys/*LL*-Glu-Lys

H_2O/ACN + 1% TFA: 100/0 → 80/20 (5 min → 15 min) → 0/100 (20 min) → 100/0(24 min).

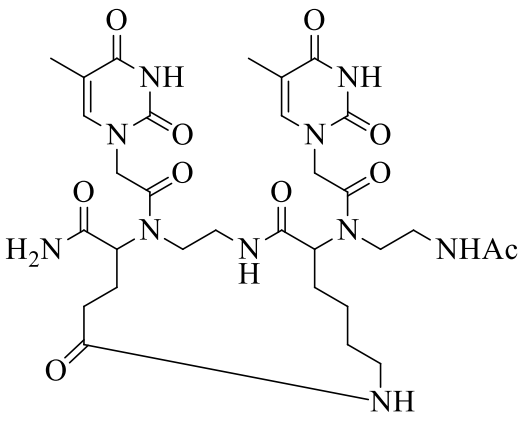

$C_{31}H_{44}N_{10}O_{10}$
MW: 716.74

R_t(*DD/LL*-Glu/Lys): 14.8 min and 15.4 min

m/z (ESI^-) = $[M-H^-]$715.05; $C_{31}H_{44}N_{10}O_{10}$ requires 716.32

β-Ala-*DD*-Glu-Lys/β-Ala-*LL*-Glu-Lys

H_2O/ACN + 1% TFA : 100/0 → 50/50(20 min) → 0/100(22 min) → 100/0(30 min)

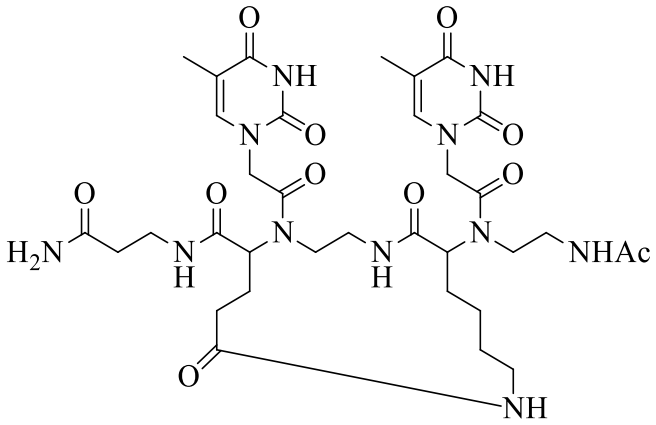

$C_{34}H_{49}N_{11}O_{11}$
MW: 787.82

R_t(*DD/LL*-Glu/Lys): 13.6 min

m/z (ESI$^+$) = [M+H$^+$]788.7; $C_{34}H_{49}N_{11}O_{11}$ requires 787.36

HRMS (ESI$^+$, MeOH) = *m/z* = [M+H$^+$]788,3684; $C_{34}H_{49}N_{11}O_{11}$ requires 788.3691[M+H$^+$]

List of References

1. Horne, W. S. & Gellman, S. H. Foldamers with heterogeneous backbones. *Acc. Chem. Res.* **41,** 1399–1408 (2008).

2. Guichard, G. & Huc, I. Synthetic foldamers. *Chem. Commun.* **47,** 5933 (2011).

3. Grotz, M. Synthese und Charakterisierung abiotischer Foldamere und ihrer Bausteine für die Nutzung in biologischen Systemen. (Würzburg, 2013).

4. Branden, C. I. & Tooze, J. *Introduction to Protein Structure*. (Garland Science, 1999).

5. Loughlin, W. A., Tyndall, J. D. A., Glenn, M. P., Hill, T. A. & Fairlie, D. P. Update 1 of : Beta-Strand Mimetics. 32–69 (2010). doi:10.1021/cr040648k

6. Pelay-gimeno, M., Glas, A., Koch, O. & Grossmann, T. N. Structure-Based Design of Inhibitors of Protein – Protein Interactions : Mimicking Peptide Binding Epitopes Angewandte. 8896–8927 (2015). doi:10.1002/anie.201412070

7. Pauling, L., Corey, R. B. & Branson, H. R. The Structure of Proteins: Two Hydrogen-Bonded Helical Configurations of the Polypeptide Chain. *PNAS* **37,** 205–211 (1951).

8. Pauling, L. & Corey, R. B. The Pleated Sheet, a new Layer Configuration of Polypeptide Chains. *PNAS* **37,** 251–256 (1951).

9. Narwani, T. J. *et al.* Recent advances on polyproline II. *Amino Acids* **49,** 705–713 (2017).

10. Berg, J. M., Tymoczko, J. L. & Stryer, L. *Biochemistry*. (W. H. Freeman, 2002).

11. Cowan, P. M., McGavin, S. & North, A. C. T. The polypeptide chain

configuration of collagen. *Nature* **176,** 1062–1064 (1955).

12. Horng, J.-C. Stereoelectronic effects on polyproline conformation. *Protein Sci.* **15,** 74–83 (2006).

13. Adzhubei, A. A., Sternberg, M. J. E. & Makarov, A. A. Polyproline-II helix in proteins: Structure and function. *J. Mol. Biol.* **425,** 2100–2132 (2013).

14. Hill, T. A., Shepherd, N. E., Diness, F. & Fairlie, D. P. Constraining cyclic peptides to mimic protein structure motifs. *Angew. Chemie - Int. Ed.* **53,** 13020–13041 (2014).

15. Robinson, J. A. Design and applications of protein epitope mimetics. *Chimia (Aarau).* **67,** 885–890 (2013).

16. Nevola, L. & Giralt, E. Modulating protein–protein interactions: the potential of peptides. *Chem. Commun.* **51,** 3302–3315 (2015).

17. Licini, G., Prins, L. J. & Scrimin, P. Oligopeptide foldamers: From structure to function. *European J. Org. Chem.* 969–977 (2005). doi:10.1002/ejoc.200400521

18. Zinzalla, G. & Thurston, D. E. Targeting protein–protein interactions for therapeutic intervention: a challenge for the future. *Future Med. Chem.* **1,** 65–93 (2009).

19. Modell, A. E., Blosser, S. L. & Arora, P. S. Systematic Targeting of Protein–Protein Interactions. *Trends Pharmacol. Sci.* **37,** 702–713 (2016).

20. London, N., Raveh, B. & Schueler-Furman, O. Druggable protein-protein interactions - from hot spots to hot segments. *Curr. Opin. Chem. Biol.* **17,** 952–959 (2013).

21. White, S. W. & Ollis, D. L. Structural Basis of Protein-Nucleic Acid Interactions. *Chem. Rev.* **87,** 981–995 (1987).

22. Lejeune, D., Delsaux, N., Charloteaux, B., Thomas, A. & Brasseur, R. Protein-

nucleic acid recognition: Statistical analysis of atomic interactions and influence of DNA structure. *Proteins Struct. Funct. Bioinforma.* **61,** 258–271 (2005).

23. Blackburn, G. M., Gait, M. J., Loakes, D. & Williams, D. M. *Nucleic Acids in Chemistry and Biology : Edition 3*. (RSC Publishing, 2006). doi:10.1039/9781847555380-00383

24. Steitz, T. A. Structural studies of protein-nucleic acid interaction: The sources of sequence-specific binding. *Q. Rev. Biophys.* **23,** 205–280 (1990).

25. Rohs, R. *et al.* Origins of Specificity in Protein-DNA Recognition. *Annu. Rev. Biochem.* **79,** 233–269 (2010).

26. Luscombe, N. M., Austin, S. E., Berman, H. M. & Thornton, J. M. An overview of the structures of protein-DNA complexes. *Genome Biol.* **1,** 1–1 (2000).

27. Varani, G. RNA - Protein Intermolecular Recognition. *Acc. Chem. Res.* **30,** 189–195 (1997).

28. Chen, Y. & Varani, G. Protein families and RNA recognition. *FEBS J.* **272,** 2088–2097 (2005).

29. Cheng, A. C., Calabro, V. & Frankel, A. D. Design of RNA-binding proteins and ligands. *Curr. Opin. Struct. Biol.* **11,** 478–484 (2001).

30. Chen, Y. & Varani, G. Engineering RNA-binding proteins for biology. *FEBS J.* **280,** 3734–3754 (2013).

31. J. Wilson, A. Inhibition of protein-protein interactions using designed molecules. *Chem. Soc. Rev.* **38,** 3289–3300 (2009).

32. Cunningham, A. D., Qvit, N. & Mochly-Rosen, D. Peptides and peptidomimetics as regulators of protein–protein interactions. *Curr. Opin. Struct. Biol.* **44,** 59–66 (2017).

33. Fahs, S., Patil-Sen, Y. & Snape, T. J. Foldamers as Anticancer Therapeutics:

Targeting Protein-Protein Interactions and the Cell Membrane. *ChemBioChem* **16,** 1840–1853 (2015).

34. Gopalakrishnan, R., Frolov, A. I., Knerr, L., Drury, W. J. & Valeur, E. Therapeutic potential of foldamers: From chemical biology tools to drug candidates? *J. Med. Chem.* **59,** 9599–9621 (2016).

35. Bautista, A. D., Craig, C. J., Harker, E. A. & Schepartz, A. Sophistication of foldamer form and function in vitro and in vivo. *Curr. Opin. Chem. Biol.* **11,** 685–692 (2007).

36. Appella, D. H., Christianson, L. A., Karle, I. L., Powell, D. R. & Gellman, S. H. beta-peptide foldamers: Robust Helix formation in a new family of beta-amino acid oligomers. *J. Am. Chem. Soc.* **118,** 13071–13072 (1996).

37. Seebach, D. *et al.* Beta-Peptides: Synthesis byArndt-Eistert homologation with concomitant peptide coupling. Structure determination by NMR and CD spectroscopy and by X-ray crystallography. Helical secondary structure of a beta-hexapeptide in solution and its stability towar. *Helv. Chim. Acta* **79,** 913–941 (1996).

38. Johnson, L. M. & Gellman, S. H. α-Helix mimicry with α/β-peptides. *Methods in Enzymology* **523,** (Elsevier Inc., 2013).

39. Mándity, I. M. & Fülöp, F. An overview of peptide and peptoid foldamers in medicinal chemistry. *Expert Opin. Drug Discov.* **10,** 1163–1177 (2015).

40. Pilsl, L. K. A. & Reiser, O. *Amino Acids*. **41,** (Springer, 2011).

41. Kritzer, J. A., Stephens, O. M., Guarracino, D. A., Reznik, S. K. & Schepartz, A. β-Peptides as inhibitors of protein-protein interactions. *Bioorganic Med. Chem.* **13,** 11–16 (2005).

42. Kritzer, J. A., Lear, J. D., Hodsdon, M. E. & Schepartz, A. Helical -Peptide Inhibitors of the p53-hDM2 Interaction. **368,** 9468–9469 (2004).

43. Hanessian, S., Luo, X. & Schaum, R. Synthesis and folding preferences of y-amino acid oligopeptides: stereochemical control in the formation of a reverse turn and a helix. *Tetrahedron Lett.* **40,** 4925–4929 (1999).

44. Seebach, D., Brenner, M., Rueping, M. & Jaun, B. CD Spectra , NMR Solution and X-ray Crystal Structures of γ -Peptides. 573–584 (2002).

45. Baldauf, C., Robert, G. & Hofmann, H. Helix Formation and Folding in γ -Peptides and Their Vinylogues. *Helv. Chim. Acta* **86,** 2573–2588 (2003).

46. Guo, L. *et al.* Characteristic structural parameters for the γ-peptide 14-helix: Importance of subunit preorganization. *Angew. Chemie - Int. Ed.* **50,** 5843–5846 (2011).

47. Douat, C. *et al.* A Cell-Penetrating Foldamer with a Bioreducible Linkage for Intracellular Delivery of DNA Angewandte. 11133–11137 (2015). doi:10.1002/anie.201504884

48. Martinek, T. A. & Fülöp, F. Peptidic foldamers: Ramping up diversity. *Chem. Soc. Rev.* **41,** 687–702 (2012).

49. Li, X. & Yang, D. Peptides of aminoxy acids as foldamers. *Chem. Commun.* 3367–3379 (2006). doi:10.1039/b602230h

50. Roy, A., Prabhakaran, P., Baruah, P. K. & Sanjayan, G. J. Diversifying the structural architecture of synthetic oligomers: the hetero foldamer approach. *Chem. Commun.* **47,** 11593 (2011).

51. Choi, S. H., Guzei, I. A. & Gellman, S. H. Crystallographic Characterization of the a/b-Peptide 14/15-Helix. *J. Am. Chem. Soc.* **129, 45,** 13780–13781 (2007).

52. Sadowsky, J. D. *et al.* (α/β+α)-peptide antagonists of BH3 domain/Bcl-x L recognition: Toward general strategies for foldamer-based inhibition of protein-protein interactions. *J. Am. Chem. Soc.* **129,** 139–154 (2007).

53. Azzarito, V., Long, K., Murphy, N. S. & Wilson, A. J. Inhibition of a-helix-mediated protein-protein interactions using designed molecules. *Nat. Chem.* **5,** 161–173 (2013).

54. Baldauf, C., Günther, R. & Hofmann, H. J. Side-chain control of folding of the homologous α-, β-, and γ-peptides into 'mixed' helices (β-helices). *Biopolym. - Pept. Sci. Sect.* **80,** 675–687 (2005).

55. Baldauf, C., Günther, R. & Hofmann, H. J. Helices in peptoids of α- and β-peptides. *Phys. Biol.* **3,** (2006).

56. Sharma, G. V. M. *et al.* A left-handed 9-helix in gamma-peptides: synthesis and conformational studies of oligomers with dipeptide repeats of C-linked carbo-gamma4-amino acids and gamma-aminobutyric acid. *Angew. Chem. Int. Ed. Engl.* **45,** 2944–7 (2006).

57. Sharma, G. V. M. *et al.* Theoretical and experimental studies on α/ε-hybrid peptides: Design of a 14/12-helix from peptides with alternating (S)-C-linked carbo-ε-amino acid [(S)-ε-Caa(x)] and L-Ala. *J. Org. Chem.* **74,** 6703–6713 (2009).

58. Muriel, A. *et al.* Title : Ribbon-like foldamers for cellular uptake and drug delivery. *ChemBioChem* **18,** 2110–2114 (2017).

59. Tew, G. N., Scott, R. W., Klein, M. L. & Degrado, W. F. Molecules : From Discovery to Practical Applications. **43,** 30–39 (2011).

60. Nepal, M., Thangamani, S., Seleem, M. N. & Chmielewski, J. Targeting intracellular bacteria with an extended cationic amphiphilic polyproline helix. *Org. Biomol. Chem.* **13,** 5930–5936 (2015).

61. Lau, Y. H., de Andrade, P., Wu, Y. & Spring, D. R. Peptide stapling techniques based on different macrocyclisation chemistries. *Chem. Soc. Rev.* **44,** 91–102 (2015).

62. Shepherd, N. E., Hoang, H. N., Abbenante, G. & Fairlie, D. P. Single turn peptide alpha helices with exceptional stability in water. *J. Am. Chem. Soc.* **127,** 2974–2983 (2005).

63. Taylor, J. W. The synthesis and study of side-chain lactam-bridged peptides. *Biopolym. - Pept. Sci. Sect.* **66,** 49–75 (2002).

64. Robertson, N. S. & Jamieson, A. G. Regulation of protein-protein interactions using stapled peptides. *Reports Org. Chem.* **5,** 65–74 (2015).

65. Fujimoto, K., Kajino, M. & Inouye, M. Development of a series of cross-linking agents that effectively stabilize α-helical structures in various short peptides. *Chem. - A Eur. J.* **14,** 857–863 (2008).

66. Chan, D. C., Fass, D., Berger, J. M. & Kim, P. S. Core Structure of gp41 from the HIV Envelope Glycoprotein. *Cell* **89,** 263–273 (1997).

67. Sia, S. K., Carr, P. a, Cochran, A. G., Malashkevich, V. N. & Kim, P. S. Short constrained peptides that inhibit HIV-1 entry. *Proc. Natl. Acad. Sci. U. S. A.* **99,** 14664–14669 (2002).

68. Judice, J. K. *et al.* Inhibition of HIV type 1 infectivity by constrained alpha-helical peptides: implications for the viral fusion mechanism. *Proc. Natl. Acad. Sci. U. S. A.* **94,** 13426–30 (1997).

69. Schafmeister, C. E., Po, J. & Verdine, G. L. Supporting Info_An All-Hydrocarbon Cross-Linking System for Enhancing the Helicity and Metabolic Stability of Peptides_Schafmeister_2000.pdf. 12364–12365 (2000).

70. Blackwell, H. E. & Grubbs, R. H. Highly efficient synthesis of covalently cross-linked peptide helices by ring-closing metathesis. *Angew. Chemie - Int. Ed.* **37,** 3281–3284 (1998).

71. Walensky, L. D. & Bird, G. H. Hydrocarbon-stapled peptides: Principles, practice, and progress. *J. Med. Chem.* **57,** 6275–6288 (2014).

72. Verdine, G. L. & Hilinski, G. J. All-hydrocarbon stapled peptides as synthetic cell-accessible mini-proteins. *Drug Discov. Today Technol.* **9,** e41–e47 (2012).

73. Justin K.Murray, S. H. G. Targeting Protein-Protein Interactions:Lessons from p53/MDM2. *Stud. Polit. Econ.* **88,** 9–30 (2007).

74. Baek, S. *et al.* Structure of the stapled p53 peptide bound to Mdm2. *J. Am. Chem. Soc.* **134,** 103–106 (2012).

75. Loughlin, W. A., Tyndall, J. D. A., Glenn, M. P. & Fairlie, D. P. Beta-Strand Mimetics. *Chem. Rev.* **104,** 6085–6117 (2004).

76. Melacini, G., Zhu, Q. & Goodman, M. Multiconformational NMR Analysis of Sandostatin (Octreotide): Equilibrium between beta -Sheet and Helical Structures. *Biochemistry* **36,** 1233–1241 (1997).

77. Pohl, E. *et al.* Structure of octreotide, a somatostatin analogue. *Acta Crystallogr. - Sect. D Biol. Crystallogr.* **51,** 48–59 (1995).

78. Veber, D. F. *et al.* A Super Active Cyclic Hexapeptide Analog of Somatostatin. *Life Sci.* **34,** 1371–1378 (1984).

79. Athanassiou, Z. *et al.* Structural mimicry of retroviral Tat proteins by constrained β-hairpin peptidomimetics: Ligands with high affinity and selectivity for viral TAR RNA regulatory elements. *J. Am. Chem. Soc.* **126,** 6906–6913 (2004).

80. Robinson, J. A. β-Hairpin Peptidomimetics : Design , Structures and Biological Activities. *Acc. Chem. Res.* **41,** 1278–1288 (2008).

81. Kussie, P. H. *et al.* Structure of the MSM2 Oncoprotein Bound to the p53 Tumor Suppressor Transactivation Domain. *Science,* **274,** 948–953 (1996).

82. Battiste, J. L. *et al.* α Helix-RNA major groove recognition in an HIV-1 Rev peptide-RRE RNA complex. *Science,* **273,** 1547–1551 (1996).

83. Moehle, K. *et al.* Design of β-hairpin peptidomimetics that inhibit binding of α-

helical HIV-1 Rev protein to the Rev response element RNA. *Angew. Chemie - Int. Ed.* **46,** 9101–9104 (2007).

84. Daly, M. *et al.* Switching the Stereochemical Outcome of 6-Endo-Trig Cyclizations; Synthesis of 2,6-Cis-6-Substituted 4-Oxopipecolic Acids. *J. Org. Chem.* **77,** 10001–10009 (2012).

85. Hol, W. G. J., Duijnen, P. T. van & Berendsen, H. J. C. The a-helix dipole and the properties of proteins. *Nature* **273,** 443–446 (1978).

86. Daley, M. Thesis: New Approaches for the Stereoselective Synthesis of N - Heterocycles. (Glasgow, 2012).

87. Harkiss, A. H. & Sutherland, A. Access to 2,6-Disubstituted 4-Oxopiperidines Using a 6-Endo-trig Cyclization: Stereoselective Synthesis of Spruce Alkaloid and (+)-241D. *J. Org. Chem.* **83,** 535–542 (2018).

88. Nicolaou, K. C., Estrada, A. A., Zak, M., Lee, S. H. & Safina, B. S. A mild and selective method for the hydrolysis of esters with trimethyltin hydroxide. *Angew. Chemie - Int. Ed.* **44,** 1378–1382 (2005).

89. Pascal, R. & Sola, R. Preservation of the protective group under alkaline conditions by using CaCl 2. Applications in peptide synthesis. *Tetrahedron Lett.* **39,** 5031–5034 (1998).

90. Aznar, F., García, A. B. & Cabal, M. P. Proline-catalyzed imino-Diels-Alder reactions: Synthesis of meso-2,6-diaryl-4-piperidones. *Adv. Synth. Catal.* **348,** 2443–2448 (2006).

91. Žari, S., Kudrjashova, M., Pehk, T., Lopp, M. & Kanger, T. Remote activation of the nucleophilicity of isatin. *Org. Lett.* **16,** 1740–1743 (2014).

92. Trost, B. M., Mahapatra, S. & Hansen, M. Palladium-catalyzed C-H activation of N-Allyl Imines: Regioselective allylic alkylations to deliver substituted aza-1,3-dienes. *Angew. Chemie - Int. Ed.* **54,** 6032–6036 (2015).

93. Alcaide, B., Almendros, P., Alonso, J. M. & Aly, M. F. A novel use of Grubbs' carbene. Application to the catalytic deprotection of tertiary allylamines. *Org. Lett.* **3,** 3781–3784 (2001).

94. Rosiak, A., Hoenke, C. & Christoffers, J. Synthesis of 3-phenyl-4-piperidones from acetophenone by shapiro and azamichael reactions and their further derivatization. *European J. Org. Chem.* 4376–4382 (2007). doi:10.1002/ejoc.200700325

95. Garro-Helion, F., Merzouk, A. & Guibé, F. Mild and Selective Palladium(0)-Catalyzed Deallylation of Allylic Amines. Allylamine and Diallylamine as Very Convenient Ammonia Equivalents for the Synthesis of Primary Amines. *J. Org. Chem.* **58,** 6109–6113 (1993).

96. Caballero, E. *et al.* Imino-Diels-Alder reactions of 1-aryl-3-(trialkylsiloxy)-1,3-butadienes in solution and the solid phase. *European J. Org. Chem.* 4004–4014 (2008). doi:10.1002/ejoc.200800284

97. Venkataraman, K. & Wagle, D. R. Cyanuric Chloride: A Useful Reagent of Converting Carboxylic Acids Into Chlorides, Esters, Amides and Peptides. *Tetrahedron Lett.* **20,** 3037–3040 (1979).

98. Kaminski, Z. J. Triazine-Based Condensing Reagents. *Biopolymers* **55,** 140–164 (2000).

99. Groß, S. *et al.* Improved Syntheses of Cyanuric Fluoride and Carboxylic Acid Fluorides. *J. Prakt. Chem.* **342,** 711–714 (2000).

100. Jansen, B. & Zangemeister-Wittke, U. Antisense therapy Antisense therapy for cancer — the time of truth. *Lancet Oncol.* **3,** 672–683 (2002).

101. Lundin, K. E., Gissberg, O. & Smith, C. I. E. Oligonucleotide Therapies: The Past and the Present. *Hum. Gene Ther.* **26,** 475–485 (2015).

102. Malik, R. & Roy, I. Making sense of therapeutics using antisense technology.

Expert Opin. Drug Discov. **6,** 507–26 (2011).

103. Hegarty, J. P. & Stewart, D. B. Advances in therapeutic bacterial antisense biotechnology. *Appl. Microbiol. Biotechnol.* **102,** 1055–1065 (2018).

104. Corey, D. R. Synthetic nucleic acids and treatment of neurological diseases. *JAMA Neurol.* **73,** 1238–1242 (2016).

105. Sharma, V. K., Sharma, R. K. & Singh, S. K. Antisense oligonucleotides: Modifications and clinical trials. *Medchemcomm* **5,** 1454–1471 (2014).

106. Stein, C. A. & Castanotto, D. FDA-Approved Oligonucleotide Therapies in 2017. *Mol. Ther.* **25,** 1069–1075 (2017).

107. Marshall, J. A. & Bundy, G. L. Nucleoside Phosphorothioates. *J. Am. Chem. Soc.* **88,** 4292–4294 (1966).

108. Dean, N. M. & Frank Bennett, C. Antisense oligonucleotide-based therapeutics for cancer. *Oncogene* **22,** 9087–9096 (2003).

109. Chan, J. H. P., Lim, S. & Wong, W. S. F. Antisense Oligonucleotides: From Design to Therapeutic Application. *Clin. Exp. Pharmacol. Physiol.* **33,** 533–540 (2006).

110. Sharma, C. & Awasthi, S. K. Versatility of peptide nucleic acids (PNAs): role in chemical biology, drug discovery, and origins of life. *Chem. Biol. Drug Des.* **89,** 16–37 (2017).

111. Nielsen, P. E., Egholm, M., Berg, R. H. & Buchardt, O. Sequence-Selective Recognition of DNA by Strand Displacement with a Thymine-Substituted Polyamide. *Scienc* **254,** 1497–1500 (1991).

112. Sugiyama, T. & Kittaka, A. Chiral peptide nucleic acids with a substituent in the N-(2-aminoethy)glycine backbone. *Molecules* **18,** 287–310 (2012).

113. Armitage, B. A. The impact of nucleic acid secondary structure on PNA

hybridization. *Drug Discov. Today* **8,** 222–228 (2003).

114. Avitabile, C. *et al.* Targeting pre-miRNA by peptide nucleic acids: A new strategy to interfere in the miRNA maturation. *Artif. DNA PNA XNA* **3,** 1–9 (2012).

115. Mehiri, M. *et al.* An Efficient Biodelivery System for Antisense Polyamide Nucleic Acid (PNA). *Oligonucleotides* **18,** 245–256 (2008).

116. Nielsen, P. E. & Egholm, M. An introduction to peptide nucleic acid. *Curr. Issues Mol. Biol.* **1,** 89–104 (1999).

117. Eriksson, M. & Nielsen, P. E. PNA-nucleic acid complexes. Structure, stability and dynamics. *Q.Rev.Biophys.* **29,** 369–394 (1996).

118. Haaima, G. *et al.* Peptide Nucleic Acids (PNAs) Containing Thymine Monomers Derived from Chiral Amino Acids: Hybridization and Solubility Properties of D-Lysine PNA. *Angew. Chemie Int. Ed. Engl.* 1939–1942 (1996). doi:10.1002/anie.199619391

119. Sforza, S., Corradini, R., Ghirardi, S., Dossena, A. & Marchelli, R. Binding of A D-Lysine-Based Chiral PNA : Direction Control and Mismatch Recognition. *European J. Org. Chem.* 2905–2913 (2000). doi:10.1002/1099-0690(200008)2000:16<2905::AID-EJOC2905>3.0.CO;2-D

120. Menchise, V. *et al.* Insights into peptide nucleic acid (PNA) structural features: the crystal structure of a D-lysine-based chiral PNA-DNA duplex. *Proc. Natl. Acad. Sci. U. S. A.* **100,** 12021–6 (2003).

121. Zhou, P. *et al.* Novel Binding and Efficient Cellular Uptake of Guanidine-Based Peptide Nucleic Acids (GPNA). *J. Am. Chem. Soc. Commun.* **125,** 6878–6879 (2003).

122. Gupta, P., Muse, O. & Rozners, E. Recognition of double-stranded RNA by guanidine-modified peptide nucleic acids. *Biochemistry* **51,** 63–73 (2012).

123. Hamzavi, R., Dolle, F., Tavitian, B., Dahl, O. & Nielsen, P. E. Modulation of the pharmacokinetic properties of PNA: Preparation of galactosyl, mannosyl, fucosyl, N-acetylgalactosaminyl, and N-acetylglucosaminyl derivatives of aminoethylglycine peptide nucleic acid monomers and their incorporation into PNA oligomers. *Bioconjug. Chem.* **14,** 941–954 (2003).

124. Hamzavi, R., Meyer, C. & Metzler-Nolte, N. Synthesis of a C-linked glycosylated thymine-based PNA monomer and its incorporation into a PNA oligomer. *Org. Biomol. Chem.* **4,** 3648–3651 (2006).

125. Aguado, G. P., Rúa, F., Branchadell, V., Nielsen, P. E. & Ortuño, R. M. Cyclobutyl-carbonyl substituted PNA: synthesis and study of a novel PNA derivative. *Tetrahedron Asymmetry* **17,** 2499–2503 (2006).

126. Dorn, S. *et al.* Side chain modified peptide nucleic acids (PNA) for knock-down of six3 in medaka embryos. *BMC Biotechnol.* **12,** (2012).

127. Gourishankar, A. & Ganesh, K. N. (α,α-dimethyl)glycyl (dmg) PNAs Achiral PNA analogs that form stronger hybrids with cDNA relative to isosequential RNA. *Artif. DNA PNA XNA* **3,** 5–13 (2012).

128. Sugiyama, T. *et al.* β-PNA: Peptide nucleic acid (PNA) with a chiral center at the β-position of the PNA backbone. *Bioorganic Med. Chem. Lett.* **21,** 7317–7320 (2011).

129. Sugiyama, T. *et al.* Peptide Nucleic Acid with a Lysine Side Chain at the β-Position: Synthesis and Application for DNA Cleavage. *Chem. Pharm. Bull. (Tokyo).* **64,** 817–823 (2016).

130. Kosynkina, L., Wang, W. & Chyau Liang, T. A Convenient Synthesis Of Chiral Peptide Nucleic Acid (PNA) Monomers. *Tetrahedron Lett.* **35,** 5173–5176 (1994).

131. Englund, E. A. & Appella, D. H. Synthesis of gamma-substituted peptide nucleic acids: a new place to attach fluorophores without affecting DNA binding. *Org.*

Lett. **7,** 3465–7 (2005).

132. Dose, C. & Seitz, O. Convergent Synthesis of Peptide Nucleic Acids by Native Chemical Ligation. *Org. Lett.* **7,** 4365–4368 (2005).

133. Sforza, S., Tedeschi, T., Corradini, R. & Marchelli, R. Induction of helical handedness and DNA binding properties of peptide nucleic acids (PNAs) with two stereogenic centres. *European J. Org. Chem.* 5879–5885 (2007). doi:10.1002/ejoc.200700644

134. Tedeschi, T., Sforza, S., Corradini, R. & Marchelli, R. Synthesis of new chiral PNAs bearing a dipeptide-mimic monomer with two lysine-derived stereogenic centres. *Tetrahedron Lett.* **46,** 8395–8399 (2005).

135. Crawford, M. J., Rapireddy, S., Bahal, R., Sacui, I. & Ly, D. H. Effect of steric constraint at the γ-backbone position on the conformations and hybridization properties of PNAs. *J. Nucleic Acids* **2011,** vol. 2011, Article ID 652702, 10 pages (2011).

136. Falkiewicz, B., Wisniowski, W., Kolodziejczyk, A. S. & Wisniewski, K. Synthesis of new chiral peptide nucleic acid (PNA) monomers. *Nucleosides Nucleotides Nucleic Acids* **20,** 1393–1397 (2001).

137. Bahal, R., Sahu, B., Rapireddy, S., Lee, C. M. & Ly, D. H. Sequence-Unrestricted, Watson-Crick Recognition of Double Helical B-DNA by (R)-MiniPEG-γPNAs. *ChemBioChem* **13,** 56–60 (2012).

138. Sahu, B. *et al.* Synthesis and Characterization of Conformationally Preorganized , (R) -Diethylene Glycol-Containing γ -Peptide Nucleic Acids with Superior Hybridization Properties and Water Solubility. *J. Org. Chem.* **76,** 5614–5627 (2011).

139. Dose, C. & Seitz, O. Single nucleotide specific detection of DNA by native chemical ligation of fluorescence labeled PNA-probes. *Bioorganic Med. Chem.* **16,** 65–77 (2008).

140. Corradini, R., Sforza, S., Tedeschi, T. & Marchelli, R. Chirality as a Tool in Nucleic Acid Recognition: Principles and Relevance in Biotechnology and in Medicinal Chemistry. *Chirality* **19,** 269–294 (2007).

141. Englund, E. A. & Appella, D. H. γ-substituted peptide nucleic acids constructed from L-lysine are a versatile scaffold for multifunctional display. *Angew. Chemie - Int. Ed.* **46,** 1414–1418 (2007).

142. Ficht, S., Dose, C. & Seitz, O. As fast and selective as enzymatic ligations: Unpaired nucleobases increase the selectivity of DNA-controlled native chemical PNA ligation. *ChemBioChem* **6,** 2098–2103 (2005).

143. Kumar, V. A. & Ganesh, K. N. Conformationally constrained PNA analogues: Structural evolution toward DNA/RNA binding selectivity. *Acc. Chem. Res.* **38,** 404–412 (2005).

144. Oleszczuk, M., Rodziewicz-Motowidło, S. & Falkiewicz, B. Restricted Rotation in Chiral Peptide Nucleic Acid (PNA) Monomers - Influence of Substituents Studied by Means of ^{1}H NMR. *Nucleosides, Nucleotides and Nucleic Acids* **20,** 1399–1402 (2001).

145. Chen, S. M., Mohan, V., Kiely, J. S., Griffith, M. C. & Griffey, R. H. Molecular dynamics and NMR studies of single-stranded PNAs. *Tetrahedron Lett.* **35,** 5105–5108 (1994).

146. Ovadia, R. *et al.* Synthesis and structural characterization of monomeric and dimeric peptide nucleic acids prepared by using microwave-promoted multicomponent reaction. *Org. Biomol. Chem.* **13,** 11052–11071 (2015).

147. Brown, S. C., Thomson, S. A., Veal, J. M. & Davis, D. G. NMR solution structure of a peptide nucleic acid complexed with RNA. *Science (80-.).* **265,** 777–780 (1994).

148. He, W. *et al.* Solution structure of a peptide nucleic acid duplex from NMR data: features and limitations.(Supporting Information). *J. Am. Chem. Soc.* **130,**

13264–73 (2008).

149. Upert, G. *et al.* The ‘fully protected backbone’ approach as a versatile tool for a new solid-phase PNA synthesis strategy. *Tetrahedron Lett.* **46,** 4081–4085 (2005).

150. Mills, J. E., Marynoff, C. A., McComsey, D. F., Stanzione, R. C. & Scott, L. The Reaction of Amines with Methylene Chloride. Evidence for Rapid Aminal Formation from N-Methylenepyrrolidinium Chloride and Pyrrolidine. *J. Org. Chem.* **52,** 1857–1859 (1987).

151. Rudine, A. B., Walter, M. G. & Wamser, C. C. Reaction of dichloromethane with pyridine derivatives under ambient conditions. *J. Org. Chem.* **75,** 4292–4295 (2010).

152. Ruan, Z., Van Kirk, K., Cooper, C. B. & Lawrence, R. M. A Novel, One-Step Palladium and Phenylsilane Activated Amidation from Allyl Ester on Solid Support. *Res. Lett. Org. Chem.* **2008,** 1–4 (2008).

153. Merrifield, B. Solid Phase Synthesis. *Science,* **232,** 341–347 (1986).

154. Palomo, J. M. Solid-phase peptide synthesis: an overview focused on the preparation of biologically relevant peptides. *RSC Adv.* **4,** 32658–32672 (2014).

155. Yadav, J. S., Balanarsaiah, E., Raghavendra, S. & Satyanarayana, M. Chemoselective hydrolysis of *tert*-butyl esters in acetonitrile using molecular iodine as a mild and efficient catalyst. *Tetrahedron Lett.* **47,** 4921–4924 (2006).

156. Nigama, S. C., Mann, A., Taddei, M. & Wermutha, C.-G. Selective Removal of the *tert*-Butoxycarbonyl Group from Secondary Amines: $ZnBr_2$ as the Deprotecting Reagent. *Synth. Commun.* **19,** 3139–3142 (1989).

157. Marcantoni, E., Massaccesi, M., Bartoli, G., Bosco, M. & Sambri, L. Selective Deprotection of *N*-Boc-Protected *tert* -Butyl Ester Amino Acids by the $CeCl_3$ $7H_2O$ - NaI System in Acetonitrile. *J. Org. Chem.* **66,** 4430–4432 (2001).

158. Evans, V., Mahon, M. F. & Webster, R. L. A mild, copper-catalysed amide deprotection strategy: Use of tert-butyl as a protecting group. *Tetrahedron* **70,** 7593–7597 (2014).

Annex I

TOCSY

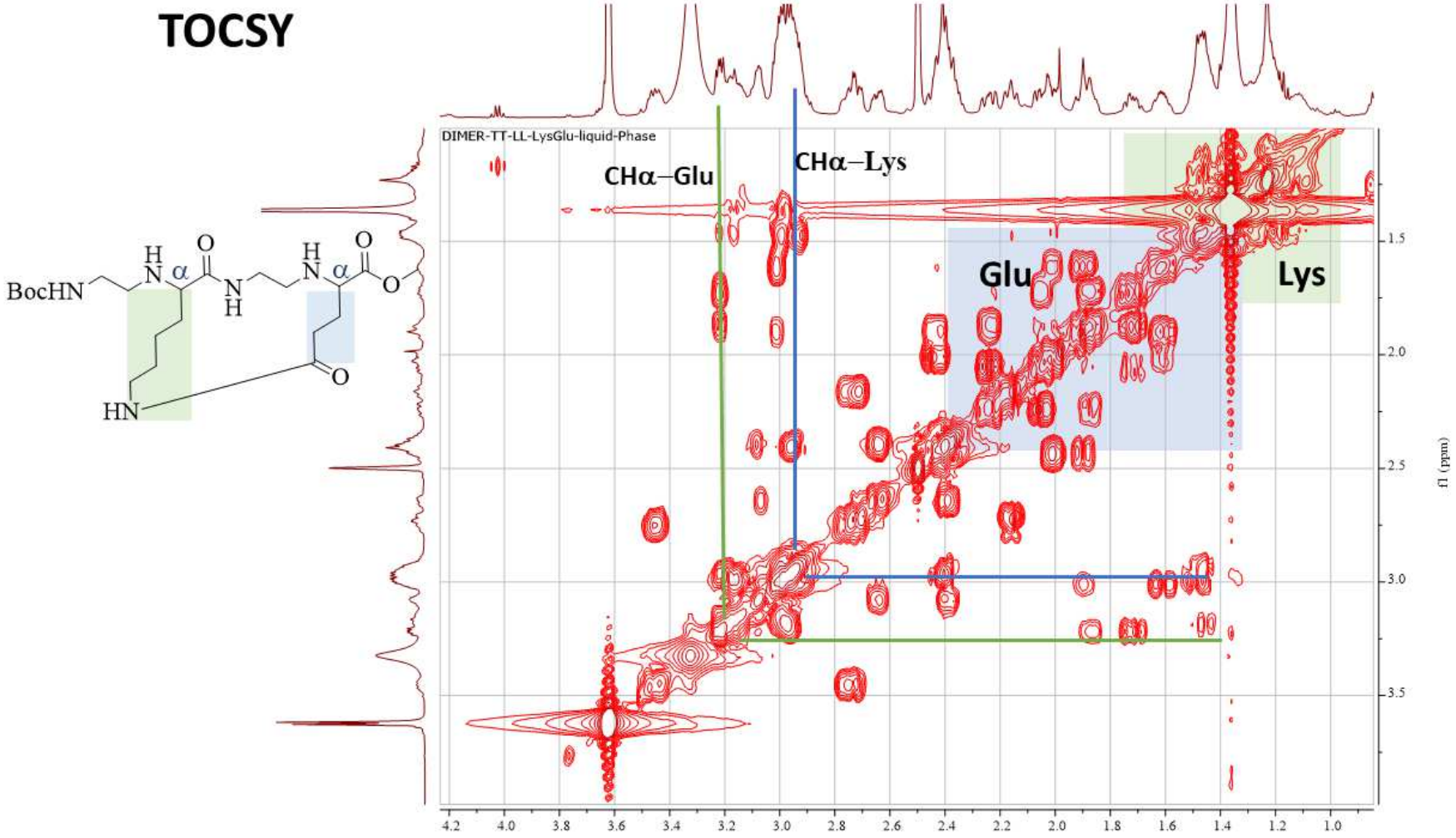
DIMER-TT-LL-LysGlu-liquid-Phase
CHα–Glu
CHα–Lys
Glu
Lys
BocHN
HN
f1 (ppm)

TOCSY

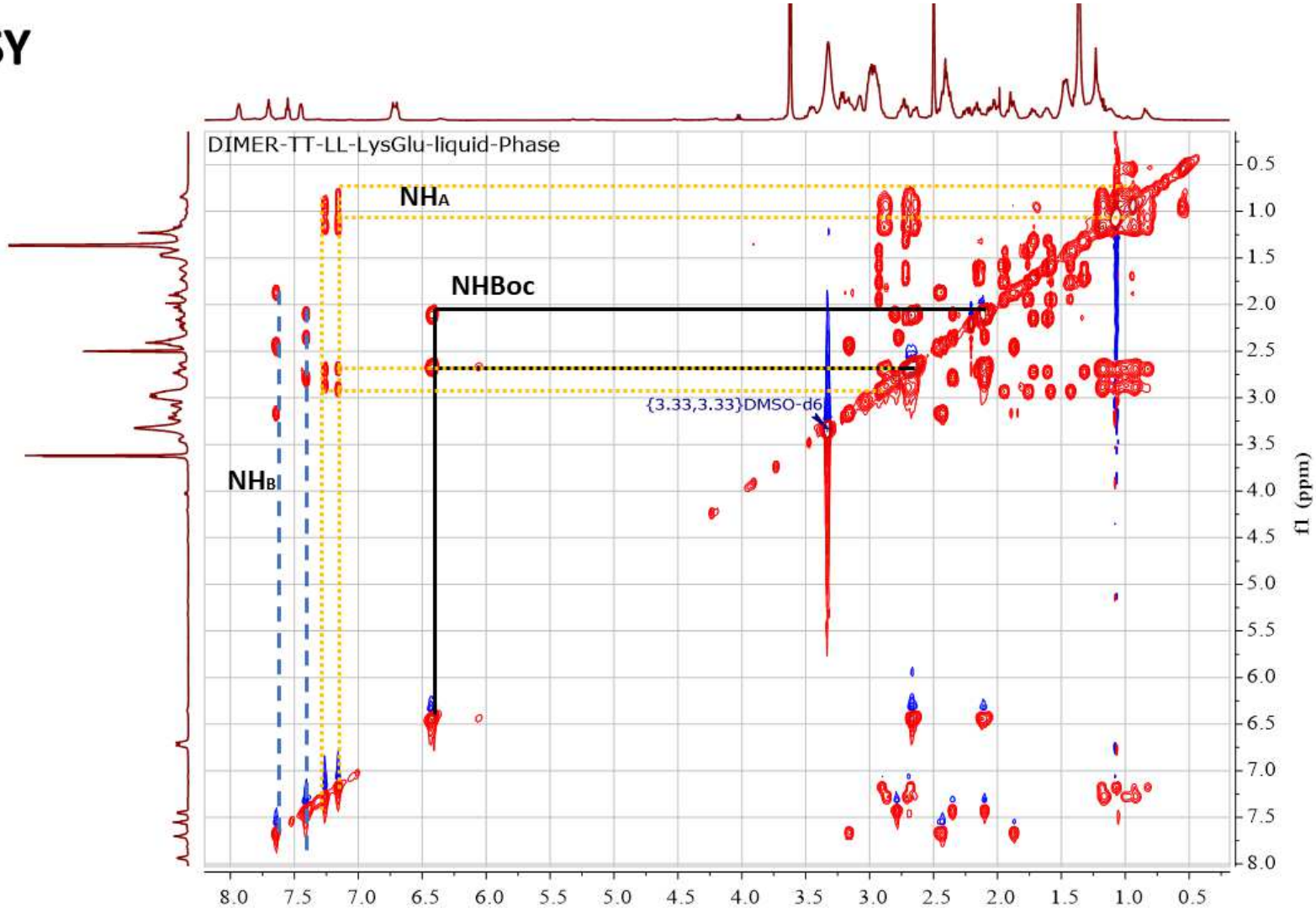
DIMER-TT-LL-LysGlu-liquid-Phase
NHA
NHBoc
NHB
{3.33,3.33}DMSO-d6
f1 (ppm)
8.0
7.5
7.0
6.5
6.0
5.5
5.0
4.5
4.0
3.5
3.0
2.5
2.0
1.5
1.0
0.5

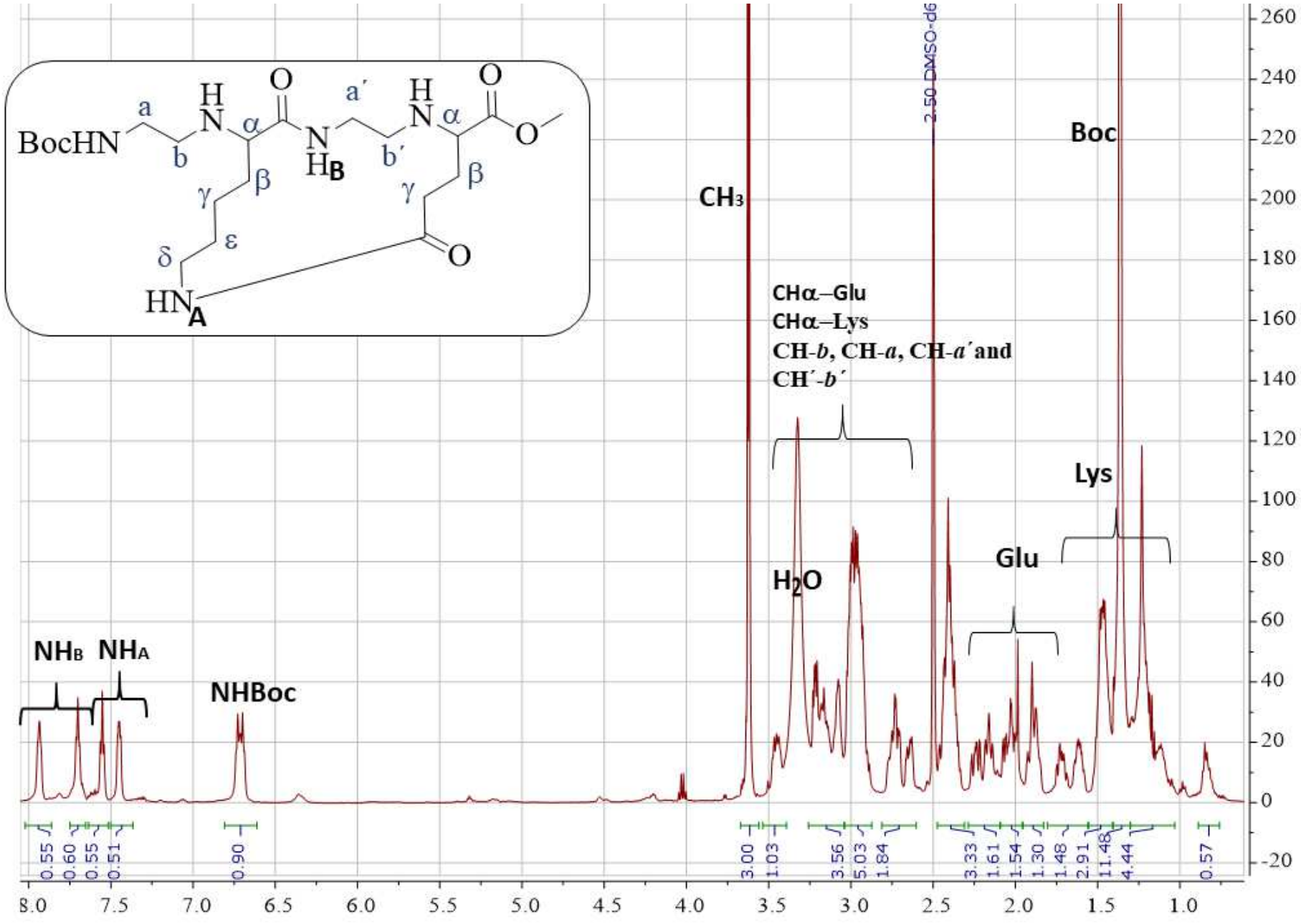
BocHN
a
b
H
N
α
O
N
H
B
a′
b′
H
N
α
O
O
γ
β
γ
β
δ
ε
O
HN
A
CH3
2.50 DMSO-d6
Boc
CHα–Glu
CHα–Lys
CH-b, CH-a, CH-a′ and
CH′-b′
Lys
Glu
H2O
NHB NHA
NHBoc
260
240
220
200
180
160
140
120
100
80
60
40
20
0
-20
0.55
0.60
0.55
0.51
0.90
3.00
1.03
3.56
5.03
1.84
3.33
1.61
1.54
1.30
1.48
2.91
11.48
4.44
0.57
8.0
7.5
7.0
6.5
6.0
5.5
5.0
4.5
4.0
3.5
3.0
2.5
2.0
1.5
1.0